swiss medical weekly

A diamond open access online journal | established in 1871 |
published by the SMW supporting association | www.smw.ch

Supplementum 306
ad Swiss Med Wkly 2026;156
November 11, 2026

Abstracts of the Swiss Oncology & Hematology Congress (SOHC)

Basel (Switzerland), November 18–20, 2026

SOHC
SWISS ONCOLOGY & HEMATOLOGY CONGRESS

SSMO SSOM SGMO · SGH+SSH · SWISS CANCER INSTITUTE



9TH SWISS ONCOLOGY AND HEMATOLOGY CONGRESS (SOHC)
BASEL, NOVEMBER 18–20, 2026

TABLE OF CONTENTS

SSH best abstract award – hemostasis, transfusion medicine, vascular, laboratory medicine, benign hematology ..... 2 S

SSH/SSMO best abstract award – experimental hematology / oncology ..... 4 S

SSH/SSMO best abstract award – clinical hemato-oncology ..... 4 S

SSMO best abstract award – clinical solid tumor oncology ..... 5 S

Oncoreha/OPS/palliative.ch/SNIO/SOHC best abstract award – nursing, supportive & palliative care, rehabilitation & survivorship and integrative oncology ..... 6 S

SSH oral presentation – hemostasis, transfusion medicine, vascular, laboratory medicine, benign hematology ..... 6 S

SSH/SSMO oral presentation – experimental hematology / oncology ..... 13 S

SSH/SSMO oral presentation – clinical hemato-oncology ..... 18 S

Oncoreha/OPS/palliative.ch/SNIO/SOHC oral presentation – nursing, supportive & palliative care, rehabilitation & survivorship and integrative oncology ..... 26 S

SSH poster presentation – hemostasis, transfusion medicine, vascular, laboratory medicine, benign hematology ..... 30 S

SSH/SSMO poster presentation – experimental hematology / oncology ..... 41 S

SSH/SSMO poster presentation – clinical hemato-oncology ..... 49 S

SSMO poster presentation – clinical solid tumor oncology ..... 58 S

Oncoreha/OPS/palliative.ch/SNIO/SOHC poster presentation – nursing, supportive & palliative care, rehabilitation & survivorship and integrative oncology ..... 62 S

Poster – hemostasis, transfusion medicine, vascular, laboratory medicine, benign hematology ..... 66 S

Poster – experimental hematology / oncology ..... 76 S

Poster – clinical solid tumor oncology ..... 85 S

Poster – nursing, supportive & palliative care, rehabilitation & survivorship and integrative oncology ..... 95 S

Index of first authors ..... 96 S

SSH BEST ABSTRACT AWARD - HEMOSTASIS, TRANSFUSION MEDICINE, VASCULAR, LABORATORY MEDICINE, BENIGN HEMATOLOGY

4544

Enhancing Gas6–TAM Signaling to Restore Immune Homeostasis in Sepsis

M. Fathi (1, 2), S. Çaku (1, 2), R. Prince (1, 2), R. Diab (1, 2), R. Etzensperger (1, 2), M. Tripodo (1, 2), T. Knopp (1, 2), B. Li (1, 2), E. Introini (1, 2), C. Keragala (3), R. Medcalf (3), C. Pfortmüller (4), R. Allam (1, 2), A. Messmer (4), A. Angelillo-Scherrer (1, 2, 3)

Department of Hematology and Central Hematology Laboratory, Bern University Hospital, Inselspital, University of Bern, Bern (1), Department for BioMedical Research, University of Bern, Bern (2), Molecular Neurotrauma and Haemostasis, Australian Centre for Blood Diseases, Monash University, Melbourne (3), Department of Intensive Care Medicine, Inselspital, Bern University Hospital, University of Bern, Bern (4)

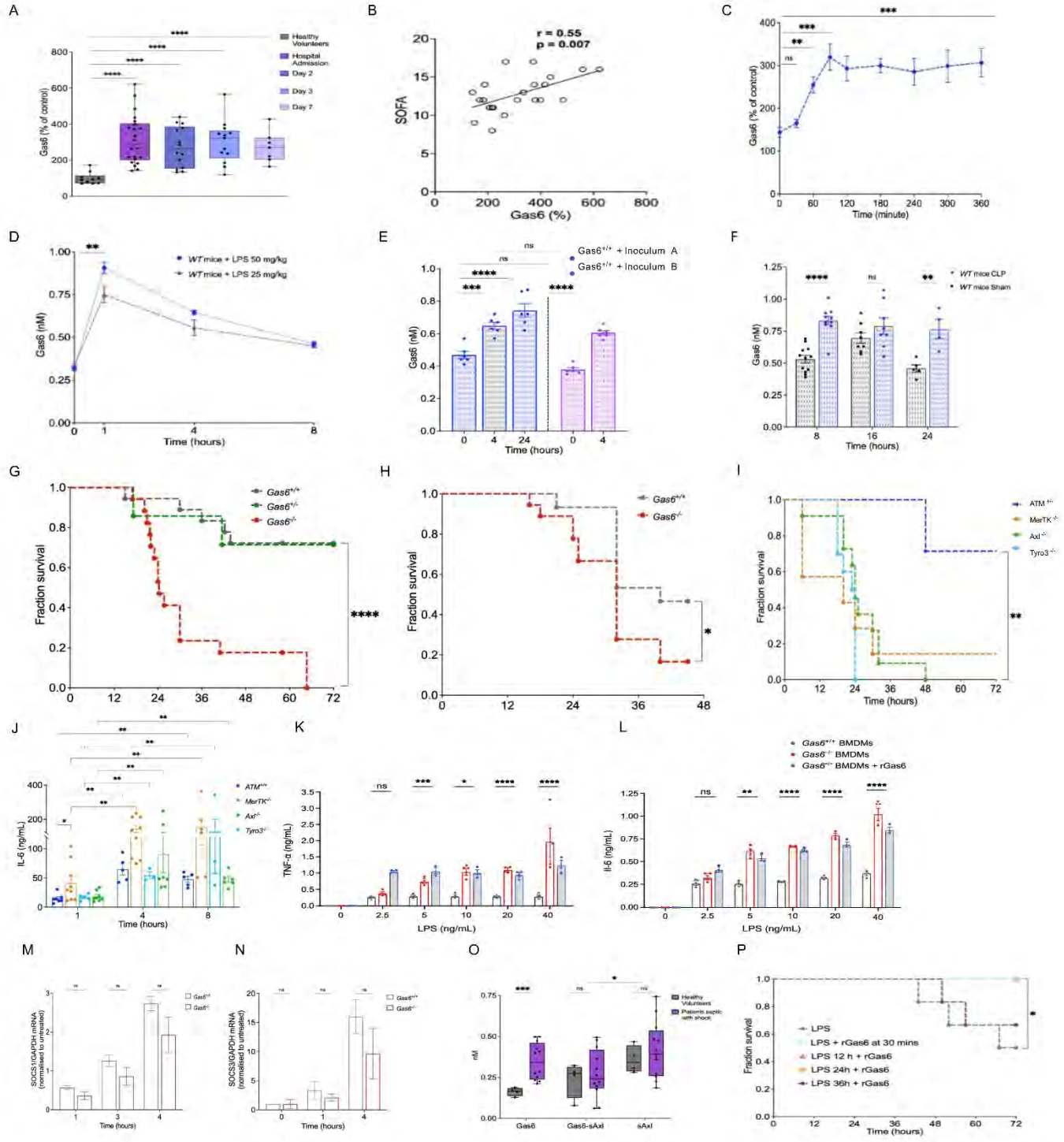
Introduction: Sepsis is characterized by dysregulated immune responses, loss of immune homeostasis, and organ dysfunction. Growth arrest-specific protein 6 (Gas6), a ligand of TAM receptors (Tyro3, Axl, MerTK), is elevated during systemic inflammation. In septic shock, Gas6 rises rapidly, remains elevated for at least seven days, and correlates with SOFA scores. However, soluble Axl (sAxl) may sequester Gas6 and limit protective TAM signaling. We investigated whether Gas6–TAM signaling is an endogenous protective pathway and whether increasing Gas6 bioavailability reduces inflammation and improves survival.

Methods: Gas6 was assessed in patients with sepsis and experimental models of systemic inflammation. LPS-induced endotoxemia was studied in $Gas6^{-/-}$ and individual TAM receptor-deficient mice by assessing survival and inflammatory cytokines. Wild-type mice received recombinant Gas6 (rGas6) after LPS challenge, and survival, Gas6, sAxl, Gas6–sAxl complexes, IL-6, and TNF-α were evaluated. Cytokine release and SOCS1/3 expression were assessed in LPS-stimulated BMDMs with or without Gas6 signaling.

Results: Gas6 was elevated in severe sepsis and septic shock, correlated with SOFA scores, and increased after LPS challenge in humans and in murine endotoxemia, E. coli peritonitis, and cecal ligation and puncture models (Fig. A-F). Despite its association with disease severity, Gas6 or individual TAM receptor deficiency increased mortality and controlled inflammatory responses, demonstrating a protective role for Gas6–TAM signaling (Fig. G-J). $Gas6^{-/-}$ macrophages showed increased TNF-α and IL-6 levels and reduced SOCS1/3 induction, while rGas6 treatment reduced TNF-α and IL-6 levels. (Fig. K-N). In septic shock, Gas6 concentrations closely matched Gas6–sAxl complexes while sAxl remained unsaturated, indicating limited free Gas6 despite elevated total Gas6 (Fig. O). Increasing Gas6 bioavailability with rGas6 improved survival following LPS challenge (Fig. P).

Conclusions: Increased Gas6 during sepsis represents a compensatory protective response constrained by sAxl-mediated sequestration. Gas6–TAM signaling provides endogenous negative feedback limiting inflammation, while increasing Gas6 bioavailability improves survival. Targeting sAxl to release endogenous Gas6 may therefore restore physiological TAM signaling and immune homeostasis in sepsis.

 Published under the CC license Attribution 4.0 International (CC BY 4.0)



Enhancing Gas6–TAMSignaling to Restore Immune Homeostasis in Sepsis: (A) Gas6 plasma levels in healthy volunteers and in patients with septic shock at hospital admission and at day 2, day 3, and day 7 (2-way ANOVA, Dunnett's multiple-comparisons test). (B) Spearman correlation and linear regression analyses assessing the relationship between plasma Gas6 levels and SOFA score in patients with septic shock. (C) Gas6 levels in plasma of healthy volunteers (n = 8) at steady state (t0) and after 15 ng/kg LPS i.v. injection (repeated-measures ANOVA and Bonferroni's multiple-comparisons test). (D) Gas6 levels in plasma of WT mice at steady state and at different time points after LPS injection (25 or 50 mg/kg; data from two independent experiments). (E) WT mice were inoculated intraperitoneally with the E. coli strain O1857 (inoculum A: 1.5×10^4 CFU; inoculum B: 1.5×10^4 to 2.5×10^5 CFU), and plasma Gas6 levels were measured at different time points (2-way ANOVA, Dunnett's multiple-comparisons test). (F) Gas6 plasma levels at 8, 16, and 24 h after CLP compared with sham-operated mice (2-way ANOVA, Bonferroni's multiple-comparisons test). (G) Kaplan–Meier plots of the survival of $Gas6^{+/+}$, $Gas6^{+/-}$, and $Gas6^{-/-}$ mice treated with LPS (25 mg/kg, i.p.). Data are pooled from multiple independent experiments (total n: $Gas6^{+/+}$ = 18, $Gas6^{+/-}$ = 17, $Gas6^{-/-}$ = 7). Log-rank Mantel–Cox test. (H) CLP survival in $Gas6^{+/+}$ and $Gas6^{-/-}$ mice. Data from three independent experiments (total n: $Gas6^{+/+}$ = 15, $Gas6^{-/-}$ = 18). Log-rank Mantel–Cox test. (I) Kaplan–Meier plots of the survival of WT ($ATM^{+/+}$) mice and mice lacking individual Gas6 receptors ($Axl^{-/-}$, $MerTK^{-/-}$, and $Tyro3^{-/-}$) treated with LPS (25 mg/kg). Data from two independent experiments (total n: $ATM^{+/+}$ = 7, $MerTK^{-/-}$ = 7, $Axl^{-/-}$ = 11, $Tyro3^{-/-}$ = 10). Log-rank Mantel–Cox test. (J) IL-6 levels in $ATM^{+/+}$, $Axl^{-/-}$, $MerTK^{-/-}$, and $Tyro3^{-/-}$ mice at 1, 4, and 8 h after LPS injection (25 mg/kg). Tukey's multiple-comparisons test. (K) 24-hour TNF-α secretion by $Gas6^{+/+}$ BMDMs, $Gas6^{-/-}$ BMDMs, and $Gas6^{-/-}$ BMDMs treated with rGas6 (400 ng/mL) following LPS stimulation (2.5–40 ng/mL; 0 ng/mL as unstimulated control). (L) 24-hour IL-6 secretion by $Gas6^{+/+}$ BMDMs, $Gas6^{-/-}$ BMDMs, and $Gas6^{-/-}$ BMDMs treated with rGas6 (400 ng/mL) following LPS stimulation (2.5–40 ng/mL; 0 ng/mL as unstimulated control). (M) Relative mRNA expression of suppressor of cytokine signaling 1 (SOCS1) quantified by qPCR using GAPDH as the housekeeping gene and normalized to untreated cells. BMDMs were stimulated with LPS (40 ng/mL) for 1, 3, and 4 h. Tukey's multiple-comparisons test. (N) Relative mRNA expression of suppressor of cytokine signaling 3 (SOCS3) quantified by qPCR using GAPDH as the housekeeping gene and normalized to baseline expression. BMDMs were assessed at 0, 1, and 4 h following LPS stimulation (40 ng/mL). (O) Plasma levels of Gas6, soluble Gas6–sAxl complexes, and sAxl in healthy volunteers and patients with septic shock (Tukey's multiple-comparisons test). (P) Kaplan–Meier plots of the survival of WT mice treated with LPS (10 mg/kg), with or without rGas6 (10 µg intravenously) administered at different time points following LPS injection (n = 6 mice per group). Log-rank Mantel–Cox test. ns, non-significant; *P < 0.05, **P < 0.01, ***P < 0.001, ****P < 0.0001.

Published under the CC license Attribution 4.0 International (CC BY 4.0)

SSH/SSMO BEST ABSTRACT AWARD - EXPERIMENTAL HEMATOLOGY / ONCOLOGY

1941

Tet2-Clonal Hematopoiesis Promotes Whereas Dnmt3a-CH Inhibits Breast Cancer Progression During Aging

K. A. Zielinska (1), N. G. Gonullu (1), J. Fullin (1), F. Prisco (2), S. Boettcher (1), F. Caiado (1), M. G. Manz (1)

Medical Oncology and Hematology, University Hospital Zurich, Zurich (1), Institute for Veterinary Pathology, University of Zurich, Zurich (2)

Introduction: Clonal hematopoiesis of indeterminate potential (CHIP) defined by the expansion of a somatic blood clone carrying mutations in leukemia-related genes frequently in DNMT3A or TET2, is a common manifestation of hematopoietic aging. CHIP incidence increases with age and is associated with multiple health hazards including increased risks of hematologic and non-hematological cancers. However, how CHIP influences solid tumor progression remains poorly understood. In this study, we hypothesized that Tet2- or Dnmt3a-driven CHIP influences breast cancer growth and metastasis by modulating the tumor immune microenvironment.

Methods: We developed a novel triple transgenic mouse model of CHIP, where floxed Tet2 or Dnmt3a R878H alleles and a reporter gene are controlled by an inducible hematopoietic-specific Cre enzyme. These were combined with a syngeneic, orthotopic, traceable breast cancer model using E0771 and Py230 cells, in young (3-4 months) and middle-aged (12-14 months) mouse cohorts. Tumor growth and metastasis were monitored longitudinally, supported by histology, flow cytometry, and single-cell RNA sequencing to elucidate molecular mechanisms.

Results: Upon aging, Tet2- and Dnmt3a-mutant CHIP have opposing impacts on breast cancer progression, with Tet2-mutant CHIP driving and Dnmt3a-mutant CHIP preventing primary tumor growth and metastasis. Dnmt3a-mutant immune infiltrates drive a robust adaptive immune tumor rejection, establishing an interferon-mediated development of MHCII high tumor associated macrophage (TAM) populations that support cytotoxic CD8+ T cell responses. In contrast, Tet2-mutant TAMs produce increased levels of innate-like inflammatory mediators IL-1 and CXCL2 imprinting an immunosuppressive phenotype that hinders efficient cytotoxic CD8+ T cell-mediated anti-tumor immune response. We further show that targeting this IL-1 / Cxcl2-mediated TAM polarization in aged mice results in the reversion of their immunosuppressive phenotypes, allowing for the establishment of a CD8+ T cell cytotoxic response capable of preventing increased tumor progression driven by an aged Tet2-mutant immune compartment.

Conclusions: These findings suggest that age and CHIP mutations synergistically influence breast cancer progression by reshaping tumor-infiltrating immune populations in a mutation-dependent manner, establishing a mechanistic link between CHIP and solid tumor immunity.

SSH/SSMO BEST ABSTRACT AWARD - CLINICAL HEMATO-ONCOLOGY

4577

Second Primary Malignancies after CAR-T-Cell Therapy: A Real-World Study from Three University Centers

J. Lechner (1), I. Shafarostova (1), L. Kolloch (2), M. Maulhardt (3), M. Kronig (1), U. Bacher (4), G. Lenz (2), T. Pabst (1)

Medical Oncology, Inselspital, Bern (1), Medicine A, University Hospital Münster, Münster (2), Medicine A, University Hospital Göttingen, Göttingen (3), Hematology, Inselspital, Bern (4)

Introduction: Chimeric antigen receptor cell (CAR-T-cell) therapy has improved treatment outcomes in relapsed/refractory B-cell malignancies but may cause serious complications. Data regarding long-term effects after CAR-T-cell therapy remains limited. Recent reports suggest an increased risk of secondary primary malignancies (SPMs).

Methods: The aim of this retrospective study was to evaluate the risk of SPMs after CAR-T-cell therapy and to assess patient (pt) outcomes.

Results: A total of 618 adult pts with hematologic malignancies (HMs) treated with CAR-T-cell therapy at three centers in Switzerland and Germany between January 2019 and October 2025 were included. The median follow-up was 37 months (range, 5-66). 34 pts (5.5%) developed SPMs. The median age was 70 years, with 65% male and 35% female pts. The median onset time of SPM following CAR-T-cell infusion was 15 months (range, 2-61). The underlying diagnoses included diffuse large B-cell lymphoma (56%), mantle cell lymphoma (17%), multiple myeloma (15%), follicular lymphoma (6%) and B-ALL (6%). The pts had received a median number of 3 prior lines of therapy (range, 1-15). CAR T-cell products administered included axicabtagene ciloleucel, tisagenlecleucel, brexucabtagene autoleucel, idecabtagene vicleucel and lisocabtagen maraleucel

Table 1 Characteristics of Patients With SPMs Following CAR T-Cell Therapy

Characteristics	Patients With SPMs
SPMs, total, n (%)	34 (5.5%)[1]
HSPMs, n (%)	10 (29%)[2]
Solid tumors, n (%)	24 (71%)[2]
HSPMs	
MDS, n (%)	8 (80%)[3]
AML, n (%)	2 (20%)[3]
Types of solid tumors	
NMSCs, n (%)	9 (26%)[2]
Squamous cell carcinoma, n (%)	5 (56%)[4]
Basal cell carcinoma, n (%)	4 (44%)[4]
Morbus Bowen, n (%)	1 (11%)[4]
Genitourinary, n (%)	3 (9%)[2]
Prostata, n (%)	2 (67%)[4]
Bladder, n (%)	1 (33%)[4]
Breast, n (%)	2 (6%)[2]
Gastrointestinal, n (%)	2 (6%)[2]
Esophageal, n (%)	1 (50%)[4]
Colorectal, n (%)	1 (50%)[4]
Oropharyngeal, n (%)	2 (6%)[2]
Lung, n (%)	1 (3%)[2]
Ovarian, n (%)	1 (3%)[2]
Melanoma, n (%)	1 (3%)[2]
CUP, n (%)	3 (9%)[2]
Multiple malignancies (all of them NMSCs), n (%)	6 (18%)[2]
Outcome	
SPMs as cause of death	6 (46%)[5]

[1]Refers to all patients.
[2]Refers to all patients with SPMs.
[3]Refers to patients with HSPMs as SPMs.
[4]Refers to patients of the respective organ system above.
[5]Refers to all deaths of patients with SPMs.
SPM – second primary malignancies, HSPM – Hematological second primary malignancies, MDS – Myelodysplastic Syndrome, AML – Acute Myeloid Leukemia, NMSC – Non-melanoma Skin Cancer, CUP – Cancer of Unknown Primary

in 38%, 24%, 18%, 15%and 6% of pts. Among pts who developed SPMs, hematologic SPMs (HSPMs) occurred in 10/34, while 24/34 developed solid tumors. Within the HSPM group, 8/10 of pts developed myelodysplastic syndrome (MDS), and 2/10 developed acute myeloid leukemia. Among pts with non-

 Published under the CC license Attribution 4.0 International (CC BY 4.0)

hematologic SPMs, non-melanoma skin cancers (NMSCs) were the most frequently observed (9/34). The remaining solid tumors included urological (3/34), breast (2/34), gastrointestinal (2/34), oropharyngeal (2/34), lung (1/34), ovarian (1/34), melanoma (1/34), and CUP (3/34). Six patients (6/34) developed multiple solid malignancies, all of which were NMSCs. At the time of the last follow-up, 38% had died, with SPMs as a cause of death in 46%. The 5-year progression-free and overall survival with SPMs were 36% and 38%, respectively (Table 1).

Conclusions: SPMs occurred in 5.5% of patients, mainly HMs and NMSCs, with no T-cell lymphomas observed. These findings support dermatological screening during follow-up, while further studies are needed to clarify risk factors and the role of prior therapies.

SSMO BEST ABSTRACT AWARD - CLINICAL SOLID TUMOR ONCOLOGY

6524

Prevention of symptomatic skeletal events (SSE) with reduced denosumab (Dmab) dose density (every 12 weeks versus every 4 weeks): A randomized phase III non-inferiority trial SAKK 96/12 (REDUSE)

R. von Moos (1), A. Müller (2), S. Hayoz (3), M. Mark (4), S. Fischer (5), R. Popescu (6), S. Rothschild (7), M. Fehr (8), C. Egger (9), S. Anchisi (10), F. Schmid (11), K. Zaman (12), C. Ackermann (13), H. Kugler (14), P. Bützberger (15), C. Uhlmann (16), M. Kueng (17), S. Wyss (18), S. Gillessen (19), A. Templeton (20), R. von Moos (21)

Tumor- und Forschungszentrum, Cantonal Hospital Graubünden, Chur (1), Onkologie, Cantonal Hospital Winterthur, Winterthur (2), Statistics, Swiss Cancer Institute, Bern (3), Oncology/Hematology, Dep. Innere Medizin, Cantonal Hospital Graubünden, Chur (4), Onkologie/Hämatologie, Health Ostschweiz, Cantonal Hospita St. Gallen, St. Gallen (5), Onkologie/Hämatologie, Tumor Zentrum Aargau and Hirslanden Klinik Aarau, Aarau (6), Onkologie/Hämatologie, Universitätsspital Basel and Cantonal Hospital Baden, Baden (7), Gynäkologie, Spital STGAG, Frauenfeld (8), Onkologie/Hämatologie, Spital Limmattal, Schlieren (9), Onkologie/Hämatologie, CHVR Hospital Valais, Sion (10), Onkologie/Hämatologie, University Hospital Zurich, Zurich (11), Onkologie/Hämatologie, Lausanne University Hospital (CHUV), Lausanne (12), Onkologie, Hospital of Thun STS AG, Thun (13), Oneologie/Hämatologie, Cantonal Hospital Aarau, Aarau (14), Onkologie/Hämatologie, Cantonal Hospital Baden, Baden (15), Onkologie/Hämatologie, Cantonal Hospital Olten, Olten (16), Onkologie/Hämatologie, HFR Fribourg – Cantonal Hospital, Fribourg (17), Competence Center, Swiss Cancer Institute, Bern (18), Onkologie, Cantonal Hospital Bellinzona (IOSI), Bellinzona (19), Onkologie, University Hospital Basel, Basel (20), Departement Direktion, Kantonsspital Graubünden, Chur (21)

Introduction: Guidelines recommend denosumab (Dmab) 120 mg every 4 weeks (Q4W) for patients (pts) with bone metastases. While a Q12W schedule is established for zoledronic acid, prospective trials evaluating a Q12W schedule for Dmab on skeletal-related events (SRE) are missing. Early dose-finding data showed similar suppression of bone-turnover markers for 60 mg Q12W and 120 mg Q4W. The REDUSE trial investigated whether a de-escalated Dmab schedule is non-inferior to standard Q4W in preventing symptomatic skeletal-related events (SSEs: symptomatic pathological fracture, radiation/surgery to bone, or spinal cord compression).

Methods: In this international, multicenter, randomized phase III trial, pts with metastatic breast cancer (BC) or metastatic castration-resistant prostate cancer (mCRPC) and ≥3 bone metastases were randomized 1:1. Arm A (standard) received Dmab 120 mg Q4W. Arm B (reduced) received 4 loading doses Q4W, followed by Q12W dosing. Primary endpoint: time to first on-trial SSE. Sample size (1,380 pts) was calculated for non-inferiority using a log-rank test with a margin of 1.20 (80% power, 5% type I error). Secondary endpoints included time to first and subsequent SSEs, and safety focusing on hypocalcemia and osteonecrosis of the jaw (ONJ).

Results: 1,380 pts were enrolled between 07/2014 and 03/2024 (784 BC, 596 mCRPC; median follow-up 37 months [42 BC, 29 mCRPC]). The trial met its primary endpoint, demonstrating non-inferiority of Q12W to Q4W. Median time to first SSE was 56.6 months (95% CI: 40.7, NR) in Arm A vs 56.5 months (95% CI: 47.7, NR) in Arm B (stratified HR 1.023 [90% CI: 0.874, 1.197]; upper limit <1.20). Non-inferiority was also shown for time to first and subsequent SSEs (stratified HR 1.043 [90% CI: 0.907, 1.198]). Safety was improved in Arm B: hypocalcemia occurred in 30% vs 46% (Arm A) and ONJ in 6.9% vs 8.5% of pts.

Conclusions: The SAKK 96/12 (REDUSE) trial demonstrates that Dmab Q12W following a 3-month loading phase is non-inferior to standard Q4W in pts with bone-metastatic BC or mCRPC. Lower rates of ONJ and hypocalcemia demonstrate a superior safety profile. Dmab Q12W represents a new standard of care, offering comparable efficacy while reducing toxicity, treatment burden, and costs.

 Published under the CC license Attribution 4.0 International (CC BY 4.0)

ONCOREHA/OPS/PALLIATIVE.CH/SNIO/SOHC BEST ABSTRACT AWARD - NURSING, SUPPORTIVE & PALLIATIVE CARE, REHABILITATION & SURVIVORSHIP AND INTEGRATIVE ONCOLOGY

0370

Multimodal Nutrition and Exercise Intervention Including a Smartphone Application: Effects on Muscle Outcomes in Patients with Advanced Cancer

L. Gafner (1), L. J. Storck (1, 2), M. Ruehlin (1), E. G. Gerrits (1, 3), Y. Krepp (2), R. Benkelmann (2), B. Rohrbach (4), C. J. Ackermann (4), A. Tan (1), M. Schmocker (5), P. J. Meffert (6), P. E. Ballmer (7, 8), M. Pless (9), C. Britschgi (9)

Center of Nutritional Medicine and Therapy, Kantonsspital Winterthur, Winterthur (1), Medizinische Klinik, Klinikum Konstanz, Konstanz (2), Clinic for Internal Medicine, Kantonsspital Winterthur, Winterthur (3), Oncology and Hematology, Spital Thun, Thun (4), Institute for Therapy and Rehabilitation, Kantonsspital Winterthur, Winterthur (5), Statistical Consulting, CORVUS, Alktalen (6), Past President, GESKES-SSNC, Winterthur (7), Praxis, am Graben, Winterthur (8), Clinic for Medical Oncology and Hematology, Kantonsspital Winterthur, Winterthur (9)

Introduction: A combined intervention consisting of nutritional counselling and structured physical exercise may improve quality of life (QoL) as well as muscle mass and strength in patients with advanced cancer who face a substantial risk of malnutrition. Mobile Health (mHealth) technologies enable remote monitoring and facilitate trial participation by limiting additional hospital visits.

Methods: After randomization, the intervention group participated in a multimodal programme with dietary counselling, exercise, and protein supplementation, while the control group received standard care. Both groups used a smartphone app for data recording. Assessments were conducted at baseline, after the three-month intervention period, and at six months to evaluate sustainability. The primary endpoint was QoL at three months (Functional Assessment of Cancer Therapy-General; FACT–G). Secondary endpoints included nutritional status, protein and energy intake, physical function, clinical outcomes, and fatigue. Skeletal muscle mass was assessed via bioelectrical impedance analysis (BIA), and muscle function using handgrip strength and the 60-second sit-to-stand test.

Results: A total of 73 patients with advanced lung or gastrointestinal (GI) cancer were enrolled at three study centres in Switzerland and Germany (62% male, 38% female; mean age 63.8 ±11.9 years; mean BMI 25.5 ±4.5 kg/m2). After three months, QoL improved in both groups, with no significant between-group difference (p = 0.734). The intervention group had significantly improved coverage of individual energy (p = 0.043) and protein (p = 0.002) requirements. There were no significant differences in muscle mass (p = 0.954), handgrip strength (p = 0.381), or the 60-second sit-to-stand test (p = 0.702).

Conclusions: Our results confirm the feasibility of the multimodal therapy in patients with advanced cancer. While the primary endpoint, QoL, was not met, the intervention group showed significantly increased coverage of individual energy and protein requirements (secondary endpoints). Explanations for the subtle differences regarding muscle outcomes may include cohort heterogeneity, selection bias, and increased motivation among the control group, who also used the study app.

	Baseline Control	Baseline Intervention	Δ 3 months Control	Δ 3 months Intervention	p =	95% CI
QoL (FACT-G), points	82.4 (±12.8)	84.3 (±12.0)	3.29	2.17	0.734	-5.5, 7.7
Energy requirement coverage, %	92.1 (±30.3)	88.1 (±25.6)	-13.8	2.4	**0.043**	-31.9, -0.5
Protein requirement coverage, %	88.7 (±39.6)	86.1 (±28.0)	-9.1	20.0	**0.002**	-47.0, -11.2
Skeletal muscle mass (BIA), kg	28.7 (±7.7)	29.6 (±6.0)	0.45	0.47	0.954	-0.9, 0.9
Handgrip strength (stronger hand), kg	33.5 (±10.3)	36.8 (±12.2)	0.00	0.86	0.381	-2.8, 1.1
60-s s sit-to-stand, repetitions	22.4 (±9.1)	24.7 (±7.3)	2.2	1.6	0.702	-2.5, 3.6

SSH ORAL PRESENTATION - HEMOSTASIS, TRANSFUSION MEDICINE, VASCULAR, LABORATORY MEDICINE, BENIGN HEMATOLOGY

6102

Protein S controlled expression as a haemostatic rebalancing strategy in factor XI deficiency

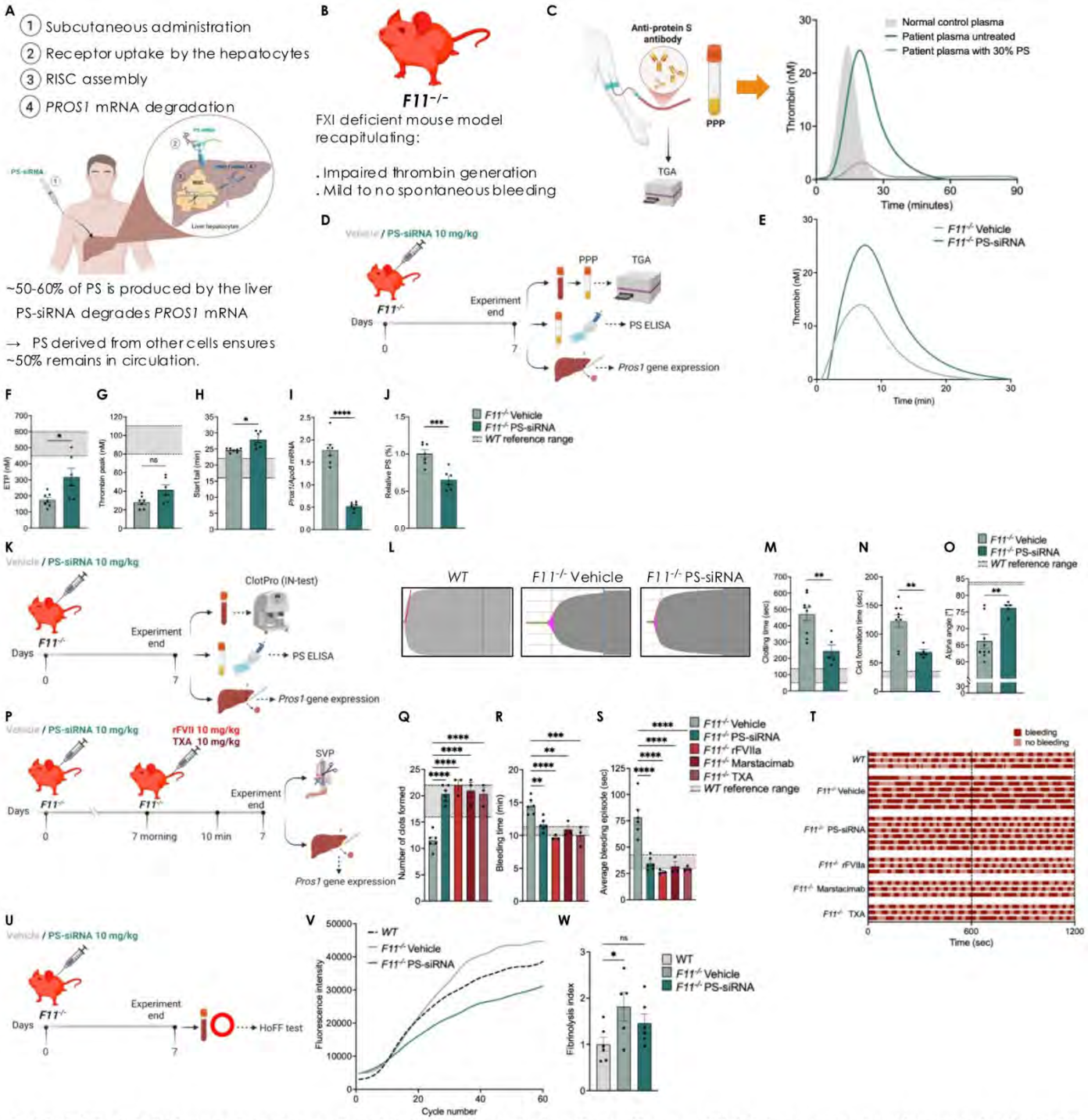
R. Diab (1, 2), M. Tripodo (1, 2), L. Calame-Longjean (1, 2), A. Staubli (1, 2), A. Casini (3), T. Renné (4), J. Kremer Hovinga (1, 2), R. Prince-Eladnani (1, 2), A. Angelillo-Scherrer (1, 2)

Department of Hematology and Central Hematology Laboratory, Inselspital, Bern University Hospital, Bern (1), Department for Biomedical Research, University of Bern, Bern (2), Division of Angiology and Hemostasis, Faculty of Medicine, Geneva University Hospitals, Geneva (3), Institute of Clinical Chemistry and Laboratory Medicine, University Medical Center Hamburg-Eppendorf, Hamburg (4)

Introduction: Factor XI (FXI) deficiency is a rare inherited bleeding disorder with impaired thrombin generation (TG) and a heterogeneous bleeding phenotype poorly predicted by FXI activity. Current prophylactic options have limited efficacy and/or thrombotic risk. Haemostatic rebalancing by attenuating endogenous anticoagulant pathways offers a non–factor replacement strategy for patients with clinically significant bleeding. Protein S (PS) limits TG through multiple anticoagulant pathways. We previously showed that liver-directed PS silencing using small interfering RNA (PS-siRNA) rebalanced haemostasis in haemophilia and Glanzmann thrombasthenia (Fig.A). Here, we assessed PS targeting in FXI deficiency (Fig.B).

Methods: Platelet-poor plasma from patients with severe FXI deficiency was spiked with an anti-PS antibody to reduce free PS to 30% or left untreated (Fig.C). TG was measured with 0.5 pM tissue factor and 2 nM thrombomodulin. F11-/- mice received a single subcutaneous dose of PS-siRNA or vehicle. On day seven, TG, viscoelastometry (ClotPro), halo fluorescence fibrinolysis, and saphenous vein puncture bleeding assays were performed.

 Published under the CC license Attribution 4.0 International (CC BY 4.0)



Protein S (PS) controlled expression enhances thrombin generation *ex vivo* in patients with severe FXI deficiency and restored haemostasis in factor XI deficient mice (*F11*$^{-/-}$). **(A)** Illustration showing the mode of action of protein S (PS) siRNA in the liver. **(B)** *F11*$^{-/-}$ mouse model used throughout the study. **(C)** Experimental overview for *ex vivo* patient thrombin generation assay (TGA). Platelet-poor plasma (PPP) from patients with FXI deficiency was either spiked with anti-PS antibody to reduce free PS to 30% or left untreated, followed by TGA in the presence of 0.5 pM tissue factor and 2 nM recombinant human thrombomodulin. Representative thrombograms are shown. **(D)** Experimental design TGA analysis. *F11*$^{-/-}$ mice received a single subcutaneous injection of 10 mg/kg PS-siRNA or vehicle (phosphate-buffered saline) on day 1. Blood was collected on day 7 for TGA. **(E)** Representative thrombograms, **(F)** endogenous thrombin potential (ETP), **(G)** thrombin peak, and **(H)** start tail, measured in PPP from PS-siRNA and vehicle-treated *F11*$^{-/-}$ mice. TG was assessed using calibrated automated thrombography in the presence of 0.5 pM tissue factor and 15 nM recombinant mouse thrombomodulin. **(I)** Quantitative real-time PCR of liver tissue to measure *Pros1* mRNA expression normalized to ApoB. **(J)** PS antigen level in plasma. *P values: ns, not significant; *P < .05; ***P < .001; unpaired t test.* **(K)** Experimental design for ClotPro analysis. *F11*$^{-/-}$ mice received PS-siRNA or vehicle as described above, followed by blood collection on day 7 for intrinsically activated ClotPro assay (IN-test; ellagic acid). **(L)** Representative clot formation curves, **(M)** clotting time, **(N)** clot formation time, and **(O)** alpha angle. *P values: **P < .01; unpaired t test.* **(P)** Experimental design for bleeding assessment. *F11*$^{-/-}$ mice received PS-siRNA or vehicle and underwent a saphenous vein puncture (SVP) on day 7. **(Q)** Number of clots formed, **(R)** total bleeding time (minutes), and **(S)** average number of bleeding episodes for the 20-minute observation period. *P values: **P < .01; ***P < .001; ****P < .0001; Brown–Forsythe analysis of variance (Anova), Dunnett's T3 multiple comparisons test.* **(T)** Stacked bar plots depicting bleeding and non-bleeding times for each experimental group across the 20-minute observation period. **(U)** Experimental design for halo fluorescence fibrinolysis (HoFF) test. *F11*$^{-/-}$ mice received PS-siRNA or vehicle as described above, followed by blood collection on day 7 for the fibrinolysis assay. **(V)** Clot lysis time, and **(W)** fibrinolysis index; *P values: ns, not significant; *P < .05; Brown–Forsythe analysis of variance (Anova), Dunnett's T3 multiple comparisons test.*

Published under the CC license Attribution 4.0 International (CC BY 4.0)

Results: In patient plasma, PS reduction to 30% increased endogenous thrombin potential versus untreated samples (575.5±205.4 vs 113.3±90.3; n = 2; Fig.C). In F11-/- mice, PS siRNA increased endogenous thrombin potential, thrombin peak, and start tail (Fig.D-J), enhanced whole-blood clot formation (Fig.K-O), increased clot number, and reduced bleeding time and episode duration to a similar extent as recombinant activated factor VII, marstacimab, or tranexamic acid (Fig.P-T). PS-siRNA also prolonged clot lysis time and reduced the fibrinolysis index, enhancing resistance to fibrinolysis (Fig.U-W).

Conclusions: Controlled PS reduction enhances haemostasis in FXI deficiency in human plasma and in vivo. By acting independently of FXI, liver-directed PS silencing represents a mechanistically distinct, non-factor replacement strategy with the potential to provide sustained haemostatic protection for patients with FXI deficiency and clinically relevant bleeding, irrespective of F11 genotype or residual FXI activity. Together with previous findings in other inherited bleeding disorders, these data support PS targeting as a broader haemostatic rebalancing strategy and warrant clinical evaluation of PS-siRNA.

9324

Controlled protein S expression using small interfering RNA rebalances haemostasis in von Willebrand disease

R. Diab (1, 2), S. Rahimi (1, 2), L. Calame-Longjean (1, 2), A. Staubli (1, 2), J. Kremer Hovinga (1, 2), J. Saub (1, 2), R. Prince-Eladnani (1, 2), A. Angelillo-Scherrer (1, 2)

Department of Hematology and Central Hematology Laboratory, Inselspital, Bern University Hospital, Bern (1), Department for Biomedical Research, University of Bern, Bern (2)

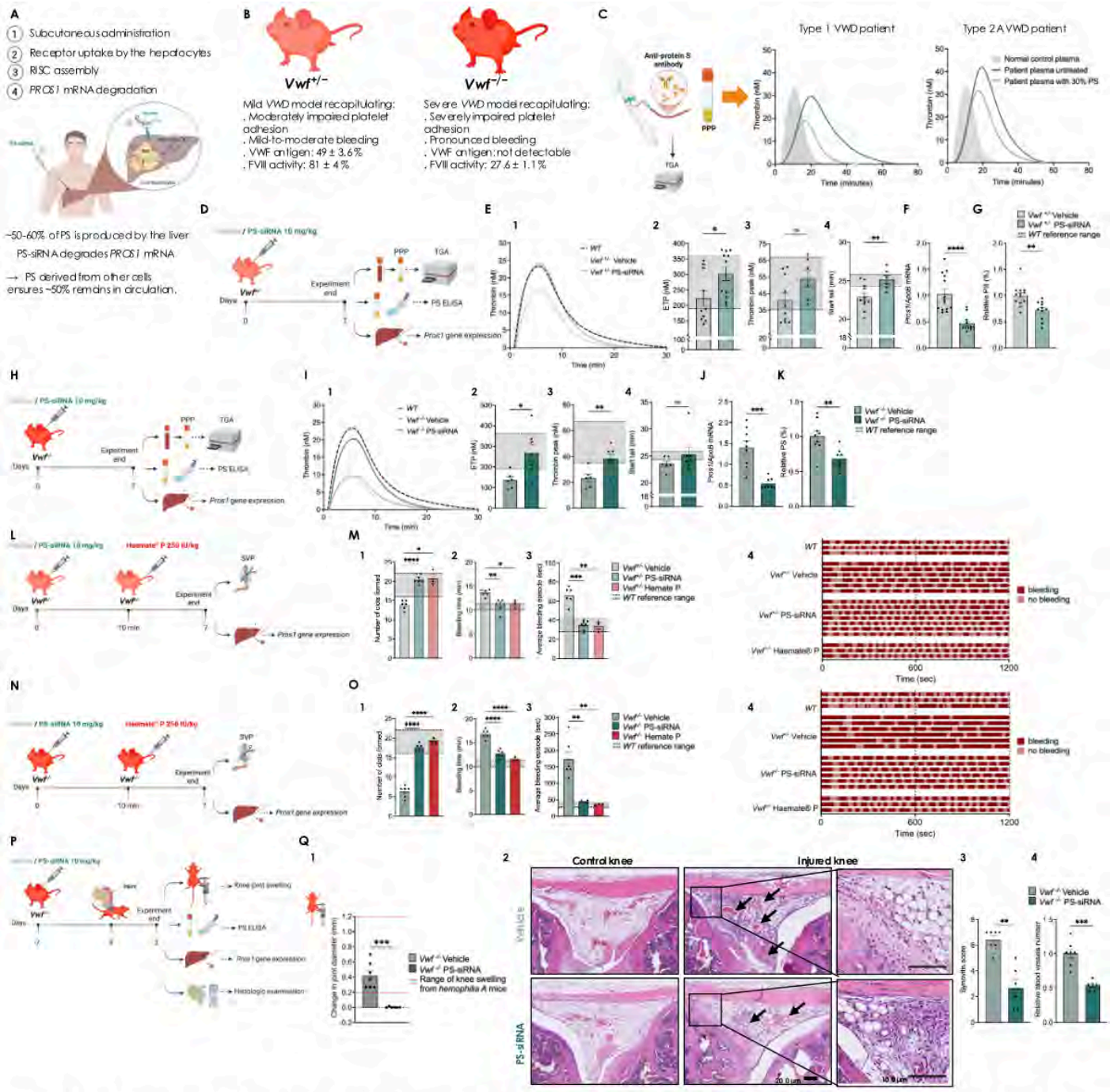
Introduction: von Willebrand disease (VWD), the most common inherited bleeding disorder, results from quantitative or qualitative defects in von Willebrand factor (VWF), impairing platelet adhesion and, in severe forms, reducing factor VIII (FVIII) levels and thrombin generation (TG). Protein S (PS) is an endogenous anticoagulant that limits TG through multiple pathways. We previously showed that liver-directed PS silencing using small interfering RNA (PS-siRNA) (Fig.A) rebalances haemostasis in haemophilia and Glanzmann thrombasthenia. Here, we investigated whether PS targeting enhances TG in plasma from patients with VWD, and whether PS-siRNA improves haemostasis in VWF-deficient mice ($Vwf^{-}/^{-}$ and $Vwf+/^{-}$) (Fig.B).

Methods: Platelet-poor plasma (PPP) from patients with mild VWD was treated with anti-PS antibody to reduce free PS to 30% or left untreated. TG was measured with 1 pM tissue factor and 2 nM thrombomodulin. $Vwf^{-}/^{-}$ and $Vwf+/^{-}$ mice received a subcutaneous injection of PS-siRNA or vehicle. On day 7, TG, viscoelastometry (ClotPro), and a saphenous vein puncture (SVP) bleeding assay were performed. $Vwf^{-}/^{-}$ mice also underwent acute hemarthrosis, followed by assessment of joint swelling and histology.

Results: In PPP from patients with mild VWD, PS reduction increased endogenous thrombin potential (ETP) versus untreated samples (Fig.C). In vivo, PS-siRNA increased ETP and thrombin peak in $Vwf^{-}/^{-}$ (Fig.D-G) and $Vwf+/^{-}$ mice (Fig.H-K). Whole-blood clot formation was unchanged, consistent with preserved FVIII activity in VWF-deficient mice. In the SVP model, PS-siRNA increased clot number and reduced bleeding time and episode duration in both $Vwf+/^{-}$ (Fig.L-M) and $Vwf^{-}/^{-}$ mice (Fig.N-O), with effects comparable to Haemate® P. PS-siRNA also reduced joint swelling, synovitis score, and synovial blood vessel density after acute hemarthrosis in $Vwf^{-}/^{-}$ mice (Fig.P-Q).

Conclusions: Targeting PS enhances haemostasis in VWD. PS reduction increased TG in patient plasma, while PS-siRNA in vivo enhanced TG, improved bleeding outcomes with efficacy comparable to VWF replacement, and protected against hemarthrosis. Together with previous findings in other inherited bleeding disorders, these data support PS targeting as a broader, non-factor replacement haemostatic rebalancing strategy with potential across VWD severity and warrant clinical evaluation of PS-siRNA.

 Published under the CC license Attribution 4.0 International (CC BY 4.0)



Protein S–small interfering RNA (PS-siRNA) enhances thrombin generation in mild von Willebrand disease (VWD) patients' *ex vivo*, restored haemostasis and protects against hemarthrosis in *VWD* murine models. (A) Illustration showing the mode of action of protein S (PS) siRNA in the liver. **(B)** von Willebrand disease mouse models used in the study. **(C)** Experimental overview for *ex vivo* patient thrombin generation assay (TGA). Platelet-poor plasma (PPP) from patients with mild VWD was either spiked with anti–PS antibody to reduce free PS levels to 30% or left untreated, followed by TGA in the presence of 1 pM tissue factor and 2 nM recombinant human thrombomodulin. Representative thrombograms are shown. **(D)** Experimental design for TGA analysis. *Vwf*$^{+/-}$ mice received a single subcutaneous injection of PS-siRNA (10 mg/kg) or vehicle (phosphate-buffered saline) on day 1. Blood was collected on day 7 for TGA. **(E) (1)** Representative thrombograms, **(2)** endogenous thrombin potential (ETP), **(3)** thrombin peak, and **(4)** start tail, measured in PPP from PS-siRNA and vehicle-treated *Vwf*$^{+/-}$ mice. **(F)** Quantitative real-time PCR of liver tissue to measure *Prcs1* mRNA expression normalized to *ApoB*. **(G)** PS antigen level in plasma. **(H)** Experimental design for TGA analysis. *Vwf*$^{+/-}$ mice received a single subcutaneous injection of PS-siRNA (10 mg/kg) or vehicle (phosphate-buffered saline) on day 1. Blood was collected on day 7 for TGA. **(I) (1)** Representative thrombograms, **(2)** endogenous thrombin potential (ETP), **(3)** thrombin peak, and **(4)** start tail, measured in PPP from PS-siRNA and vehicle-treated *Vwf*$^{+/-}$ mice. TG was assessed using calibrated automated thrombography in the presence of 1 pM tissue factor and 15 nM recombinant mouse thrombomodulin. **(J)** Quantitative real-time PCR of liver tissue to measure *Prcs1* mRNA expression normalized to *ApoB*. **(K)** PS antigen level in plasma. *P values: ns, not significant; *P < .05; **P < .01; ***P < .001; ****P < .0001; unpaired t test.* **(L)** Experimental design for bleeding assessment. *Vwf*$^{+/-}$ mice received PS-siRNA, vehicle or Haemate® P and underwent a saphenous vein puncture (SVP) on day 7. **(M) (1)** Number of clots formed, **(2)** total bleeding time (minutes), and **(3)** average number of bleeding episodes for the 20-minute observation period. **(4)** Stacked bar plots depicting bleeding and non-bleeding times for each experimental group across the 20-minute observation period. **(N)** Experimental design for bleeding assessment. *Vwf*$^{+/-}$ mice received PS-siRNA, vehicle or Haemate® P and underwent a saphenous vein puncture (SVP) on day 7. **(O) (1)** Number of clots formed, **(2)** total bleeding time (minutes), and **(3)** average number of bleeding episodes for the 20-minute observation period. *P values: *P < .05; **P < .01; ***P < .001; ****P < .0001; Brown–Forsythe analysis of variance (Anova), Dunnett's T3 multiple comparisons test.* **(4)** Stacked bar plots depicting bleeding and non-bleeding times for each experimental group across the 20-minute observation period. **(P)** Schematic of experimental design. Seven days after single subcutaneous injection of PS-siRNA (10 mg/kg) or vehicle (phosphate-buffered saline) in *Vwf*$^{+/-}$ mice, right knees were injured using a 30-gauge needle; knee diameters were measured 72 hours later. Blood and knees were collected at the end of the experiment. **(Q) (1)** Difference between the knee diameter. *P values: **P < .001;* unpaired t test. **(2)** Microscopic evaluation (Haematoxylin and Eosin stain) of the knee intra-articular space of a representative, uninjured leg (control leg) and injured leg. Squares indicate regions with synovial hyperplasia; arrows indicate synovial blood vessels, **(3)** relative blood vessels number, and **(4)** synovitis score. The synovitis score is a cumulative score obtained by using a 3-point (0, 1, and 2) scoring system of synovial hyperplasia, vascularity, and blood presence based on examination of histological sections. *P values; **P < .01; ***P < .001;* unpaired t test.

Published under the CC license Attribution 4.0 International (CC BY 4.0)

0418

Protein S as a tissue-directed modulator of the synovial and myeloid response in haemophilic arthropathy

S. Rahimi (1, 2), R. Diab (1, 2), M. Prummer (3), P. Nicholson (4), R. Prince-Eladnani (5, 2), A. Angelillo-Scherrer (5, 2)

Department of Hematology and Central Hematology Laboratory, Inselspital, Bern University Hospital, University of Bern, Bern (1), Department for Bio-Medical Research, University of Bern, Bern (2), NEXUS Personalized Health Technologies, ETH, Zürich (3), Next Generation Sequencing Platform, University of Bern, Bern (4), 1) Department of Hematology and Central Hematology Laboratory, Inselspital, Bern University Hospital, University of Bern, Bern (5)

Introduction: Haemophilia A (HA), caused by factor VIII deficiency, is complicated by recurrent hemarthrosis (RH), driving haemophilic arthropathy with progressive synovitis and cartilage and bone destruction. Despite advances in bleeding prevention, no treatment restores joint health once arthropathy is established. Protein S (PS) is a natural anticoagulant whose reduction rebalances haemostasis in HA. Beyond coagulation, PS acts through TAM-family receptors regulating macrophage and stromal-cell function, suggesting a direct role in joint responses to bleeding. We investigated whether PS modulates haemophilic arthropathy beyond haemostatic rebalancing.

Methods: Using a mouse model of RH, we performed bulk RNA sequencing of synovium from wild-type (WT; F8+/+Pros1+/+), HA (F8−/−Pros1+/+), and HA PS-deficient (F8−/−Pros1−/−) mice under healthy conditions, in contralateral non-injured joints, and after RH injury (Fig. A). Transcriptomic analyses and cell-type deconvolution were complemented by assessment of inflammation, macrophage function, circulating monocytes, and bone architecture.

Results: RH induced a macrophage/fibroblast-driven program in WT synovium involving extracellular-matrix organization, collagen deposition, wound healing, angiogenesis, and inflammation. This response was blunted in HA but restored toward the WT signature in HA PS-deficient mice (Fig. B). Cell-type deconvolution showed injury-induced fibroblast expansion in WT and HA PS-deficient synovium that was absent in HA (Fig. C). Compared with HA, HA PS-deficient mice showed reduced synovial inflammatory cytokines (Fig. D), less macrophage infiltration (Fig. E), enhanced macrophage erythrocyte phagocytosis (Fig. F), fewer inflammatory blood monocytes, and better-preserved bone architecture, even without injury (Fig. G,H).

Conclusions: These data identify PS as a modulator of RH pathogenesis and haemophilic joint responses. PS deficiency not only rebalances haemostasis but also restores injury-responsive stromal and macrophage programs, reduces inflammation, promotes erythrocyte clearance, and preserves bone architecture. Thus, targeting PS may provide dual haemostatic and tissue-protective effects and represent a potential disease-modifying strategy for haemophilic arthropathy. Ongoing PS-siRNA studies will assess whether therapeutic PS silencing reproduces these effects.

 Published under the CC license Attribution 4.0 International (CC BY 4.0)

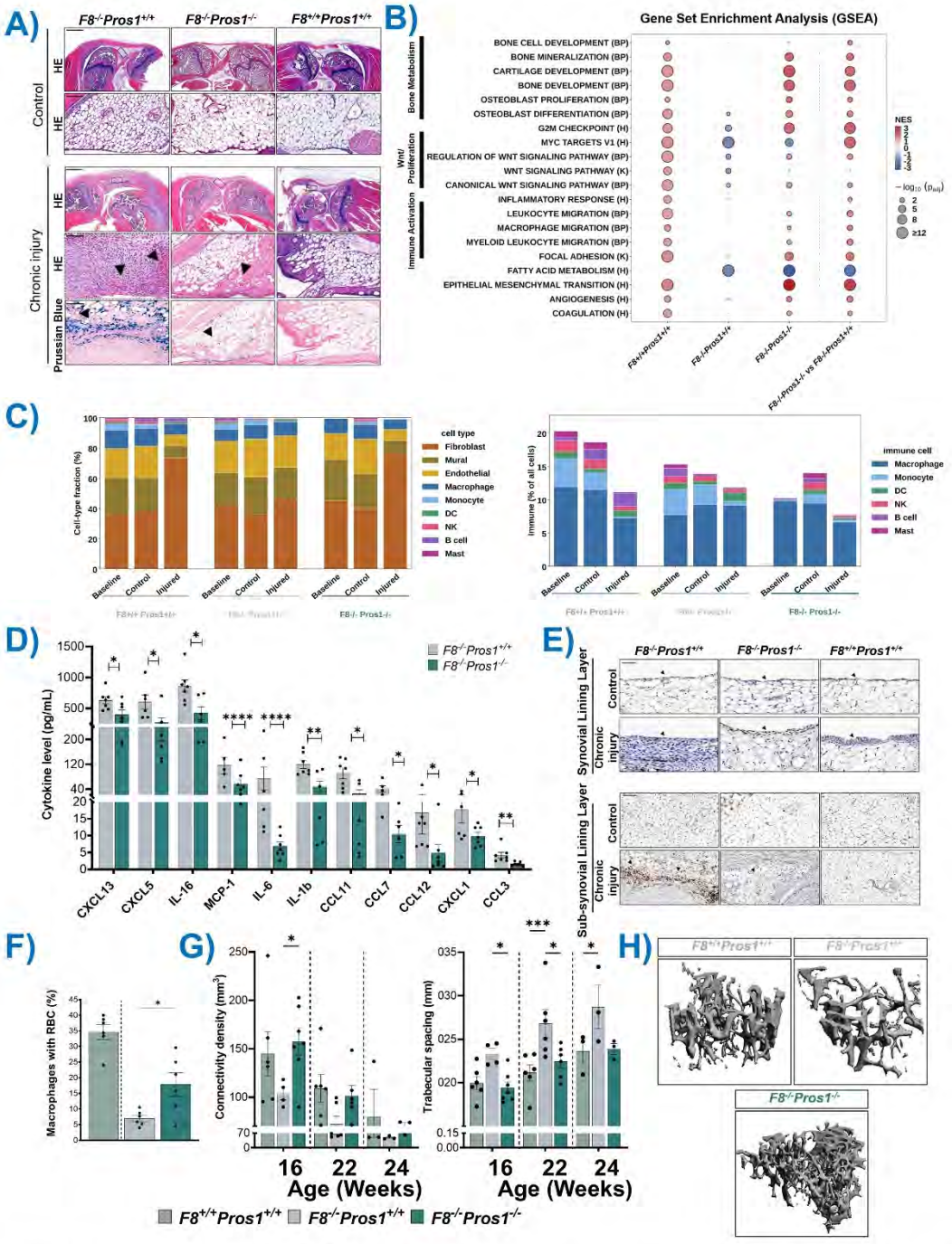


Figure Legend - Protein S deficiency reduces inflammation and enhances synovial repair through macrophage phagocytic activity and fibroblast activation in haemophilia A mice. A) Representative histological images of uninjured (control) and injured knee joints. Hematoxylin and eosin (H&E) staining revealed marked red blood cell extravasation (black arrowheads) in the injured joints of *F8*$^{-/-}$*Pros1*$^{+/+}$ mice. Consistently, Prussian Blue staining demonstrated increased hemosiderin deposition (arrowheads) in *F8*$^{-/-}$*Pros1*$^{+/+}$ mice compared with *F8*$^{+/+}$*Pros1*$^{+/+}$ and *F8*$^{-/-}$*Pros1*$^{-/-}$ mice, indicating enhanced iron accumulation following recurrent joint bleeding. Scale bar = 200 µm. B) Gene set enrichment analysis (GSEA) dot plots revealed significant modulation of pathways associated with bone metabolism, WNT signaling and cell proliferation, inflammation, angiogenesis, coagulation, fatty acid metabolism, and epithelial-to-mesenchymal transition in *F8*$^{+/+}$*Pros1*$^{-/-}$ mice. In addition, *Pros1* deficiency reversed transcriptomic signatures associated with hemarthrosis in *F8*$^{-/-}$*Pros1*$^{+/+}$ mice, resulting in a profile more similar to *F8*$^{+/+}$*Pros1*$^{+/+}$ mice (n = 3). C) Cell-type deconvolution revealed that *F8*$^{-/-}$*Pros1* mice had a higher fibroblast population and reduced immune cell infiltration in the synovium compared to *F8*$^{-/-}$*Pros1*$^{+/+}$ mice, but showed levels similar to *F8*$^{+/+}$*Pros1*$^{+/+}$ mice; this was consistent with the GSEA, in which extracellular matrix and inflammatory processes were differentially regulated. D) Cytokine profiling of knee joint lavage samples revealed significantly increased levels of pro-inflammatory cytokines in *F8*$^{-/-}$*Pros1*$^{+/+}$ mice compared with *F8*$^{-/-}$*Pros1*$^{-/-}$ mice following recurrent hemarthrosis. Data are presented as mean ± SEM (n = 4-6 per group); *p< .05, **p< .01, ****p < .0001. E) Representative CD68 immunostaining (macrophage marker) of uninjured (control) and injured knee joints was performed to evaluate macrophage distribution within the synovial lining layer (SLL) and sub-synovial lining layer (sub-SLL). Following recurrent hemarthrosis, *F8*$^{-/-}$*Pros1*$^{+/+}$ mice exhibited a complete absence of CD68-positive macrophages in the SLL, accompanied by marked macrophage infiltration in the sub-SLL, compared with *F8*$^{-/-}$*Pros1*$^{-/-}$ and *F8*$^{+/+}$*Pros1*$^{+/+}$ mice. Arrowheads indicate the distribution of CD68-positive macrophages. F) Quantification of senescent RBC engulfment demonstrated significantly greater phagocytic activity in *F8*$^{-/-}$*Pros1*$^{-/-}$ BMDMs than in *F8*$^{-/-}$*Pros1*$^{+/+}$ BMDMs; however, phagocytic activity remained lower than that observed in wild-type (*F8*$^{+/+}$*Pros1*$^{+/+}$) BMDMs. Data are presented as mean ± SEM (n = 6); *P < .05. f) µCT analysis of knee joints revealed increased trabecular connectivity density in *F8*$^{-/-}$*Pros1*$^{-/-}$ mice at 16 weeks of age, along with (G) reduced trabecular spacing compared with *F8*$^{-/-}$*Pros1*$^{+/+}$ mice. However, trabecular spacing remained consistently higher in *F8*$^{-/-}$*Pros1*$^{-/-}$ mice at 22 and 24 weeks. (H) Representative reconstructed µCT images illustrating trabecular bone architecture in mice at 16 weeks of age. All data are shown as mean mean ± SEM (n= 3-6). *p< .05, **p< .01, ***p < .001.+

Published under the CC license Attribution 4.0 International (CC BY 4.0)

0479

Diagnostic utility of platelet function testing by flow cytometry in patients with bleeding disorders of unknown cause (BDUC)

K. Haeri (1), D. Bertaggia Calderara (1), A. Aliotta (1), A. P. Batista Mesquita Sauvage (1), D. Shehwar (1), A. Casini (2), L. Alberio (1)

Division and Central Laboratory of Hematology, Lausanne University Hospital (CHUV) and University of Lausanne, Lausanne (1), Division of Angiology and Hemostasis, Department of Medicine, University Hospitals of Geneva, University of Geneva, Geneva (2)

Introduction: Up to 70% of patients with clinically relevant bleeding tendency remain without an identifiable cause after standard laboratory work-up (assessing coagulation factors and platelet aggregation) and are classified as having a bleeding disorder of unknown cause (BDUC). We investigated diagnostic utility of platelet function testing by flow cytometry in BDUC patients.

Methods: 44 patients from the SwissBUC study were included (86% female; median age, 39.5 years [IQR, 29.5–46.75 years]; range, 20–63 years). Platelet structure and functions were assessed by flow cytometry. Surface expressions of glycoproteins (GP) IIb-IIIa (fibrinogen receptor), Ib-IX (von Willebrand factor receptor), VI and Ia (collagen receptors) were evaluated with fluorophore-conjugated receptor-specific antibodies. Functional assays included: (i) Procoagulant COAT platelets generation quantified as Annexin-V+/PAC1- after simultaneous COllagen-And-Thrombin (THR) stimulation; (ii) Dense granule content and secretion assessed by mepacrine loading and release following activation by THR or GPVI-specific agonist convulxin (CVX); (iii) α-granule secretion (P-selectin expression) and GPIIb-IIIa activation (PAC1 binding) to ADP (0.5, 5, 50 µM), THR (0.005, 0.05, and 0.5 U/ml), or CVX (5, 50, and 500 ng/ml). The results were compared with internal reference ranges from healthy individuals (n = 60).

Results: We identified following abnormalities, which may coexist in a patient: low GPVI expression (n = 9); reduced COAT platelet generation (n = 20); dense granule anomalies (decreased content n = 2; decreased CVX-induced secretion n = 6); decreased α-granule secretion to ADP (n = 16); reduced GPIIb-IIIa activation after THR (n = 3); reduced GPIIb-IIIa activation after CVX (n = 17). Several patients had ≥2 abnormalities within the same activation pathway (CVX n = 15; ADP n = 5; THR n = 2). Four patients were within reference ranges.

Conclusions: Platelet flow cytometry identified abnormalities in 40/44 BDUC patients that had not been detected by conventional platelet assays. The most prevalent abnormalities were decreased response to CVX (granule secretion and/or GPIIb-IIIa activation), decreased alpha-granule secretion to ADP, and decreased potential to generate COAT platelets. The latter is specifically treatable, supporting flow cytometry as a complementary test in BDUC patients.

9754

Early coagulation recovery after therapeutic LMWH in term pregnancy: implication for neuraxial timing

H. Legardeur (1), A. Cuénoud (2), M. G. Zermatten (3), P. Schoettker (2), A. Aliotta (3), F. Grandoni (3), L. Alberio (3), D. Baud (1), M. Gavillet (3)

Woman-Mother-Child, Lausanne University Hospital, Lausanne (1), Anesthesiology, Lausanne University Hospital, Lausanne (2), Haematology, Lausanne University Hospital, Lausanne (3)

Introduction: Guidelines recommend a 24-hour delay between the last therapeutic low-molecular-weight heparin (LMWH) dose and neuraxial anaesthesia. This interval is the same as in non-pregnant patients undergoing elective surgery and does not consider pregnancy-associated hypercoagulability. Moreover, this requirement imposes planned delivery, or general anaesthesia when urgent caesarean delivery is required, both increasing thromboembolic and anaesthesiologic risk. We therefore aimed to characterize the evolution of anti-factor Xa activity, coagulation markers and global coagulation potential during the 24h following the last therapeutic LMWH dose in term pregnant persons.

Methods: Single-centre observational study including 26 consecutive term pregnant individuals receiving weight-adjusted LMWH, 27 non-anticoagulated term pregnant, and 20 non-pregnant, non-anticoagulated controls. Serial anti-Xa activity, in vivo and ex vivo thrombin generation markers were determined at 4-hours intervals over the 24h after the last LMWH dose.

Results: Both in vivo and ex vivo thrombin generation assays confirmed the net procoagulant status associated with term pregnancy. Already 12 hours after the last injection, and despite detectable anti-Xa activity (median 0.35 IU/ml), in vivo coagulation markers and thrombin generation parameters were restored to levels comparable to nonpregnant non-anticoagulated controls. No participant with anti-Xa <0.4 IU/mL demonstrated impaired endogenous thrombin potential. Detectable anti-Xa activity persisted in 58% of participants at 24h (median 0.13 IU/ml), when epidural is considered safe, further highlighting the limitation of purely pharmacokinetics approach in this setting.

Conclusions: Our data suggest that the anticoagulant effect of LMWH may be attenuated within hours of administration in the pregnancy-associated procoagulant milieu. Given the small sample size and reliance on a surrogate biological marker, these findings should be interpreted cautiously. They nevertheless raise the possibility that a uniform 24-hour delay may be overly conservative and support further evaluation of individualized approaches to neuraxial anaesthesia timing and peripartum management.

3563

Mitochondrial Calcium Uniporter: a key modulator for the generation of Procoagulant platelets

D. Shehwar (1), S. Barki (2), D. B. Calderara (1), K. Haeri (1), A. Aliotta (1), M. R. Alam (2), L. Alberio (1)

Department of Laboratory Medicine and Pathology, Lausanne University Hospital (CHUV), Lausanne (1), Department of Biochemistry, Quaid-i-Azam University, Islamabad (2)

Introduction: Procoagulant platelets are a subpopulation of highly activated platelets that promote thrombin generation. They exhibit negatively-charged phosphatidylserine (PS) on their surface, facilitating the formation of tenase and prothrombinase complexes. Dual platelet stimulation with thrombin (THR) and convulxin (CVX) (agonist of the collagen receptor GPVI) leads to persistently high cytosolic calcium, which is transported to the mitochondria via mitochondrial calcium uniporter (MCU), eventually triggering mitochondrial depolarization and opening of mitochondrial permeability transition pores (mPTP), leading to the procoagulant transformation. The aim of this study was to target MCU to modulate the formation of procoagulant platelets.

Methods: MCU was inhibited by treating platelets with Ru265. Platelets were stimulated with increasing concentrations of THR and CVX individually or in combination (THR+CVX). Platelet procoagulant properties were assessed by flow cytometry using PAC1 (binding activated fibrinogen receptor) and Annexin V (binding negatively charged PS). Mitochondrial function and

 Published under the CC license Attribution 4.0 International (CC BY 4.0)

cytosolic calcium were determined using TMRM and calcium ion indicators (Fluo-4 and Fluo-5N), respectively.

Results: THR alone (0.5, 5 and 10 U/ml) generated predominantly aggregating platelets (90% PAC1+/Annexin V-), with only 5% displaying a procoagulant phenotype (Annexin V+/PAC1-), with no change in presence of Ru265. Low dose CVX (2 ng/ml) generated predominantly aggregating platelets (80%) with only 4% procoagulant platelets, with significant reduction to 70% in the former and no change in the latter in the presence of Ru265. CVX at 500 ng/ml induced 90% aggregating and 15% procoagulant platelets, with no change in the former and significant reduction to 10% in the latter by Ru265. Of note, the combination of THR (0.5 U/ml) and CVX (500 ng/ml) induced 40% aggregating and 60% procoagulant platelets. In presence of Ru265 aggregating platelets increased to 60% and procoagulant decreased to 40%. Ru265 showed a dose and time dependent decrease in cytosolic and supramaximal cytosolic Ca2+, and prevented mitochondrial depolarization.

Conclusions: Our data demonstrates that MCU inhibition reduces procoagulant platelet formation by preventing calcium-dependent mitochondrial depolarization, thus maintaining the platelets in an aggregating activation state.

SSH/SSMO ORAL PRESENTATION - EXPERIMENTAL HEMATOLOGY / ONCOLOGY

4599

Targeting oncogene-driven phosphatidic acid metabolism to treat acute myeloid leukaemia

T. Gremelspacher (1, 2), J. Koren (1, 2), A. Sonrel (1, 2), H. Hao-Shen (1, 2), S. Herrenschmidt (1, 2), N. C. Bentires-Alj (1, 2), J. Tossounidis (1, 2), I. Cervenka (1, 2), C. C. Widmer (3), J. Buescher (4), P. Apostolova (1, 2)

Department of Biomedicine, University of Basel, Basel (1), Department of Hematology, University Hospital of Basel, Basel (2), Department of Hematology and Laboratory Medicine, University Hospital of Basel, Basel (3), Max-Planck-Institute, Immunobiology and Epigenetics, Freiburg (4)

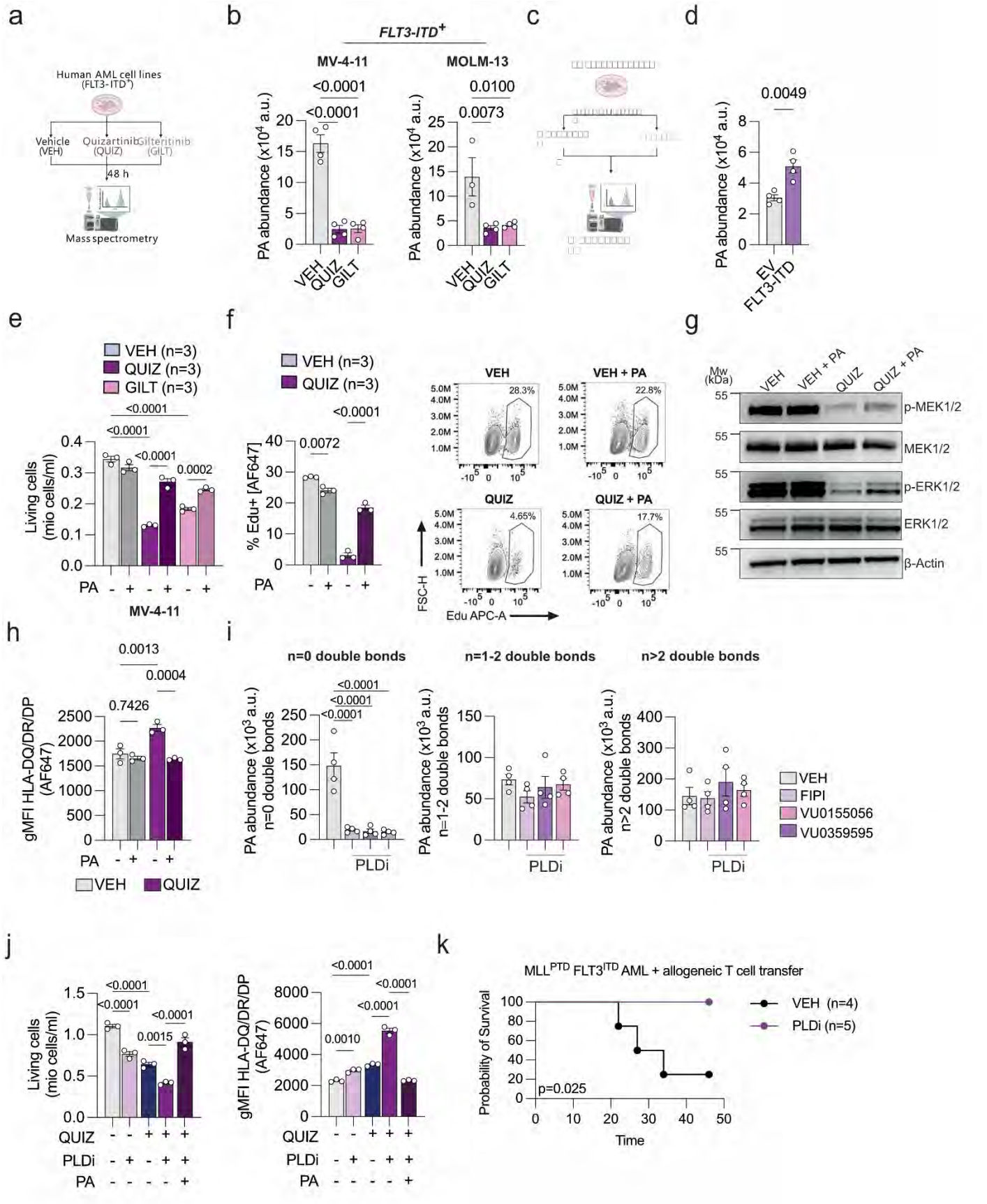
Introduction: Acute myeloid leukaemia (AML) is an aggressive malignancy driven by genetic alterations in haematopoietic stem and progenitor cells. Mutations in Fms-like tyrosine kinase 3 (FLT3) are frequent and associated with poor prognosis. Despite advances in allogeneic haematopoietic stem cell transplantation (allo-HSCT) and specialised treatments like FLT3 inhibition (FLT3i), resistance and relapse remain major challenges. Metabolic rewiring may cooperate with oncogenic signalling not only to promote AML cell survival and proliferation but also to help leukaemic cells evade immune control. We hypothesised that oncogenic FLT3 signalling induces leukaemia-promoting lipid metabolism programs that may represent a targetable vulnerability.

Methods: High-coverage liquid chromatography–mass spectrometry lipidomics was used to profile FLT3-dependent changes in AML cells. The effects of exogenous phosphatidic acid (PA), inhibition of PA synthesis through phospholipase D (PLDi), and combined PLDi and FLT3i were assessed using cellular proliferation, cell-cycle, signalling and human leucocyte antigen class II (HLA-II) expression assays. Leukaemia-bearing mice received PLDi in combination with allogeneic T cells to assess effects in vivo.

Results: Genetic and pharmacological models (Fig. 1a-d) showed that oncogenic FLT3 signalling induced the accumulation of the bioactive lipid PA. Exogenous PA attenuated FLT3i-induced growth inhibition by sustaining cell-cycle progression and MAPK signalling (Fig. 1e-g). Notably, PA also reduced HLA-II surface expression (Fig. 1h), suggesting a potential role in immune evasion. We could identify PLD as a major contributor to PA synthesis. PLDi depleted saturated PA species (Fig. 1i), impaired AML cell proliferation and increased HLA-II expression. These effects were potentiated by additional FLT3i, highlighting the therapeutic potential of targeting both oncogenic signalling and lipid metabolism (Fig. 1j). PLDi also significantly prolonged survival in AML-bearing mice, supporting its therapeutic potential in vivo (Fig. 1k).

Conclusions: Our findings identify PA metabolism as a previously unrecognised link between oncogenic FLT3 signalling, AML growth and reduced immune recognition. Targeting PLD-dependent PA synthesis may offer a new treatment strategy by restricting leukaemic proliferation and restoring features required for an anti-leukaemic immune response.

 Published under the CC license Attribution 4.0 International (CC BY 4.0)



Published under the CC license Attribution 4.0 International (CC BY 4.0)

2668

LILRB2 Contributes to CAR T-cell Dysfunction and Is a Novel Therapeutic Target in Acute Myeloid Leukemia

S. Brunn (1), M. Chambovey (1), N. Raymann (1), M. Ponzo (1), S. Alberio (1), A. Baumann (1), L. Raas (1), C. Pellegrino (1), J. M. Ellegast (1), J. Deuel (1), M. G. Manz (1), C. F. Magnani (1)

Medical Oncology and Hematology, University Hospital Zurich, Zurich (1)

Introduction: Acute myeloid leukemia (AML) is an aggressive hematologic malignancy with poor outcomes. Although chimeric antigen receptor (CAR) T-cell therapies have shown major clinical benefit in other cancers, their efficacy in AML has been limited by the lack of targets that can be safely engaged without causing myeloablation, and by an immunosuppressive tumor microenvironment. In this context, leukocyte immunoglobulin-like receptor-B2 (LILRB2) has emerged as an immunosuppressive receptor, but its impact on CAR T-cell function and suitability as a therapeutic target remains unclear. In this project, we aimed to characterize the expression profile of LILRB2 on leukemic blasts and healthy cells, and to investigate the impact of LILRB2 expression on CAR T-cell phenotype and functional activity. In addition, we sought to evaluate the therapeutic potential of LILRB2-targeted CAR T cells as a treatment strategy for AML.

Methods: (Included in the results section)

Results: We found that LILRB2 is expressed in 65% of AML patients blasts, highly expressed on tumor-associated myeloid cells, and largely absent from healthy hematopoietic stem and progenitor cells. Through knockout and overexpression models in vitro and in vivo, we showed that LILRB2 impairs anti-CD33 directed CAR T-cell killing, expansion, and cytokine production, while promoting their exhaustion and differentiation. Using antibody-mediated LILRB2 blockade, these effects could be partially reversed. Transcriptomic analyses revealed suppression of immune-related pathways and induction of DNA damage response and senescence in CAR T cells. Hence, we designed anti-LILRB2 CAR T cells, which showed potent cytotoxicity in vitro and robust antitumor activity in vivo, including tumor eradication in xenograft models, without detectable toxicity in humanized mice.

Conclusions: Collectively, our results identify LILRB2 as a key regulator of CAR T-cell dysfunction and support LILRB2 targeting as a promising therapeutic strategy warranting further study in AML.

1863

Genome-wide CRISPR screening identifies a lactate–OXPHOS synthetic lethality in T-cell acute lymphoblastic leukaemia

S. Patel (1), N. Baran (2), A. Lodi (3), M. Chomczyk (4), V. Mohanty (5), M. Dede (5), Y. Huynh (3), M. Collins (3), M. I. Gadallah (3), P. Sharma (1), J. H. Park (6), J. S. Enriquez (7), I. Veletic (1), Y. Dhungana (8), Y. Zhou (9), P. Thandapani (10), K. Dunner, Jr (11), J. M. Henderson (12), J. R. Zickus (7), A. Skwarska (13), D. Dymkowska (14), C. Ramage (1), K. Hayes (1), Z. Zeng (1), G. Alatrash (10), S. Konoplev (15), E. J. Jabbour (1), G. Borthakur (1), R. E. Davis (12), J. E. Marszalek (16), B. A. Kaipparettu (6), J. Yu (17), K. Chen (5), P. Bhattacharya (7), S. Tiziani (3), M. Konopleva (13)

Department of Leukemia, The University of Texas MD Anderson Cancer Center, Houston (1), Hematology and hematological central laboratory, Inselspital, Bern (2), Department of Nutritional Sciences, The University of Texas at Austin, Austin (3), Experimental Hematology, Institute of Hematology and Transfusion Medicine, Warsaw (4), Department of Bioinformatics and Computational Biology, The University of Texas MD Anderson Cancer Center, Houston (5), Department of Molecular and Human Genetics, Baylor College of Medicine, Houston (6), Department of Cancer Systems Imaging, The University of Texas MD Anderson Cancer Center, Houston (7), Department of Pathology, St. Jude Children's Research Hospital, Memphis (8), Department of Hematopoietic Biology and Malignancy, University of Texas MD Anderson Cancer Center, Houston (9), Department of Hematopoietic Biology and Malignancy, The University of Texas MD Anderson Cancer Center, Houston (10), Department of Cancer Biology, The University of Texas MD Anderson Cancer Center, Houston (11), Department of Lymphoma and Myeloma, The University of Texas MD Anderson Cancer Center, Houston (12), Department of Oncology, Department of Cell Biology, Albert Einstein College of Medicine, Bronx (13), Nencki Institute of Experimental Biology, Polish Academy of Sciences, Warsaw (14), Department of Hematopathology, The University of Texas MD Anderson Cancer Center, Houston (15), Therapeutics Discovery Division, The University of Texas MD Anderson Cancer Center, Houston (16), Department of Computational Biology, St. Jude Children's Research Hospital, Memphis (17)

Introduction: T-cell acute lymphoblastic leukaemia (T-ALL) carries a poor prognosis in relapsed or refractory settings, underscoring the need for novel therapeutic strategies. Monocarboxylate transporter 1 (MCT1, encoded by SLC16A1) is highly expressed across T-ALL genetic subtypes and mediates lactate efflux. AZD3965, an MCT1 inhibitor in Phase I/II clinical trials, offers direct translational potential. We hypothesised that pharmacological MCT1 inhibition would create a metabolic trap exploitable by co-targeting oxidative phosphorylation (OXPHOS).

Methods: A genome-wide CRISPR-Cas9 dropout screen was conducted in PF382 T-ALL cells treated with the MCT1 inhibitor AZD3965. Hits were analysed by MAGeCK and DrugZ. Synergy between AZD3965 and the complex I inhibitor IACS-010759 was quantified by Bliss independence analysis in five T-ALL cell lines and primary patient samples. Mitochondrial function was assessed by Seahorse metabolic profiling, flow cytometry (reactive oxygen species, mitochondrial membrane potential, apoptosis), NMR-based metabolomics, respiratory chain enzyme assays, and transmission electron microscopy. Resistance mechanisms were characterised by chronic sub-lethal exposure. Activity of a triple metabolic blockade was evaluated in vitro and in a xenograft model.

Results: The screen identified OXPHOS and mitochondrial translation as the principal synthetic lethal pathways under AZD3965. AZD3965 plus IACS-010759 demonstrated strong Bliss synergy across all T-ALL lines and primary samples. The combination caused progressive mitochondrial exhaustion: elevated cellular and mitochondrial reactive oxygen species, collapse of mitochondrial membrane potential, reduced oxygen consumption rate, and apoptotic cell death. NMR metabolomics confirmed intracellular lactate accumulation and impaired TCA cycle flux. Chronic exposure generated resistance characterised by CD36- and CPT1-driven fatty-acid oxidation (FAO), providing alternative ATP. Addition of the CPT1 inhibitor

Published under the CC license Attribution 4.0 International (CC BY 4.0)

etomoxir reversed resistance and restored parental sensitivity. In vivo, the combination reduced leukaemia burden and prolonged survival.

Conclusions: Genome-wide CRISPR screening uncovers a clinically actionable lactate–OXPHOS synthetic lethality in T-ALL exploitable by AZD3965/IACS-010759. FAO-mediated metabolic plasticity drives acquired resistance, overcome by triple blockade, supporting clinical evaluation of this strategy.

7057

An AI-Based Live-Cell Imaging Platform for Dynamic, Immune-Informed Functional Precision Medicine in Acute Myeloid Leukemia

W. Checinska (1), I. Lukic (2), F. Wolpert (2), M. Saric (1), V. Cecconi (1), S. Ambrosini (1), G. Kalweit (2, 3), M. Kalweit (2, 3, 4), S. Kreutmair (1, 5, 6)

Institute of Experimental Immunology, University of Zurich, Zurich (1), (CRIION), Collaborative Research Institute Intelligent Oncology, Freiburg (2), IMBIT//BrainLinks-BrainTools, University of Freiburg, Freiburg (3), Department of Computer Science, University of Freiburg, Freiburg (4), The LOOP Zurich, University of Zurich, Zurich (5), Department of Medical Oncology and Hematology, University Hospital Zurich, Zurich (6)

Introduction: Despite the success of immunotherapy in many cancers, acute myeloid leukemia (AML) remains largely refractory. Combinatorial immune perturbations tailored to individual immune profiles are needed. However, current ex vivo platforms are limited by poor immune-subpopulation resolution and lack of temporal insight into immune-cancer-dynamics.

Methods: We established a novel microscopy-based platform combining time-lapse brightfield imaging with AI-driven vision-based analysis to dynamically monitor treatment responses. Individual cells were segmented and characterized using a multi-model feature extraction pipeline, generating high-dimensional representations of cellular morphology. A linear classifier (logistic regression) trained on frozen ConvNeXtV2, SwinV2 and DinoBloom features (4,608 dimensions) was used for cell-type/viability prediction. The model was trained using heterogeneous co-culture image datasets, including seven AML cell lines and immune subpopulations.

Results: First, an algorithm discriminating AML blasts from peripheral blood mononuclear cells (PBMCs) was trained on 248,235 cells and achieved accuracies of 0.887 (AML) and 0.926 (PBMCs): overall accuracy 0.907, AUC 0.967, on 114,601 held-out cells from wells disjoint from training. Brightfield-based viability assessment trained on 44,621 cells achieved high accuracy (0.952 live; 0.529 apoptotic, AUC 0.889), measured against reporter labels, and ranging from AUC 0.820-0.902 across all eight populations imaged. Second, the model was refined to resolve major PBMC subpopulations (monocytes, NK/T/B lymphocytes, and residual cells) enabling immune cell-specific attribution of treatment effects. The model was trained on 32,425 cells for cell type detection (held-out accuracy 0.705, macro F1 0.714, MCC 0.725) and 56,588 cells for viability assessment (0.882 live, 0.859 apoptotic, AUC 0.938). Third, T cell subsets were isolated using releasable fluorescent antibodies, enabling subsequent cell-tracking dye staining and temporal analysis of cell-cell interactions, underscoring the platform's functional relevance to identify new therapeutic vulnerabilities.

Conclusions: This platform represents a significant advance in ex vivo perturbation testing by providing dynamic, single-cell resolution data across the cancer-immune ecosystem, aiming to advance precision immunotherapy for AML.

7965

Exploiting the IGHV4-34 BCR clonotype for precision targeting of aggressive B-cell lymphoma using T-cell engagers and antibody-drug conjugates

B. Besemer (1), C. Schultheiss (1, 2), M. Binder (1, 2)

Department of Biomedicine, University of Basel, Basel (1), Division of Medical Oncology, University Hospital Basel, Basel (2)

Introduction: The immunoglobulin heavy-chain variable region gene IGHV4-34 is frequently used in a stereotyped B-cell receptor (BCR) configuration and is found in 30% of activated B-cell-like diffuse large B-cell lymphoma (ABC-DLBCL). Current B-cell malignancy therapies predominantly target general B-cell lineage antigens, whereas clonotypic BCR motifs allow selective targeting of malignant B-cell clonotypes while sparing healthy B cells and reducing treatment escape through antigen loss. Here we assessed whether the IGHV4-34-specific antibody 9G4 could serve as a platform for precision immunotherapy.

Methods: 9G4 specificity was assessed using immune repertoire and single-cell sequencing of 9G4-sorted healthy-donor B cells. A CD3-directed, Fc-containing 9G4 bispecific antibody (bsAb) was evaluated in T-cell co-cultures with IGHV4-34-positive and IGHV4-34-negative B-cell lymphoma cell lines. Target-cell killing, T-cell activation and effector molecule secretion were quantified by flow cytometry and multiplex analysis. 9G4 internalisation was assessed by imaging flow cytometry, and the efficacy of a 9G4-based antibody-drug conjugate (ADC) carrying a monomethyl auristatin E payload was evaluated.

Results: 9G4-positive B cells were enriched for IGHV4-34 rearrangements across immunoglobulin isotypes and light-chain pairings in healthy-donor B cells, confirming clonotype specificity. The 9G4×CD3 bsAb selectively activated T cells and induced killing of IGHV4-34-positive ABC-DLBCL (OCI-LY3) and B-lymphoblastic lymphoma (U698M) cell lines, while sparing IGHV4-34-negative Raji cells. The bsAb activity was retained in the presence of human plasma and polyclonal IgG, as well as with patient-derived T cells as effectors. Further, we found that 9G4-mediated target binding induced rapid internalisation into acidic compartments in IGHV4-34-positive cell lines through macropinocytosis without impairing T-cell-mediated cytotoxicity. Exploiting this property, a 9G4-based ADC selectively induced apoptosis of IGHV4-34-positive OCI-LY3 and U698M cells, but not IGHV4-34-negative Raji cells, with activity comparable to the EMA-authorised ADC polatuzumab vedotin.

Conclusions: These data establish IGHV4-34 as an internalising, clonotype-defined vulnerability accessible through complementary T-cell redirection and payload-delivery strategies, supporting further development of 9G4-based therapeutics for aggressive B-cell lymphoma.

 Published under the CC license Attribution 4.0 International (CC BY 4.0)

1983

Reprogramming of non-CAR T cells predicts and drives CD19-CAR T cell therapy-associated toxicities in B-cell lymphoma patients

S. Ambrosini (1), T. Wertheimer (2, 1), M. Moore (1), J. Chabbey (1), W. Mamozai (3), S. Stolz (3), M. Lin (1), M. Kauffmann (1), M. Schaefer (1, 4, 5), C. Ulutekin (1), F. Ingelfinger (2, 6), S. Reisenauer (3), H. Baniadam (7), M. P. Carbo (3), O. Gutwein (3, 8), M. Saric (1), C. Merten (1), C. Alberti (1), A. Sethi (1), S. Unger (1), N. Wolfensberger (3), V. Papadopoulou (3), P. Hockl (3), M. G. Manz (3, 9), A. Müller (10), C. C. Widmer (11), W. Huber (7, 12), T. Zenz (3, 9, 12), B. Becher (1, 9, 12), S. Kreutmair (1, 3, 9, 12)

Institute of Experimental Immunology, University of Zurich, Zurich (1), Department of Haematology, University Medical Center Freiburg, Freiburg (2), Department of Medical Oncology and Hematology, University Hospital Zurich, Zurich (3), Department of Immunology and Immunotherapy, Icahn School of Medicine at Mount Sinai, New York (4), Department of Biology, ETH Zurich, Zurich (5), German Cancer Consortium (DKTK) Partner site Freiburg, University Hospital Heidelberg, Heidelberg (6), Genome Biology Unit, European Molecular Biology Laboratory, Heidelberg (7), Gray Faculty of Medicine, Tel Aviv University, Tel Aviv (8), Comprehensive Cancer Center Zurich, University Hospital Zurich, Zürich (9), Department of Blood Group Serology and Transfusion Medicine, Medical University Vienna, Vienna (10), Department of Hematology, University Hospital Basel, Basel (11), The LOOP Zurich, University of Zurich, Zurich (12)

Introduction: Immune-mediated toxicities of chimeric antigen receptor (CAR) T cell therapy, including cytokine release syndrome (CRS), immune effector cell-associated neurotoxicity syndrome (ICANS) and hematotoxicity (ICAHT) remain major causes of non-relapse morbidity and mortality. The contribution of the patient's immune contexture, comprising CARpos and CARneg immune cells, remains poorly understood.

Methods: Using high dimensional longitudinal single-cell spectral flow cytometry, we profiled CARpos and CARneg immune compartments across 295 peripheral blood samples from a total of 45 patients with relapsed/refractory B-cell lymphoma enrolled in two independent cohorts receiving CD19-directed CAR T-cell therapy.

Results: We show that CARneg T cells are not passive bystanders but undergo dynamic, toxicity-specific reprogramming and actively contribute to CAR T cell-associated immunopathology. Severe ICANS was partly encoded before infusion: an effector, Th1-skewed CARneg $CD4^+$ T-cell program present at apheresis preceded severe neurotoxicity and was subsequently recapitulated in CARpos $CD4^+$ T cells after infusion. CARneg T cells emerged as key cytokine sources (TNF, GM-CSF, IL-2), shaping an inflammatory host-environment with subsequent ICANS. Early ICAHT reflects a cytotoxic, marrow-tropic bystander T cell switch upon CAR T cell therapy, whose persistence, coinciding with CD47 "don't-eat-me" retention, distinguished resolving from late hematotoxicity.

Conclusions: These findings challenge the CARpos T cell-centric model and position CARneg T cells as predictive correlates that shapes subsequent CARpos T cell states, and immunopathologic effector in CAR T cell therapy-associated toxicity.

8746

Computationally Designed ZAP70 Kinase Off-Switch Enables Rapid, Selective and Reversible Control of CAR- and TCR-T Cells

M. Hafezi (1), A. Semilietof (1), L. Hadadi (1), E. Dorchies (1), T. Que (1), P. Reichenbach (1), P. Guillaume (1), R. Genolet (1), E. Gray-Gaillard (1), C. Arber (1), B. Gentner (1), V. Zoete (1), O. Michielin (2), M. Irving (1)

Department of fundamental oncology, Ludwig Institute for Cancer Research University of Lausanne and Lausanne University Hospital (CHUV), Lausanne (1), Department of Oncology, Geneva University Hospital, Geneva, Switzerland, Geneva (2)

Introduction: Adoptive T-cell transfer (ACT) therapies are transforming the clinical landscape in oncology and autoimmunity, but treatment-related toxicities remain a major safety concern that limits their broader clinical application. As existing safety switches are largely designed around individual receptors or modalities, a broadly applicable pharmacological strategy enabling precise, selective, and reversible control across both TCR- and CAR-T cell platforms remains an unmet need. We therefore aimed to develop a universal pharmacological off-switch for engineered T cells.

Methods: We computationally reprogrammed the ATP-binding pocket of ZAP70, a proximal protein tyrosine kinase shared by TCR and CAR signalling, to generate a drug-responsive kinase switch that preserves signalling function while conferring sensitivity to clinically approved kinase inhibitors. Endogenous ZAP70 was replaced with the engineered variant, and the effects of clinically approved kinase inhibitors on TCR- and CAR-mediated T-cell activation were evaluated in vitro and in vivo.

Results: The engineered ZAP70 variant rendered T cells selectively sensitive to subtherapeutic concentrations of clinically approved kinase inhibitors while preserving TCR and CAR signaling in the absence of drug. Replacement of endogenous ZAP70 enabled rapid, selective, and reversible pharmacological control of both TCR- and CAR-mediated T-cell activation in vitro and in vivo.

Conclusions: We establish a kinase-based pharmacological off-switch that enables unified, rapid, selective, and reversible control of both TCR- and CAR-engineered T cells. This platform provides a broadly applicable and clinically adaptable approach for enhancing the safety and tunability of adoptive T-cell therapies.

 Published under the CC license Attribution 4.0 International (CC BY 4.0)

SSH/SSMO ORAL PRESENTATION - CLINICAL HEMATO-ONCOLOGY

7092

Real-world evidence of CAR T-cell treatment in Switzerland: a nationwide registry analysis

C. Arber (1), J. van den Berg (2), H. Baldomero (2), L. Barras (3), M. Daskalakis (4), T. Demont (3), M. Fehr (5), S. Gerull (6), T. Güngör (7), J. Halter (2), R. Merki (8), G. Nair (9, 10), U. Novak (11), T. Pabst (11), C. Renner (12), D. Schneidawind (13), F. Simonetta (14), G. Stüssi (15), S. Zeerleder (8), J. R. Passweg (2), A. Holbro (2, 16)

Department of Oncology, Lausanne University Hospital, Lausanne (1), Hematology, University Hospital Basel, Basel (2), National Data Management and Research Centre for Stem Cell Transplantation and Cellular Therapy (NDRC), Swiss Transfusion SRC, Bern (3), Hematology and Central Hematology Laboratory, Inselspital, Bern (4), Medical Oncology and Hematology, Cantonal Hospital St. Gallen, St. Gallen (5), Hematology, Cantonal Hospital Aarau, Aarau (6), Division of Stem Cell Transplantation, University Children's Hospital Zurich, Zurich (7), Hematology, Cantonal Hospital Lucerne, Lucerne (8), Swiss Blood Stem Cells, Swiss Transfusion SRC, Bern (9), Medical Oncology and Hematology, Cantonal Hospital Winterthur, Winterthur (10), Medical Oncology, Inselspital, Bern (11), Clinic for Hematology and Oncology, Hirslanden Hospital, Zurich (12), Medical Oncology and Hematology, University Hospital Zurich, Zurich (13), Hematology, Geneva University Hospital, Geneva (14), Oncology Institute of Southern Switzerland (IOSI), Cantonal Hospital Bellinzona, Bellinzona (15), Regional Blood Transfusion Service, Swiss Red Cross, Basel (16)

Introduction: Chimeric antigen receptor T-cell (CAR T) therapy has rapidly expanded across products and indications, but its implementation in Switzerland has not been systematically described. We analysed real-world registry data of CAR T-cell use and outcomes in Switzerland.

Methods: Multicentre analysis of the Swiss Blood Stem Cell Transplantation and Cellular Therapy (SBST)/EBMT CAR T registry, covering all standard-of-care CAR T infusions from January 2019 to December 2025 (data cut March 2026; trial [n = 28] and compassionate-use [n = 12] treatments excluded). Outcomes were assessed per patient at first infusion: complete response (CR) by day 100, overall survival (OS, Kaplan-Meier) and non-relapse mortality (NRM, competing risk), with 95% confidence intervals (CI); CAR T requests not resulting in infusion (slot requests) were described.

Results: In total, 894 CAR T infusions were administered to 883 patients across 11 centres. Annual infusions increased from 41 in 2019 to 230 in 2025, and active centres from 4 to 11. Six products were used (Table 1): tisa-cel accounted for 39/41 infusions in 2019 but only 6/230 in 2025, while axi-cel was the most frequent overall (n = 310). Non-Hodgkin lymphoma accounted for 591/894 infusions (66%; DLBCL n = 477, mantle cell n = 43, follicular n = 40, primary CNS n = 16, other n = 15), multiple myeloma for 229 (26%), B-ALL for 55 (6%) and other entities for 19 (2%). Across all indications (n = 882, excluding one patient with prior CAR T abroad; median follow-up 23 months), the CR rate was 59% (95% CI 55-62; lymphoma 60%, myeloma 48%), 12-month OS 74% (71-77; lymphoma 71%, myeloma 81%) and 12-month NRM 4.8% (3.4-6.4; lymphoma 4.8%, myeloma 6.1%); in B-ALL, CR rate was 94% and 12-month OS 86%. Of 82 CAR T requests (79 patients, 8 centres) not resulting in infusion of the requested product, 12 patients later received CAR T; 67 had not by the end of 2025, mainly because they died before infusion (n = 36, 54%), became too ill (n = 14, 21%) or manufacturing failed (n = 12, 18%).

Conclusions: CAR T-cell therapy use in Switzerland expanded more than fivefold between 2019 and 2025 and evolved to a multi-product, multi-indication landscape, with outcomes comparable to published real-world cohorts. The registry provides a framework for further analyses of access, safety and outcomes. Updated and extended analyses will be presented at the meeting.

Product	Swissmedic first approval	2019	2020	2021	2022	2023	2024	2025	Total
Kymriah (tisa-cel)	18.10.2018	39	38	36	38	18	12	6	**187**
Yescarta (axi-cel)	17.04.2019	2	26	34	44	86	66	52	**310**
Tecartus (brexu-cel)	25.08.2021	–	–	1	14	14	20	14	**63**
Abecma (ide-cel)	20.08.2021	–	–	–	32	49	47	14	**142**
Breyanzi (liso-cel)	28.03.2022	–	–	–	–	5	36	63	**104**
Carvykti (cilta-cel)	08.08.2022	–	–	–	–	–	7	81	**88**
Total		**41**	**64**	**71**	**128**	**172**	**188**	**230**	**894**
Indication									
Non-Hodgkin lymphoma		32	60	62	87	111	120	119	**591**
Multiple myeloma		–	–	–	31	49	54	95	**229**
B-ALL		8	4	9	9	5	12	8	**55**
Other		1	–	–	1	7	2	8	**19**
Other characteristics									
Active centres		4	6	9	10	9	10	11	–
Median age (years)		61	67	61	64	67	68	66	–
Apheresis to infusion (days, median)		63	46	47	48	46	47	54	–

Table 1. Standard-of-care CAR T infusions in Switzerland by product, indication and year.

3999

Context-Free Blast Classification Fails at the WHO 20% AML Threshold: Observer, AI, and Clinical Validation

S. H. Hahn (1), S. B. Balabanov (1), J. D. Deuel (1), S. H. Hahn (1)

Medical Oncology and Hematology, University of Zurich, Zurich (1)

Introduction: Accurate blast enumeration is critical for AML diagnosis at the WHO 20% threshold. AI-based classifiers are structurally constrained to context-free single-cell analysis. Using BlastenBlaster (www.blastenblaster.com)—a gamified training platform for single-cell bone marrow image classification—we experimentally imposed analogous context-free conditions on human observers to enable systematic comparison between AI and human blast quantification.

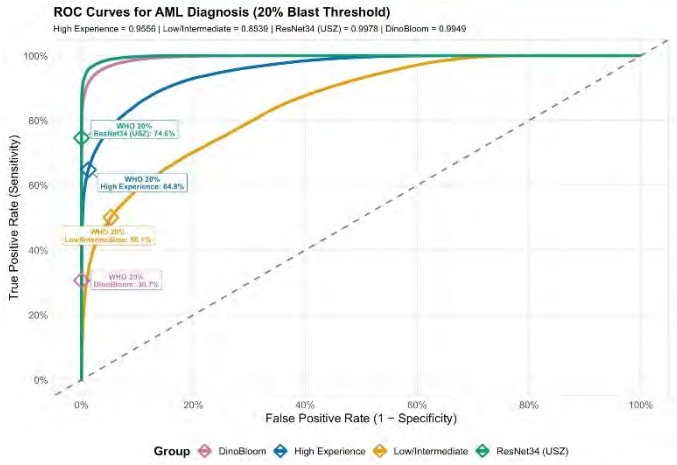
Methods: 29,927 single-cell bone marrow classifications by 25 observers (stratified by experience into two groups; inter-rater agreement Fleiss' κ = 0.57, overall accuracy 72.6%) were used to construct observer-specific confusion matrices. Two AI classifiers (ResNet34 [in-house] and DinoBloom [open-source]) were characterised analogously. Monte Carlo simulation (100,000 cases; 500-cell differential) modelled diagnostic performance across the blast spectrum and derived AUC for all four groups. Paired blast sensitivity (observer majority vote vs. AI) was compared using McNemar's test (2,627 cells, 106 slides). Clinical validation used 77 first-diagnosis AML specimens from a routine clinical AI system.

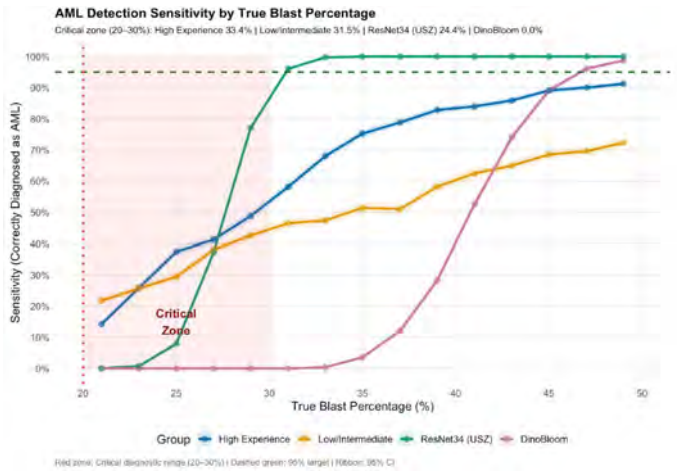
Results: Despite near-perfect simulation AUCs (Human High-experience 0.956, Human Low/intermediate 0.854, ResNet34 0.998, DinoBloom 0.995), all groups failed critically at the WHO 20% threshold—most severely in the 20–30% blast zone. Threshold sensitivities were 64.8%, 50.1%, 74.6%, and 30.7%, respectively; in the critical zone (20–30% true blasts), they collapsed to 33.4%, 31.5%, 24.4%, and 0.0%—AI systems showing the steepest decline. Paired cell-level blast sensitivity: observer majority vote 95.2% vs. ResNet34 69.6% (McNemar p <0.001) and DinoBloom 47.0% (p <0.001). In clinical validation,

 Published under the CC license Attribution 4.0 International (CC BY 4.0)

a DinoBloom-based clinical AI system systematically underestimated blasts (bias −20.8 pp, 95% LoA −51.2 to +9.6, Bland-Altman, n = 75); sensitivity 0.761 (95% CI 0.662–0.859).

Conclusions: Context-free blast classification—whether by human observers or AI—fails systematically at the WHO 20% diagnostic threshold and introduces clinically consequential misclassification risk. AI systems may require slide-level morphological context integrated into training paradigms and clinical decision support to become reliable diagnostic tools.





0361

Increased allele frequency of a LAG3 germline variant is associated with male-predominance and favorable outcome after ASCT in myeloma

A. Mena (1), K. Seipel (1), P. Horum (1), M. Hoffmann (1), M. Bertschinger (1), I. Shafarostova (1), U. Bacher (2), T. Pabst (1)

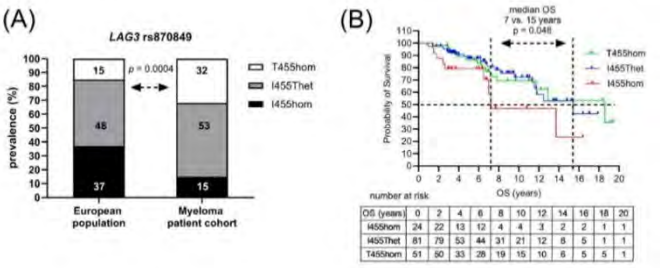
Medical Oncology, Inselspital, Bern (1), Hematology, Inselspital, Bern (2)

Introduction: The incidence of multiple myeloma (MM) is higher in males than females, suggesting sex-related difference. LAG3 and CTLA4 are immune checkpoint proteins and inhibitory regulators of T-cells. We investigated LAG3 rs870849 and CTLA4 rs231775 polymorphisms in transplant-eligible MM patients and their association with genetic risk and treatment outcome after high-dose chemotherapy and autologous stem cell transplantation (HDCT/ASCT).

Methods: Peripheral blood samples from 171 transplant-eligible MM patients were analysed by Sanger sequencing, and allele frequencies were compared to the European reference population.

Results: We found that CTLA4 rs231775 had an allele frequency identical to the European population (0.36) and was not associated with MM susceptibility. In contrast, LAG3 rs870849 occurred at a significantly increased allele frequency of 0.59 compared with 0.39 in the European population. Interestingly, LAG3 allele frequencies were higher in males than females (0.61 vs. 0.53). Gene-risk analyses demonstrated significant associations between LAG3 rs870849 and MM in dominant, recessive and codominant models. In the codominant model, homozygous T455 carriers had an odds ratio (OR) of 5.4 compared with homozygous I455 carriers, while male-specific genetic risk exceeded female-specific risk (OR 6.8 vs. 3.6). Baseline clinical characteristics were largely comparable between genotype groups. However, T455hom LAG3 patients comprised a higher proportion of male patients and higher frequencies of light-chain myeloma and patients with renal dysfunction. Following HDCT/ASCT, treatment outcomes differed according to LAG3 genotype, with median progression-free survival of 2.6, 3.3 and 3.4 years and median overall survival of 7, 15 and 18 years in the I455hom, I455Thet and T455hom LAG3 genotypes, respectively. In contrast, CTLA4 rs231775 genotypes were not associated with genetic risk or clinical outcome.

Conclusions: LAG3 rs870849 was enriched in transplant-eligible MM patients, particularly in males, and was associated with favourable treatment outcome following HDCT/ASCT. These findings identify LAG3 rs870849 as a potential male-predominant germline susceptibility variant and support further investigation of LAG3 as a biomarker for risk stratification and therapeutic strategies in MM.



0342

Myeloid neoplasms post cytotoxic cancer treatment in a Swiss population

J. Veillard (1), G. Tsilimidos (2), S. Meyer (3), S. Masouridi-Levrat (4, 5), C. Widmer (6), M. Fleury (7), S. Mathes (3), W. Rim (3), M. Christen (3), A. Ducrot (4, 5), G. de Fraipont (8), I. Ameti (9), M. Cuendet (5, 8, 10, 11), O. Michielin (5, 8, 10), Y. Chalandon (4, 5), J. Passweg (6), S. Pradervand (5, 8, 10), S. Blum (2)

Division of Clinical Pathology, Department of Diagnostics, Geneva University Hospitals (HUG), Geneva University Hospital, Geneva (1), Service and Central Laboratory of Hematology, Department of Oncology and Department of Laboratory Medicine and Pathology, Lausanne University Hospital (CHUV) and Lausanne University (UNIL), Lausanne University Hospital, Lausanne (2), Department of Hematology and Central Hematology Laboratory, University Hospital Inselspital Bern, University of Bern, Inselspital, Bern (3), Division of Hematology, University Hospital of Geneva (HUG), Geneva University Hospital, Geneva (4), Faculty of Medicine, University of Geneva, Geneva (5), Division of Hematology, University Hospital Basel (USB), University Hospital Basel, Basel (6), Department of Oncology, Lausanne University Hospital (CHUV) and Lausanne University (UNIL), Lausanne University Hospital, Lausanne (7), Service of Precision Oncology, Department of Oncology, Geneva University Hospitals (HUG), Geneva University Hospital, Geneva (8), Service of Radiology, Department of Diagnostics, Geneva University Hospitals (HUG), Geneva University Hospital, Geneva (9), SIB, Swiss Institute of Bioinformatics, Lausanne (10), Department of Physiology and Biophysics, Weill Cornell Medicine, New York (11)

Introduction: Myeloid neoplasms post-cytotoxic treatment (MN-pCT) are myeloid malignancies arising after cytotoxic treatment mostly used for cancer treatment. Myelodysplastic neoplasms (MDS) and acute myeloid leukemias (AML) are the

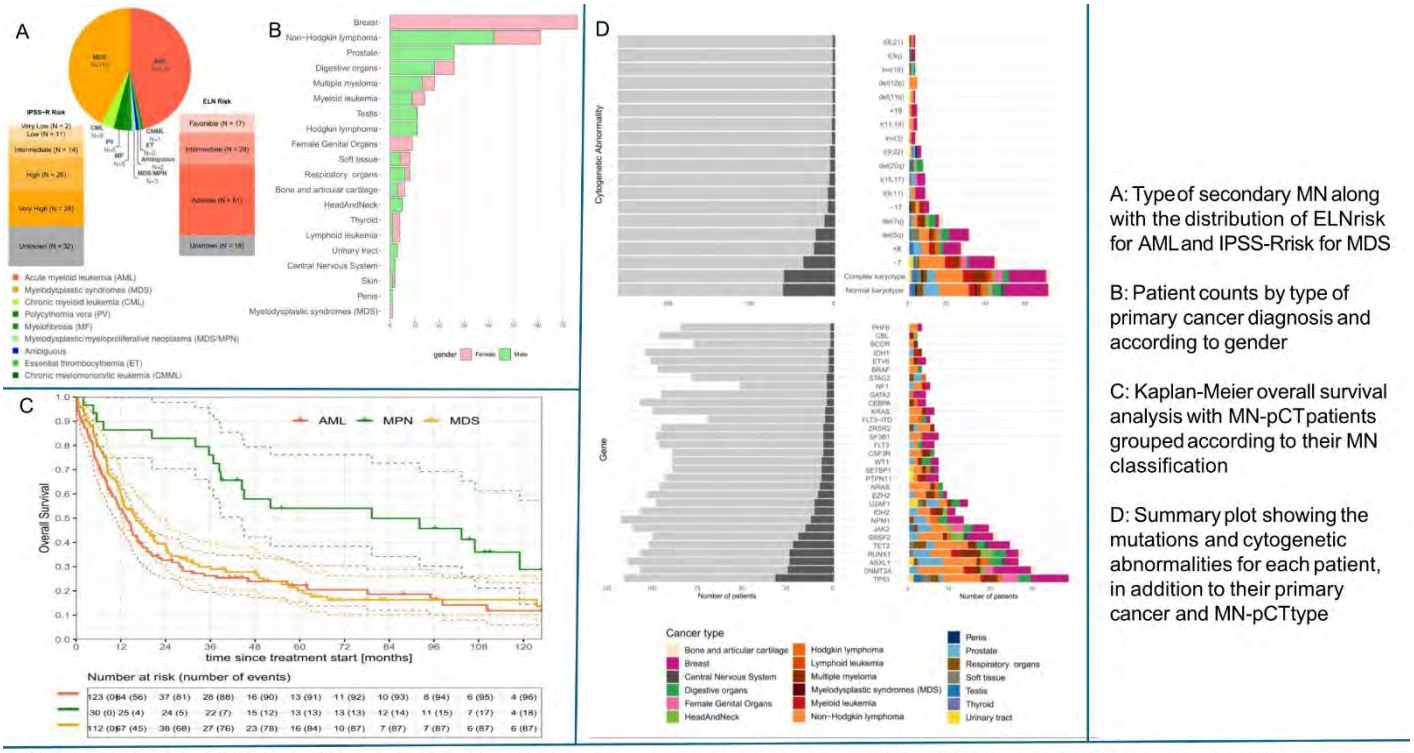
Published under the CC license Attribution 4.0 International (CC BY 4.0)

commonest forms. The objective of the this study is to document and describe the MN-pCT incidence and outcomes in the Swiss population for the first time.

Methods: Most studies in MN-pCT use already diagnosed patient cohorts to analyze prognosis and treatment. For this study, a reverse approach was followed, screening every oncologic patient receiving cytotoxic treatment over a periode of twenty years in four Swiss university hospitals. Datasets were collected through structured algorithms by the Swiss Personalized Health Network. Cases were validated by hematologists and statistical analyses were performed to calculate risk of MN-pCT through standardized incidence ratio (SIR), drug and primary cancer related hazard ratios, and survivals curves.

Results: 205,443 oncologic patients from four Swiss university hospitals, during a period of 20 years, were screened. 267 MN-pCT cases were identified, mostly AML and MDS of adverse risk scores, with also 30 myeloproliferative neoplasms (MPN). SIR for the cohort was 14.2 with soft-tissue sarcomas and cartilage cancers having the highest (62.3 and 100.1 respectively). Alkylating agents and cytotoxic antibiotics showed an enrichment of MN-pCT cases (adjusted P <0.001). No correlation was found between chemotherapeutic agents and cytogenetic anomalies, with TP53 mutations and complex karyotypes being highly common. Both MDS and AML cases had adverse outcomes with a median overall survival (OS) of 1.3 and 1.11 years respectively. MPN cases had much longer OS of more than 6 years. 57.3% of MN-pCT patients received treatment, mostly hypomethylating agents or intensive chemotherapy. Neither strategy resulted in different survival in both fit and unfit for hematopoietic stem cell transplantation patients.

Conclusions: Inverse approach enabled MN-pCT risk estimation, revealing higher-than-expected associations and confirming the adverse prognosis of MN-pCT. An increased number of MPN cases was found, a feature rarely reported in the literature. These findings emphasize the importance of long-term monitoring of cancer survivors exposed to cytotoxic therapies, as well as further investigation into the clonal evolution of MN-pCTs.



A: Type of secondary MN along with the distribution of ELN risk for AML and IPSS-R risk for MDS

B: Patient counts by type of primary cancer diagnosis and according to gender

C: Kaplan-Meier overall survival analysis with MN-pCT patients grouped according to their MN classification

D: Summary plot showing the mutations and cytogenetic abnormalities for each patient, in addition to their primary cancer and MN-pCT type

Abbreviations: AML= acute myeloid leukemia, ELN= European Leukemia Net, IPSS-R=revised international prognosis scoring system, MDS= myelodysplastic neoplasm, MN = myeloid neoplasm, MPN= myeloproliferative neoplasm, pCT= post cytotoxic treatment

1664

Efficacy and Safety of Ruxolitinib Combined With Extracorporeal Photopheresis for Chronic Graft-versus-Host Disease

C. Koch (1), M. G. Manz (1), M. G. Naegeli (2), D. Schneidawind (1)

Department of Medical Oncology and Hematology, University Hospital Zurich, Zurich (1), Department of Dermatology, University Hospital Zurich, Zurich (2)

Introduction: Chronic graft-versus-host disease (cGvHD) remains a leading cause of long-term morbidity following allogeneic hematopoietic stem cell transplantation. Ruxolitinib (RUX) is the current standard treatment for steroid-refractory or -dependent (SR) cGvHD, whereas extracorporeal photopheresis (ECP) remains frequently utilized in clinical practice. However, data on the combined use of RUX-ECP are scarce. We aimed to compare the efficacy and safety of combined RUX-ECP therapy with ECP monotherapy in patients with SR-cGvHD.

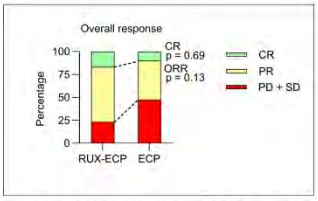
Methods: We conducted a retrospective single-center study including patients with SR-cGvHD treated with RUX-ECP (n = 30) or ECP alone (n = 21) between 2012 and 2025. cGvHD manifestations, severity, and treatment responses were evaluated according to NIH consensus criteria. Clinical outcomes included overall and organ-specific response rates, time to response, corticosteroid reduction, survival outcomes, relapse incidence, and treatment-related adverse events.

Results: Overall response rates were numerically higher with RUX-ECP than with ECP (77% vs. 52%; p = 0.13) with complete responses in 17% and 10% of patients, respectively (p = 0.69). Patients receiving RUX-ECP responded significantly earlier than those treated with ECP alone (median 2.6 vs. 12.3 months; p = 0.0249). Favorable response trends with RUX-ECP were observed in gastrointestinal, ocular, and cutaneous SR-cGvHD. Survival outcomes, including overall survival, relapse incidence, non-relapse mortality, and event-free survival, were comparable between treatment cohorts. Corticosteroid taper-

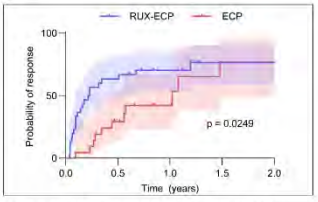
Published under the CC license Attribution 4.0 International (CC BY 4.0)

ing was substantially improved with RUX-ECP, with steroid discontinuation achieved in 69% of patients at 12 months compared with 10% in the ECP group (p = 0.005). Median corticosteroid reduction was also greater with combination therapy (88% vs. 30%; p = 0.0026). Adverse events were manageable and consistent with the established safety profile of ruxolitinib.

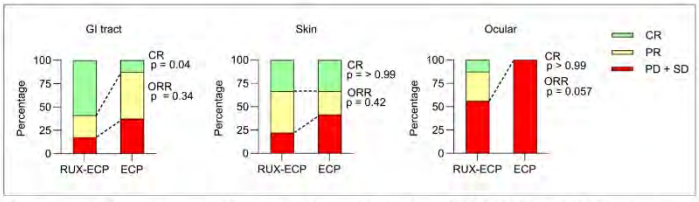
Conclusions: The RUX-ECP combination was associated with high response rates, more rapid clinical responses, and superior corticosteroid-sparing effects compared with ECP alone in patients with SR-cGvHD. Clinical benefits were maintained without compromising survival outcomes, and treatment was generally well tolerated. These findings support further prospective evaluation of combined immunomodulatory strategies in cGvHD management.



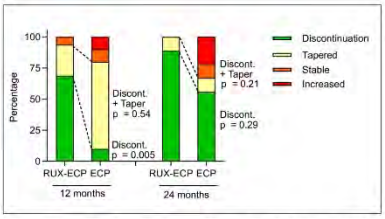
Overall response rates of the RUX-ECP and ECP cohort



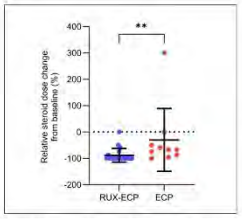
Time to first response of the RUX-ECP and ECP cohort



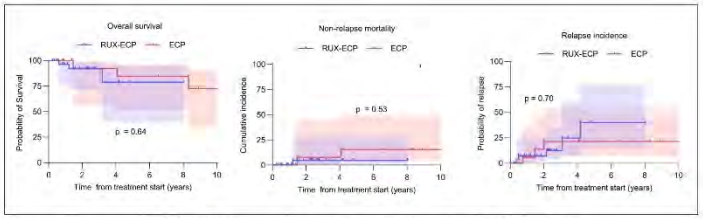
Organ-specific responses (GI-tract, skin, ocular) of the RUX-ECP and ECP cohort



Steroid reduction / discontinuation of the RUX-ECP and ECP cohort after 12 and 24 months



Relative steroid doses at 12 months RUX-ECP or ECP



Clinical outcomes (OS, NRM, relapse incidence) after RUX-ECP or ECP

3596

CAR T-Cell Therapy versus Autologous Stem Cell Transplantation in Aggressive B-Cell Lymphomas

D. Hugi (1), I. Shafarostova (1), M. Kronig (1), M. Bertschinger (1), K. Seipel (1), U. Bacher (2), T. Pabst (1)

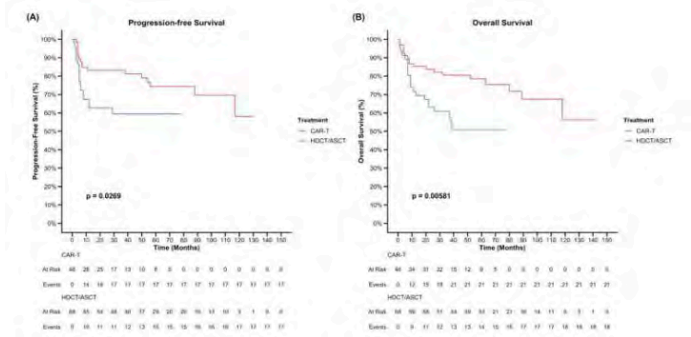
Medical Oncology, Inselspital, Bern (1), Hematology, Inselspital, Bern (2)

Introduction: Traditionally, high-dose chemotherapy followed by autologous stem cell transplantation (HDCT/ASCT) has been the standard of care (SOC) in second-line treatment of aggressive B-cell lymphomas. However, outcomes have remained poor, especially in patients with refractory disease. More recently, chimeric antigen receptor (CAR) T-cell therapy has become a well-established treatment option of relapsed/refractory (r/r) aggressive B-cell lymphomas. Despite this development, it remains unclear whether HDCT/ASCT or CAR T-cell therapy is more effective in chemosensitive disease.

Methods: In this retrospective observational study, we compared the efficacy of HDCT/ASCT versus CAR T-cell therapy in patients with r/r aggressive B-cell lymphomas, who were in a complete remission (CR) or partial remission (PR) after salvage chemotherapy, thereby suggesting chemosensitive disease. Patients received CAR T-cell therapy or HDCT/ASCT between January 2014 and May 2024 at a single Swiss academic centre. The primary endpoints were progression-free survival (PFS) and overall survival (OS).

Results: With a median follow-up of 39.5 months in the CAR T-cell therapy group and 71.5 months in the HDCT/ASCT group, median PFS and OS were not reached in either cohort. HDCT/ASCT was associated with an improved 2-year PFS (83% vs. 63%; p = 0.0269) and OS (84% vs. 63%; p = 0.00581), as well as a trend to a lower rate of early relapse (16% vs. 35%; p = 0.0854) as compared to CAR T-cell therapy. Moreover, death occurred in 46% of CAR T-cell patients and in 27% of HDCT/ASCT patients (p = 0.0445). The cumulative incidence of non-relapse mortality (NRM) was significantly higher in the CAR T-cell patient group compared to the HDCT/ACST group (15% vs. 6% at 12 months, p = 0.0130).

Conclusions: In contrast to randomized studies in unbiased DLBCL relapse cohorts, our findings suggest that HDCT/ASCT may result in superior clinical outcomes compared to CAR T-cell therapy in patients with r/r aggressive B-cell lymphomas who demonstrate chemosensitive disease following salvage chemotherapy. NRM in patients treated with CAR T-cell therapy appears to be relevant. Prospective studies are warranted to define the optimal treatment strategy for this patient population.



Published under the CC license Attribution 4.0 International (CC BY 4.0)

SSMO ORAL PRESENTATION - CLINICAL SOLID TUMOR ONCOLOGY

0304

Darovasertib Plus Crizotinib vs Investigator's Choice as First-Line Treatment for Patients with HLA-A2 Negative Metastatic Uveal Melanoma: Primary Results from the OptimUM-02 trial

M. Orloff (1), E. Ramelyte (2), M. O. Butler (3), P. Rutkowski (4), L. Di Guardo (5), M. S. Carlino (6), B. Chmielowski (7), L. Kennedy (8), K. Montazeri (9), J. Sacco (10), E. Rossi (11), V. Atkinson (12), R. Haq (13), M. McKean (14), G. Cole (15), H. Patel (15), L. Kwei (15), J. Sachdev (15), D. M. Beaupre (15), S. Piperno-Neumann (16)

Thomas Jefferson, University Hospital, Philadelphia PA (1), Department of Dermatology, University Hospital Zurich, Zurich (2), Departments of Medicine and Immunology, Princess Margaret Cancer Centre, University of Toronto, Toronto (3), Department of Soft Tissue, Bone and Melanoma Cancers, Maria Sklodowska-Curie National Research Institute of Oncology, Warsaw (4), Department of Oncology and Hematology, . Fondazione IRCCS Istituto Nazionale dei Tumori di Milano, Milano (5), The University of Sydney and the Melanoma Institute, Westmead and Blacktown Hospitals, Westmead (6), University of California Los Angeles, Jonsson Comprehensive Cancer Center, Los Angeles, CA (7), Taussig Cancer Center, Cleveland Clinic Foundation, Cleveland, OH (8), Mass General Brigham Cancer Institute, Massachusetts General Hospital, Boston, MA (9), Department of Medical Oncology, The Clatterbridge Cancer Centre NHS Foundation Trust, Birkenhead, Wirral (10), Fondazione Policlinico Universitario A.Gemelli, IRCCS, Rome (11), University of Queensland, Princess Alexandra Hospital, Brisbane (12), Center for Ocular Melanoma, Dana-Farber Cancer Institute, Boston, MA (13), Sarah Cannon Research Institute, Sarah Cannon Research Institute, Nashville, TN (14), IDEAYA Biosciences, IDEAYA Biosciences, South San Francisco, CA (15), Department of Medical Oncology, Institut Curie Research University, Paris (16)

Introduction: Uveal melanoma (UM) is the most common ocular cancer in adults with up to 50% of patients developing metastasis with high mortality. No FDA-approved systemic treatments exist for HLA-A*02:01 (HLA-A2) -negative metastatic UM (mUM). Darovasertib (darova) is a first-in-class, oral PKC inhibitor that showed encouraging clinical outcomes in a prior phase 1/2 study in combination with the MET inhibitor crizotinib (crizo).

Methods: OptimUM-02 is an open-label study of HLA-A2 negative first-line mUM patients who were randomized 2:1 to receive darova 300 mg plus crizo 200 mg BID or investigator's choice (IC) of treatment (pembrolizumab, ipilimumab + nivolumab, or dacarbazine). The primary endpoint for efficacy for phase 2 was progression-free survival (PFS) by RECIST (BICR). Other endpoints included investigator assessed PFS (PFSinv), objective response rate (ORR), duration of response (DOR), disease control rate (DCR: CR+ PR + SD ≥ 12 weeks), and safety.

Results: Overall 338 patients received at least one dose of study treatment (safety population), 313 comprised the efficacy population. The median PFS by BICR was 6.9 months for darova+crizo (5.6, 8.3) and 3.1 months for IC (1.8, 4.2); HR: 0.42, p <.0001. Median PFSinv was 6.7 months (5.6, 8.2) and 2.7 months (1.7, 4.1) resp; HR 0.36, p <0.0001. BICR ORR {37.1% [CR 2.4%; PR 34.8%] vs. 5.8% [CR 0%, PR 5.8%], DCR (73.3% vs 31.1%), DOR (median 6.8 months vs. Non-Evaluable) all favored darova+crizo (p-value <0.0001). The most common treatment emergent adverse events (AEs) for darova+crizo were diarrhea (89.5%), nausea (78.2%), peripheral edema (70.7%), & vomiting (53.6%). In the IC arm, these were nausea (41.4%), diarrhea (36.3%), fatigue (33.3%), AST & ALT elevation (31.1%). AEs led to discontinuation & dose reduction of darova in 3.8% & 23.8% and crizo in 10.9% & 27.2% subjects. In the IC arm, 19.2% discontinued due to AEs. Treatment related serious AEs occurred in 9.2% and 25.3% on darova + crizo and IC respectively.

Conclusions: In patients with HLA-A2-negative-mUM treated in the first-line setting, darova+crizo demonstrated a clinically and significantly longer PFS, and improved ORR and DCR compared with the investigator's choice treatment. AEs were consistent with the previously reported safety profiles in each arm. These results support a potential new therapeutic standard for a disease with limited treatment options and poor prognosis.

8276

Trends in Treatment and Survival for Localised Low and Intermediate-Risk Prostate Cancer Patients in Switzerland

E. Camarillo-Retamosa (1), E. Bastiaannet (2), L. Wildis (3, 4), K. Staehel (3, 4), B. Gosztony (1), D. Menges (2, 5), S. Rohrmann (2), A. Lorch (1), N. Miglino (1), M. A. Puhan (2), T. Mehra (1, 6)

Medical Oncology and Hematology, University of Zurich and University Hospital of Zurich, Zurich (1), Epidemiology, Biostatistics and Prevention Institute, University of Zurich, Zurich (2), NICER, National Institute for Cancer Epidemiology and Registration, Zurich (3), NACR, National Agency for Cancer Registration, Zurich (4), Medical Epidemiology and Biostatistics, Karolinska Institutet, Stockholm (5), Medical Clinic, Zuger Kantonsspital AG, Baar (6)

Introduction: Localised prostate cancer is heterogeneous, ranging from indolent to aggressive forms. In localised low- and intermediate-risk cases, seminal trials found no survival differences between definitive treatment and active monitoring. This study aimed to analyse trends in treatment patterns and cancer–specific survival among Swiss patients with localised low- and intermediate-risk prostate cancer.

Methods: We conducted a population-based observational cohort study using data from the National Agency for Cancer Registration (NACR). Adult patients diagnosed between 2000 and 2021 with prostate cancer (ICD-10 C61) were pre-selected, but only those meeting the criteria for localised low- and intermediate-risk according to the current European Association of Urology (EAU) Guidelines on Prostate Cancer (i.e. reported Stage T1 and T2, N0–Nx, cM0 disease, Gleason Score ≤7 and PSA <20 ng/ml) were selected. Treatments were categorised, and Prostate Cancer Specific Survival (PCSS) was calculated for the entire cohort and over time.

Results: A total of 28252 patients fulfilled the inclusion criteria and were included in the analysis. No treatment was registered in 37.4% of patients, while active monitoring was documented in 1.8%. Surgery alone was the most common active treatment (41.4%). Radiotherapy +/- hormonal treatment was recorded in 16.3%. Treatment patterns changed over the years; between 2000-2010 and 2011-2021, the proportion of no recorded treatment or active monitoring increased by 6.7%, radiotherapy +/- hormonal therapy decreased by 4.7%, and surgery alone increased by 1.7%. Variations in trends in treatment patterns were significant between regions. At a median follow-up of approximately 6 years, ten-year prostate cancer-specific survival (PCSS) was 97.6% (95% confidence interval (CI) 97.3% - 97.9%), with a slight increase between 2000-2010 and 2011-2021 being observed (96.7% to 98.2%, age-adjusted hazard ratio (HR) 0.91, 95% confidence interval (CI) 0.90-0.93, P <0.001).

Conclusions: The rate of surgery remains high with a small increase over time. Regional differences in treatment trends are substantial and require further analysis. Documentation of treatment strategies within cancer registries, particularly active monitoring, was limited. Long-term outcomes in Swiss patients with early-stage prostate cancer are excellent, with increasing prostate cancer-specific survival.

 Published under the CC license Attribution 4.0 International (CC BY 4.0)

9726

Predictive and Prognostic Evaluation of Tumor Microenvironment and Systemic Inflammation in Relapsed/Metastatic Head and Neck Cancer

T. Andermatt (1, 2), C. Schultheiss (1, 2), B. Ehret (3), C. Delley (3), M. Daniel (3), A. Eklund (3), S. Chevrier (3), A. Brandt (1), M. S. Matter (4), M. Binder (1, 2)

Division of Medical Oncology, University Hospital Basel, Basel (1), Laboratory of Translational Immuno-Oncology, Department of Biomedicine, University of Basel, Basel (2), Research Department, Navignostics, Horgen (3), Division of Pathology, University Hospital Basel, Basel (4)

Introduction: *Only a subset of patients with relapsed/metastatic head and neck squamous cell carcinoma (R/M HNSCC) derive benefit from immune checkpoint inhibitors (ICI), and predictive biomarkers are lacking. While the tumor microenvironment (TME) influences ICI response across cancer entities, data in R/M HNSCC remain scarce. Systemic inflammatory markers and circulating cytokines have been associated with poor survival, but their relationship to the TME and ICI response remains unclear. We aimed to assess associations between TME features and plasma markers and their respective predictive and prognostic value.*

Methods: The cohort comprised 75 R/M HNSCC patients from the FOCUS trial treated with ICI. Pretreatment tumor tissue was profiled by imaging mass cytometry (IMC) using a 44-marker panel to characterize immune cell populations, activation states, and spatial organization. Pretreatment and on-treatment plasma samples were analyzed by flow cytometry for circulating cytokines and immune-related proteins.

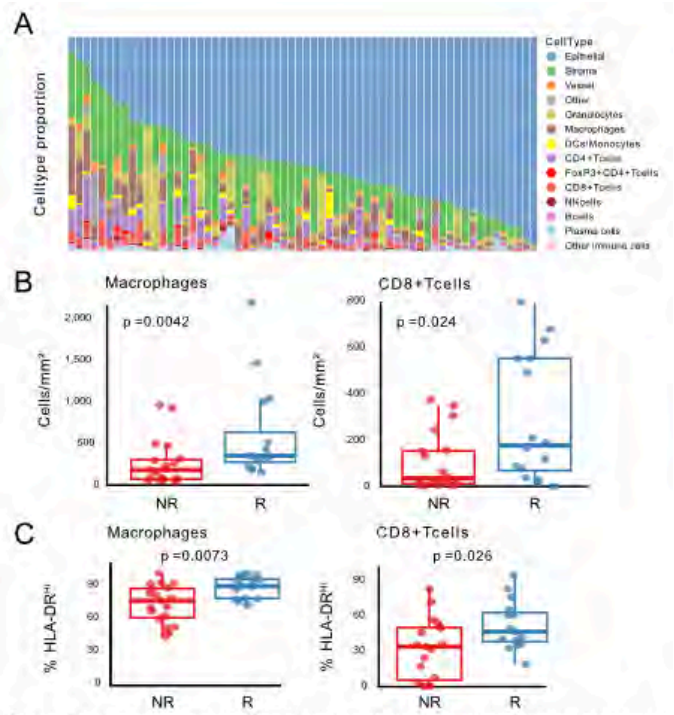


Fig. 1. The tumor microenvironment is linked to immunotherapy response in HNSCC. A) The bar plot shows the proportional cell type composition of each pretreatment HNSCC sample as analyzed by imaging mass cytometry. **B)** Macrophages and CD8+ T cells are enriched in responders. Box plots show the density of individual cell types per patient in responders (R) and non-responders (NR). **C)** Activated immune cell populations are enriched in responders. Box plots show the percentage of cells within each cell type exhibiting high HLA-DR expression in responders (R) and non-responders (NR). Each dot represents an individual patient. P-values were calculated using the Mann–Whitney U test.

Results: In the pretreatment TME, granulocyte abundance, particularly in necrotic areas, was associated with ICI non-response, whereas macrophages, CD4+ and CD8+ T cells were enriched in responders. Macrophages and FoxP3+ CD4+ T cells in the stromal compartment were associated with improved OS, whereas FoxP3+ CD4+ T-cell abundance in necrotic areas was associated with worse OS. Clusters of ≥10 closely located CD4+ T cells were observed exclusively in responders. Granulocytes, macrophages, NK cells, and CD8+ T cells with high HLA-DR expression were enriched in responders. Plasma profiles changed during treatment but were generally not predictive of response. Higher on-treatment levels of sCD25, CXCL13, and sTIM3 were associated with worse OS. Pretreatment CXCL13 correlated with lower stromal cell density, higher intratumoral macrophage density, and lower tumor cell density in necrotic areas, whereas sCD25 and sTIM3 showed no associations with TME features.

Conclusions: IMC revealed distinct, spatially defined immune cell populations associated with ICI response and OS. HLA-DR^high immune subsets were enriched in responders, supporting a potential role of pre-activated immunity in treatment response. Circulating immune-related proteins were prognostic for OS. Notably, circulating CXCL13 was associated with poor OS, contrasting with its favorable prognostic association in the tumor microenvironment.

6516

Feasibility and Clinical Utility of Patient-Matched Real-World Evidence Reports for Molecular Tumor Board Recommendations

L. A. Boos (1, 2), E. Camarillo-Retamosa E (1, 2), C. Doerig (3), M. Sarwary (1, 2), S. Rizzo (4), N. Miglino (1, 2), L. Fábregas-Ibáñez (5), B. Bodenmiller (6, 7), S. Chevrier (8), A. S. Eklund (8), M. Nowak (5), S. Rahmani-Khajouei (5), M. Bodmer (3), D. Glinz (3), I. Opitz (2, 9), S. Ulrich (2, 10), M. Guckenberger (2, 11), L. Hempel (1), P. Rahimzadeh (1, 2), B. Gosztonyi (1, 2), U. Richter (1), L. Bankel (1), A. Wicki (1, 2)

Medical Oncology, University Hospital Zurich, Zurich (1), Faculty of Medicine, University of Zurich, Zurich (2), ., Hoffmann-La Roche Ltd, Basel (3), ., Genentech, South San Francisco, CA (4), Pathology - Molecular Tumor Profiling, University Hospital Zurich, Zurich (5), Department of Quantitative Biomedicine, University of Zurich, Zurich (6), Institute of Molecular Systems Biology, Federal Institute of Technology Zurich, Zurich (7), ., Navignostics AG, Horgen (8), Department of Thoracic Surgery, University Hospital Zurich, Zurich (9), Department of Pulmonology, University Hospital Zurich, Zurich (10), Department of Radio oncology, University Hospital Zurich, Zurich (11)

Introduction: Comprehensive genomic profiling provides increasing numbers of identifiable molecular subgroups across cancers, many of which are too rare for prospective randomised trials. The current granular molecular diagnostics have led to profiles not covered in guidelines or trial data, creating evidence gaps in routine care. Structured real-world data (RWD) may help address this need. Its role in molecular tumor board (MTB) workflows remains insufficiently explored.

Methods: Structured patient-matched RWD reports were integrated into the workflow of the MTB. RWD reports were generated using a predefined matching algorithm linking clinico-genomic features from our institutional database to patient cohorts in the de-identified Flatiron Health–Foundation Medicine NSCLC Clinico-Genomic Database. The feasibility, plausibility and clinical utility to inform treatment recommendations were assessed by MTB oncologists using a structured questionnaire on the utility and actionability of each RWD report. Descriptive statistics summarised the outcomes.

Results: For all 200 included patients with advanced NSCLC, a matched RWD report was generated. The presented data were judged to be plausible by the participating clinicians. Reports contained unique information considered relevant for potential treatment personalisation in 77%. RWD-based recommendations differed from initial MTB treatment recommendations recorded prior to having access to the RWD report in 21%. Discordance occurred in 16% of first-line, 22% of second line and 24% of third-line or later recommendations and was more frequent in cases without classical actionable oncogenic drivers. The re-

Published under the CC license Attribution 4.0 International (CC BY 4.0)

port increased clinicians' confidence in their initial MTB treatment recommendations in 54.8%. In all cases, clinicians indicated that they could not have retrieved equivalent information presented in the RWD report from any other source within 15 minutes.

Conclusions: Patient-matched RWD reports can be integrated into the MTB workflow with the potential for a clinically meaningful impact, informing decision-making and treatment recommendations. These findings support further exploration of RWD as a complementary evidence source in precision oncology.

6127

Diagnostic and Treatment Indicators for Prostate Cancer: Analysis of Swiss Cancer Registry Data from 2020–2023

G. L. Eggebrecht (1, 2), E. S. Pedersen (1, 2), K. Steigmiller (1, 2), C. Würmschimmel (3), D. S. Engeler (4), S. Boxler (5), D. Menges (6, 7), M. Weber (1, 2), M. Schaffner (1, 2), A. Abo El Ela (1, 2), K. Staehelin (1, 2)

National Agency for Cancer Registration, (NACR), Zurich (1), National Institute for Cancer Epidemiology and Registration, (NICER), Zurich (2), Department of Urology, Lucerne Cantonal Hospital, Lucerne (3), Department of Urology, Cantonal Hospital St. Gallen, St. Gallen (4), Praxis im Engeriedspital, Boxler & Spahn, Bern (5), Epidemiology, Biostatistics and Prevention Institute (EBPI), Univeristy of Zurich, Zurich (6), Department of Medical Epidemiology and Biostatistics (MEB), Karolinska Institut, Stockholm (7)

Introduction: Background and Objective: Prostate cancer is the most common cancer among men in Switzerland. The quality of prostate cancer treatment is regularly assessed and monitored in certified cancer centres. However, little is known about the nationwide quality of care. Analysing population-based cancer data collected in cancer registries can fill this gap. We aimed to comprehensively describe the burden, diagnostic characteristics, treatment patterns and survival of prostate cancer in Switzerland.

Methods: Methods: This analysis was based on the Swiss national cancer registry data and included all malignant primary cases of prostate cancer (ICD-10: C61) diagnosed in Switzerland between 2020 and 2023. Analyses included evaluation of detection method, risk group at diagnosis according to European Association of Urology, case discussion at a tumour board, first treatment, and 3-year survival.

Results: Results: The sample included 35717 cases of primary prostate cancer with median age at diagnosis of 70.7 years (interquartile range: 64.3-76.6). Only 268 (0.8%) were younger than 50 years at diagnosis. The most common method of detection was opportunistic screening (n = 26862; 76%). Most cases were categorised into low risk (n = 4912; 14%) or intermediate risk (n = 8943; 25%) while 9500 (27%) were in the high risk localised or locally advanced group and 4010 (11%) were in the high-risk metastatic group. Older age was associated with higher risk group. Related to care, treatment decision in a tumour board was registered for 19931 (56%) and was negatively associated with older age (45% among the ≥80-year-olds) and positively associated with risk group (75% for high risk locally advanced; 65% for high risk metastatic). The most common first treatment was radical prostatectomy alone (n = 11332; 32%) or in combination (n = 755; 2.1%). Active surveillance was documented for 7028 cases (20%). Survival was high with 90% age-standardised observed and 96% relative 3-year survival.

Conclusions: Conclusion: Most prostate cancers in Switzerland were detected early and categorised as low- or intermediate-risk at diagnosis, most frequently following opportunistic screening and characterised by high short-term relative survival. Overall, the findings indicate favourable diagnostic and care outcomes but also highlight opportunities for improvement, particularly regarding the proportion of cases discussed at a tumour board.

5483

Integrating Tumor-Informed ddPCR with Comprehensive cfDNA Sequencing for Longitudinal ctDNA Monitoring in Gastrointestinal Cancers

S. Hussung (1, 2), A. S. De Oliveira Gomes (1), M. Geissmann (1), L. Grossmann (1), D. Seidl (3), S. Gächter (3), M. Nowak (3), M. Schaufelberger (3), C. Mennicke (3), S. Rahmani-Khajouei (3), C. Pistoni (1), T. Brezina (1, 2), M. Zoche (3), H. Moch (3, 4), A. Weber (3, 5), R. Fritsch (1, 2)

Medical Oncology and Hematology, University Hospital Zurich, Zurich (1), Medical Oncology and Hematology, University of Zurich, Zurich (2), Institute of Pathology and Molecular Pathology, University Hospital Zurich, Zurich (3), Institute of Pathology and Molecular Pathology, University of Zurich, Zurich (4), Institute of Molecular Cancer Research (IMCR), University of Zurich, Zurich (5)

Introduction: Circulating tumour DNA (ctDNA) enables minimally invasive monitoring in gastrointestinal (GI) cancers, but routine implementation is limited by technological heterogeneity, cost, and lack of standardisation. We evaluated tumour-informed personalised droplet digital PCR (ddPCR) for longitudinal ctDNA monitoring and its complementarity with comprehensive cell-free DNA (cfDNA) sequencing.

Methods: Tumour tissue from 17 patients with GI malignancies underwent comprehensive genomic profiling to identify patient-specific ddPCR targets. Personalised ddPCR assays were applied to serial plasma samples and compared with comprehensive cfDNA sequencing. Concordance, variant allele frequencies (VAFs), longitudinal ctDNA kinetics, radiological response, exploratory survival outcomes, and temporal genomic changes were assessed.

Results: Forty-six targets representing 37 unique variants were selected. Of 33 newly developed ddPCR assays, 28 (84.8%) were successfully established, with at least one trackable tumour-derived variant available for every patient. Overall, 119 plasma samples were analysed by ddPCR with 100% technical success; 40 of 41 cfDNA sequencing analyses were successful (97.6%). Among 27 paired plasma samples, 26 were concordant (96.3%), with positive and negative percent agreements of 93.8% and 100%, respectively. VAFs correlated strongly between methods (Spearman ρ = 0.888; P <.0001). Among seven baseline ctDNA-positive patients evaluable longitudinally, four achieved molecular clearance; all four also demonstrated objective radiological response at first restaging. In an exploratory 8-week landmark analysis, non-increasing ctDNA was associated with longer overall survival (P = .0149). Serial cfDNA sequencing revealed temporal genomic changes in seven of eight patients, including treatment-emergent resistance alterations.

Conclusions: Personalised ddPCR enabled robust longitudinal ctDNA monitoring with high concordance to comprehensive cfDNA sequencing, while sequencing provided complementary information on genomic evolution and resistance. Combining targeted ddPCR monitoring with comprehensive cfDNA sequencing may provide a pragmatic strategy for longitudinal molecular assessment in GI cancers.

 Published under the CC license Attribution 4.0 International (CC BY 4.0)

ONCOREHA/OPS/PALLIATIVE.CH/SNIO/SOHC ORAL PRESENTATION - NURSING, SUPPORTIVE & PALLIATIVE CARE, REHABILITATION & SURVIVORSHIP AND INTEGRATIVE ONCOLOGY

5494

Benefit of Short-term Interventions for Cancer Patients addressing Dignity, Meaningfulness and Mindfulness in Acute Care: Results of a Randomized Controlled Trial

G. M. Meinlschmidt (1), K. K. Klatte (2), R. S. Schaefert (1), H. C. Chochinov (3), G. R. Rodin (4), S. E. Eckstein (2)

Psychosomatic Medicine, University Hospital Basel, Basel (1), Palliative Care, University Hospital Basel, Basel (2), Psychiatry, University of Manitobia, Toronto (3), Psychiatry, University of Toronto, Toronto (4)

Introduction: The diagnosis of cancer poses a threat to fundamental existential human needs, including the confrontation with death, uncertainty, loss of autonomy, feeling a burden to others, and loss of meaning given often profound changes in personal goal orientations and roles. It was shown that perception of dignity plays an important role in coping with an uncurable disease. Focusing on patients with a terminal illness, we have developed a modular approach for the acute care setting consisting of Dignity Therapy, modified Managing Cancer and Living Meaningfully (CALM) Therapy, and a mindfulness-based intervention (MBI) to address the individual needs of this heterogenous group of patients. We hypothesize that patients receiving a personalized short-term intervention show better outcomes in terms of mental well-being than those receiving standard specialized palliative consultation services (SSPC) only.

Methods: We aimed to randomize 40 patients from the palliative care consulting service of the University Hospital Basel (life expectancy <18 months) to receive either the modular short-term intervention and SSPC or SSPC alone. Patients in the intervention group chose one of the offered modules, consisting of two sessions. Changes in mental well-being pre-versus post-intervention were measured by the Patient Dignity Inventory (PDI) in both groups. Secondary outcomes include the Patient Health Questionnaire-9 (PHQ-9), the Integrated Palliative Care Outcome Scale (IPOS) and semi-structured interviews.

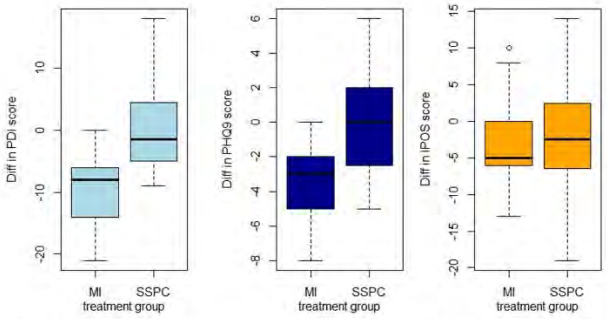


Figure 1: Boxplot of differences between treatment groups in cancer patients for A) PDI scores, B) PHQ9 scores, and C) IPOS scores. *Abbrev.: MI, Modular Intervention; SSPC, Standard Specialized Palliative Consultation Services; PDI, Patient Dignity Inventory; PHQ-9 , Patient Health Questionnaire-9; IPOS, Integrated Palliative Care Outcome Scale.*

Results: Over the recruitment period of 19 months, 42 patients overall and 40 cancer patients completed the study. Breast cancer patients (27.3%) and glioblastoma patients (18.3%) represented the largest subgroups within our study. In the simple regression analysis of the 40 cancer patients, the beta coefficient for treatment arm, estimating the difference in treatment between arms, was -9.78. The difference in PDI score change as well as the PHQ9 score change between groups were significant (p-value <0.001), while changes in IPOS were similar in both groups. Analysis of the post-intervention interview showed a high patient-perceived benefit of the intervention, especially in dignity and overall helpfulness.

Conclusions: Quantitative and qualitative analysis of included cancer patient data shows a clear benefit of the modular short-term intervention in terms of increased dignity and quality of life.

Table 1: Demographics of included cancer patients (n =42, one death, one withdrawal due to health decline)

	Mean (SD)/ count (Percentages) All	SSPC	MI
Age	67.1 (13.0)	67.3 (15.6)	66.7 (9.4)
Gender			
Male	15 (35.7 %)	8 (38.1 %)	7 (33.3 %)
Female	27 (64.3 %)	13 (61.9 %)	14 (66.7 %)
Relationship status			
Married or living with partner	25 (59.5 %)	13 (61.9 %)	12 (57.1 %)
Living alone (single or widowed)	17 (40.5 %)	8 (38.1 %)	9 (42.9 %)
Religion			
Christian	24 (57.1 %)	9 (42.9 %)	15 (71.4%)
Other	2 (4.8 %)	1 (4.8 %)	1 (4.8 %)
No confession	16 (38.1 %)	11 (52.4 %)	5 (23.8)
Education Level			
Obligatory	2 (4.8 %)	2 (9.5) %	-
Apprenticeship	19 (45.2 %)	11 (52.4 %)	8 (38.1 %)
High School	11 (26.2 %)	5 (23.8 %)	6 (28.6 %)
College/University	10 (23.8 %)	3 (14.3 %)	7 (33.3 %)
Primary disease/ cancer site			
Breast cancer	12 (28.6 %)	4 (19.0 %)	8 (38.1 %)
Glioblastoma	8 (19.0 %)	4 (19.0 %)	4 (19.0 %)
Uterine cancer	4 (9.5 %)	3 (14.3 %)	1 (4.8 %)
Lung cancer	4 (9.5 %)	3 (14.3 %)	1 (4.8 %)
Prostate cancer	3 (7.1 %)	1 (4.8 %)	2 (9.5 %)
Other cancer sites	11 (21.4 %)	6 (28.8 %)	5 (24.0 %)
Time between primary diagnosis and study participation	4.0 years (6.0) (median 1.26)	3.3 years (4.8) (median 1.3)	4.7 years (7.2) (median 1.2)
< 6 months	16 (38.6 %	9 (42.9 %)	7 (33.3 %)
> 6 months	26 (62.0 %)	12 (57.1 %)	14 (66.7 %)
< 12 months	20 (47.6 %)	10 (47.6 %)	10 (47.6 %)
>12 months	22 (52.4 %)	11 (52.4 %)	11 (52.4 %)

Abbrev.: MI, Modular Intervention; SSPC, Standard Specialized Palliative Consultation Services

2652

Psychosocial support needs and utilization of support among survivors of cancer in young adulthood in Switzerland: a report from the Adolescent and Young Adult (AYA) Psychosocial Health Study

K. Roser (1), M. Ospelt (1), M. Blum (2), O. Gautschi (3, 4), L. Mader (5), W. Mingrone (6), M. Mousavi (2), B. Müller (3), M. Vetter (7), C. Bolliger (1)

Faculty of Health Sciences and Medicine, University of Lucerne, Lucerne (1), -, Cancer Registry of Eastern Switzerland, St. Gallen (2), Department for Medical Oncology, Cantonal Hospital of Lucerne, Lucerne (3), Department for Medical Oncology, University of Bern, Bern (4), Cancer Registry Bern and Solothurn, University of Bern, Bern (5), Department for Oncology, Cantonal Hospital Olten, Olten (6), Center for Oncology and Hematology, University Hospital Basel, Basel (7)

Introduction: The psychosocial needs of survivors of cancer in young adulthood in Switzerland remain poorly understood. With this study, we aimed to (1) describe psychosocial support needs of young adult cancer survivors (YACS) during treatment and survivorship, (2) determine whether these needs change from treatment to survivorship, and (3) identify characteristics associated with unmet needs.

Published under the CC license Attribution 4.0 International (CC BY 4.0)

Methods: We included survivors aged 21-39 years at diagnosis, diagnosed at least two years prior to our questionnaire survey. We used descriptive statistics to analyze distributions of psychosocial support needs during treatment and survivorship. McNemar's tests assessed changes in these needs over time, and logistic regressions identified determinants of unmet needs.

Results: A total of 131 YACS (mean age at study = 37.5 years; 61% female) participated in our study. Most YACS reported that their needs were met in all support domains, both during treatment and survivorship. During treatment, unmet needs were highest for insurance support (n = 30; 23%), support for friends (n = 20; 15%) and family (n = 17; 13%). During survivorship, unmet needs were most pronounced for insurance support (n = 15; 12%), information on cancer and late effects (n = 10; 8%), and work-related support (n = 9; 7%). Intrapersonal needs (e.g., information, psychological), remained stable, while unmet interpersonal (e.g., family, friends), and institutional/systemic (e.g., insurance, work) support needs declined during survivorship. Younger age and shorter time since diagnosis were associated with unmet intrapersonal needs during survivorship, while male sex predicted unmet interpersonal needs during treatment.

Conclusions: Although most support needs are met, targeted efforts are needed to address the remaining unmet needs of Swiss YACS in order to ensure they receive adequate survivorship care.

9193

Direct medical costs of de-escalated denosumab in patients with bone metastases: within-trial analysis of the non-inferiority trial SAKK 96/12 REDUSE

E. Antonini (1), S. Stoffel (1), A. Mueller (2), S. Hayoz (3), M. Mark (4, 5), S. Fischer (6), R. Popescu (7), S. Rothschild (8), M. Fehr (9), C. Egger-Arnet (10), S. Anchisi (11), F. Schmid (12), K. Zaman (13), C. Ackermann (14), S. Wyss (15), A. J. Templeton (16), S. Gillessen (5), R. von Moos (17), M. Schwenkglenks (1)

Department of Public Health, University of Basel, Basel (1), Department of Medical Oncology, KSW - Kantonsspital Winterthur, Winterthur (2), Statistics, Swiss Cancer Institute, Bern (3), Oncology/Hematology Department, KSGR - Kantonsspital Graubünden, Chur (4), Istituto Oncologico della Svizzera Italiana (IOSI), EOC, Bellinzona and Faculty of Biosciences, Università della Svizzera Italiana (USI), Lugano (5), Department of Medical Oncology and Hematology, Kantonsspital St. Gallen, St. Gallen (6), Dept. of Medical Oncology, Haematology, Supportive and Palliative Care, Tumor Zentrum Aargau, Aargau (7), Medical Oncology Department, Universitätsspital Basel, Basel (8), Gynäkologie und Geburtshilfe, Spital Thurgau AG - Kantonsspital Frauenfeld, Frauenfeld (9), Medical Oncology Dept, Spital Limmattal, Schlieren (10), Oncology department, Spital Thurgau AG - Kantonsspital Frauenfeld, Frauenfeld (11), Department of Urology, USZ - University Hospital Zürich, Zürich (12), Oncology Dept., CHUV - Centre Hospitalier Universitaire Vaudois, Lausanne (13), Department of Oncology and Haematology, Spital STS AG Onkologiezentrum Thun-Berner Oberland, Thun (14), Department of Clinical Operations, Swiss Cancer Institute, Bern (15), Department of Medical Oncology, St. Claraspital AG, Basel (16), Oncology/Hematology Dept.,, KSGR - Kantonsspital Graubünden, Chur (17)

Introduction: The randomizedrandomised multicenter phase III trial SAKK 96/12 REDUSE compared guideline-recommended denosumab (Dmab; 120 mg every 4 weeks; Arm A) with a de-escalated schedule (every 4 weeks for 3 doses, then every 12 weeks; Arm B) in patients with bone metastases (BM) from advanced breast or castration-resistant prostate cancer. The trial met its primary clinical endpoint of non-inferiority, as presented at ASCO 2026. This economic sub-study of REDUSE evaluates within-trial direct medical costs from a Swiss statutory health insurance system perspective.

Methods: BM-related healthcare resource use was valued in 2025 Swiss francs (CHF) using Swiss costs for Dmab acquisition and administration, hospital stays, rehabilitation, nursing home and home care, outpatient care, radiotherapy, concomitant medications (excluding anticancer therapies), symptomatic skeletal events and osteonecrosis of the jaw. Mean costs per patient were analysed with a gamma generalised linear model and logarithmic link (Gamma GLM), adjusting for tumour type, performance status, country group, and follow-up time.

Results: We included 1,333 intention-to-treat patients (Arm A, n = 667; Arm B, n = 666); mean follow-up time was 25.0 and 26.9 months, respectively. Observed mean Dmab acquisition and administration costs per patient were CHF 14,134 in Arm A and CHF 6,671 in Arm B, implying a reduction of 53%. Observed total costs were CHF 42,193 in Arm A and CHF 37,989 in Arm B. The smaller reduction in total costs was partially driven by the longer observation time and associated accumulation of healthcare costs in Arm B. In the Gamma GLM considering follow-up time, adjusted total costs were CHF 41,264 (95% confidence interval (CI) 37,696 to 44,715) in Arm A and CHF 36,283 (CI 33,251 to 39,630) in Arm B. The adjusted difference was CHF -4,981 (CI -9,583 to -8) and adjusted ratio 0.879 (CI 0.783 to 0.988).

Conclusions: Compared with standard Dmab dosing every 4 weeks, the de-escalated Dmab strategy was associated with lower within-trial direct medical costs, driven by reduced Dmab costs. These findings support a substantial cost containment potential of Dmab de-escalation in patients with bone metastases.

5619

A tailored digital intervention for BRCA1 and BRCA2 family support: the DIALOGUE cluster-randomized trial

L. C. Schiess (1), C. Barton (1), B. Moon (2), S. Aissaoui (3, 4), F. Brugnoletti (5), N. Bürki (6), M. Caiata Zufferey (7), M. Cattaneo (1), P. O. Chappuis (5, 8), F. Ciorba (9), V. Duong (1), R. Graffeo (10), U. Hasler-Strub (11), K. Heinimann (12, 13), J. Kim (14), S.-W. Kim (15), K. Leunig (16), M. C. Lim (17), C. Monnerat (18), J. S. Park (19, 20), M. Rabaglio (21), J. M. Ryu (22), R. Saccilotto (1), S. Schlooz (21), S. Schmid (23), C. Uhlmann Nussbaum (24), U. Zürrer-Härdi (25), S. Kim (2), M. C. Katapodi (1)

Faculty of Medicine, Clinical Research, University of Basel, Basel (1), College of Nursing, Yonsei University, Seoul (2), Breast Center, Cantonal Hospital Fribourg, Fribourg (3), The Breast Centre, Hirslanden Clinique de Grangettes, Geneva (4), Unit of Oncogenetics, Division of Precision Oncology, University Hospitals of Geneva, Geneva (5), Women's Clinic, University Hospital Basel, Basel (6), Department of Business Economics, Health and Social Care, University of Applied Sciences and Arts of Southern Switzerland, Manno (7), Division of Genetic Medicine, University Hospitals of Geneva, Geneva (8), Department of Mathematics and Computer Science, University of Basel, Basel (9), Oncology Institute of Southern Switzerland, Ente Ospedaliero Cantonale (EOC), Bellinzona (10), Onkologie/Hämatologie, Kantonsspital Graubünden, Chur (11), Institute for Medical Genetics and Pathology, University Hospital Basel, Basel (12), Department of Biomedicine, Research Group Human Genomics, University of Basel, Basel (13), College of Medicine, Asan Medical Center, Department of Surgery, University of Ulsan, Seoul (14), Breast Care Center, Department of Breast Surgery, Daerim St Mary's Hospital, Seoul (15), Senologie /Genetische Beratung, Affidea brustCare Brust-Zentrum Zürich, Zürich (16), Center for Gynecologic Cancer Research Institute and Hospital, Division of Tumor Immunology, National Cancer Center, Goyang (17), Department of Medical Oncology, Hospital of Jura, Delemont (18), Department of Internal Medicine, Division of Medical Oncology, Yonsei University College of Medicine, Seoul (19), Cancer Prevention Center, Hereditary Cancer Clinic, Yonsei Cancer Center, Seoul (20), Department of Medical Oncology, Inselspital, Bern (21), Samsung Medical Center, Department of Surgery, Division of Breast Surgery, Sungkyunkwan University School of Medicine, Seoul (22), Medizinische Onkologie, Luzerner Kantonsspital, Luzern (23), Medizinische Onkologie, Kantonsspital Olten, Olten (24), Tumorzentrum Brustzentrum, Kantonsspital Winterthur, Winterthur (25)

Introduction: Families affected by BRCA1 and BRCA2 pathogenic variants report unmet needs for ongoing psychosocial support and support for cascade genetic testing. We evaluated whether a digital tailored platform, the Family Gene Toolkit™

 Published under the CC license Attribution 4.0 International (CC BY 4.0)

v2.0, provided better educational, psychosocial comprehensive support compared to a generic website (control).

Methods: DIALOGUE is a parallel, family-level cluster-randomized trial conducted in Switzerland and Korea. Probands with a BRCA1 or BRCA2 germline pathogenic variant were allocated to the intervention or the control. Their relatives were randomized to the same arm. The intervention provided tailored information on cancer genetics, coping, self-efficacy for managing cancer risk and family communication. Outcomes were assessed at baseline (T1), two months (T2) and six months (T3).

Results: A total of 136 probands (intervention = 73; control = 63) and 46 relatives (intervention = 21; control = 25) participated in the trial. Knowledge of cancer genetics increased in both groups, with no differences in change scores at T2 and T3. In analyses adjusted for T1 values, problem-focused coping was higher in the intervention group at T2 (p = .03) and avoidant coping was lower at T3 (p = .02). Self-efficacy for managing cancer risk increased in the intervention group at both T2 and T3 (both p = 0.01). The proportion of eligible relatives invited through the platform did not differ between the intervention and the control groups (p = 0.70). However, of 21 relatives untested at T1, three underwent genetic testing during T2 and T3, all in the intervention group.

Conclusions: Participants benefited from having access to a digital platform explaining cancer genetics. The additional improvements in coping with genetic testing results and self-efficacy in managing cancer risk suggest that the Family Gene Toolkit™ v2.0 provides potential benefits to help with psychosocial adaptation and cascade testing of family members. Further inquiries will evaluate the implementation potential of the digital platform.

4298

Impact of HCP Supervision on Sensitive Quality-of-Life-Questionnaire (QLQ) Item-Scoring by Cancer Patients: Results from the Prospective Randomized Cross-over IMSUP Study

D. P. de Jong-Bakker (1), A. C. Meyer-Gerspach (2, 3), J. Antonov (4), F. A. de Jong (5), A. J. Templeton (6, 1, 3)

Medical Oncology Research Group, St. Clara Research Ltd., Basel (1), Metabolics and Gastroenterology Research Group, St. Clara Research Ltd., Basel (2), Faculty of Medicine, University of Basel, Basel (3), Clinical Research, Lindenhofgruppe, Bern (4), Medical Oncology and Hematology, Health Ostschweiz (HOCH), Kantonsspital St. Gallen, St. Gallen (5), Medical Oncology, St. Claraspital, Basel (6)

Introduction: PROs are increasingly collected digitally at home, but also under HCP supervision on paper or tablet in the hospital. We assessed whether QLQ administration mode affects scoring of sensitive sexual and financial domains.

Methods: IMSUP is a multicentre randomised cross-over study in adult cancer pts on systemic therapy (NCT06490393). Pts were randomised 1:1 to complete PROs (QLQ-C30, QLQ-SH22 and a local financial toxicity tool) under HCP supervision on paper followed by digital completion at home before the next cycle, or vice versa. Pt preference was assessed at baseline and after both QLQ sets. Calculation of domain scores followed EORTC guidance; differences (Δs) were analysed using the paired Wilcoxon signed-rank test. Absolute Δs of ≥3 points were considered relevant, (BH-adjusted) P <.05 statistically significant.

Results: Of 226 included pts (mean age 62.2 yrs [32% ≥70]; 113/113 m/f), 206 completed both QLQ sets; 9 only one (6 for medical reasons, 3 withdrew consent). For sensitive domains, HCP-supervised completion was associated with reporting of less severe concerns: Sexual Satisfaction 40.2 vs 43.9 (SS, 8Qs; Δ = -3.7, Padj = .034); Sexual Pain 14.0 vs 15.9 (SP, 3Qs; Δ = -1.9, Padj = .163); Financial Toxicity 24.0 vs 27.2 (FIN, 4Qs; Δ = -3.2, Padj = .030). For the non-sensitive QLQ-C30 comparator, HCP supervision gave a higher QoL score (C30, 13 domains; 74.4 vs 72.1, Δ = 2.3, P = .017). Preference for supervision decreased from 38.3% to 29.1% after both QLQ sets (P = .022). Digital completion required less HCP time (22.5 vs 6.4 min, P <.001), but more pts needed reminders (14.0 vs 28.0%; P <.001). Sensitive items had higher non-response rates, but less so with supervision (SS: 22 vs 26%, P = .059; SP: 20 vs 25%, P = .023; FIN: 8 vs 11%, P = .049; C30: 2 vs 1.6%, P = .582).

Conclusions: HCP-supervised paper completion of QLQs was associated with a consistent shift towards more favourable scoring by cancer pts, particularly reporting less severe concerns/negative feelings on sensitive domains (absolute Δ ≥3 points). Although pts preferred digital completion at home, limited digital access/literacy, efforts to obtain returned PROs and sensitive-item non-response warrant consideration. The mode effect is superimposed on QLQ results and may contribute to differences across administration modes. These findings should inform trial design and comparisons across/within studies and pts, especially for sensitive PROs.

Table 1: Paired analyses in the prospective multicentre randomised cross-over IMSUP study (NCT06490393; 226 patients)

	HCP-supervised completion on paper	Digital completion at home	Wilcoxon signed-rank *P*-value (BH-adjusted)	Paired *N*
QLQ-SH22 Sexual Satisfaction domain score (SS, mean [SD]) Lower score indicates more favourable status (8 items)	40.2 (23.4)	43.9 (21.8)	*P*=.023 (*P*=.034)	*N*=129
QLQ-SH22 Sexual Pain domain score (SP, mean [SD]) Lower score indicates more favourable status (3 items)	14.0 (24.0)	15.9 (24.7)	*P*=.163 (*P*=.163)	*N*=130
Financial Toxicity domain score (FIN, mean [SD]) Lower score indicates more favourable status (4 items)	24.0 (18.9)	27.2 (18.2)	*P*=.010 (*P*=.030)	*N*=188
QLQ-C30 Composite QoL score (C30, mean [SD]) Higher score indicates more favourable status (13 domains)	74.4 (15.3)	72.1 (14.4)	*P*=.004	*N*=186
Direct HCP time spent (mean [SD])	22.5 min (9.5)	6.4 min (8.6)	*P*<.001	*N*=206
Patients reminded to complete their QLQ set (*N*, %) Missed appointment or not completed digitally as agreed	*N*=30, 14.0%	*N*=60, 28.0%	*P*<.001	*N*=214
Completed QLQ sets (*N*) Missing due to medical reasons (11), digital skills (3), or consent withdrawal (6)	*N*=213	*N*=208		*N*=206
QLQ-SH22 Sexual Satisfaction domain (SS) Item non-response (% SS items of completed QLQs, mean [SD])	22.0% (30.7)	26.0% (33.3)	*P*=.059	*N*=206
QLQ-SH22 Sexual Pain domain (SP) Item non-response (% SP items of completed QLQs, mean [SD])	19.6% (31.2)	24.8% (35.4)	*P*=.023	*N*=206
Financial Toxicity domain (FIN) Item non-response (% FIN items of completed QLQs, mean [SD])	7.8% (18.5)	10.9% (22.4)	*P*=.049	*N*=206
QLQ-C30 Composite score (C30) Item non-response (% C30 items of completed QLQs, mean [SD])	1.9% (10.0)	1.6% (7.3)	*P*=.582	*N*=206

 Published under the CC license Attribution 4.0 International (CC BY 4.0)

4533

From evidence to recommendations: the long shadow of childhood cancer

K. Roser (1), M. Ospelt (1), E. M. Tinner (2, 3), M. Hendriks (1), L. Mader (4), S. Kälin (1)

Faculty of Health Sciences and Medicine, University of Lucerne, Lucerne (1), Division of Pediatric Hematology and Oncology, Department of Pediatrics, Inselspital, University Hospital Bern, Bern (2), Standort Liestal, University Clinic of Medicine, Kantonsspital Baselland, Liestal (3), Cancer Registry Bern Solothurn, University of Bern, Bern (4)

Introduction: Childhood cancer affects the daily lives of survivors and their families in numerous ways, including socio-economic consequences. The objective of this project was to investigate insurance, legal, and financial hardships after childhood cancer and provide evidence-based recommendations using a three-step approach: 1) synthesizing existing international evidence on parents' and survivors' hardships; 2) exploring the lived experiences of survivors and parents in Switzerland; and 3) developing and prioritizing evidence-informed recommendations through a structured stakeholder dialogue.

Methods: In-depth information on insurance, legal, and financial hardships after childhood cancer was collected through systematic literature reviews (step 1) and focus group discussions with survivors and parents of survivors (step 2). In step 3, based on findings from the systematic reviews and focus groups, relevant stakeholders discussed recommendations to mitigate these hardships and implement respective measures in Switzerland.

Results: Two systematic reviews comprising 82 publications indicated that many survivors and parents experience insurance and financial hardships, whereas legal hardships were less frequently investigated and reported. In 11 focus groups, 11 survivors and 18 parents described numerous, often interrelated, insurance, legal, and financial hardships encountered during survivorship. During the stakeholder dialogue involving three experts, one survivor and one parent, 15 recommendations were developed and rated. Informative checklists targeted at different advocacy groups were rated highest in terms of relevance and feasibility. These checklists could offer key information across the cancer continuum, including frequently asked questions and relevant contact points, tailored to different target groups.

Conclusions: The findings from the systematic reviews and focus groups highlight the substantial and interrelated socio-bureaucratic hardships faced by survivors and parents. The hardships and the set of recommendations emphasize the need for sustained support beyond active treatment, and targeted educational and policy-level interventions to alleviate long-term burdens. They further underscore the importance of initiatives such as the Right to be Forgotten in Switzerland and across Europe.

6260

Posttraumatic growth and resilience among survivors of cancer in young adulthood in Switzerland: a report from the Adolescent and Young Adult (AYA) Psychosocial Health Study

K. Roser (1), L. Mader (2), M. Mousavi (3), M. Blum (3), B. Müller (4), M. Vetter (5), C. Bolliger (1)

Faculty of Health Sciences and Medicine, University of Lucerne, Lucerne (1), Cancer Registry Bern and Solothurn, University of Bern, Bern (2), -, Cancer Registry of Eastern Switzerland, St. Gallen (3), Department for Medical Oncology, Cantonal Hospital of Lucerne, Lucerne (4), Center for Oncology and Hematology, Cancer Center Baselland, Cantonal Hospital Baselland, Liestal (5)

Introduction: Survivors of young adult cancer (YACS) face distinct psychosocial challenges. Posttraumatic growth (PTG) and resilience may aid adaptation, though their relationship and relevance in this age group remain insufficiently understood. We aimed to (1) describe PTG and resilience among Swiss YACS and (2) investigate the associations of PTG with resilience, sociodemographic, and cancer-related characteristics.

Methods: We included survivors aged 21-39 years at diagnosis, diagnosed at least two years prior. We conducted a questionnaire survey using the Posttraumatic Growth Inventory (PTGI; range:0-105) and the Connor-Davidson Resilience Scale (CD-RISC 10; range:0-40). Data were analyzed using descriptive statistics and linear regression.

Results: A total of 131 YACS (62% female; mean age at study = 37.6 years, SD = 5.1) were included. The PTG sum score was 54.6 (SD = 23.0, range:1-101), and YACS reported most PTG in appreciation of life (mean = 3.3, 95% confidence interval: 3.2-3.6) and least in spiritual change (1.1, 0.9-1.3). The mean resilience score was 28.06 (SD = 5.91, range:10-39), and YACS reported the highest score for the item "Achieving goals despite obstacles" (3.2, 2.6-3.0), and the lowest for the item "see humorous side of things" (2.1, 2.0-2.3). PTG was higher among females and those who received chemotherapy, while resilience showed no significant association with PTG.

Conclusions: These findings suggest that PTG and resilience are distinct but complementary adaptation processes in YACS. With higher PTG linked to female gender and chemotherapy, and resilience showing no direct association with PTG, personalized psychosocial support remains essential to help survivors navigate their unique cancer experiences and promote well-being.

 Published under the CC license Attribution 4.0 International (CC BY 4.0)

SSH POSTER PRESENTATION - HEMOSTASIS, TRANSFUSION MEDICINE, VASCULAR, LABORATORY MEDICINE, BENIGN HEMATOLOGY

3933

Fibrinogen variants, but not common FXIII or fibrinogen polymorphisms, influence clot permeability in hereditary dysfibrinogenaemia

A. Couzens (1), R. Marchi (2), T. Simurda (3), L. Ardillon (4), C. Biron Andreani (5), M. Daniel (6), E. De Maistre (7), N. Drillaud (8), B. Frotscher (9), A. Vega (10), A. Lebreton (10), M. Neerman-Arbez (1), A. Casini (11)

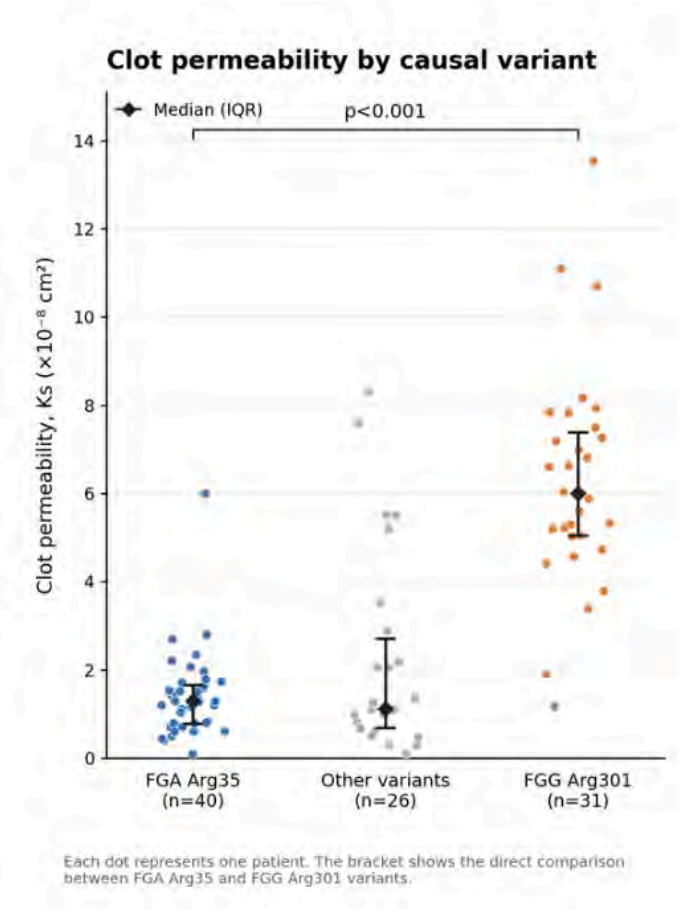
Department of Genetic Medicine and Development, University of Geneva, Geneva (1), Department of Medicine, University of Geneva, Geneva (2), Department of Hematology and Transfusiology, National Centre of Hemostasis and Thrombosis, Martin (3), Laboratoire d'Hématologie-Hémostase, CHRU de Tours Hôpital Trousseau, Tours (4), Service d'Hématologie biologique, CHU de Montpellier Hôpital Saint-Eloi, Montpellier (5), Service d'Hémostase, CHU de Lille - Centre de Biologie Pathologie Pierre-Marie Degand, Lille (6), Haemostasis Unit, University Hospital of Dijon, Dijon (7), Centre Régional de Traitement de l'Hémophilie, CHU de Nantes Hôtel Dieu, Nantes (8), Centre Régional de Traitement de l'Hémophilie, CHU de Nancy Hôpitaux de Brabois, Nancy (9), Service d'Hématologie biologique, CHU de Clermont-Ferrand Hôpital d'Estaing, Clermont-Ferrand (10), Division of angiology and hemostasis, University Hospitals of Geneva, Geneva (11)

Introduction: Hereditary dysfibrinogenaemia shows marked clinical heterogeneity, the biological determinants of which remain poorly defined. Fibrin clot properties may contribute, but the influence of common genetic modifiers, particularly factor XIII (FXIII) and fibrinogen polymorphisms, is uncertain. We assessed whether causal fibrinogen variants and common polymorphisms affect clot properties and are associated with bleeding phenotype

Methods: In this multicentre international cross-sectional study, patients with molecularly confirmed dysfibrinogenaemia were characterised by whole-exome sequencing. Bleeding phenotype was assessed using the International Society on Thrombosis and Haemostasis Bleeding Assessment Tool (ISTH-BAT). Clot polymerisation and lysis were assessed by turbidimetry and permeability by the Darcy constant (Ks). Analyses focused on frequent causal variants at FGA Arg35 and FGG Arg301 and on the F13A1 Val34Leu, FGB -455G>A, and FGA Thr312Ala polymorphisms.

Results: Ninety-nine patients were included; 40 carried an FGA Arg35 variant and 31 an FGG Arg301 variant. Turbidimetric polymerisation and lysis parameters did not differ significantly between causal variant groups. None of the common polymorphisms was significantly associated with clot properties. By contrast, permeability differed markedly by causal variant. FGG Arg301 carriers had higher permeability than non-carriers (Ks 6.3 ± 2.5 vs 1.7 ± 1.7; p <0.001), whereas FGA Arg35 variants were associated with lower permeability (Ks 1.4 ± 1.0). Permeability also differed significantly between the Arg301 and Arg35 groups (p <0.001). No consistent association was observed between causal variants, polymorphisms or clot parameters and ISTH-BAT score (permeability: R^2 = 2.7%; p = 0.142).

Conclusions: Causal fibrinogen variants, but not the common FXIII and fibrinogen polymorphisms studied, influence clot permeability in congenital dysfibrinogenaemia. The absence of an association with ISTH-BAT score indicates that clot properties alone do not explain clinical heterogeneity and supports a multifactorial model involving additional haemostatic determinants.



7060

Longitudinal Changes in Lymphocyte Subsets in Donors After Leukapheresis for Donor Lymphocyte Infusion: A Retrospective Swiss Cohort Study

M. Bürgin (1), K. Frei (2), J. Lansel (2), M. Florova (3), G. Tayfun (4), D. Schneidawind (3), S. Waldvogel (5), A. Holbro (6), L. Infanti (6), A. Buser (6), J. Passweg (1), G. Nair (2), J. Lötscher (1)

Division of Hematology, University Hospital Basel, Basel (1), Swiss Blood Stem Cells Registry, Blutspende SRK Schweiz, Bern (2), Department of Medical Oncology and Hematology, University Hospital Zurich, Zurich (3), Department of Stem Cell Transplantation, University Children's Hospital Zurich, Zurich (4), Blood Transfusion Service SRC, Geneva University Hospital, Geneva (5), Blood Transfusion Center North-Western Switzerland, Swiss Red Cross, Basel (6)

Introduction: Donor lymphocyte infusion (DLI), an established cellular therapy after allogeneic haematopoietic cell transplantation, requires leukapheresis from donors who previously donated stem cells. However, the effects of DLI leukapheresis on donor lymphocyte (Lc) counts and subsets, and the risk of persistent lymphopenia, remain insufficiently characterised. We therefore assessed longitudinal changes in Lc subsets following DLI donation and explored factors associated with incomplete Lc recovery.

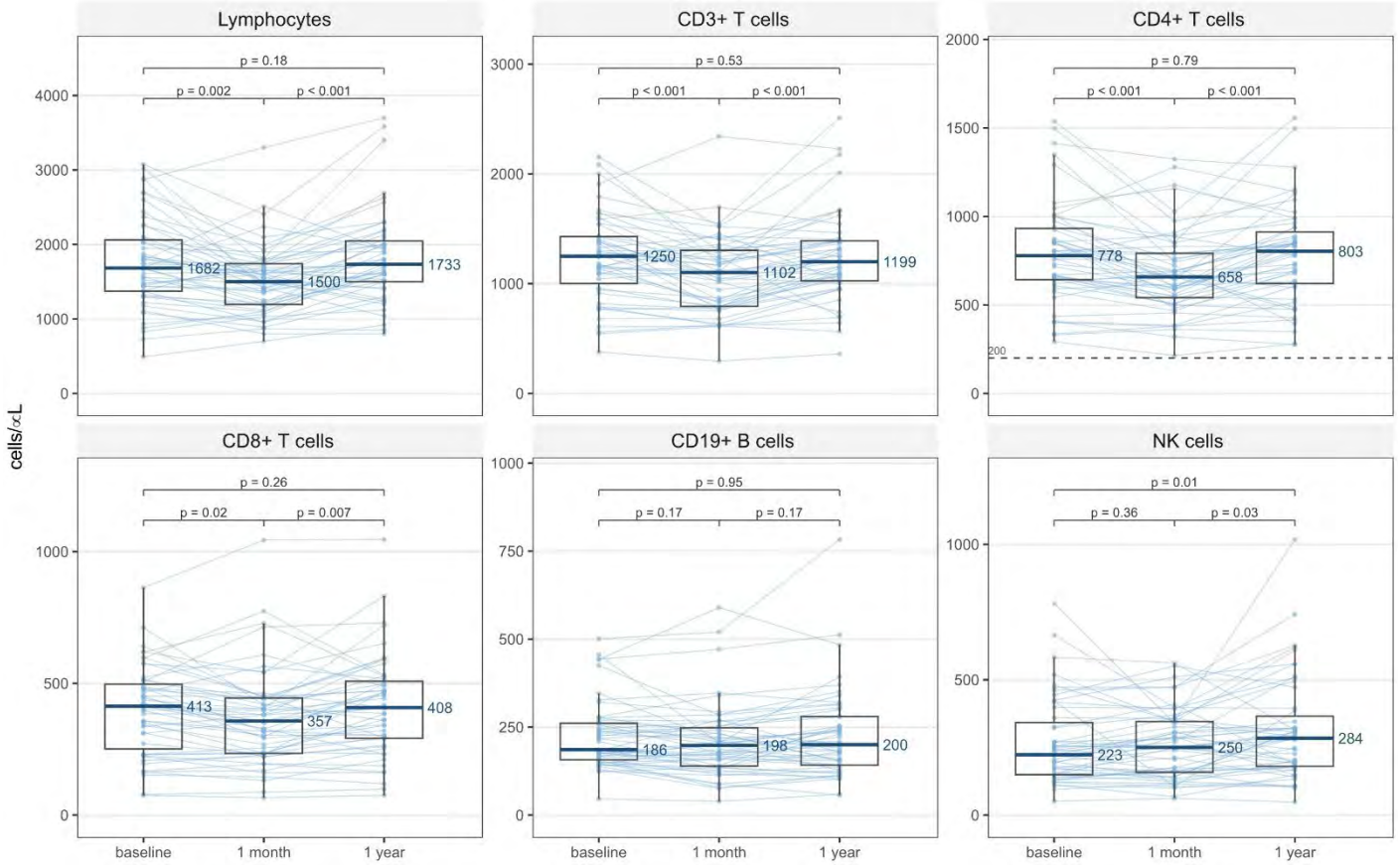
Methods: We conducted a retrospective multicentre national cohort study of healthy donors undergoing leukapheresis for DLI donation in Switzerland between November 2017 and April 2024. Complete blood counts and Lc subsets (CD3+, CD4+, CD8+, CD19+ B cells and NK cells) were assessed at baseline,

Published under the CC license Attribution 4.0 International (CC BY 4.0)

at 1 month (1mt) and 1 year (12mt). We examined associations between donor- and donation-related factors and lower Lc counts. Self-reported symptoms and serious adverse events were assessed by questionnaire and treating physicians, respectively.

Results: Among 153 donors, 51 had complete Lc subset data and formed the primary analysis cohort. Absolute Lc, CD3+, CD4+ and CD8+ counts decreased significantly at 1mt and returned to baseline by 12mt at the population level, whereas B and NK cells did not decrease significantly. CD4+ T cells showed the greatest decline, with a median decrease of 15% at 1mt; no donor developed a clinically relevant CD4+ count <200 cells/µL. After donation, eight donors (15.7%) had at least one Lc subset below the reference range at both 1mt and 12mt; three (5.9%) had normal baseline counts, whereas five (9.8%) already had low baseline counts. In exploratory analyses, older age and a shorter interval between stem cell and DLI donation were associated with lower Lc subset counts at 1mt and 12mt. Three serious adverse events were reported, but none were attributed to DLI donation. Self-reported symptoms were generally mild and self-limiting.

Conclusions: DLI leukapheresis was associated with a transient, reversible reduction in Lc counts at the population level. Pre-existing lymphopenia, older age and shorter intervals between stem cell and DLI donation showed trends towards prolonged, albeit mild, Lc subset abnormalities in a minority of donors. Together with the absence of severe CD4+ lymphopenia and DLI-related serious adverse events, these findings support the safety of DLI donation.



Published under the CC license Attribution 4.0 International (CC BY 4.0)

4250

Uncontrolled thrombin generation drives purpura fulminans in protein S deficiency

M. Tripodo (1, 2), R. Prince-Eladnani (1, 2), S. Calzavarini (1, 2), M. D. Reina Caro (1, 2), J. A. Fernández (3), J. H. Griffin (3), A. Angelillo-Scherrer (1, 2)

Clinic of Hematology & Central Hematology Laboratory, Inselspital, Bern (1), DBMR, University of Bern, Bern (2), Department of Molecular Medicine, The Scripps Research Institute, La Jolla (3)

Introduction: Purpura fulminans (PF) is a life-threatening thrombohaemorrhagic syndrome characterized by microvascular thrombosis, haemorrhagic necrosis, and multiorgan injury. Severe congenital protein S (PS) deficiency causes neonatal PF. PS has anticoagulant and Tyro3/MerTK-mediated cellular functions, but their respective roles in PF remain unclear. Based on previous work showing that genetic ablation of factor VIII (F8) or factor IX rescues PS-deficient (Pros1–/–) mice from death, we investigated how uncontrolled coagulation promotes vascular injury, inflammation, and lymphatic dysfunction.

Methods: Conditional PS depletion was induced by Poly I:C in Pros1lox/–Mx1-Cre+ and Pros1lox/loxMx1-Cre+ mice. Pros1+/+ and Pros1+/– mice received warfarin. Pros1+/+ and Pros1–/– embryos were analysed by histology and whole-mount confocal immunofluorescence to assess blood and lymphatic vessels and macrophages. Coagulation-dependent effects were assessed in F8–/–Pros1–/– embryos; fatty acid β-oxidation was inhibited with etomoxir.

Results: Poly I:C reduced PS to 16.6±2% in Pros1lox/–Mx1-Cre+ mice without inducing PF-like lesions. Warfarin reduced survival in Pros1+/– versus Pros1+/+ mice (8% vs 88%) (Fig. A) and promoted PF-like lesions (Fig. B). Pros1–/– embryos showed extensive vascular/endothelial damage and haemorrhage (Fig. C), accompanied in the skin by macrophage accumulation, inflammation-associated lymphangiogenesis, lymphatic enlargement, and dysfunction (Fig. D). F8–/–Pros1–/– embryos showed preserved vascular architecture, demonstrating that limiting thrombin generation prevents vascular damage despite PS absence (Fig. E). Etomoxir reduced lymphatic expansion and hemorrhage despite persistent systemic coagulopathy (Fig. F).

Conclusions: Complete PS deficiency causes uncontrolled thrombin generation, leading to vascular injury, inflammation, macrophage accumulation, and secondary lymphatic dysfunction. Rescue by F8 deficiency indicates that loss of PS anticoagulant activity, rather than Tyro3/MerTK-mediated functions, is the primary driver of PF. Inflammation-driven lymphangiogenesis contributes to disease severity but is secondary to the coagulation defect (Fig. G). These findings identify dysregulated coagulation as the central mechanism and inflammatory and lymphatic responses as potential complementary therapeutic targets.

 Published under the CC license Attribution 4.0 International (CC BY 4.0)

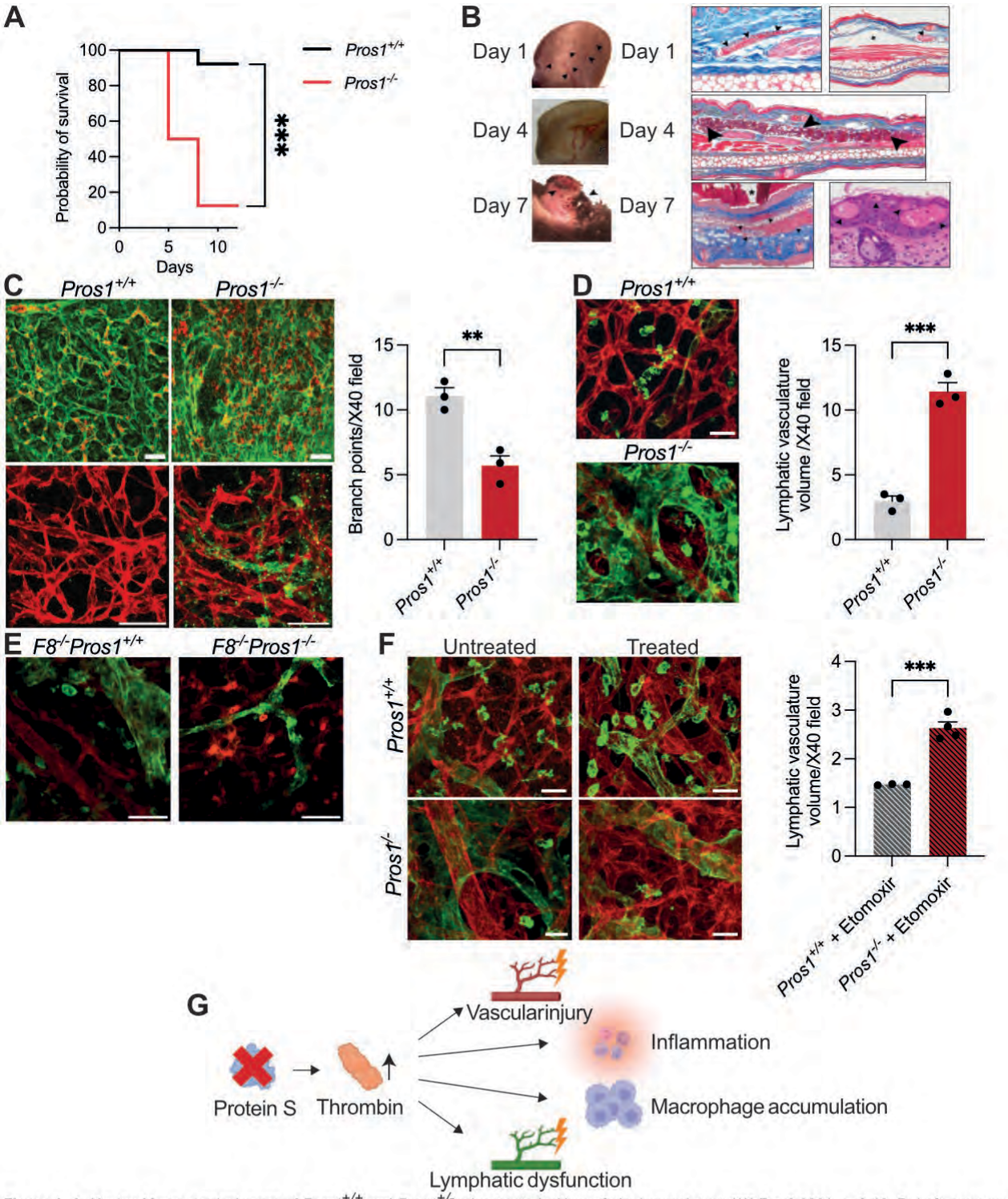


Figure 1. A, Kaplan-Meyer survival curve of *Pros1*$^{+/+}$ and *Pros1*$^{+/-}$ mice treated with warfarin, log-rank test, **** P < 0.0001, n=8-13. **B**, Left: progression of vascular changes in *Pros1*$^{+/-}$ warfarin-treated mice. Arrow heads indicate vasculature and lesions on the ear tissue. Right: Masson-trichrome staining of ears during the progression of vascular changes in *Pros1*$^{+/-}$ warfarin-treated mice. Arrow heads indicate bleeding areas in vessels. Stars indicate areas of edema. **C**, Left: confocal microscopy of dorsal skin in *Pros1*$^{+/+}$ embryos, and *Pros1*$^{-/-}$ embryos. Stainings used, upper panel: VE-cadherin (green, staining adhesion cells in endothelium) and Ter119 (red, staining erythroid cells); lower panel: fibrin (green) and Pecam1 (red, staining endothelial cells). Scalebar in VE-cadherin + Ter110: 50 µm. Scalebar in fibrin + Pecam1 staining: 10 µm. Right: Quantification of branch points per 40X field in *Pros1*$^{+/+}$ and *Pros1*$^{-/-}$ embryos. n=3, unpaired t-test. ** P< 0.01. **D**, Left: confocal microscopy of embryonic vasculature stained with Lyve1 and Pecam1 in *Pros1*$^{+/+}$ embryos, and *Pros1*$^{-/-}$ embryos. Scalebar: 30 µm. Right: volume of lymphatic vasculature per 40X field in *Pros1*$^{+/+}$ and *Pros1*$^{-/-}$ embryos. Unpaired t-test. *** P< 0.0005, n=3. **E**, Confocal microscopy of dorsal skin in *F8*$^{-/-}$*Pros1*$^{+/+}$ embryo and *F8*$^{-/-}$*Pros1*$^{-/-}$ embryos, stained with Lyve1 (green, immunostaining of the lymphatic endothelium) and Pecam1 (red, immunostaining of endothelial cells). Scalebar: 50 µm. **F**, Left: confocal microscopy of vasculature in etomoxir treated and untreated *Pros1*$^{+/+}$ and *Pros1*$^{-/-}$ E16 embryos, stained with Lyve1 (green, staining lymphatic vasculature) and Pecam1 (red, staining endothelial cells). Scalebar: 30 µm. Right: Volume of lymphatic vasculature per 40X field in *Pros1*$^{+/+}$ and *Pros1*$^{-/-}$ embryos treated with etomoxir. n = 3-4, unpaired t-test. *** P< 0.001. **G**, Representative scheme of the effect of protein S deficiency on vasculature and cells. Complete PS deficiency causes uncontrolled thrombin generation, leading to vascular injury, inflammation, macrophage accumulation, and secondary lymphatic dysfunction.

Published under the CC license Attribution 4.0 International (CC BY 4.0)

0706

Usefulness and performance of procoagulant platelet flow cytometry and multiple electrode aggregometry for detecting platelet-activating HIT antibodies

L. Hayenga (1), F. J. Gomez (1), E. Matthey-Guirao (1), M. G. Zermatten (1), L. Alberio (1), A. Aliotta (1)

Central Hematology Laboratory, Lausanne University Hospital - CHUV, Lausanne (1)

Introduction: Heparin-induced thrombocytopenia (HIT) is a severe immune-mediated prothrombotic disease caused by platelet-activating anti-platelet factor 4 (PF4)/heparin antibodies. Immunoassays are sensitive but cannot reliably distinguish pathogenic from non-activating antibodies, while reference functional assays are technically demanding and poorly accessible. We evaluated two more accessible functional assays (i) HIT-induced procoagulant platelet flow cytometry (HIT-PCP) and (ii) heparin-induced multiple electrode aggregometry (HIMEA), against established gold-standard functional testing.

Methods: Plasma from 35 patients investigated for HIT and 11 healthy controls were analysed. Samples were classified according to immunoassay (IA) and reference functional assay (FA) results as healthy controls, IA−, IA+/FA−, or IA+/FA+. HIT-PCP was quantified in donor platelet-rich plasma with buffer, low-dose heparin (0.5 IU/mL), and high-dose heparin (100 IU/mL). HIMEA was performed in hirudinated whole blood with saline, low-dose heparin (1 IU/mL), and high-dose heparin (200 IU/mL). ROC analysis determined optimal diagnostic cut-offs.

Results: Both assays discriminated IA+/FA+ samples from healthy controls and functionally negative samples. IA+/FA+ samples showed the characteristic HIT-dependent response, with marked platelet activation at low heparin concentrations and suppression at high heparin concentrations. For HIT-PCP, a 32% cut-off yielded 92% sensitivity and 93% specificity; responses ≥47% were exclusively observed in functionally positive samples, corresponding to 100% positive predictive value (PPV). For HIMEA, a 170 U cut-off yielded 100% sensitivity and 94% specificity; responses >300 U were exclusively associated with functionally positive samples, corresponding to 100% PPV.

Conclusions: HIT-PCP and HIMEA provide rapid, highly accurate functional detection of platelet-activating HIT antibodies while preserving the defining heparin-dependent response. Their high diagnostic performance and compatibility with available flow cytometry or electrode aggregometry platforms support their implementation as accessible and rapid alternatives to traditional functional testing.

5661

Newly detected red cell alloantibodies in pregnancy: anti-D, -c or -K were found in only one in five women but accounted for all severe cases

D. Y. Duygu Yildiz Özkaya (1), P. R. Piet-Lennart Rosenstock (1), M. D. Michael Daskalakis (1), K. J. Jalowiec (1)

Department of Haematology and Central Haematology Laboratory, Inselspital, Bern (1)

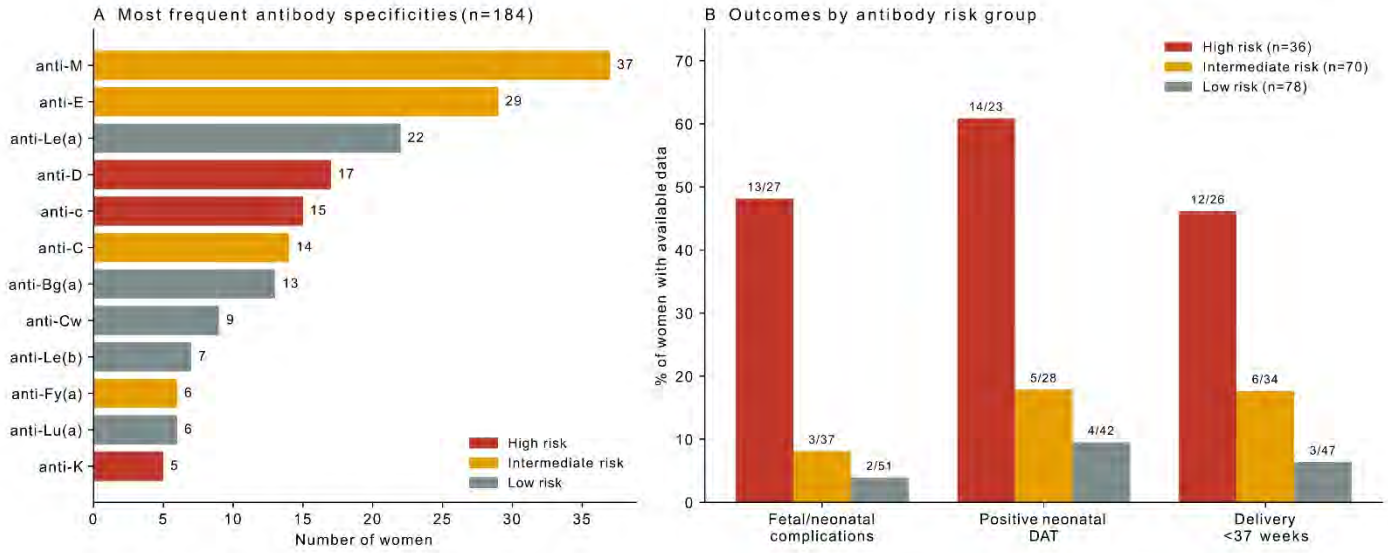
Introduction: Antenatal detection of a red cell alloantibody triggers work-up, monitoring and counselling, although only some specificities cause haemolytic disease of the fetus and newborn (HDFN). We analysed the clinical relevance and timing of detection of red cell antibodies in pregnancy.

Methods: Retrospective single-centre analysis of all red cell antibodies newly detected at a university hospital laboratory between 2018 and 2024. Based on British Society for Haematology guidance, antibodies were classified as high risk (anti-D, anti-c, anti-K), intermediate risk (other specificities for which fetal assessment is proposed, e.g. anti-E, -C, -M, -Fya) or low risk (routine obstetric care or enzyme-only reactivity, e.g. Lewis, P1, Bg, Lutheran, Cw). High-risk and all other pregnancies were compared using Fisher's exact test.

Results: From 1962 newly detected antibodies, 184 pregnant women were identified. Of these, 36 (20%) had high-risk antibodies; 70 (38%) had intermediate-risk and 78 (42%) exclusively low-risk antibodies. Fetal or neonatal complications occurred in 13/27 (48%) high-risk pregnancies versus 5/88 (6%) in all others, and delivery before 37 weeks in 12/26 (46%) versus 9/81 (11%) (both $p < 0.001$); no complication in the low-risk group was plausibly antibody-mediated. In 45/108 pregnancies (42%), including 10/23 (43%) with high-risk antibodies (6 with complications), the antibody was first detected at our centre within one week before delivery, mostly due to late referral to our clinic. Anti-D remained the leading cause of severe HDFN (complications in 9/15, including hydrops fetalis). Anti-K (n = 5) caused the most severe courses, including one intrauterine fetal death; all 5 intrauterine transfusions were for anti-D or anti-K.

Conclusions: Only 20% of women with newly detected alloantibodies had high-risk antibodies (anti-D, -c, -K), yet these caused most complications and all severe courses, while 42% had only low-risk antibodies without antibody-related morbidity. Late detection mainly reflected late referral, underlining the need for early referral and transfer of antenatal antibody results. National obstetric guidance advises rescreening only RhD-negative women at 28 weeks, whereas transfusion guidance advises rescreening all women, acknowledging scarce evidence; harmonised, specificity-based recommendations deserve evaluation.

 Published under the CC license Attribution 4.0 International (CC BY 4.0)



Risk groups according to British Society for Haematology guidance (2025). High risk: anti-D, anti-c, anti-K. Intermediate risk: other specificities for which fetal assessment is proposed (e.g. anti-E, -C, -M, -Fya, -Jka). Low risk: routine obstetric care or no association with HDFN (e.g. Lewis, P1, Bg, Lutheran, Cw) or enzyme-only reactivity; panel A is coloured by specificity only. High risk vs all others: p<0.001 for each outcome (Fisher's exact test). DAT, direct antiglobulin test; HDFN, haemolytic disease of the fetus and newborn.

4588

Lupus Anticoagulant–Hypoprothrombinemia Syndrome: A laboratory diagnostic approach and frequency in 2499 patients

A. Aliotta (1), E. Matthey-Guirao (1), F. J. Gomez (1), L. Alberio (1), M. G. Zermatten (1)

Central Hematology Laboratory, Lausanne University Hospital - CHUV, Lausanne (1)

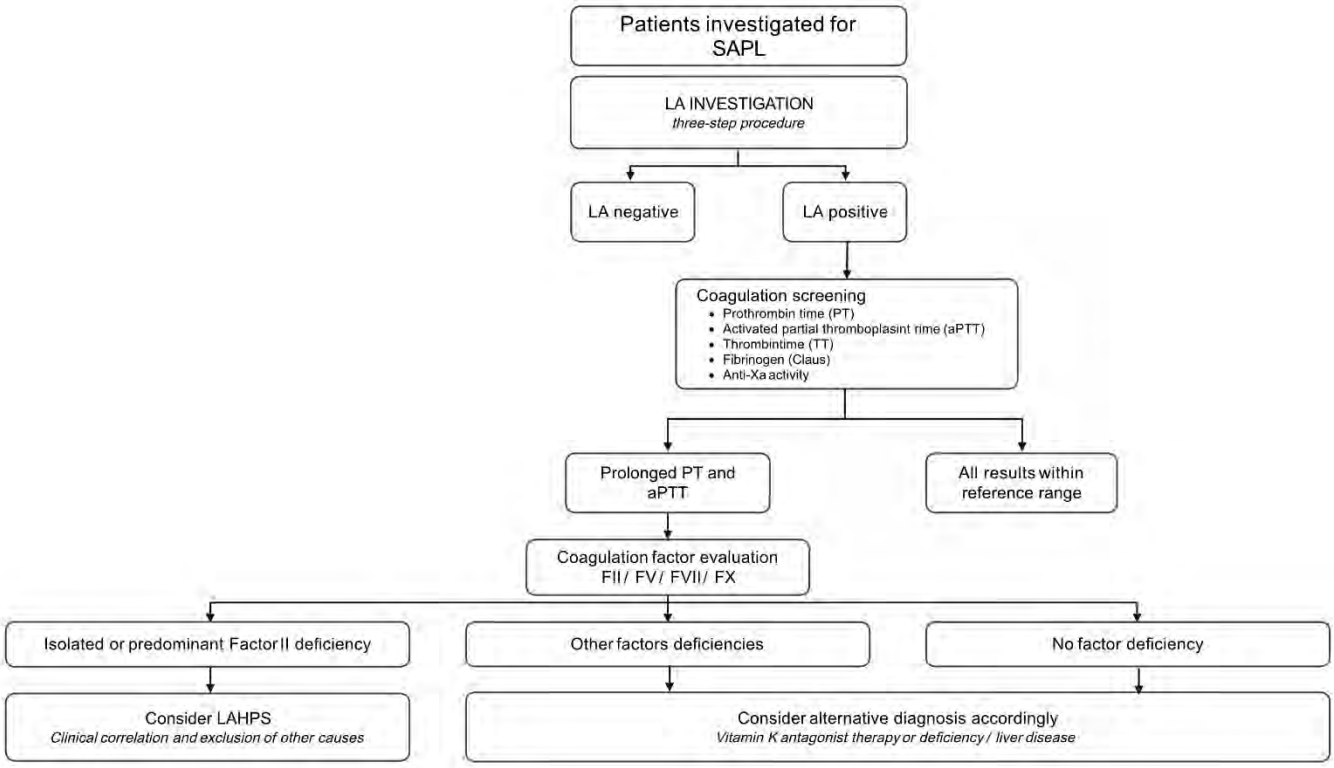
Introduction: Lupus anticoagulant–hypoprothrombinemia syndrome (LAHPS) is a rare, acquired bleeding disorder characterized by lupus anticoagulant (LA) associated with factor II deficiency. Its incidence in routine practice is unknown, and diagnosis is challenging because prolonged clotting times have multiple competing causes. We aimed to estimate the frequency of LAHPS among patients undergoing LA testing and to evaluate a practical stepwise laboratory approach for its recognition.

Methods: We retrospectively reviewed 2989 consecutive LA investigations corresponding to 2499 unique patients performed in a tertiary hemostasis laboratory. LA was screened by a lupus sensitive activated partial thromboplastin time, aPTT (PTT-LA) and a diluted Russel viper venom time, DRVVT assay (LA1/LA2). Patients with confirmed LA positivity were screened for concomitant prolongations of prothrombin time (PT) and routine aPTT. Potential anticoagulant interference, fibrinogen activity, and PT-mixing were assessed before performing targeted factor assays.

Results: LA was confirmed in 99 of 2499 patients (4.0%). Among these, 25 had concomitant PT and aPTT prolongation. Stepwise evaluation identified two patients with acquired factor II deficiency consistent with LAHPS, corresponding to an incidence of 0.8 per 1000 patients investigated and 2.0% among LA-positive patients. The diagnostic workflow distinguished LAHPS from more common causes of prolonged clotting times (VKA n = 14, anti-Xa anticoagulants n = 6, cirrhosis n = 1, LA interfering with PT n = 2) and restricted factor testing to selected patients with unexplained abnormalities.

Conclusions: LAHPS is rare in routine laboratory practice. In LA-positive patients, unexplained prolongation of both PT and aPTT should prompt exclusion of anticoagulant interference and other acquired causes, followed by targeted coagulation factor assays. This stepwise approach facilitates recognition of LAHPS while limiting unnecessary investigations.

Published under the CC license Attribution 4.0 International (CC BY 4.0)



2673

Effects of Dual Pathway Inhibition on blood clot properties

A. CASINI (1, 2), M. LAVERGNE (1), S. NOLLI (1), J.-L. RENY (1, 3), P. FONTANA (1, 2)

Geneva Platelet Group, Faculty of Medicine, University of Geneva, Geneva (1), Division of Angiology and Haemostasis, Geneva University Hospitals, Geneva (2), Division of General Internal Medicine, Geneva University Hospitals, Geneva (3)

Introduction: Patients with stable atherosclerotic vascular disease remain at risk of recurrent cardiovascular events. Dual pathway inhibition (DPI) with aspirin and low-dose rivaroxaban reduces this risk, but increases the risk of bleeding events. Interindividual variability in the biological response to DPI remains poorly understood and may contribute to differences in the balance between thrombotic and bleeding risks. We therefore aimed to identify whole-blood assays capable of detecting interindividual variability in clot properties during DPI.

Methods: Blood samples from 30 healthy donors were exposed in vitro to four conditions: control, aspirin (500 µM), rivaroxaban (40 ng/mL), or the combination (DPI). Three whole-blood assays assessed clot formation, contraction, and lysis: Whole Blood Thrombin Generation (WBTG), Whole Blood Thrombodynamics (WBTd), and Halo Fluorescence Fibrinolysis (HoFF), respectively. Assays were compared based on reproducibility and sensitivity to interindividual differences.

Results: All assays showed good reproducibility, with intra-assay coefficients of variation below 15% for the main parameters. WBTG showed that rivaroxaban and DPI, but not aspirin alone, significantly reduced thrombin generation compared to control: the amount of thrombin generated decreased by about 12%, thrombin peak decreased by 20%, and lag time increased by 167%. WBTd showed that aspirin, rivaroxaban, and DPI similarly reduced clot contraction extent (about 7%) and rate (about 8%) compared to control. Using the HoFF test, neither antithrombotic (alone or in combination) significantly affected fibrinolysis. WBTG showed the greatest interindividual variability, with a coefficient of variation of 33.8% for thrombin generation and 31.8% for thrombin peak.

Conclusions: These findings indicate that DPI exerts distinct effects on coagulation, with rivaroxaban modulating thrombin generation, and both agents affecting clot contraction, while fibrinolysis appears largely unaffected. WBTG showed the greatest reproducibility and sensitivity to interindividual differences in response to DPI. Therefore, WBTG appears to be the most suitable assay to explore interindividual variability in the biological response to DPI.

9779

Inter-individual variability of haemostatic correction in patients receiving emicizumab: Bleeding risk and implications for treatment monitoring

F. Monnin-Respen (1), A. P. Batista Mesquita Sauvage (1), F. J. Gomez (1), C. Pereira Portela (1), A. Aliotta (1), L. A. Gautier (1), D. Shehwar (1), K. Haeri (1), M. G. Zermatten (1), L. Alberio (1), D. Bertaggia Calderara (1)

Division of Hematology and Central Hematology Laboratory, Lausanne University Hospital (CHUV) and University of Lausanne (UNIL), Lausanne (1)

Introduction: Despite the good protection offered by emicizumab in haemophilia A (HA), some patients experience breakthrough bleeding. Routine tests are inadequate for monitoring emicizumab-induced haemostatic correction, as they normalize at subtherapeutic drug concentrations. Global-coagulation-assays have been proposed to assess emicizumab pharmacodynamics. We aimed to characterize individual thrombin generation (TG) profiles in patients on emicizumab prophylaxis and explore their relationship with steady-state drug concentrations and bleeding complications.

Methods: TG was assessed by calibrated-automated-thrombogram in platelet-poor-plasma from 11 patients with HA (mean age 51.5 years, range 23-78) including 7 with severe and 4 with

 Published under the CC license Attribution 4.0 International (CC BY 4.0)

moderate HA, in presence of 1 pM tissue-factor and 4 uM phospholipids. Samples were collected during annual follow-up visits on emicizumab prophylaxis. Plasma emicizumab concentration was measured using a modified one-stage assay.

Results: Mean steady state emicizumab concentration was 54±9 ug/mL, with no difference between severe and moderate HA patients. TG profiles varied markedly among individuals, with no correlation between emicizumab concentration and TG parameters (endogenous thrombin potential ETP, r = 0.23; peak height PH, r = 0.22), and were unexplained by coagulation factor activities. All severe HA patients had lower median TG parameters (ETP = 429 nM*min, p <0.0001; PH 26.9 nM, p = 0.001) compared to moderate HA patients (ETP = 831 nM*min; PH 42.2nM). No bleeding occurred in moderate HA. Two severe HA patients with low TG profiles had joint bleeding and a third one suspected joint microbleeds, although similar low TG values were observed in severe patients without bleeding. Patients with bleedings were older, had joints damage and started prophylaxis later in life than patients without documented bleeding.

Conclusions: There is an important inter-individual variability in the haemostatic response to similar levels of emicizumab. Despite a low TG profile, severe HA patients without additional risk factors appear to be protected against bleeding. In contrast, low TG seems to be insufficient to protect from bleeding older patients who had initiated prophylaxis later in life and had established damaged joints. In this context, TG assessment associated with clinical joint evaluation might be a useful complementary biomarker to support individualized treatment decision.

Table: Clinical Characteristics of patients with severe HA

Patients with spontaneous bleeding during Hemlibra® prophylaxis										
Patients	**Age (years)**	**Age at prophylaxis initiation (years)**	**Prophylaxis**	**Documented Joints damage**	**Score HEAD US (Year)**	**Score HJHS (Year)**	**Joint Prothesis**	**Available Joint Imaging data**	**Bleeding events**	**Physical activity**
P03	70	66	Hemlibra® since 2022 Previously rFVIII on demand	Yes, severe degradation Disabling arthropathy knees, ankles elbows	Not available	Not available	Yes (knee/ hip)	2022 CT: Left elbow hemarthrosis, bilateral hip/ankle arthropathy; bilateral TKA 2025 MRI: Severe destructive left elbow arthropathy	Occurred during occasional more intense physical activity	Light
P05	75	67	Hemlibra® since 2022 Between 2018 and 2022 rFVIII prophylaxis Previously rFVIII on demand	Yes, severe degradation	Not assessable because of multiple prothesis	Not available	Yes (bilateral knees and ankles)	2022 US: Elbow, resolving right hemarthrosis; bilateral chronic synovitis and severe osteochondral degeneration	Bleeding occurred using crutches	None
P09	59	37, Refacto 56, Hemlibra®	Hemlibra® since 2023 Previously prophylaxis low dose rFVIII (2 instead of 3 weekly injections as recommended)	Yes, severe degradation	23 (2026)	Not available	No		Suspected microbleeding with swollen elbow	None
Patients without spontaneous bleeding during Hemlibra ®prophylaxis										
P02	29	23	Hemlibra® since 2020 Previously rFVIII prohylaxis since childhood Between 2016 and 2020 on demand treatment with rFVIII	Absent	0 (2022) 0 (2026)	2 (2022)	No	2019 MRI: Left hip no evidence of hemarthrosis	None	Yes (only since Hemlibra®)
P06	27	Initiated in childhood	Hemlibra® from 2022 Previously rFVIII prophylaxis since childhood	Absent	Not available	Not available	No	2017 US: Left elbow hemarthrosis 2018 MRI: Left elbow, no synovial or cartilaginous abnormalities	None	Fitness since adolescence
P10	23	Initiated in childhood	Hemlibra® since 2020 Previously prophylaxis with rFVIII since childhood	Absent	0 (2021) 0 (2020) 0 (2024)	2 (2021)	No		None	Swimming 5/week
P11	78	64	Hemlibra® since 2024 Previously prophylaxis from 2012 with rFVIII	Present	Not assessable because of multiple prothesis	Not available	Yes, (bilateral knees and ankles; hip)		None	None

Abbreviations: CT, computed tomography; HEAD-US, Haemophilia Early Arthropathy Detection with ultrasound score (not assessable in patients with extensive joint prothesis; HJHS, Haemophilia Joint Health Score; MRI, magnetic resonance imaging; TKA, total knee arthroplasty; US, ultrasound

Published under the CC license Attribution 4.0 International (CC BY 4.0)

6249

Immunoassay Discordance in Heparin-Induced Thrombocytopenia Confirmed by Platelet-activation Assay: a 12-Year Retrospective Review

R. Nieves-Ortega (1), A. Aliotta (1), M. G. Zermatten (1), L. Alberio (1)

Hematology, Lausanne University Hospital, Lausanne (1)

Introduction: Diagnosis of heparin-induced thrombocytopenia (HIT) combines clinical pre-test probability with immunoassays (IAs) detecting anti-PF4/heparin antibodies, followed by confirmatory platelet-activation assays. Because IAs offer high sensitivity, a negative result is widely regarded as sufficient to rule out HIT. However, several reports have described rare cases of confirmed HIT despite negative IAs. This study aims to characterize the incidence of HIT confirmed by heparin-induced platelet activation assay (HIPA) and at least one negative IA.

Methods: We retrospectively reviewed all cases of suspected HIT analysed at our institution between May 2014 and September 2026. Pre-test probability of HIT was assessed with the 4T score. Testing for anti-PF4/heparin antibodies followed our institution's algorithm, sequentially performing a chemiluminescent IA (CLIA) and a particle gel IA (PaGIA). The latter was replaced by a latex immune-turbidimetric assay (LIA) from December 2021. All samples with a positive IA according to our in-house cut-offs (CLIA ≥0.33 U/ml, PaGIA titer ≥1 and/or LIA ≥0.7 U/ml) and/or a 4T score ≥6 underwent enzyme-linked immunosorbent assay (ELISA) testing and were sent to a reference laboratory for a confirmatory HIPA. We reviewed all cases with a positive HIPA and at least one negative IA (ELISA, CLIA, PaGIA and/or LIA).

Results: Of 4253 samples tested for suspected HIT, 771 (18.1%) underwent confirmatory platelet-activation testing, and 262 (6.2%) had HIT confirmed by a positive HIPA. Among HIPA-confirmed cases, 18 (6.9%) had at least one negative IA according to the manufacturer's cutoff: 9 with CLIA <1.0 U/mL, 12 with LIA <1.0 U/mL or a PaGIA titer <1 and 2 with a negative ELISA. Table 1 shows the distribution of IA profiles among these patients. No sample tested negative on all IAs. These 18 patients had a median age of 66 years, 9 (50%) were female, and the median 4T score was 4.5 (interquartile range 4 – 6).

Conclusions: A small but clinically relevant proportion of HIPA-confirmed HIT cases had at least one negative IA, although none tested negative across all of them. These findings support the use of complementary IAs in diagnostic algorithms to reduce the risk of false-negative results associated with reliance on a single IA.

CLIA	LIA/PaGIA	ELISA	n (%)
+	-	+	8 (44.4)
-	+	+	5 (27.8)
-	-	+	3 (16.7)
+	-	-	1 (5.6)
-	+	-	1 (5.6)

Table 1. Immunoassay profiles of the eighteen patients with HIPA-confirmed HIT and at least one negative immunoassay. *CLIA = chemiluminescent IA, LIA = latex immune-turbidimetric assay, PaGIA = particle gel immunoassay, ELISA = enzyme-linked immunosorbent assay.*

6195

Bivalirudin in heparin-induced thrombocytopenia: An analysis of 515 treatment days in 22 patients

T. Veyron (1), A. Valentin (2), E. Matthey-Guirao (1), F. J. Gomez (1), A. Aliotta (1), L. Alberio (1), M. G. Zermatten (1)

Service and Central Laboratory of Hematology, Lausanne University Hospital, Lausanne (1), VIB/AI, KU Leuven, Leuven (2)

Introduction: Bivalirudin is used to treat heparin-induced thrombocytopenia (HIT), particularly in patients with hepatic impairment or third-space fluid accumulation, but evidence on its efficacy remains limited.

Methods: We reviewed a case series of patients treated with bivalirudin for suspected HIT at a Swiss university hospital between 12.2021 and 05.2024. HIT was diagnosed using a published algorithm combining 4T score, anti-PF4/heparin immunoassays and the heparin-induced platelet aggregation assay (HIPA). Initial bivalirudin doses were 0.06, 0.04, and 0.02 mg/kg/h for estimated glomerular filtration rates (CKD-EPI) of >60, 30–60, and 15–30 mL/min, respectively. The target plasma concentration was 0.8–1.5 µg/mL, measured three hours after initiation or dose adjustment. Vitamin K antagonists (VKA) were started after platelet count recovery and overlapped for at least five days and continued until INR 3.0–4.0 on two consecutive days.

Results: Twenty-two patients (46% females; median age 64 years, IQR 52–69; Table 1) received bivalirudin for suspected HIT over 515 treatment days. HIT was confirmed in 19 (10 HIPA-positive; 9 on clinical/immunoassay criteria); 10 patients had HIT with thrombosis at presentation. Two patients had previously received argatroban, and three also received intravenous immunoglobulin. Platelet counts normalized after a median of 4 days; D-dimer levels also declined rapidly. Two patients (9.1%) developed thrombotic events during bivalirudin treatment (one pulmonary embolism after <24 hours; one radial artery occlusion after 18 treatment days). Five patients (22.7%) developed bleeding complications under treatment (two [9.1%] clinically relevant non-major bleedings; three [13.6%] major bleedings). Bivalirudin levels at bleeding were therapeutic (0.7–1.2 µg/mL). One patient died during bivalirudin therapy due to advanced cancer, and one underwent transhumeral amputation. Following transition to VKA, INR decreased by a median of 2.1 three hours after discontinuation of bivalirudin.

Conclusions: In this case series, bivalirudin treatment led to a rapid recovery in platelet count and a reduction in D-dimers. Two thrombotic events (9%) occurred during treatment. Bleeding complications (22.7%) were relatively low given the high-risk profile of HIT patients and occurred at therapeutic bivalirudin levels. Bivalirudin appears to be effective and relatively safe in patients with HIT.

 Published under the CC license Attribution 4.0 International (CC BY 4.0)

Patient characteristics	
Females, % (n/N)	46 (10/22)
Age, years; median (IQR; range)	64.0 (52–69; 34–84)
HIT diagnosis features	
4T score; median (IQR; range)	5.0 (4.0–6.0; 3–7)
CLIA, U/mL; median (IQR; range)	3.29 (0.68–10.64; 0–29.4)
PaGIA, titer; median (IQR; range)	16 (16–16; 16–16)
HIPA positive, n (%)	10 (45.5)
Type of HIT	
HIT without thrombosis, n (%)	9 (41)
HIT-T, n (%)	10 (45)
Treatments	
Bivalirudin only	19
Argatroban prior to bivalirudin	2
IVIG	3
Plasmapheresis	0
Bivalirudin treatment, days	515
Median duration (days)	18
IQR duration (days)	12; 31.5
Range duration (days, min; max)	5; 48
Complications under bivalirudin	
Arterial thromboembolic events, n (%)	1 (4.5)
Venous thromboembolic events, n (%)	1 (4.5)
Bleeding events, CRNMB, n (%)	2 (9.1)
Bleeding events, major, n (%)	3 (13.6)
Outcomes	
Limb amputation, n (%)	1 (4.5)
In-hospital mortality, n (%)	1 (4.5)

0462

In vivo pharmacological effects of apixaban and edoxaban in patients with liver cirrhosis

L. A. Gautier (1), C. Pereira Portela (1), D. Bertaggia Calderara (1), L. Veuthey (1), A. Aliotta (1), M. G. Zermatten (1), E. Mdawar-Bailly (2), S. Cuénoud (2), D. Moradpour (2), M. Fraga (2), L. Alberio (1)

Département médecine de laboratoire et pathologie (DMLP), Lausanne University Hospital, Lausanne (1), Département de médecine, service de gastroentérologie et hépatologie, Lausanne University Hospital, Lausanne (2)

Introduction: While several patients with liver cirrhosis (LC) require long-term anticoagulation because of atrial fibrillation or venous thromboembolism, data on direct oral anticoagulants (DOAC) remain limited. Here, we evaluated the pharmacological profiles of two DOAC in this population.

Methods: This monocentric clinical trial enrolled 47 non-anticoagulated patients with Child A (n = 36) and B (n = 11) LC, randomised to receive either apixaban 5 mg BID (n = 24) or edoxaban 60 mg OD (n = 23) for 7 days, and 16 control patients with Child A (n = 12) and B (n = 4) LC on long-term DOAC therapy without intervention. Pharmacokinetic and pharmacodynamic parameters were measured at day (d)1, 3, 8, and 9. Preliminary results include DOAC peak and trough concentrations, ex vivo thrombin generation (TG) parameters, and in vivo markers of coagulation (prothrombin fragments 1+2 [F1+2], thrombin–antithrombin complexes [TAT], D-dimers [DD]).

Results: The interventional cohort included 70% male patients, all with preserved renal function. 55% were thrombocytopenic (median platelet count 127 G/L). DOAC concentrations exhibited distinct profiles, with median peak and trough levels of 158 and 97 ng/mL for apixaban, and 204 and 17 ng/mL for edoxaban, respectively. At d8, 45% of the participants taking apixaban had very low trough levels below the 10th percentile of patients without LC [1], a finding also observed in 30% of the patients with LC receiving long-term anticoagulation. No patient had trough concentrations above the values observed in patients without LC [1]. Ex vivo TG parameters changed in line with DOAC levels ($p < 0.0001$). At d8, F1+2 and DD were significantly decreased (-32% and -29%, respectively; $p < 0.05$). F1+2 and DD decreased by 30% and 32% with edoxaban ($p < 0.01$ and $p = 0.17$), and 32% and 23% with apixaban ($p < 0.001$ and $p < 0.05$). Patients with thrombocytopenia exhibited less DD reduction compared to those without (6% versus 37%; $p < 0.05$) (Figure 1), a similar trend was shown between Child A and B (33% versus 7% reduction, $p = 0.06$).

Conclusions: Edoxaban showed higher peak and lower trough levels than apixaban. Based on F1+2 and DD, both DOAC appeared effective in patients with LC. Noteworthy, thrombocytopenia and LC severity seem to correlate with a lower DD reduction, suggesting a possible differential anticoagulant efficacy.

[1] de Vries et al. Thromb Haemost 2025;125:563–573.

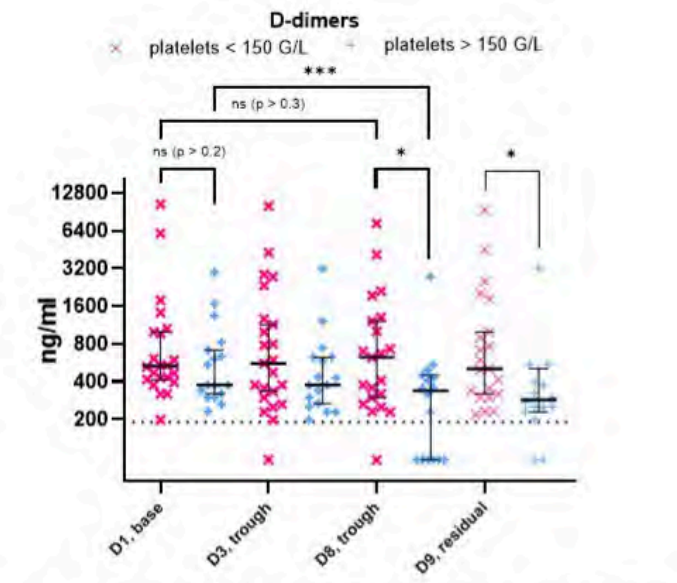


Figure 1. Anticoagulant effect assessed by D-dimer levels according to platelet levels during anticoagulant treatment; median with 95% confidence interval, ns: p>0.05, *: 0.01<p<0.05, **: 0.001<p<0.01. D: day

4555

Predicting the need for a second collection day in allogeneic peripheral blood stem cell donation

M. Baldenweg (1), E. Mathier (2), A. Bachofner (3), P. Hockl (3), D. Schneidawind (3), T. Benoit (3)

Faculty of Medicine, University Zürich, Zurich (1), Department of Biosystems Science and Engineering, ETH Zurich, Basel (2), Department of Medical Oncology and Haematology, University Hospital Zurich, Zurich (3)

Introduction: Most healthy allogeneic peripheral blood stem cell donors achieve the collection target in a single apheresis, although all are commonly scheduled for two collection days at our institution. We aimed to determine whether the need for a second collection day can be predicted early enough to support apheresis capacity planning.

Methods: We retrospectively analysed 366 allogeneic stem cell donors undergoing peripheral blood stem cell collection between 2020 and 2024. Donors were grouped according to the actual number of apheresis days performed; the collection target was ≥4.0 × 10^6 $CD34^+$ cells/kg recipient body weight. Demographic, donor/recipient, laboratory and collection parameters were evaluated using univariable and multivariable Firth-

 Published under the CC license Attribution 4.0 International (CC BY 4.0)

penalised logistic regression. Predictive performance was assessed by the area under the receiver operating characteristic curve (AUC).

Results: 350/366 donors (95.6%) completed collection in one day, while 16 (4.4%) required more than one collection day. Pre-apheresis CD34⁺ concentration in peripheral blood after G-CSF mobilisation was strongly associated with collection outcome and alone discriminated single-day from multi-day collection with an AUC of 0.98 (95% CI 0.95–0.99). Importantly, donor characteristics available at baseline also carried predictive information: in univariable analysis, female sex, shorter donor height and a lower donor/recipient weight ratio were associated with multi-day collection. A multivariable model excluding pre-apheresis CD34⁺ achieved a cross-validated AUC of 0.89 (95% CI 0.81–0.97), suggesting that the risk of requiring a second collection day may be estimated before the morning-of-collection CD34⁺ result is available.

Conclusions: Although pre-apheresis CD34⁺ concentration in peripheral blood after G-CSF mobilisation remains the strongest predictor of single-day collection, donor and recipient characteristics available at baseline may enable earlier identification of donors at risk of requiring a second collection day. Such prediction could support more efficient apheresis capacity planning and reduce the need to schedule every allogeneic peripheral blood stem cell donation for two collection days. Prospective validation is warranted before implementation in clinical practice.

2877

Recurrent venous thromboembolism in patients with hereditary and acquired thrombophilia after discontinuing anticoagulation – a systematic review and meta-analysis

K. Vrotniakaite-Bajerciene (1), T.-F. Wang (2), E. Sabri (2), A. Angelillo-Scherrer (1), G. Le Gal (2), M. Carrier (2)

Department of Hematology and Central Hematology Laboratory, Inselspital, Bern (1), Department of General Internal Medicine, Ottawa Hospital Research Institute, Ottawa (2)

Introduction: The role of thrombophilia in clinical decision making regarding secondary venous thromboembolism (VTE) prevention is still uncertain. We aimed to investigate the associations between hereditary and acquired thrombophilia and recurrent VTE after discontinuation of anticoagulation following initial VTE treatment.

Methods: A systematic review and meta-analysis was conducted to evaluate the risk of recurrent VTE in patients with and without thrombophilia including factor V Leiden (FVL) mutation, prothrombin gene G20210A mutation (PTM), antithrombin, protein C, protein S deficiencies (ATD, PCD, PSD), and antiphospholipid antibody syndrome (APS). Eligible studies included randomized trials and cohort studies reporting recurrent VTE after discontinuing anticoagulation following completion of initial VTE treatment. Study-level incidence rates (IR) per 100 patient-years, incidence rate ratios (IRR), and adjusted hazard ratio (aHR) were calculated or extracted and pooled using random-effects models. Certainty of evidence was assessed using the Grading of Recommendations, Assessment, Development and Evaluation (GRADE) approach.

Results: Fifty-one studies (n = 34,623 patients; 42.3% female; 33.5% with unprovoked index VTE) were included. Overall, 9,270 patients (26.8%) had at least one thrombophilia. Patients with APS, compound heterozygous FVL/PTM, and homozygous FVL mutation had the highest rates of recurrent VTE after stopping anticoagulation, with IR of 11.9 (95% CI 8.4–16.9, I2 = 59%), 8.6 (95% CI 5.9–12.6, I2 = 74%), and 8.5 (95% CI 4.8–15.1, I2 = 37%) per 100 person-years, respectively, compared to 4.2 (95% CI 3.6–4.9, I2 = 95%) per 100 person-years among patients without thrombophilia (Table 1). High-risk thrombophilias, including APS, ATD, PCD, homozygous FVL, and compound heterozygous FVL/PTM were associated with an approximately 2-3-fold increased risk of recurrent VTE, whereas low-risk thrombophilias (FVL or PTM), were associated with an approximately 50% increased risk (Figure 1). Heterogeneity and the certainty of evidence was predominantly moderate. Evidence regarding PSD was inconclusive.

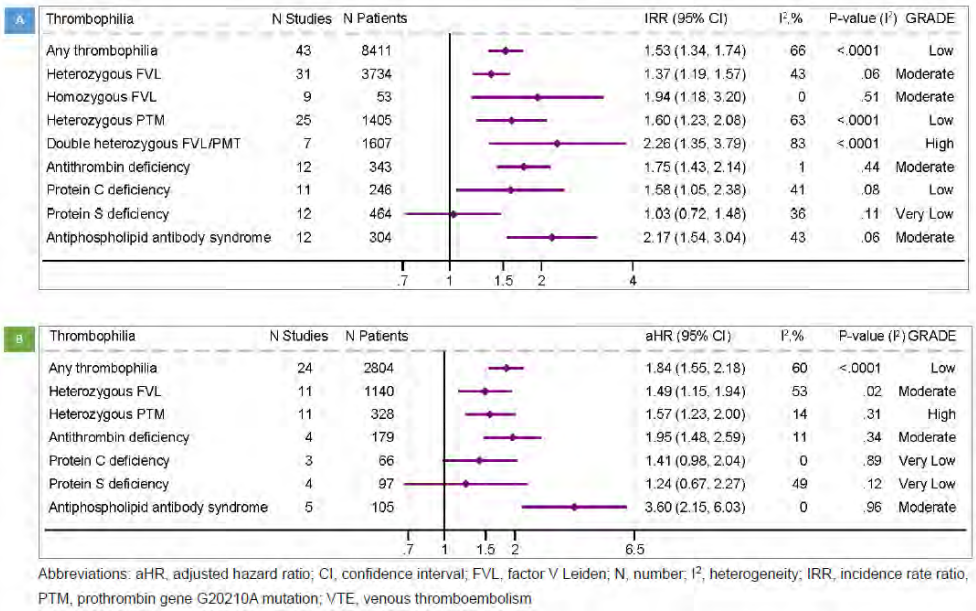
Table 1. Incidence rates of recurrent venous thromboembolism per 100 patient-years in patients with and without thrombophilia after discontinuing anticoagulation

Type of Thrombophilia	N Studies	N Patients	Incidence rate per 100 patient-years (95% CI)	I^2, %	P-value I^2
No thrombophilia	43	20941	4.2 (3.6 – 4.9)	95	<.0001
Any thrombophilia	49	9063	6.8 (5.8 – 7.8)	88	<.0001
Heterozygous FVL mutation	34	3909	6.5 (5.2 – 8.0)	87	<.0001
Homozygous FVL mutation	11	97	8.5 (4.8 – 15.1)	37	0.10
Heterozygous PTM mutation	27	1433	6.7 (5.1 – 8.8)	73	<.0001
Homozygous PTM mutation	2	19	6.7 (3.2 – 14.0)	0	0.64
Double heterozygous FVL/PTM mutation	8	1635	8.6 (5.9 – 12.6)	74	0.003
Antithrombin deficiency	15	387	7.9 (6.1 – 10.2)	41	0.05
Protein C deficiency	14	340	6.5 (5.0 – 8.4)	24	0.19
Protein S deficiency	15	569	5.9 (4.9 – 7.2)	6	0.38
Antiphospholipid antibody syndrome	12	304	11.9 (8.4 – 16.9)	59	0.005

Abbreviations: CI, confidence interval; FVL, factor V Leiden; I^2 – heterogeneity; N, number; PTM, prothrombin gene G20210A mutation

Conclusions: Both hereditary and acquired thrombophilia are associated with an increased risk of recurrent VTE after discontinuation of anticoagulation. The derived prognostic estimates can help individualize risk assessment of recurrent VTE and support shared decision-making regarding extended anticoagulation.

Figure 1. IRR (A) and aHR (B) of recurrent VTE, thrombophilia vs. no-thrombophilia



Abbreviations: aHR, adjusted hazard ratio; CI, confidence interval; FVL, factor V Leiden; N, number; I^2, heterogeneity; IRR, incidence rate ratio, PTM, prothrombin gene G20210A mutation; VTE, venous thromboembolism

Published under the CC license Attribution 4.0 International (CC BY 4.0)

SSH/SSMO POSTER PRESENTATION - EXPERIMENTAL HEMATOLOGY / ONCOLOGY

7001

Tissue-specific partial reprogramming in the aged hematopoietic compartment

A. Alonso Calleja (1), A. Jimenez Sanchez (1), C. Bataclan (1, 2), F. Schyrr (1), S. Ferreira Lopes (1), T. Smirnova (3), K. Kioseoglou (1), M. C. Galavotti (1), G. Desdín-Mico (1), O. Naveiras (1, 3, 4)

Department of Biomedical Sciences, University of Lausanne, Lausanne (1), School of Life Sciences, Ecole Polytechnique Fédérale de Lausanne, Lausanne (2), Hematology Service, Departments of Clinical Oncology and Laboratory Medicine and Pathology, Cantonal University Hospital of Lausanne, Lausanne (3), Department of Fundamental Oncology, University of Lausanne, Lausanne (4)

Introduction: Haematopoietic stem and progenitor cells (HSPCs) self-renew and generate all blood lineages, but aging impairs their regenerative capacities, limiting their clonal output. Transient in vivo expression of the Yamanaka factors (Oct4, Sox2, Klf4, and c-Myc; collectively OSKM or 4F) induces partial reprogramming (PR), a molecular program which has been shown to rejuvenate multiple tissues. The cell-autonomous impact of PR in HSPCs remains unexplored due to lack of an HSPC-specific model. We hypothesised that in vivo PR restores HSPC regenerative capacity, and generated two doxycycline-inducible, Vav1-driven mouse models (4FVav1 and 4F3Vav1) to study transient PR in the hematopoietic compartment.

Methods: Following toxicity and safety assays, we established a PR protocol for the haematopoietic system to evaluate its short-term effects in both young and aged mice. Both strains and controls (4F) were subjected to this regimen. We performed comprehensive molecular and functional characterisation, including single-cell RNA sequencing (scRNA-seq) for HSPCs from bone marrow (BM) and immune cells from spleen (SP), complete blood counts (CBC), colony-forming unit (CFU) assays and competitive transplantation.

Results: The protocol has no signs of haematopoietic neoplasia, although excessive cycles caused teratomas in 4F3Vav1 mice. In the PR cohort, a total of 52,106 cells for BM and 41,360 for SP were annotated to major progenitor and immune cell populations. Our analysis demonstrated that both strains reached a similar level of PR (defined by the co-expression of Sox2 and Klf4) in the BM (~25%) and no expression in the SP (<1%). Mainly HSPCs were reprogrammed, while mature immune cells were found resistant to reprogramming. Furthermore, PR induced a transient increase in immunophenotypic hematopoietic progenitor populations in BM. PR transiently reduced platelets and enhanced CFU potential in vitro and clonal output in vivo. Long-term assessment following consecutive PR cycles revealed recovery of platelet counts and restoration of the HSPC compartment upon doxycycline withdrawal, accompanied by enhanced activity of more primitive progenitor populations.

Conclusions: In summary, both models achieved HSPC-specific PR, boosting progenitor activity without malignant transformation.

0387

The CD19 CAR T Hinge Region Influences Avidity and Cytotoxicity in CD19 SNP Variants in B-cell Lymphoma

L. Hörtensteiner (1, 2, 3), H. Mandhair (1, 2), S. Fischer (1), K. Seipel (1), F. S. Krebs (4, 5), V. Zoete (4, 5), U. Novak (1, 2), T. Pabst (2), M. Wehrli (1, 2)

DBMR, University of Bern, Bern (1), Medical Oncology, Inselspital, Bern (2), Cell Biology, Graduate School of Cellular and Biomedical Sciences, Bern (3), Department of Fundamental Oncology, University of Lausanne, Lausanne (4), Molecular Modelling Group, Swiss Institute of Bioinformatics, Lausanne (5)

Introduction: Outcomes after CD19-directed chimeric antigen receptor (CAR) T-cell therapy in relapsed/refractory diffuse large B-cell lymphoma (DLBCL) are heterogeneous, and no biomarker guides the choice between products. The germline CD19 polymorphism rs2904880, encoding Val174 (V174) or Leu174 (L174), has been linked to differential responses to FMC63-based CAR T cells. We investigated how the CAR hinge architecture modulates the interaction with CD19 variants and how this relates to clinical outcomes.

Methods: We modelled the FMC63-CD19 complex in silico (PDB 7URV) and quantified CD19 surface expression on B-cell lymphoma lines carrying V174/V174 or V174/L174. Two FMC63-based CARs differing only in the hinge domain (CD8 vs CD28) were compared for proliferation, cytotoxicity (Incucyte and luciferase-based) and avidity (z-Movi). We further analysed a single-center retrospective cohort of 91 patients with r/r DLBCL, stratified by CD19 genotype and CAR product.

Results: In silico, L174 induced distinct conformational changes and additional hydrophobic contacts within the FMC63-CD19 interface. CD19 surface expression was higher in V174/L174 than in V174/V174 cells. Both constructs proliferated similarly. Cytotoxicity against V174/V174 targets was comparable, whereas the CD28-hinge CAR killed V174/L174 cells more efficiently. Avidity was overall higher for the CD8-hinge CAR, with stronger binding to V174/V174 than to V174/L174 despite lower CD19 expression, consistent with an inverse relationship between very high avidity and optimal cytotoxicity. Clinically, V174/V174 patients had inferior overall survival compared with V174/L174 carriers. Among V174/V174 patients, axi-cel (CD28 hinge/transmembrane) was associated with longer survival than tisa-cel, whereas V174/L174 carriers tended to do better with tisa-cel.

Conclusions: A single germline amino acid change in CD19 reshapes the CAR-target interface, and the hinge domain determines how the CAR handles it. Very high avidity is not the same as better killing, which has direct consequences for CAR design. The genotype-dependent differences between axi-cel and tisa-cel suggest that CD19 genotyping may help guide product selection and warrant prospective validation.

 Published under the CC license Attribution 4.0 International (CC BY 4.0)

5635

T cell receptor repertoire architecture and benefit from immune checkpoint inhibition

C. Schultheiss (1), L. Braun (2), P. Schmidt-Barbo (3), M. Kalweit (4), A. Stein (5), R. Zeiser (2), M. Binder (6)

Medical Oncology, University Hospital Basel, Basel (1), Department of Hematology, Oncology and Stem Cell Transplantation, University Medical Center Freiburg, Freiburg (2), Department Biomedicine, University Hospital Basel, Basel (3), Department of Computer Science, University of Freiburg, Freiburg (4), University Cancer Center Hamburg (UCCH), Hematology-Oncology Practice Eppendorf (HOPE), Hamburg (5), Medical Oncology, University of Basel, Basel (6)

Introduction: Immune checkpoint blockade (ICB) is a therapeutic mainstay across cancers, yet only 10-15% of patients achieve durable benefit. T cell dysfunction contributes to resistance and we still lack reliable biomarkers informing on T cell functionality and outcome under ICB. The only routinely used biomarker is tumor PD-L1 positivity (CPS score) that has shown insufficient reliability for individual treatment decisions. Building on trial-specific links between peripheral T cell receptor (TCR) architecture and outcome, we set out to determine reproducible benefit-associated features across four prospective ICB trials and tested their relationship with tumor control in a transplanted mouse model.

Methods: We analysed blood TCR repertoires from 266 patients with metastatic gastrointestinal or head and neck cancer in AVETUX, RAP, INTEGA, and FOCUS. TRB sequencing covered 226 baseline and 155 pre-cycle 2 samples. Metrics included richness, clonality, Shannon diversity, V/D/J usage, CDR3 length and Kidera factors. Benefit was primarily overall survival at or above the trial median. Progression-free survival or response was used when follow-up was insufficient. Logistic-regression and random-forest classifiers combined repertoire metrics with top-n clonotype features using a stratified 75/25 split and three-fold cross-validation. In a syngeneic MC38 model, serial blood and endpoint tissue TCR repertoires were related to tumor burden after anti-PD-1 or control treatment.

Results: Across all cohorts, richness was lower in patients than age-matched healthy donors. Pooled clonality remained stable on treatment, whereas richness increased. Patients with favorable outcomes had higher baseline richness (median 1,434 vs 1,199), and only this group increased during cycle 1. The association was reproduced across all trials. Richness alone yielded an AUC of 0.64. Full repertoire composition using a random forest and the top 10 clonotypes improved held-out AUC to 0.74 versus approximately 0.60 for CPS (pan-cancer, n = 1,267). Anti-PD-1 slowed MC38 growth. Intratumoral richness inversely correlated with endpoint tumor weight in control.

Conclusions: Peripheral TCR architecture was reproducibly associated with ICB benefit and full repertoire composition outperformed CPS and richness alone. Serial blood analysis may provide clinically relevant predictive information on the effector compartment.

8223

Combined heterozygous RAG1/RAG2 mutations are linked to immunodeficiency and loss of tolerance

A. J. Jauch (1), O. Bignucolo (2), M. Bosticardo (3), F. Pala (3), O. Delmonte (3), M. Dölz (4), M. Ghraichy (5), B. Meyer (6), R. Higgins (7), A. Ghosh (7), I. Heijnen (8), J. Dirks (6), V. von Niederhäusern (9), F. Baldin (10), F. Maquardsen (10), U. Boglarka (11), K. Csomos (11), M. Talib (11), J. Trück (9), L. Jörg (12), A. MacPherson (13), J. R. Passweg (6), J. Halter (6), W. V. Bonilla (14), K. S. Lang (15), C. T. Berger (16), A. Navarini (17), A. Oxenius (18), C. Hess (19), J. E. Walter (11), L. D. Notarangelo (3), M. Recher (10)

Department of Haematology and Immunodeficiency Laboratory, Department of Biomedicine, University Hospital Basel, Basel (1), Swiss Institute of Bioinformatics, SIB and miri dynamics, Lausanne and Basel (2), National Institutes of Health, Laboratory of Clinical Immunology and Microbiology, National Institute of Allergy and Infectious Diseases, Bethesda, MD 20892, USA (3), Department of Biomedicine, Molecular Immune Regulation Laboratory, Basel (4), Division of Immunology, University Children's Hospital, University of Zurichand Children's Research Center, Zürich (5), Department of Haematology, University Hospital Basel, Basel (6), Division of Dermatology and Dermatology Laboratory, Department of Biomedicine, University Hospital Zurich, Zürich (7), Division of Medical Immunology, Laboratory Medicine, University Hospital Basel, Basel (8), Division of Immunology and Children's Research Center, Universitäts- Kinderspital Zürich, Zürich (9), Immunodeficiency Laboratory, Department of Biomedicine and University Center for Immunology, University Hospital Basel, Basel (10), Johns Hopkins All Children's Hospital, University of South Florida, Saint Petersburg, FL (11), Division of Allergology and Clinical Immunology, Inselspital, Bern (12), Department of Visceral Surgery and Medicine and Maurice Müller Laboratories, Department for Biomedical Research, Inselspital, Bern (13), Division of Experimental Virology, Department Biomedicine, University Hospital Basel, Basel (14), Institute of Immunology, University of Duisburg-Essen, Duisburg (15), Translational Immunology, Department of Biomedicine, University Hospital Basel, Basel (16), Division of Dermatology and Dermatology Laboratory, Department of Biomedicine, University Hospital Basel, Basel (17), Institute of Microbiology, ETH, Zürich (18), Immunobiology Laboratory, Department of Biomedicine, University Hospital Basel, Basel (19)

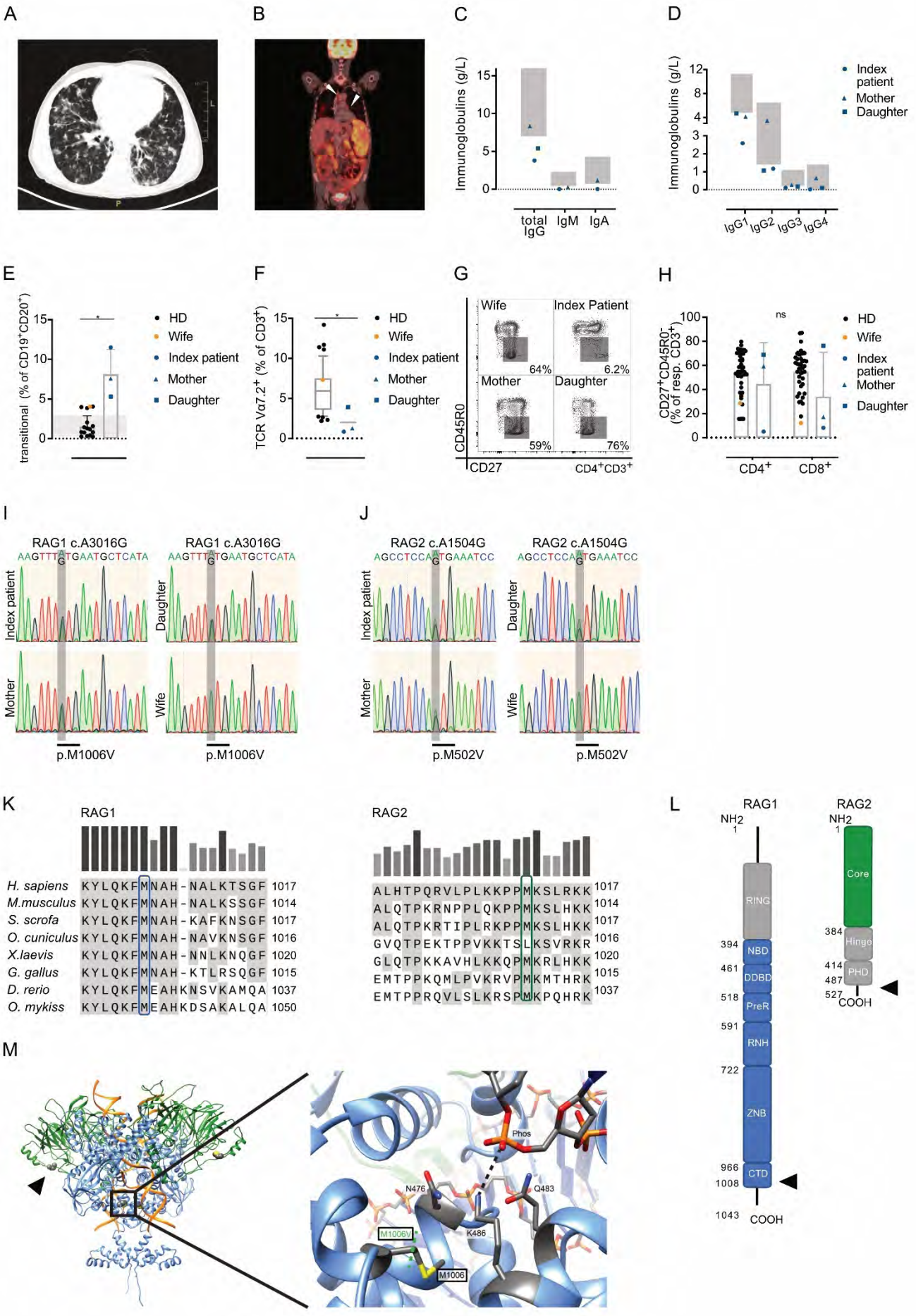
Introduction: Recombination-activating genes 1 and 2 (RAG1/2) are essential for V(D)J recombination, which generates the diverse repertoire of B- and T-cell receptors. Patients harboring homozygous or combined heterozygous hypomorphic RAG1 and/or RAG2 mutations suffer from variable immunodeficiencies, including severe combined immunodeficiency (SCID), Omenn syndrome, and combined immunodeficiency with granulomas and/or autoimmunity (CID-G/AI). While homozygous or compound heterozygous RAG mutations are well-studied, the effects of combined heterozygous mutations remain not understood.

Methods: Here we describe three individuals from the same Caucasian family carrying double heterozygosity for two missense mutations in the RAG1 and RAG2 genes.

To examine the in vivo impact of single or double heterozygous mutations in the RAG1/2 genes, we characterized two mouse models carrying a hypomorphic missense mutation in Rag1 (RAG1mut) or Rag2 (RAG2mut) with regard to their impact on the lymphocyte development, the T cell repertoire composition, the capacity to respond to lymphocytic choriomeningitis virus (LCMV) infection and the infection-induced immune dysregulation

Results: One of the three individuals suffered from a complicated form of CID ultimately requiring allogeneic bone marrow transplantation, while the other individuals were clinically more silent but shared some of the phenotypical immune dysregulations. We demonstrate that decreasing RAG functionality by 40% seen in mice with double heterozygous Rag1/2 mutations leads to alterations in lymphocyte development, the T cell receptor repertoire and the adaptive immune response towards virus infection. Several manifestations of immune-dysregulation observed in the double heterozygous Rag mutant mice

 Published under the CC license Attribution 4.0 International (CC BY 4.0)



Published under the CC license Attribution 4.0 International (CC BY 4.0)

were mirrored in the human patients carrying two heterozygous RAG1/RAG2 mutations.

Conclusions: This study for the first time documents an additive-immunodeficiency and immune-dysregulation associated with combined heterozygous RAG1/RAG2 hypomorphic mutations.

Figure 1: Qualitative changes in the B cell and T cell compartments in patients carrying two heterozygous mutations in *RAG1* and *RAG2*. (A) Computer tomography (CT) scan of the index patient, axial plane of the chest. The representative scan displays bronchiectasis, nodules, and ground-glass changes. (B) Positron emission tomography (PET)-CT scan coronal plane of the index patient, documented bi-pulmonary consolidations with metabolic activity and mediastinal/hilar lymphadenopathy (white arrows) as well as splenomegaly. Wall thickening of the ascending colon. (C and D) Immunoglobulin measurements in the three patients (gray box indicates the respective in-house reference range). (E) Transitional B cells (CD38+IgM+IgD+) were enumerated within the B cell population by flow cytometry. Gray indicates the in-house reference range of healthy donors (HD). (F) Assessment of the proportion of peripheral blood T cells expressing the TCR Va7.2, healthy controls and CID patients (combined immunodeficiency) were partially already published (Jauch et al., 2023) (G) Representative flow cytometric contour plots of naïve CD4+ T cells (CD27+CD45R0-, gray box). The number next to the box indicates the percentage within the CD4+CD3+ cell population. (H) Enumeration of naïve CD4+ and CD8+ T cells in the index patient, his mother, his daughter and the healthy wife. Sanger sequencing confirmed the heterozygous missense mutation in (I) recombination-activating gene 1 (*RAG1*) and (J) *RAG2* in the three patients. Heterozygosity is seen as superimposed peaks in the chromatogram. (K) Multiple protein alignment for RAG1 resp. RAG2 from different vertebrates. (L) Schematic illustration of the human RAG1 and RAG2 proteins. The two mutations are indicated with black arrows. The catalytic core domain is colored in blue for RAG1 and green for RAG2. Amino acid numbers refer to19. CTD (carboxy-terminal domain), DDBD (dimerization and DNA-binding domain), NBD (nonamer-binding domain), PHD (plant homeodomain domain), preR (pre-RNase H), RING (really interesting new gene, zinc-finger domain), RNH (catalytic RNase H). (M) Molecular representation of the structure of the human RAG1-RAG2 heterotetramer in ribbons bound to DNA. Blue colored ribbons represent RAG1 (AA338-1010, the structure was constructed with SWISS-MODEL20), green represents RAG2 (AA1-527 , the structure was constructed using the ROBETTA algorithm21) and orange highlights the DNA helix. In RAG2 the M502 is indicated by a black arrow. The zoom-in view for RAG1 indicates the proximity of M1006 to K486 and the DNA (phosphate). The green dashed line represents the limit of a much smaller Val side-chain at position 1006. By the residual change to M1006V, the interaction between K486 and the DNA might be destabilized. Significance was computed with a non-parametric Mann-Whitney test in (f) and with multiple comparison correction for (g/h/i).

6113

ASPP2κ uncouples PD-L1 expression from interferon-driven T cell recruitment in triple-negative breast cancer - a candidate mechanism of primary checkpoint resistance

K. M. Kampa-Schittenhelm (1), C. Wincek (1), A. Ruiba (1), W. Liu (1), K. Jahankhani (1), S. Kembu Chettiar Ravichandran (1), B. Ludewig (2), W. Jochum (3), M. M. Schittenhelm (1)

Medical Oncology and Hematology, Cantonal Hospital St. Gallen, St. Gallen (1), MFZ, Cantonal Hospital St. Gallen, St. Gallen (2), Pathology, Cantonal Hospital St. Gallen, St. Gallen (3)

Introduction: Immune checkpoint blockade is the only approved immunotherapy in metastatic TNBC and is restricted to PD-L1-positive tumours, yet most of these patients derive no durable benefit, while in the early setting benefit is independent of PD-L1. What underlies primary resistance in the PD-L1-positive group is unknown. We have identified ASPP2κ, an oncogenic splice variant of the tumor suppressor ASPP2 that is C-terminally truncated, lacking important interaction domains. ASPP2κ is expressed in tumor but not in healthy tissue promoting tumor progression and drug resistance. We here demonstrate that ASPP2κ expression shapes the tumor immune microenvironment of TNBC and specifically, that it dissociates PD-L1 expression from the interferon-driven recruitment of cytotoxic T cells.

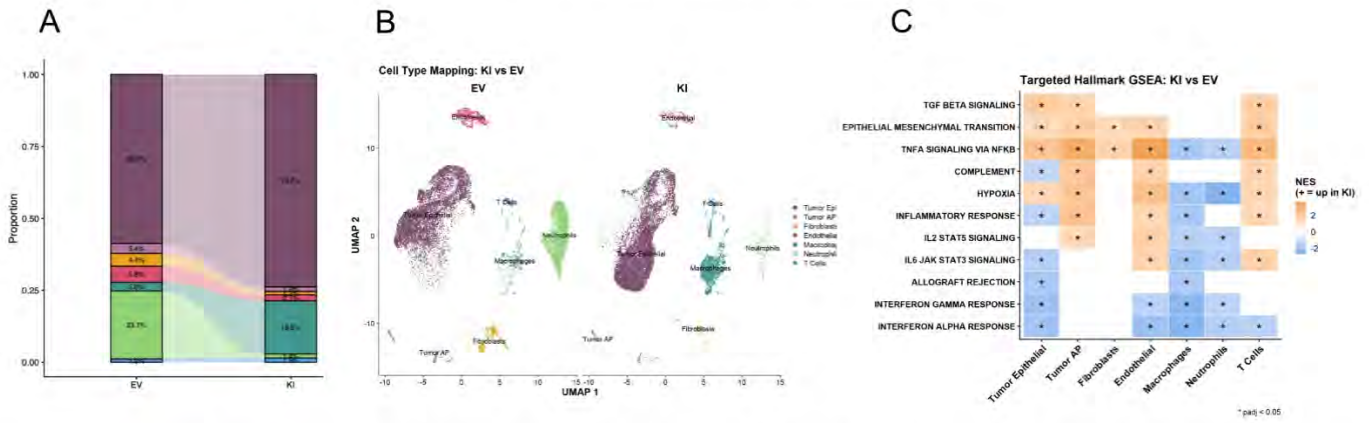
Methods: ASPP2κ expression was quantified by isoform-specific qRT-PCR in native TNBC and healthy breast tissue (n = 75). NSG ASPP2κ-knockdown and immune-competent 4T1 TNBC mouse models were generated. Bulk RNA-seq was performed on ASPP2κ-KD vs. control cells and tumors derived from the 4T1 model were analysed by single-cell RNA-seq, flow cytometry, immunohistochemistry and serum cytokine arrays.

Results: ASPP2κ is highly expressed in TNBC, with no meaningful expression in healthy tissue. Bulk and sc. RNA-seq identified PD-L1 (CD274) as ASPP2κ-dependent together with a PI3K/AKT signature; in vitro and ex vivo analyses confirmed this regulation to be tumor cell-intrinsic and interferon-independent. In vivo, ASPP2κ-expressing tumors presented with elevated PD-L1 and loss of interferon-driven, T cell-recruiting signalling: IFN-γ, TNF-α and the CXCR3 ligands CXCL9/10/11 were suppressed. Granulocytic cells were largely lost, tumour-associated macrophages expanded, T cells were present but exhausted, and MCP-1/CCL2 was induced.

Conclusions: ASPP2κ generates a PD-L1-high but immune-excluded state in which PD-L1 is elevated without an interferon response. This distinguishes it from adaptive immune resistance and identifies oncogene-driven, innate resistance. Tumors carrying this configuration would be expected to be refractory to checkpoint blockade while still meeting the biomarker criterion applied in the clinic. Since ASPP2κ is present specifically in tumors, expression of ASPP2κ is both, a candidate for stratification within the PD-L1-positive population and a potential therapeutic target.

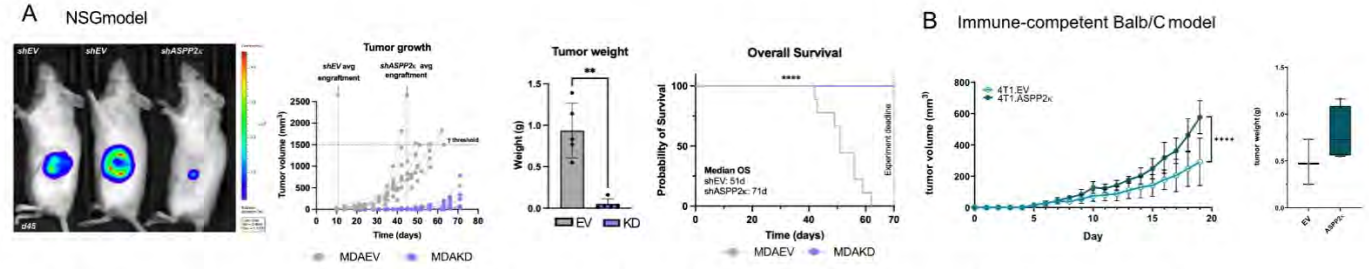
 Published under the CC license Attribution 4.0 International (CC BY 4.0)

Figure 1 Expression of ASPP2κ reshapes the tumor immune microenvironment



ASPP2κ reshapes the tumor immune microenvironment (scRNA-seq 4T1_ASPP2κ_KI vs. EV, BALB/c, day 20). (A) Relative abundance of the annotated cell populations in EV and KI tumors, showing loss of the granulocytic compartment and expansion of macrophages in ASPP2κ-expressing tumors. (B) UMAP embedding of all cells, split by genotype, with the seven annotated populations color-coded. (C) Targeted hallmark GSEA (KI vs. EV) per cell population. Normalized enrichment score, orange indicates upregulation in KI. Asterisks mark adjusted $p < 0.05$. Note the loss of interferon-α and interferon-γ response signatures alongside enrichment of EMT and TNFA/NF-κB signaling (*unpublished*)

Figure 2 Expression of ASPP2κ promotes tumor growth in independent mouse models



In vivo modeling. (A) Xenotransplantation of MDA-MB-231 ASPP2k-knockdown (KD) cells into a NSG mouse model. *(A.1)* Representative IVIS imaging of tumor engraftment in a total of 18 mice. *(A.2)* Tumor growth, tumor weight *(A.3) and (A.4)* overall survival (OS), according to ASPP2k expression. (B) Orthotopic transplantation of ASPP2k overexpressing murine 4T1 (KI) and control (EV) cells into immune-competent Balb/C mice confirm tumor growth and survival in dependency of ASPP2k.

1820

Modulating the bone marrow adipocytes differentiation axis to target measurable residual disease in pediatric and young adult T-ALL

C. Bataclan (1), A. Martins (1), R. Benhassine (2), U. Koch (3), F. Radtke (3), S. Ferreira Lopes (1), T. Smirnova (4), O. Naveiras (1, 4)

Department of Biomedical Sciences, Faculty of Biology and Medicine, University of Lausanne, Lausanne (1), Department of Fundamental Oncology (DOF), Centre Hospitalier Universitaire Vaudois, Lausanne (2), SV ISREC UPRAD, Ecole Polytechnique Fédérale de Lausanne, Lausanne (3), Service et Laboratoire central d'hématologie, Centre Hospitalier Universitaire Vaudois, Lausanne (4)

Introduction: Measurable residual disease (MRD) is a major predictor of relapse in T-cell acute lymphoblastic leukaemia (T-ALL). Following intensive chemotherapy, bone marrow (BM) aplasia is associated with increased adipogenesis, potentially creating transient niches supporting residual leukaemic cells. We hypothesise that remodelling along the stromal-to-adipocyte differentiation axis generates transient microenvironmental states promoting MRD persistence under therapeutic pressure. We therefore investigate in vitro how distinct stages along this axis influence T-ALL persistence and establish an in vivo model to address the contribution of the adipogenic BM niche.

Methods: T-ALL cell lines were co-cultured with human bone marrow stromal cells (hBMSCs) at different stages of adipogenic differentiation, exposed to IC50 or IC90 doxorubicin or vincristine, with or without dexamethasone. Cell recovery was quantified by flow cytometry. Primary NOTCH1-driven murine T-ALL blasts were secondary-transplanted to characterise tissue tropism and BM infiltration. Secondary transplantation into BMAd-Cre;DTA mice will subsequently be used to investigate T-ALL engraftment and persistence following BMAd depletion.

Results: Stromal support varied according to T-ALL cell line, therapeutic pressure and adipogenic stage. While NOTCH1-WT cells showed no consistent differentiation-dependent pattern, NOTCH1-mutant cells displayed preferential support from

 Published under the CC license Attribution 4.0 International (CC BY 4.0)

early-to-intermediate stages. Under high therapeutic pressure, specific stages of stromal remodelling increased viable NOTCH1-mutant T-ALL cell numbers by up to 8-fold versus no-stroma controls, while further adipogenic maturation markedly reduced this support. The protective phenotype was observed across distinct chemotherapeutic conditions and further enhanced by dexamethasone. In vivo, secondary transplantation of primary NOTCH1-driven T-ALL cells into C57BL/6 recipient mice confirmed infiltration of leukaemic blasts into the BM, with leukaemic cells also detected in adipocyte-rich BM regions.

Conclusions: Our preliminary results indicate that T-ALL support varies dynamically across the BM adipogenic differentiation axis, with early-to-intermediate stages promoting leukaemic persistence under therapeutic pressure. The validated BM-tropic T-ALL model provides the basis to directly investigate whether BMAd depletion alters leukaemic engraftment and persistence in vivo.

9797

Hematon Units from liquid biopsies enable robust 3D imaging of human bone marrow niche heterogeneity

Y. Zhang (1), R. Sarkis (2, 3), C. Bataclan (2, 3), L. Angenendt (1), V. Basset (4), T. Smirnova (4), E. Boeri (2), N. Piazzon (5), D. Maison (5), M. Constanza (4), N. Dewarrat (4), S. Cherix (6), O. Spertini (4), S. Blum (4), B. Deplancke (3), L. de Leval (5), T. Schroeder (1), O. Naveiras (2, 4)

Department of Biosystems and Engineering, ETH-Zurich, Basel (1), Department of Biomedical Sciences, Faculty of Biology and Medicine, University of Lausanne, Lausanne (2), Insistute of Bioengineering, School of Life Sciences, EPFL, Lausanne (3), Department of Laboratory Medicine and Pathology, Hematology Service, Lausanne University Hospital, Lausanne (4), Department of Laboratory Medicine and Pathology, Institute of Pathology, Lausanne University Hospital, Lausanne (5), Department of Orthopedics and Traumatology, Lausanne University Hospital, Lausanne (6)

Introduction: The bone marrow (BM) stromal niche is a diverse microenvironment that regulates haematopoiesis in health and disease, yet technical and accessibility barriers have kept it poorly characterised in humans. We assessed whether human hematon units (HU), multicellular functional spheroids obtained from routine diagnostic BM aspirates, can serve as an accessible ex vivo model to resolve and quantify human BM stromal heterogeneity across homeostasis, acute myeloid leukaemia (AML), and regeneration after induction chemotherapy.

Methods: We developed and validated an immunohistochemistry panel of fifteen BM niche markers on decalcified formalin-fixed paraffin-embedded (FFPE) tissue sections, delineating endosteal, perivascular, adipocytic, and parenchymal stromal subniches. We then applied multiplex whole-mount 3D immunofluorescence imaging to intact HUs, enabling volumetric quantification of stromal and vascular compartments in control marrow and in longitudinally sampled AML patients at diagnosis, aplasia, and haematopoietic recovery.

Results: Marker expression and spatial patterns were concordant between tissue sections and HUs and revealed pronounced stromal heterogeneity. We describe in situ co-expression patterns of human stromal cell surface markers together with their spatial and micro-anatomic localisation. Volumetric analysis of HUs across AML treatment resolved reproducible, compartment-specific remodelling: endothelial (CD31) and CD90+ stromal compartments were reduced during disease and aplasia, while myeloid (S100A8/A9) and progenitor populations recovered progressively, revealing differential vulnerability and regenerative trajectories across distinct niche compartments.

Conclusions: HUs constitute a primary, decalcification-free ex vivo model that captures the composition and spatial organisation of the human BM stroma. Readily obtained from routine liquid biopsies, they offer an accessible platform to quantify niche remodelling in physiological and malignant haematopoiesis, with potential for future culture-based and functional assays.

3911

Scalable single-cell Functional Precision Medicine via AI-driven morphological profiling across hematological and solid tumors

B. D. Hale (1, 2), R. Wegmann (1, 2), M. Wyss (1), P. Hanns (3, 4), R. Lima (3, 4), M. Nunez (3, 4), V. Heinzelmann-Schwarz (3, 4), B. Snijder (2), F. Jacob (3, 4), Y. Severin (1, 5)

Hematology & Solid tumor research, Prevision Medicine AG, Zurich (1), Snijder Lab, Botnar Institute of Immune Engineering, Basel (2), Department of Biomedicine, University Hospital Basel, Basel (3), Department of Biomedicine, University of Basel, Basel (4), Department of Biology, ETH Zurich, Zurich (5)

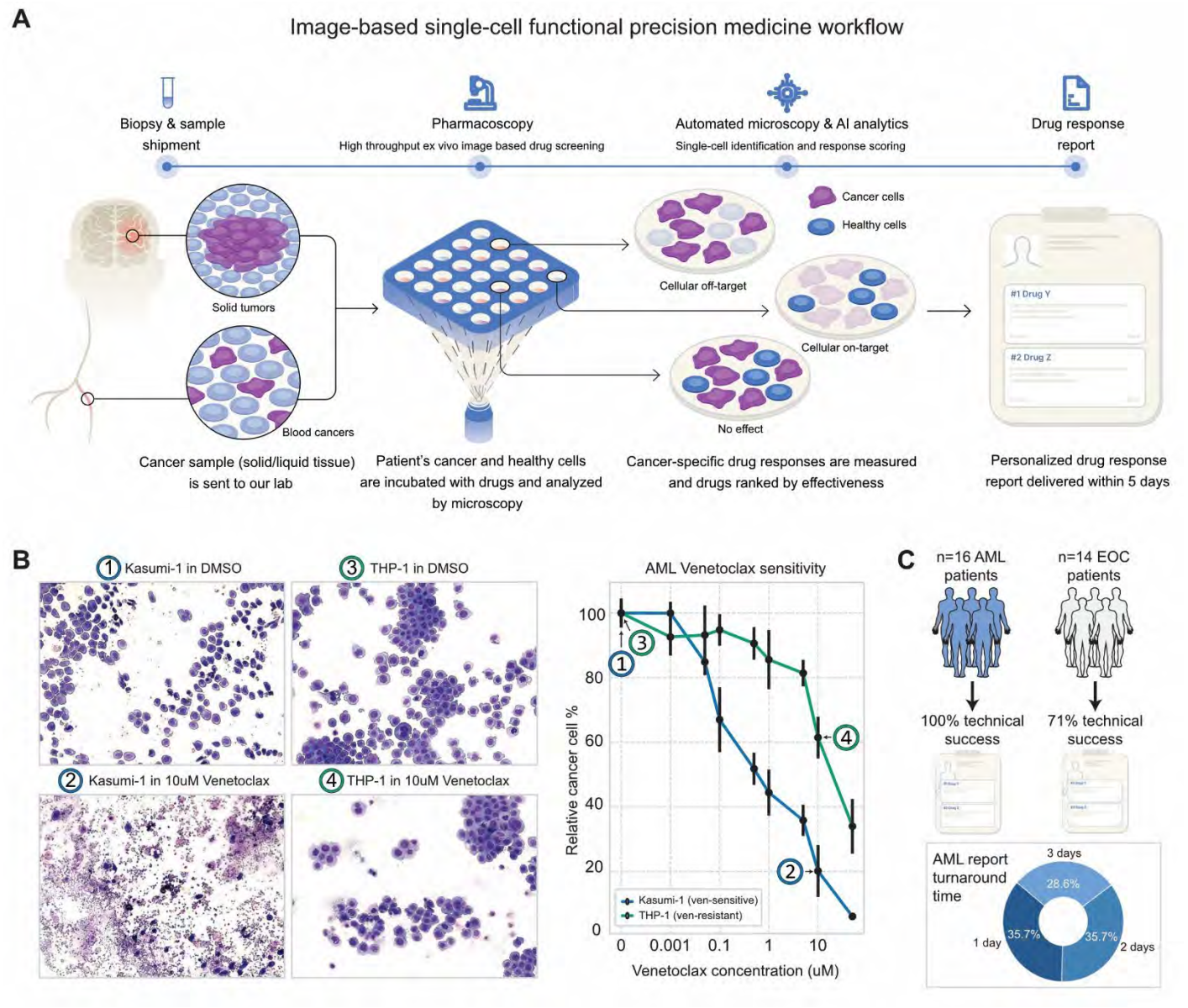
Introduction: Genomic profiling fails to identify actionable therapies for >50% of cancer patients. Image-based single-cell Functional Precision Medicine (scFPM) tools address this gap by directly measuring ex vivo drug responses on primary cells. This approach has already demonstrated increased overall survival in leukemia and lymphoma patients across two interventional clinical trials (EXALT-1 and DARTT-1). However, reliance on immunofluorescence (IF) microscopy creates cost, infrastructure, and throughput bottlenecks. To overcome this, we engineered a scalable scFPM platform replacing IF with histological staining and AI-driven morphological profiling. We validated our assay across hematological and solid malignancies, evaluated diverse drug classes (small molecules, antibody-drug conjugates [ADCs] and bi-specific T-cell engagers [BiTEs]), and demonstrated clinical feasibility regarding success rates and turnaround time.

Methods: Primary cells and co-cultures incubated on drug-coated plates for 24 hours, and dried directly onto the plates via controlled evaporation prior to fixation and histological staining. An automated, cloud-deployed pipeline using custom-trained deep learning networks segmented and classified cell types via morphological profiling. We evaluated the workflow in cell lines (acute myeloid leukemia [AML], multiple myeloma [MM] and epithelial ovarian cancer [EOC]) and T-cell co-cultures and validated it on primary AML (n = 16) and EOC (n = 14) patient samples.

Results: The AI pipeline accurately distinguished malignant, immune and apoptotic cell populations. In co-cultures, the platform quantified expected sensitivity profiles to venetoclax (AML) and dexamethasone (MM), aligned EOC responses to ADCs with target expression, and captured T-cell-mediated killing by BiTEs within 24 hours. In primary samples, technical success was 100% in AML and 71% in EOC, delivering actionable drug screening reports in an average of <3 days. Maintaining the clinically validated readout, the platform achieved a 75% reduction in imaging time, 50% lower reagent costs, 95% reduced data storage, 80% lower equipment costs, and 20-fold faster cellular classification versus IF.

Conclusions: Overall, we validated our AI-driven scFPM platform across diverse drug modalities to deliver rapid, cost-effective, and clinically actionable drug response profiles in primary hematological and solid tumors.

 Published under the CC license Attribution 4.0 International (CC BY 4.0)



6292

Decoding Cell Fate: Autophagy-Apoptosis Crosstalk in Pediatric Immune Thrombocytopenia

C. Bitsina (1), T. Stein (1), M. Seiler (2), A. Balduini (3), C. di Buduo (3), M. Schmugge (1), F. D. Franzoso (1)

Division of Hematology, University Children's Hospital Zurich, Zurich (1), Division of Emergency Medicine, University Children's Hospital Zurich, Zurich (2), Department of Molecular Medicine, University of Pavia, Pavia (3)

Introduction: Immune thrombocytopenia (ITP) is among the most prevalent acquired autoimmune bleeding disorders, with suboptimal treatment responses in a subset of pediatric patients. Abnormalities in megakaryopoiesis and platelet production are implicated in ITP pathophysiology. Previous studies, including those from our group, have demonstrated a role for platelet apoptosis in ITP, whereas the contribution of other signaling pathways, such as autophagy, remain to be elucidated. Using in vitro models of megakaryopoiesis and thrombopoiesis, we aimed to determine the pathogenic roles of interplay mechanisms between apoptotic changes and dysregulated autophagy in ITP.

Methods: MEG-01 cell line and megakaryocytes (MKs) differentiated from CD34+-selected peripheral blood mononuclear cells (PBMCs) from healthy controls (HCs) and ITP patients were used. MK differentiation and platelet production were assessed by flow cytometry and RT-qPCR. Apoptosis (CASP3, CASP8, CASP9, BCL2, BAX) and autophagy (ULK1, BECN1, ATG5, LC3B, p62) markers were analyzed by RT-qPCR, immunoblotting and confocal microscopy. BAX -siRNA silencing was performed to investigate its role in apoptosis as well as potential implications for autophagy regulation in primary MKs. Autophagic flux was evaluated by chloroquine treatment and transfection with the LC3B-GFP-mCherry reporter in MEG-01 cells and CD34+-derived MKs exposed to control or ITP-derived plasma. Autophagy flux dynamics were further assessed in a 3D-bone-marrow model using LC3B-GFP-mCherry-transfected-MEG-01 cells and primary MKs.

Results: ITP-derived plasma increased BCL2 and BECN1 and reduced p62 expression in MEG-01 cells and HC-derived MKs, while LC3B-GFP-mCherry assays and chloroquine-induced LC3/p62 accumulation indicated enhanced autophagic activity in ITP-plasma-treated cells. MKs from ITP patients showed significant upregulation of apoptosis (CASP3, CASP8, CASP9, BAX) and autophagy (ULK1, BECN1, ATG5, LC3B) markers and

Published under the CC license Attribution 4.0 International (CC BY 4.0)

higher LC3 puncta abundance than HCs, indicating an increased autophagic flux. In ITP-derived MKs, siRNA-mediated BAX silencing resulted in a significant reduction in BECN1 expression compared with HCs.

Conclusions: Our findings implicate dysregulated apoptosis-autophagy crosstalk in impaired platelet production in ITP, highlighting potential mechanisms underlying platelet disorders.

0426

Tumour-restricted IL-2 delivery via an immunocytokine enhances CAR T-cell efficacy in solid tumour models

C. Pellegrino (1), C. F. Magnani (2)

Department of Biology, Philochem AG, Otelfingen (1), Department of Medical Oncology and Hematology, University Hospital Zürich (USZ) and University of Zürich (UZH), Zürich (2)

Introduction: Chimeric antigen receptor (CAR) T-cell therapies achieve durable responses in B- and plasma-cell malignancies but remain largely ineffective against solid tumours, owing to limited tumour homing, restricted intratumoral expansion, and early CAR T-cell attrition. Cytokines such as interleukin-2 (IL-2) can enhance CAR T-cell activity, but systemic administration causes dose-limiting toxicity. We evaluated whether tumour-restricted IL-2 delivery could overcome these barriers and improve CAR T-cell efficacy in two preclinical solid tumour models.

Methods: CAR T cells targeting carbonic anhydrase IX (CAIX) in renal cell carcinoma (RCC) or carcinoembryonic antigen (CEA) in colorectal adenocarcinoma (COAD) were generated and assessed in vitro. Combination with an IL-2 immunocytokine directed against the extra-domain B (ED-B) of fibronectin, which is expressed on tumour-associated endothelial cells and cancer-associated fibroblasts, was evaluated in NSG mice bearing RCC or COAD xenografts.

Results: CAR T cells showed potent in vitro cytotoxicity against RCC and COAD cell lines but limited in vivo activity, being effective only at high doses. Combining CAR T cells with the IL-2 immunocytokine improved tumour control without systemic toxicity. Targeted IL-2 delivery required low cytokine exposure, thereby improving the therapeutic index and showed improved efficacy compared to equimolar dose of non-targeted systemic IL-2. Improved activity in vivo was associated with increased intratumoral CAR T-cell infiltration and expansion. Co-delivering of the immunocytokine lead to remodeling of the tumor microenvironment towards a more inflammatory and T-cell permissive status.

Conclusions: Tumour-restricted IL-2 delivery enhances intratumoral CAR T-cell proliferation and antitumor activity, while allowing precise control over cytokine timing and dosing. This strategy represents a versatile, clinically translatable approach to improve CAR T-cell efficacy in solid tumours.

4225

Decoding In-Human CAR T-Cell Re-Expansion: Single-Cell Multi-Omics-Guided Engineering of Next-Generation anti-BCMA CAR-T Cells in Multiple Myeloma

S.-Y. Lee (1), L. Hörtensteiner (2, 3, 1), J. M. Hölzl (2, 3, 1), A. Nater (4), M. C. Kreuzer (4, 5), H. Mandhair (2, 1), M. Hoffmann (1), P. Nicholson (5), U. Novak (2, 1), M. Wehrli (2, 1)

Medical Oncology, Inselspital, Bern (1), DBMR, Tumor Immunology, University of Bern, Bern (2), Cell Biology, Graduate School for Cellular and Biomedical Sciences, Bern (3), Interfaculty Bioinformatics Unit, University of Bern, Bern (4), Next Generation Sequencing (NGS) Platform, University of Bern, Bern (5)

Introduction: Anti-BCMA CAR T cells induce deep responses in relapsed/refractory multiple myeloma, but most patients relapse without antigen loss, so durability depends on whether infused cells persist and re-expand. What allows an individual CAR T-cell clone to re-expand in a patient has rarely been examined at clonal resolution in humans. We used an exceptional idecabtagene vicleucel (ide-cel) responder as an in-human discovery engine for next-generation anti-BCMA CAR T cell design.

Methods: The index patient (triple-class refractory, six prior relapses) reached the highest peak transgene level among the 50 ide-cel patients treated at our center (757,927 copies/ug DNA) and was in complete remission for more than 900 days, with repeated CAR T re-expansion, before passing away from causes unrelated to myeloma. We collected blood cells from the infusion product and on days 450, 786, and 861, then sorted them into CAR+ and CAR- cells. All cells underwent paired 5′ single-cell RNA and TCR sequencing; CAR integration sites in the CAR+ cells were mapped using long-read sequencing.

Results: We observed that the CAR T cells could be distinguished into two populations, one with a low CAR expression and mainly CD8 T cells, the other with a high CAR expression and mainly CD4 T cells. We also detected clonal dominance among CAR+, but not CAR- T cells. For these clones, we compared gene expression after versus before expansion, as well as before expansion versus before contraction. Future expanders were differing from future contractors by 580 genes that define a metabolic fitness and proliferative priming axis, including the upregulation of NAMPT, PRDX3, NDUFS2 and MKI67. After expansion, these clones mounted a robust activation response with intact physiological brakes, including FOS, JUN, DUSP1 and ZFP36. TNFRSF4/OX40 was identified as one of the most frequent integration sites and was also strongly upregulated before expansion versus before contraction.

Conclusions: Anti-BCMA CAR T cells may induce durable responses if their persistence and expansion can be enhanced. Our study identifies metabolic fitness and a robust, yet brake-intact, activation response as the state underlying CAR T-cell re-expansion. It also identifies NAMPT, AP-1 balance, and OX40 as engineering targets for next-generation anti-BCMA CAR T cells. These findings are derived from a single patient and should be considered hypothesis-generating.

 Published under the CC license Attribution 4.0 International (CC BY 4.0)

SSH/SSMO POSTER PRESENTATION - CLINICAL HEMATO-ONCOLOGY

3012

Serum Immunoglobulin Changes in Multiple Myeloma Patients Treated with CAR T-Cell Therapy

A. Burger (1), U. Bacher (2), M. Hoffmann (1), M. Bertschinger (1), K. Seipel (1), C. Schild (2), I. Shafarostova (1), T. Pabst (1)

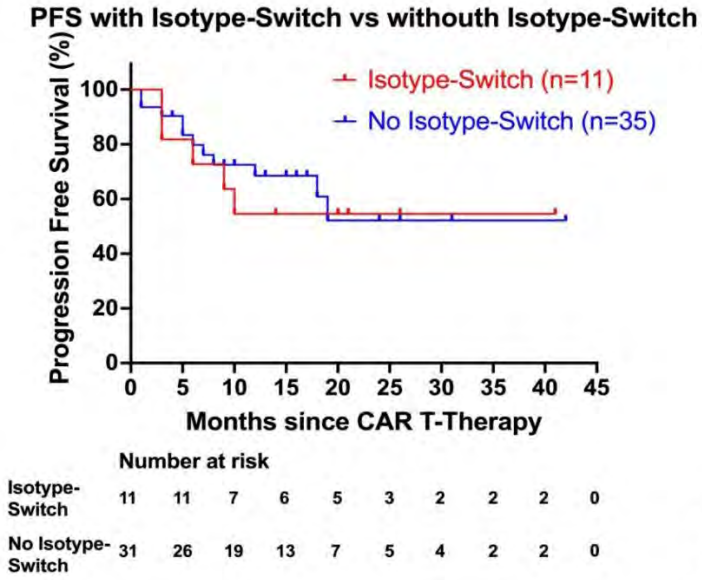
Medical Oncology, Inselspital, Bern (1), Hematology, Inselspital, Bern (2)

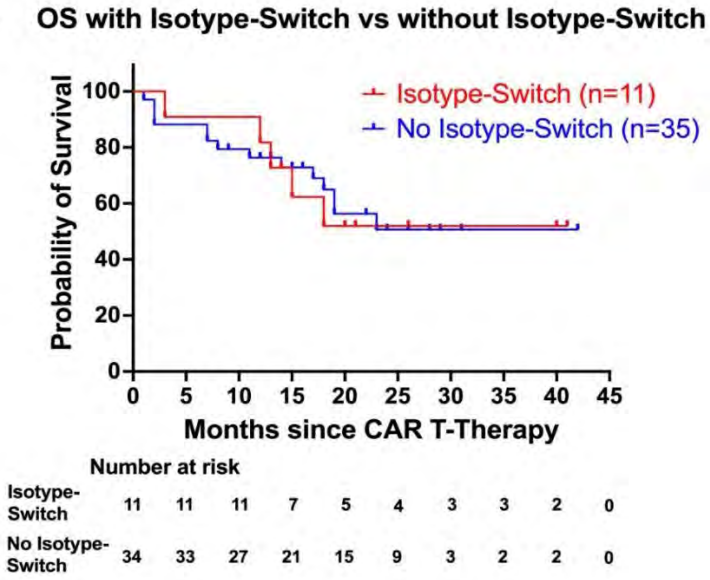
Introduction: Chimeric antigen receptor (CAR) T-cell therapy has emerged as an effective treatment for relapsed or refractory multiple myeloma (RRMM), with high response rates of 80-95%. Serum immunoglobulin changes have been observed throughout conventional multiple myeloma (MM) treatment, including after immunomodulatory drugs, proteasome inhibitors, and autologous stem cell transplantation. However, the clinical significance of new abnormal protein bands (APBs) following CAR T-cell therapy is largely unexplored.

Methods: We retrospectively analyzed consecutive MM patients who received CAR T-cell therapy at a single academic center between May 2021 and February 2024. Serum paraprotein (M-protein) patterns were assessed using immunofixation electrophoresis (IFE) before and after CAR T-cell treatment. Patients were grouped based on serum immunoglobulin changes.

Results: Among 46 patients, 9 (19.6%) developed new APBs following CAR T-cell therapy. Among the 26 patients who experienced clinical relapse, 4 (15.4%) had APBs, 19 (73%) were paraprotein-positive with the same immunoglobulin pattern, and 3 (11.5%) showed no evidence of a paraprotein in IFE. Among the 20 patients who did not experience clinical relapse, 5 (25%) developed APBs, 3 (15%) retained the same paraprotein, and 12 (60%) had no detectable paraprotein. The median time to the appearance of APBs following CAR T-cell infusion was 7 months (range: 2–17 months). Patients with APBs were more frequently classified as R-ISS Stage II (66.7%) than those without (37.8%), and t(4;14) was more prevalent among patients with APBs (33.3%) than those without (8.1%). There were no significant differences in progression-free survival (PFS, p = 0.87) or overall survival (OS, p = 0.95) between patients with and without APBs (see Figure 1).

Conclusions: Appearance of APBs following CAR T-cell therapy in patients with MM is a frequent finding. While APBs are common, they are not necessarily associated with disease relapse or worse outcomes in terms of PFS or OS. Changes in serum immunoglobulin profiles should not be interpreted as biochemical relapse. Larger, prospective, multi-center studies are needed to further investigate this phenomenon.





7978

Lower stem-cell yields after daratumumab-VRD induction in a predominantly vinorelbine-mobilised multiple myeloma cohort

A. Genthon (1), J. Dereme (1), E. E. Kampouri (2), E. Gagliarducci (3), A. Cairoli (1), M. Nabergoj (1), S. Barelli (1), J. Schoumans (4), N. Lauriers (1), P.-Y. Bochud (2), N. Rufer (3), H. Auner (1)

Service and Central Laboratory of Haematology, Lausanne University Hospital (CHUV), Lausanne (1), Service of infectious disease Department of Internal Medicine, Lausanne University Hospital (CHUV), Lausanne (2), Department of medicine, Interregional Blood Transfusion SRC, Epalinges (3), Oncogenomic Laboratory Department of Laboratories and Pathology, Lausanne University Hospital (CHUV), Lausanne (4)

Introduction: Vinorelbine plus granulocyte colony-stimulating factor (G-CSF) is widely used in Switzerland for peripheral blood stem-cell mobilisation in multiple myeloma. Daratumumab-containing induction has been associated with lower CD34+ cell yields. We examined this association in a cohort predominantly mobilised with vinorelbine.

Methods: This retrospective single-centre study included 200 consecutive patients with newly diagnosed multiple myeloma undergoing first autologous stem-cell transplantation between 2020 and 2025. Patients received bortezomib, lenalidomide and dexamethasone (VRD, n = 97) or daratumumab-VRD (D-VRD, n = 103). Vinorelbine plus G-CSF was used in 191 patients; vinorelbine was omitted in 7 due to pre-existing neuropathy (mobilisation data were missing for 2). All 200 patients were analysed. The primary endpoint was inadequate collection (<4 x 10^6 CD34+ cells/kg). Secondary endpoints included total yield, collection of ≥6 x 10^6 CD34+ cells/kg, achievement of this

Published under the CC license Attribution 4.0 International (CC BY 4.0)

target in a single apheresis, plerixafor use, more than one apheresis and collection failure (<2 x 10^6 CD34+ cells/kg).

Results: Baseline characteristics were similar between groups. Before transplantation, 81.3% of VRD and 87.4% of D-VRD patients achieved at least a very good partial response (p = 0.247). Median CD34+ yield was lower after D-VRD (4.96 versus 7.84 x 10^6 cells/kg; adjusted median difference -2.85, 95% CI -4.50 to -2.21). Inadequate collection occurred in 19.4% after D-VRD versus 4.1% after VRD and remained associated with D-VRD after adjustment for age, R-ISS and pre-transplant response (adjusted OR 6.57; 95% CI 2.04-21.10; p = 0.002). D-VRD patients were less likely to reach ≥6 x 10^6 CD34+ cells/kg overall (adjusted OR 0.15; 95% CI 0.08-0.29; p <0.001) or in a single apheresis (adjusted OR 0.14; 95% CI 0.07-0.28; p <0.001). Plerixafor use and more than one apheresis were more frequent after D-VRD (adjusted OR 3.37; 95% CI 1.02-11.16; p = 0.046 and adjusted OR 7.46; 95% CI 3.34-16.62; p <0.001, respectively). Collection failure occurred in 2 D-VRD patients and in no VRD patients.

Conclusions: In this cohort predominantly mobilised with vinorelbine plus G-CSF, D-VRD was associated with less efficient collection. Most D-VRD patients achieved a transplant-compatible yield, but had lower CD34+ yields, more frequent plerixafor use and a greater need for multiple apheresis procedures.

	VRD	D-VRD	Total	p
N	97 (48.5%)	103 (51.5%)	200 (100.0%)	
Age at transplantation	61 [55-66]	58 [54-64]	60 [54-65]	0.154
Age group				
<65 ans	67 (69.1%)	80 (77.7%)	147 (73.5%)	0.169
≥65 ans	30 (30.9%)	23 (22.3%)	53 (26.5%)	
Sex				
Female	41 (42.3%)	36 (35.0%)	77 (38.5%)	0.288
Myeloma subtype				
A	20 (20.6%)	16 (15.5%)	36 (18.0%)	0.762
D	1 (1.0%)	2 (1.9%)	3 (1.5%)	
G	56 (57.7%)	60 (58.3%)	116 (58.0%)	
Light chain only	18 (18.6%)	24 (23.3%)	42 (21.0%)	
M	1 (1.0%)	1 (1.0%)	2 (1.0%)	
non secretory	1 (1.0%)	0 (0.0%)	1 (0.5%)	
Light chain				
Kappa	55 (56.7%)	65 (63.1%)	120 (60.0%)	0.373
Kappa + Lambda	0 (0.0%)	1 (1.0%)	1 (0.5%)	
Lambda	42 (43.3%)	37 (35.9%)	79 (39.5%)	
R-ISS				
1	42 (44.7%)	35 (35.7%)	77 (40.1%)	0.313
2	40 (42.6%)	44 (44.9%)	84 (43.8%)	
3	12 (12.8%)	19 (19.4%)	31 (16.1%)	
Disease response pre-ASCT				
<VGPR	18/96 (18.8%)	13/103 (12.6%)	31/199 (15.6%)	0.247
≥VGPR	78/96 (81.3%)	90/103 (87.4%)	168/199 (84.4%)	
Missing	1 (1.0%)	0 (0.0%)	1 (0.5%)	
Conditioning regimen				
Melphalan 140 mg/m²	2 (2.1%)	1 (1.0%)	3 (1.5%)	0.657
Melphalan 160 mg/m²	2 (2.1%)	1 (1.0%)	3 (1.5%)	
Melphalan 200 mg/m²	92 (95.8%)	101 (98.1%)	193 (97.0%)	
Vinorelbine				
Non	2 (2.1%)	5 (4.9%)	7 (3.5%)	0.562
Inconnu	1 (1.0%)	1 (1.0%)	2 (1.0%)	

Outcomes	Adjusted effect of D-VRD vs VRD	p
CD34+ yield (median)	-2.85 x10^6/kg [-4.50 to -2.21]	<0.001
Target ≥4 ×10^6/kg	OR 0.15 [0.05-0.49]	0.002
Target ≥6 ×10^6/kg	OR 0.15 [0.08-0.29]	<0.001
Optimal success[1]	OR 0.14 [0.07-0.28]	<0.001
Plerixafor use	OR 3.37 [1.02-11.16]	0.046
More than one apheresis	OR 7.46 [3.34-16.62]	<0.001

[1]CD34+≥6×10^6/kg collected in one apheresis.

VRD: Velcade, Revlimid, dexamethasone; D-VRD: daratumumab, Velcade, Revlimid, dexamethasone; R-ISS: revised international scoring system; VGPR: very good partial response.

Published under the CC license Attribution 4.0 International (CC BY 4.0)

4212

Donor-Derived Cytogenetic Alterations After Allogeneic Hematopoietic Stem Cell Transplantation: A Retrospective Single-Center Cohort Study

R. Rasiah (1), S. Kathirchelvan (1), J. Passweg (1), J. Halter (1), M. Stoikou (2), B. C. Glaeser (2), S. Cichon (2), D. Juskevicius (1), F. Wenzel (2), C. C. Widmer (1)

Hematology, University Hospital Basel, Basel (1), Institute of Medical Genetics and Pathology, University Hospital Basel, Basel (2)

Introduction: Cytogenetic analysis is essential for diagnosis and risk stratification of hematologic malignancies. While karyotyping at diagnosis establishes the cytogenetic baseline, the value of routine post-transplant cytogenetic assessment after allogeneic hematopoietic stem cell transplantation (allo HCT) remains unclear. We investigated the frequency and clinical relevance of post-transplant cytogenetic abnormalities, with particular focus on donor-derived alterations.

Methods: We retrospectively analyzed adult patients undergoing allo HCT between January 2020 and December 2024 at our institution. Cytogenetic data at diagnosis, before transplantation and after allo HCT were extracted from diagnostic reports. Only patients with complete diagnostic and post-transplant datasets were included. Donor versus recipient origin was determined by sex chromosome configuration in sex-mismatched transplants and supported by molecular data in sex-matched cases.

Results: Of 557 patients with available data, 324 had complete datasets. Before transplantation, 63 patients (19.4%) showed abnormal cytogenetics. After allo HCT, 290 patients (89.5%) had a normal donor-derived karyotype. Cytogenetic abnormalities were detected in 34 karyograms from 33 patients. Twenty-eight were classified as disease-related recipient abnormalities, supported by concomitant molecular relapse and decreasing chimerism. Donor-derived alterations were identified in six cases (1.8%). Four showed isolated loss of chromosome Y, consistent with an age-related donor phenomenon. Two patients had donor-derived translocations. One developed a clonal t(10;17)(q26;q21) three months after allo HCT without evidence of neoplasia during three years of follow-up, suggesting a constitutional origin. The second developed donor-derived AML within three years despite persistent 100% donor chimerism; notably, karyotyping at three months had been normal

Conclusions: Clinically relevant cytogenetic abnormalities after allo HCT are uncommon, and donor-derived alterations are rare. Most donor-associated findings, particularly loss of chromosome Y, likely represent age-related phenomena without immediate clinical consequences. Routine post-transplant cytogenetic surveillance for donor-derived abnormalities appears to have limited diagnostic yield and should be interpreted within the broader clinical context.

7940

Determinants and clinical impact of Hemophagocytic Lymphohistiocytosis in Acute Myeloid Leukemia patients

M. Gavillet (1), A. Guillet (2), S. Bibert (2), M. Nabergoj (1), E. Kampouri (2), S. Blum (1), P.-Y. Bochud (2)

Hematology, Lausanne University Hospital, Lausanne (1), Infectious Disease, Lausanne University Hospital, Lausanne (2)

Introduction: Hemophagocytic lymphohistiocytosis (HLH) is a life-threatening hyperinflammatory syndrome increasingly recognized in hematologic malignancies of lymphoid lineage. However, data on HLH complicating acute myeloid leukemia (AML) and myelodysplastic syndromes with increased blasts (MDS-IB) remain limited. We aimed to evaluate the incidence, risk factors, and clinical impact of HLH in a large prospective cohort of hematologic patients receiving intensive chemotherapy.

Methods: We analyzed adult patients with AML/MDS-IB patients prospectively enrolled in the MINCO registry at Lausanne University Hospital (CHUV) between 2007 and 2025. HLH episodes were identified prospectively and validated using the HScore. Analyses were performed per chemotherapy course. Logistic regression models were used to identify risk factors for HLH and its clinical impact.

Results: The study included 841 chemotherapy courses in 412 AML/MDS-IB patients. Thirty-four HLH episodes occurred (incidence 4.1%). In multivariable analysis, factors independently associated with HLH included purine-based chemotherapy regimens compared with standard "7+3" induction whether prescribed as a front-line induction (OR = 11.4, 95%CI 4.1-32) or a salvage therapy regimen (OR = 12.8, 95%CI 4.3-38), both highly significant (P <0.001) and agranulocytosis within 3 days after admission (OR = 2.66, 95% CI 1.3-5.6, P = 0.01). Using a matched case-control design, we also showed that ≥3 microbiologically documented infections (MDI, OR = 9.23, 95%CI 2.2-40, P = 0.001) and higher doses of corticosteroids (≥0.5 mg prednisone equivalent per kg of body weight, OR = 5.64, 95% CI 1.4-24, P = 0.02) were more frequent prior to HLH than during the equivalent time at risk in controls. HLH was also associated with worse outcomes, including prolonged hospitalization (median 43 vs. 29 days, P <0.001) and agranulocytosis (29 vs. 18 days; P <0.001), increased occurrence of severe infections (qSOFA ≥2, 23.5% vs 18.6%, P = 0.04) and transfers to ICU (23.5% vs. 6.9% P = 0.02) and markedly higher overall mortality (20.6% vs. 2.9%; P = 0.02).

Conclusions: HLH is a severe and likely underrecognized complication of AML therapy. Its occurrence appears strongly linked to treatment-related immunosuppression, particularly purine-based regimen. Given its major adverse prognostic impact, heightened clinical awareness and earlier recognition are essential in this high-risk population.

8285

Direct Oral Anticoagulants versus Aspirin for Thromboprophylaxis in Multiple Myeloma Patients Receiving Immunomodulatory Therapy: An Updated Systematic Review and Meta-Analysis

P. Barrera (1), R. Adhikari (2), R. Zahid (3)

Facultad de Medicina, Universidad de Buenos Aires, Buenos Aires (1), School of Medicine, Augusta University, Georgia (2), College of Medicine, FMH College of Medicine and Dentistry, Lahore (3)

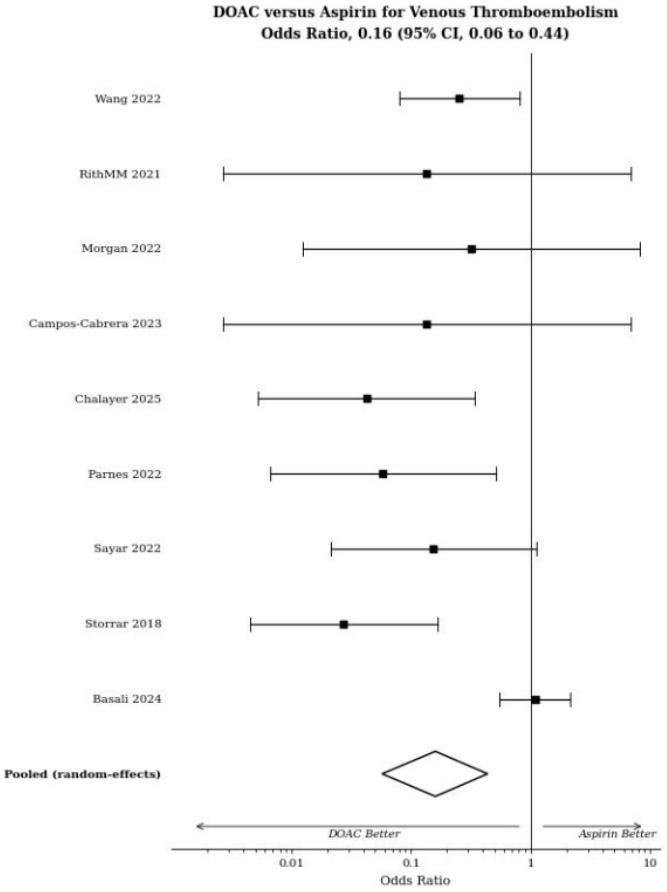
Introduction: Multiple myeloma (MM) patients face up to a 20-fold higher risk of venous thromboembolism (VTE) than the general population, further elevated by immunomodulatory drug (IMiD)-based regimens, underscoring the need for optimal prophylaxis. Direct oral anticoagulants (DOACs) are increasingly used for thromboprophylaxis, but comparative evidence against aspirin remains limited. A prior meta-analysis of 10 studies (1,026 patients) reported a significant DOAC benefit; we expanded the evidence base to 18 studies and applied the Peto odds ratio method to account for the high prevalence of zero-event arms, comparing DOACs against aspirin and low-molecular-weight heparin (LMWH) for VTE prophylaxis in MM.

Methods: We searched PubMed, Cochrane CENTRAL, and Embase without date restriction, cross-referenced against three prior reviews. Eighteen studies met inclusion criteria (2 randomised, 16 observational). Random-effects meta-analysis used the Peto odds ratio (OR), given extensive zero-event study arms. Sensitivity analyses included leave-one-out influence testing and subgroup analysis by design.

 Published under the CC license Attribution 4.0 International (CC BY 4.0)

Results: Nine of ten eligible studies (1,029 patients: 447 DOAC, 582 aspirin) yielded an estimable odds ratio; one had zero events in both arms. DOAC prophylaxis was associated with significantly reduced VTE odds versus aspirin (OR 0.16, 95% CI 0.06–0.44, p = 0.0004; k = 9). Heterogeneity was substantial (I^2 = 69%). Leave-one-out analysis identified one discordant retrospective cohort as responsible for nearly all heterogeneity; its exclusion yielded OR 0.11 (95% CI 0.05–0.24, I^2 = 0%). Subgroup and sensitivity analyses ruled out study design and population indirectness as explanations. DOAC versus LMWH also favoured DOAC (OR 0.07, 95% CI 0.01–0.41, p = 0.003; k = 2). International Society on Thrombosis and Haemostasis (ISTH)-defined major bleeding did not differ meaningfully between DOAC and aspirin (1.2% vs. 1.0%, single informative pair).

Conclusions: DOAC prophylaxis is associated with a large, consistent reduction in VTE odds versus aspirin in MM, with no signal of increased bleeding. The effect withstood extensive sensitivity testing, including exclusion of the one discordant cohort (OR 0.11, I^2 = 0%), positioning DOACs as a strong candidate alternative to aspirin pending confirmation in adequately powered randomised trials.



1859

Earlier Cytokine Release Syndrome Onset Is Associated With Greater Longitudinal Cumulative Chimeric Antigen Receptor T-Cell Expansion After Tisagenlecleucel

D. M. Devin Meier (1), G. W. Gertrud Wiedemann1 (1), J. R. Jean-Benoît Rossel (2), U. B. Vera Ulrike Bacher (1), T. P. Thomas Pabst (3), I. C. Ioannis Chanias (1), B. L. Benjamin Lüscher (1), A. S. Anne Angelillo-Scherer (1), M. D. Michael Daskalakis (1), K. J. Katarzyna Aleksandra Jalowiec (1)

Department of Haematology and Central Haematology Laboratory, Inselspital, Bern (1), University of Bern, Department of Clinical Research, Bern (2), Department of Medical Oncology, Inselspital, Bern (3)

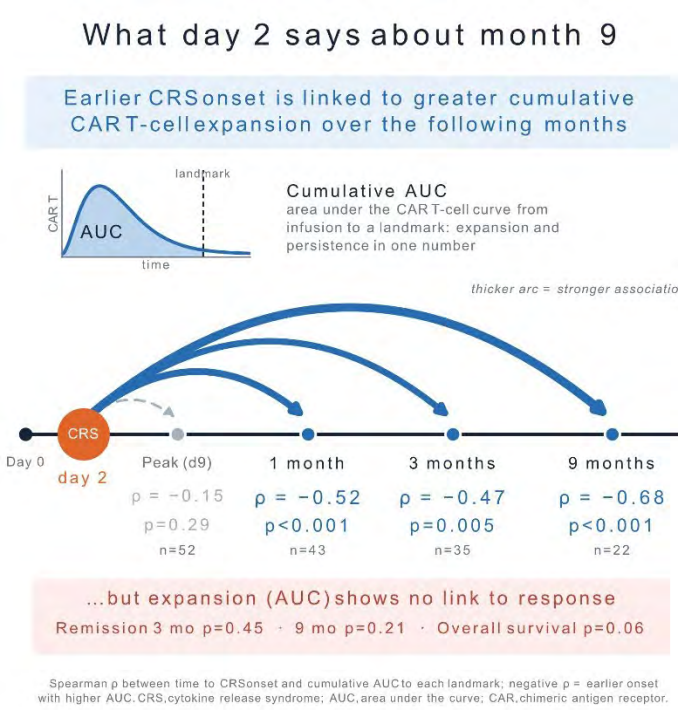
Introduction: Chimeric antigen receptor (CAR) T-cell expansion can be summarised by its peak or by the 28-day area under the curve (AUC). Both have been related mainly to toxicity severity, not its timing. Whether integration over longer windows adds information is unknown. We asked whether cumulative AUC over successive landmarks after tisagenlecleucel (tisa-cel) is associated with the timing of cytokine release syndrome (CRS), whether it reflects CRS grade, neurotoxicity, remission or survival, and whether transduction efficiency relates to AUC.

Methods: We retrospectively analysed all 71 patients treated with tisa-cel at a single centre (2018–2023). Peripheral blood CAR transgene levels were quantified serially by droplet digital polymerase chain reaction. Cumulative AUC was calculated by trapezoidal integration to 1, 3 and 9 months, to the observed expansion peak and to the last measurement; landmarks not reached were not extrapolated. Remission was assessed at 3 and 9 months. Analyses (Spearman, Kruskal-Wallis, Mann-Whitney U) were exploratory, uncorrected for multiplicity.

Results: Patients had diffuse large B-cell lymphoma (82%), follicular lymphoma (10%) or acute lymphoblastic leukaemia (8%). CRS occurred in 76% (median onset day 2); expansion peaked at median day 9. Time to CRS onset correlated inversely with cumulative AUC at 1 month (ρ = −0.52, p <0.001, n = 43), 3 months (ρ = −0.47, p = 0.005, n = 35) and 9 months (ρ = −0.68, p <0.001, n = 22), but not with AUC to the observed peak (ρ = −0.15, p = 0.29, n = 52) or at the last measurement (ρ = −0.18, p = 0.20, n = 52). CRS grade differed by AUC at 1 month only (p = 0.037). AUC was not associated with remission at 3 or 9 months (p = 0.45; p = 0.21) or with overall survival (p = 0.06). Immune effector cell-associated neurotoxicity analyses were inconsistent and underpowered. Transduction efficiency correlated modestly with 9-month AUC only (ρ = 0.41, p = 0.03, n = 30).

Conclusions: Earlier CRS onset was consistently associated with greater cumulative CAR T-cell expansion over fixed monthly landmarks, but not with expansion integrated to the peak or to the last measurement, i.e. windows of variable length. CRS timing may thus indicate the expansion trajectory early, whereas expansion was unrelated to remission or survival. Since later landmarks favour longer-surviving patients, multicentre validation is warranted.

Published under the CC license Attribution 4.0 International (CC BY 4.0)



5670

Efficacy and Safety of Venetoclax Bridging Therapy Prior to CAR T-Cell Therapy in Patients with t(11;14) Multiple Myeloma

N. Hodel (1), M. Bertschinger (1), M. Hoffmann (1), I. Shafarostova (1), U. Bacher (2), T. Pabst (1)

Medical Oncology, Inselspital, Bern (1), Hematology, Inselspital, Bern (2)

Introduction: Chimeric antigen receptor (CAR) T-cell therapy has revolutionized the treatment landscape of multiple myeloma (MM). Bridging treatment plays a crucial role in reducing tumour burden, improving the effector-to-target cell ratio, and lowering CAR T-cell therapy-related toxicities. Venetoclax is a highly selective and potent inhibitor of the anti-apoptotic protein B-cell lymphoma 2 (BCL-2) and has demonstrated rapid and high response rates in patients harbouring t(11;14) translocation.

Methods: In this retrospective single-centre case series we analysed patients with t(11;14)-positive relapsed MM who received Venetoclax bridging therapy before CAR T-cell therapy between May 2022 and April 2026. The primary endpoint was overall response rate (ORR) before CAR T-cell therapy.

Results: We included 8 heavily pretreated patients. 63% (5/8) had received ≥ 4 prior lines of therapy, and 88% (7/8) had previously undergone autologous stem cell transplantation. Venetoclax was used as monotherapy in 6/8 (75%) patients and in combination therapy in 2/8 (25%). Venetoclax was well tolerated, with no cases of tumor lysis syndrome or transfusion support during bridging therapy. None of the patients developed neutropenia. The ORR was 88%, no patient experienced disease progression during bridging therapy. The median time to response was 45 days. Seven patients (88%) received idecel and one patient (13%) received cilta-cel. Following CAR T-cell infusion, grade 1 CRS occurred in 5/8 (63%) patients, with no cases of higher-grade CRS (≥ grade 2). Grade 1 ICANS occurred in 1/8 (13%) patient. Cytopenias were mild, 1/8 (13%) patient required red blood cell transfusion after CAR T-cell therapy. Infections occurred in 50% (4/8) patients. No cases of hemophagocytic lymphohistiocytosis (HLH) were documented. Hypogammaglobulinemia was diagnosed in 3/8 (38%) patients. Following CAR T-cell therapy, all patients achieved at least a complete response (CR), with 4/8 (50%) patients achieving a stringent CR. The median PFS after CAR T-cell therapy was 363 days, the median OS after one year 75% (Figure 1 and 2).

Conclusions: In this analysis, Venetoclax demonstrated a high ORR and rapid time to response in a heavily pretreated patient population. No unexpected safety signals were observed during or after Venetoclax therapy, supporting its potential as a an effective and feasible bridging strategy in patients with t(11;14) MM.

Figure 1. Progression-Free Survival (PFS)

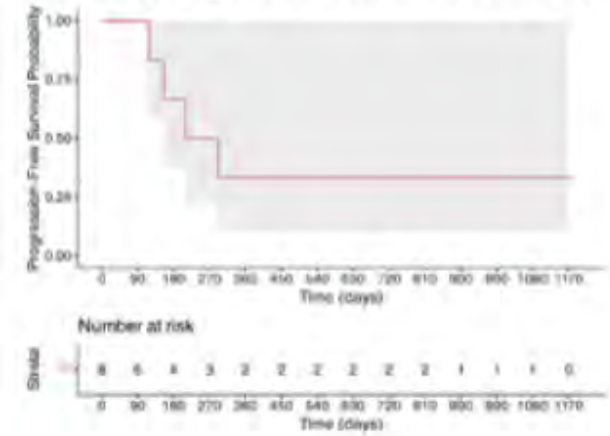
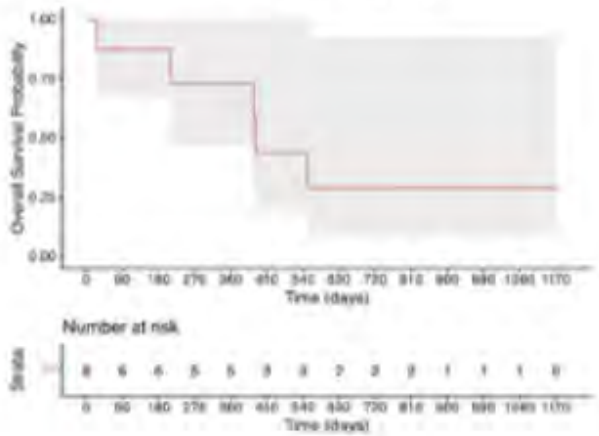


Figure 2. Overall Survival (OS)



Published under the CC license Attribution 4.0 International (CC BY 4.0)

2800

Single-cell deterministic multimodal interconnected RNA-sequencing and imaging reveals recurrent versus divergent profiles in acute myeloid leukemia with recurrent genetic abnormalities

T. F. Ferrari (1), G. T. Tsilimidos (2), O. N. Naveiras (2), B. D. Deplancke (1)

SV-IBI, Ecole Polytechnique Fédérale de Lausanne, Lausanne (1), Service et Laboratoire central d'hématologie, Lausanne University Hospital, Lausanne (2)

Introduction: IRIS is a platform capable of coupled single-cell (SC) flow-imaging and RNA sequencing. We leveraged its capacities to profile acute myeloid leukemia (AML), aiming to define cell phenotypes indicative of the RNA state in leukemic subtypes and determine reproducibility for image-based diagnostics.

Methods: We profiled 12 NPM1 mutated (NPM1m), 7 KMT2A rearranged (KMT2Ar), 4 myelodysplasia related (MR) and 5 Healthy control blood samples at diagnosis. RNA integration determined multilevel specific and shared profiles, from which donor and cohort-level deviations were determined. Through per cell matching of imaging, we created a linked feature space, revealing cohort and donor-recurrent and divergent phenotypes, variable through hematopoiesis.

Results: Recurrent cohort-level cores defining AML RNA profiles were uncovered and linked to imaging profiles. The strongest transcriptional differences between NPM1m and KMT2Ar, reoccurring across multiple donors and remaining significant after permutation, occurred in early myeloid progenitors. Differentially expressed genes included ELMO1, RUNX1, ETV6, FNBP1, ARHGAP25 and TRIO. Morphologically, NPM1m showed small, fine-grained nuclear chromatin textures, consistent with the disruption of nucleolar architecture after NPM1 cytoplasmic delocalization, strongest in stem cells, compared to KMT2A and MR samples. NPM1m cells also showed changes in endoplasmic reticulum (ER) and mitochondrial (Mt) features, recurring in >90% of donors, suggesting that the canonical NPM1m state is a coordinated cellular architecture rather than an isolated nuclear phenotype. In contrast, the KMT2Ar morphology shows larger chromatin bodies and spatial relationships of the nucleus and imaged organelles, including increased perinuclear Mt and ER signal. KMT2Ar had higher heterogeneity in RNA phenotype, emphasized through the myeloid window, whilst retaining recurrent morphology. RNA deviations appear donor-specific and compatible with fusion partner variability. MR morphology was dominated by Mt organization rather than nuclear morphology, with its core distinguished by recurrent changes in Mt texture.

Conclusions: We found that different SC-based morphotypes correspond not only to distinct RNA differentiation profiles but also to underlying genotypic heterogeneity in AML. These subtle phenotypic differences could be leveraged to predict genetic aberrations in diagnostics.

7881

A Digital Learning Ecosystem Improves Access to Structured Postgraduate Education in Academic Haematology and Oncology

N. Karantzelis (1), T. M. Benoit (1), M. Liu (1), R. Schwotzer (1), A. Wicki (1), M. G. Manz (1)

Department of Medical Oncology and Haematology, University Hospital Zurich, Zurich (1)

Introduction: Providing structured postgraduate medical education within trimmed medical-efficiency clinical environments is challenging. We evaluated the implementation, utilisation and user acceptance of a digital learning ecosystem combining an institutional Learning Management System (LMS) with a weekly educational newsletter at a Swiss tertiary academic centre.

Methods: A digital learning ecosystem (Figure 1) was implemented at the Department of Medical Oncology and Haematology of a university hospital in 01/2026. The pull-based LMS provides on-demand access to recorded case lectures, journal clubs, FMH and FAMH educational content, instructional videos, multiple-choice questions and further literature. A push-based weekly newsletter promoted learner engagement and educational activities. LMS analytics were collected during the first six months after implementation. User acceptance was assessed using an anonymous cross-sectional survey with Likert-scale and free-text questions in 06/2026. Subgroup analyses were performed according to professional seniority.

Results: During the first six months, 41 users enrolled in 162 LMS courses, generating 224 video views. 27 participants completed the survey, including 13 residents, 10 attending or senior attending physicians and four additional healthcare professionals, including FAMH specialists. Acceptance was high across all career stages. The newsletter received the highest rating (4.83/5), followed by platform usability (4.50/5), support for educational activities (4.42/5), contribution to structured postgraduate education (4.32/5) and content quality (4.19/5). Willingness for continued use and recommendation were both high (8.3/10). No meaningful differences were observed between residents and attending physicians. Lack of protected educational time was identified as the main barrier to more frequent use. Participants recommended expanding the platform to interprofessional education and a regional training network involving two major teaching hospitals.

Conclusions: A digital learning ecosystem integrating an institutional LMS with a weekly educational newsletter achieved high acceptance across different career stages. This scalable approach may improve access to structured postgraduate education and facilitate interprofessional and multi-institutional continuing medical education. The platform is being further refined to meet evolving educational needs.

 Published under the CC license Attribution 4.0 International (CC BY 4.0)

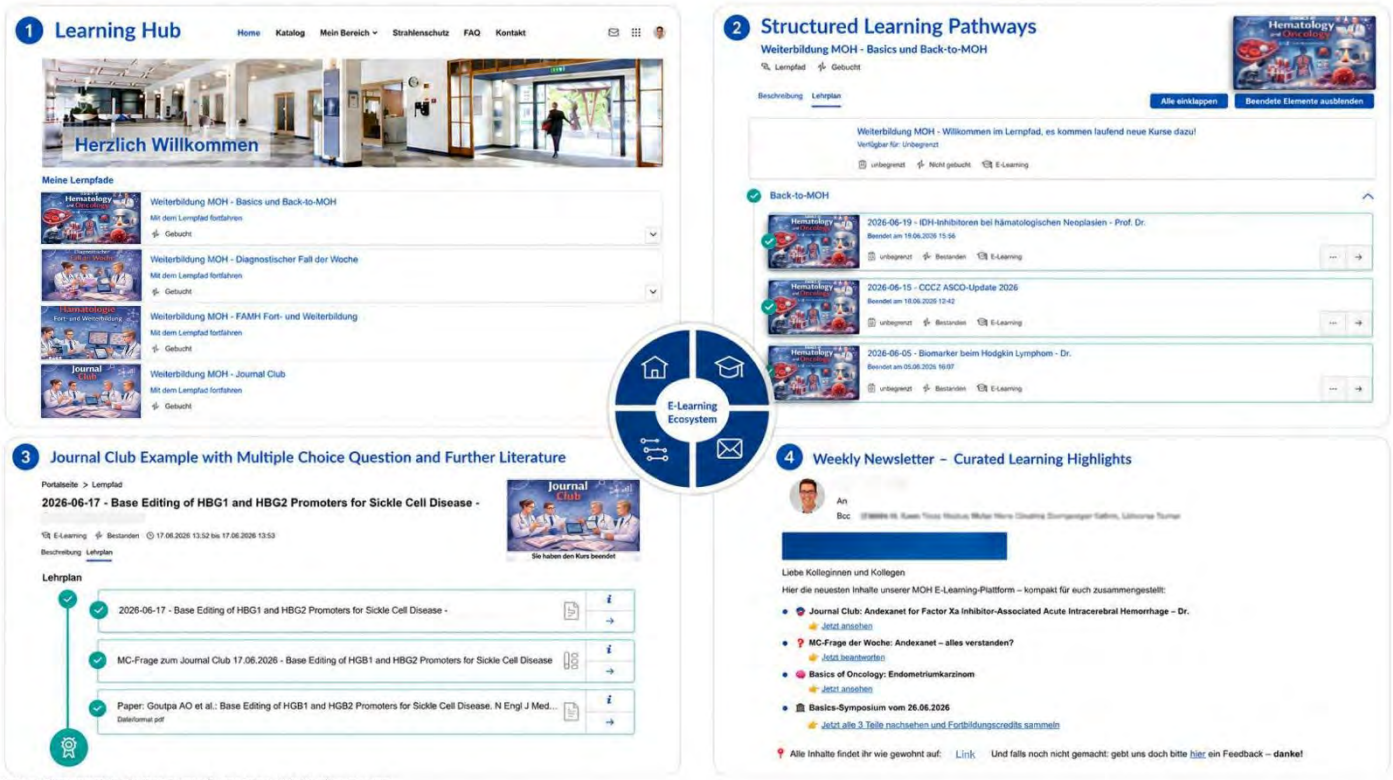


Figure1. Overviewof the Digital LearningEcosystem and Its KeyComponents

6540

Do SSH-SSMO/SOHC Abstracts Make It to Print? Publication and Authorship Outcomes

S. Mikula (1), D. Taussky (1, 2), D. Benzaquen (1), A. Champion (1), A. Sabbah (3)

Radiation oncology, Hôpital de La Tour, Meyrin (1), Radiation oncology, Centre hospitalier de l'Université de Montreal, Montreal (2), Division of surgical and interventional sciences, McGill University, Montreal (3)

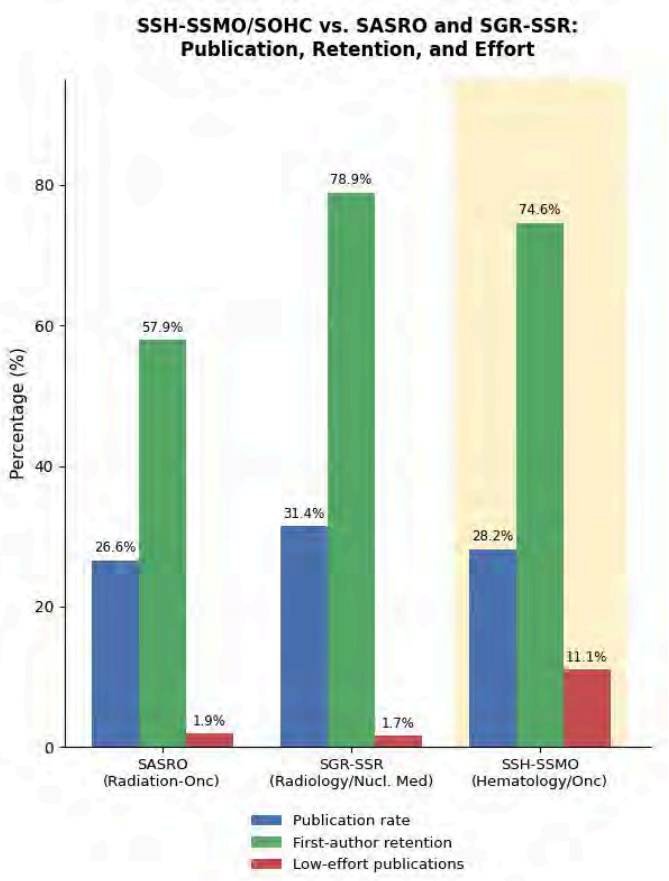
Introduction: To evaluate publication conversion and first-author retention, comparing Hematology/Oncology (SSH-SSMO/SOHC) performance against Radiology/Nuclear Medicine (SGR-SSR) and Radiation-Oncology (SASRO), identifying factors influencing publication and authorship continuity.

Methods: A bibliometric analysis included 1,591 abstracts presented at SSH-SSMO (n = 418), SASRO (n = 402) and SGR-SSR (n = 771) from 2017–2019 and 2022–2023. The publication status was determined via PubMed. Associations between specialty, year, presentation type, gender, institutional affiliation, and publication effort tier were evaluated using chi-square tests, logistic regression, Firthpenalized models, and Kaplan–Meier time-to-publication analysis.

Results: Overall, 467 abstracts were published, with SSH-SSMO showing a publication rate (28.2%) comparable to that of other societies. 49.8% of first authors were female, and gender differences in publication rate were minor (26.0% for females vs 32.5% for males, p = 0.19), which stayed stable over time.Institutional affiliation did not predict publication. SSH-SSMO showed high first-author retention at publication (74.6%), lower than SGR-SSR (78.9%) but substantially higher than SASRO (57.9%). In logistic regression using SSH-SSMO as the reference group and adjusting for conference year, SSH-SSMO retained first authorship at more than twice the odds of SASRO (aOR 2.13, 95% CI 1.20–3.70; p = 0.009), and comparable odds to SGR-SSR (aOR 0.80 95% CI 0.47–1.35; p = 0.40). Gender, presentation type and affiliation did not influence retention. Effort distribution (low: case reports/letters; medium: retrospective studies; high: prospective/randomized trials) differed significantly across specialties (p <0.001). Hematology/oncology produced a disproportionate share of low-effort outputs (11.1%, vs 1.9% for Radiation-Oncology and 1.7% for Radiology/Nuclear Medicine) and the lowest proportion of high-effort publications (26.3%, vs 29.5% and 34.9%, respectively). This is the most distinctive weakness of the hematology/oncology output profile.

Conclusions: SSH-SSMO/SOHC demonstrates publication rates and first-author retention comparable to those of other Swiss societies, but shows a disproportionate share of low-effort publications. Targeted initiatives to support more substantive outputs may strengthen SOHC's scientific impact and visibility.

 Published under the CC license Attribution 4.0 International (CC BY 4.0)



5467

Safety and Tolerability of Bispecific Antibody Therapies Versus CAR-T Cell Therapy: A Systematic Review and Meta-Analysis

M. M. Bilal (1), A. Hizomi (2), S. K. Ayaanuddin (2)

Medicine, Caucasus international University, TBILISI (1), Medicine, Tbilisi State University, TBILISI (2)

Introduction: This systematic review and meta-analysis evaluate the relative incidence of (CRS) and (ICANS) between bispecific antibody therapies and CAR-T cell therapy to facilitate evidence-based treatment selection.

Methods: A systematic search was conducted across PubMed, Embase, and the Cochrane Library for clinical trials and observational cohort studies published between January 2021 and May 2026. Studies evaluating FDA/EMA-approved CAR-T (tisagenlecleucel, axicabtagene ciloleucel) or bispecific antibodies (glofitamab, talquetamide, mosunetuzumab) for lymphoma or multiple myeloma reporting detailed safety profiles were included. Study quality was assessed using QUADAS-2. A random-effects meta-analysis calculated pooled odds ratios (OR) for any-grade and severe (Grade ≥3) CRS and ICANS. Subgroup analyses stratified by disease stage and study design were performed to assess potential confounding by indication.

Results: Of 742 screened records, 34 studies comprising 4,812 patients were included (CAR-T: n = 2,150; BiTEs: n = 2,662). The pooled analysis revealed that any-grade CRS was significantly lower in patients treated with bispecific antibodies compared to CAR-T cell therapy (58.4% vs 81.2%; OR 0.32, 95% CI: 0.22–0.47, p <0.001). Severe CRS (Grade ≥3) occurred in 1.8% of the bispecific cohort versus 6.9% in the CAR-T cohort (OR 0.26, 95% CI: 0.12–0.56, p = 0.004). The incidence of any-grade ICANS was substantially reduced with bispecific antibodies compared to CAR-T therapy (9.2% vs 28.6%; OR 0.18, 95% CI: 0.11–0.29, p <0.001), with Grade ≥3 ICANS occurring in less than 1% of the bispecific antibody group. Subgroup analyses stratified by disease stage and refractory status yielded consistent findings, supporting the observation that lower neurotoxicity is an inherent property of bispecific antibody mechanisms. Heterogeneity between bispecific agents was noted, with glofitamab showing greater toxicity than talquetamide; however, all remained substantially lower than CAR-T comparators.

Conclusions: Bispecific antibodies demonstrate significantly more favourable safety profiles for CRS and neurotoxicity versus CAR-T therapies. These findings suggest bispecific antibodies offer more manageable treatment with reduced intensive care requirements, particularly valuable for centres lacking specialised cellular therapy infrastructure. Direct prospective head-to-head trials are warranted

8136

Efficacy and Safety of Venetoclax-Based Therapy Versus Intensive Chemotherapy in Newly Diagnosed Acute Myeloid Leukemia: A Systematic Review and Meta-Analysis

M. M. Bilal (1), S. K. Ayaanuddin (2), A. Hizomi (2)

Medicine, Caucasus international University, TBILISI (1), Medicine, Tbilisi State University, TBILISI (2)

Introduction: Venetoclax combined with hypomethylating agents has emerged as standard-of-care for newly diagnosed acute myeloid leukaemia (AML) in elderly and unfit patients. However, direct efficacy and safety comparisons with intensive chemotherapy remain limited. This meta-analysis evaluates treatment outcomes between venetoclax-based therapy and conventional chemotherapy in newly diagnosed AML

Methods: Systematic search of PubMed, Embase, and Cochrane Library (January 2018–May 2026) for randomised controlled trials and prospective cohort studies comparing venetoclax-hypomethylating agent therapy with intensive chemotherapy in newly diagnosed AML. Quality assessment via QUADAS-2 for observational studies and Cochrane Risk of Bias tool for RCTs. Random-effects meta-analysis calculated pooled odds ratios (OR) and 95% confidence intervals (CI) for complete remission (CR), CR with incomplete count recovery (CRi), overall survival (OS) at 2 years, and grade ≥3 adverse events

Results: 12 studies (2,847 patients; venetoclax-based n = 1,524; intensive chemotherapy n = 1,323) were included. CR/CRi rates were comparable between venetoclax and intensive chemotherapy (72.3% vs 68.9%; OR 1.18, 95% CI: 0.91–1.53, p = 0.22). Two-year overall survival was significantly higher with venetoclax therapy (65.4% vs 52.1%; OR 1.72, 95% CI: 1.31–2.26, p <0.001), particularly in patients ≥75 years. Severe adverse events (grade ≥3) occurred less frequently with venetoclax-based therapy (58.2% vs 71.8%; OR 0.56, 95% CI: 0.42–0.76, p = 0.001), with lower rates of febrile neutropaenia and infectious complications. Subgroup analyses confirmed consistent overall survival benefit across age groups and cytogenetic risk categories.

Conclusions: Venetoclax-hypomethylating agent therapy demonstrates superior overall survival compared with intensive chemotherapy in newly diagnosed AML, with significantly more favourable tolerability. These findings support expanding access to venetoclax-based regimens beyond elderly populations and reinforce paradigm shift away from intensive chemotherapy in AML management. Future studies should explore optimal sequencing and identify biomarkers predicting treatment response.

Published under the CC license Attribution 4.0 International (CC BY 4.0)

7085

Treatment choice in chronic lymphocytic leukaemia (CLL): physician and patient preferences in Switzerland

S. Müller (1), D. Feltrin (2), N. Heim (1), B. Peschke (3)

Institute of Marketing Management, ZHAW School of Management and Law, Winterthur (1), Commercial Department, AstraZeneca AG, Baar (2), Medical Department, AstraZeneca AG, Baar (3)

Introduction: Treatment choice in chronic lymphocytic leukaemia (CLL) increasingly requires shared decision-making given the growing range of targeted therapies. Prior studies often used discrete choice experiments (DCE) and identified progression-free survival (PFS) and treatment-related severe infection risk as key drivers of physician and patient treatment preferences. This first Swiss preference study builds on previous results, adding treatment-related fatigue as a novel attribute, to assess whether similar priorities apply in a different healthcare setting.

Methods: A choice-based conjoint (CBC) survey was administered to CLL physicians and patients across all three Swiss language regions (Mar 2023–Nov 2024). Respondents evaluated hypothetical treatment profiles defined by eight attributes: PFS, minimal residual disease, administration regimen, follow-up frequency, treatment-related diarrhoea, treatment-related severe infection risk, treatment-related hypertension risk, and treatment-related fatigue (see Table for the levels for each attribute). Relative importance (RI) values and part-worth utilities were estimated for physicians (n = 33) and patients (n = 27) based on a Hierarchical Bayes (HB) estimation; group differences were tested statistically.

Results: Treatment-related fatigue was the most important attribute for both physicians (RI: 20.8%) and patients (RI: 18.8%), ranking ahead of PFS (RI physicians: 19.5%; RI patients: 17.7%). Treatment-related diarrhoea ranked third for physicians (RI: 18.3%); administration regimen ranked third for patients (RI: 14.0%). For both physicians and patients, oral administration for 12 months and oral therapy for 24 months – two distinct levels – showed the highest part-worth utilities. Treatment-related severe infection risk ranked fourth for both groups (RI physicians: 12.6%; RI patients: 12.4%).

Conclusions: Treatment-related fatigue emerged as the leading attribute for both physicians and patients, ahead of PFS. Together with the shared preference for oral over intravenous administration, this indicates that day-to-day treatment burden, in addition to efficacy and safety, drives CLL treatment choice. These findings support fatigue management and oral regimen as priorities for shared decision-making. The small sample size limits precision, warranting confirmation in larger Swiss cohorts.

Attributes	RI			Levels	Part-worth utilities		
	Physicians	Patients	Sig.		Physicians	Patients	Sig.
PFS	19.5	17.7	p>0.10	24 mo	-3.48	-2.06	p<0.01
				36 mo	-1.59	-1.44	p>0.10
				48 mo	+1.44	+0.91	p>0.10
				60 mo	+3.63	+2.58	p<0.01
MRD	8.7	8.7	p>0.10	Detectable	-1.16	-1.05	p>0.10
				Undetectable	+1.16	+1.05	p>0.10
Administration regimen	8.7	14.0	p<0.01	IV 6 mo	-0.45	-0.61	p>0.10
				Oral 12 mo	+1.06	+1.47	p>0.10
				Oral 24 mo	+1.00	+1.67	p<0.05
				Oral continuous	-0.38	-1.81	p<0.01
				IV 6 mo + Oral 12 mo	-0.20	-0.71	p<0.05
				IV 6 mo + Oral 24 mo	-0.48	+0.74	p<0.01
				IV 6 mo + Oral cont.	-0.54	-0.74	p>0.10
Follow-up frequency	4.3	6.6	p<0.01	Monthly	+0.14	+0.15	p>0.10
				Quarterly	-0.12	+0.40	p<0.05
				Half-yearly	-0.01	-0.55	p<0.05
Treatment-related diarrhoea	18.3	12.4	p<0.01	0x/day	+2.38	+0.50	p<0.01
				1-2x/day	+1.85	+1.30	p<0.05
				3-7x/day	-4.23	-1.79	p<0.01
Treatment-related severe infection risk	12.6	12.4	p>0.10	5%	+2.12	+1.82	p>0.10
				15%	+0.37	-0.76	p<0.01
				30%	-2.49	-1.06	p<0.01
Treatment-related hypertension risk	7.0	9.4	p<0.01	0%	+0.03	-0.32	p>0.10
				5%	+1.08	+1.10	p>0.10
				10%	-0.05	+0.35	p>0.10
				15%	-1.07	-1.13	p>0.10
Treatment-related fatigue	20.8	18.8	p>0.10	None	+2.99	+1.75	p<0.01
				Mild	+1.64	+0.66	p<0.05
				Moderate	+0.17	+0.47	p>0.10
				Severe	-4.80	-2.88	p<0.01

Published under the CC license Attribution 4.0 International (CC BY 4.0)

SSMO POSTER PRESENTATION - CLINICAL SOLID TUMOR ONCOLOGY

3009

Multimodal AI Recurrence Risk Stratification Is Maintained in Patients Aged ≥70 Years With Breast Cancer

E. D. Chiru (1), L. Sojak (1), S. Muenst (2), J. Witowski (3), K. Zeng (3), C. Tang (3), C. Kurzeder (4), M. Vetter (1)

Oncology and Hematology, Cantonal Hospital Baselland, Liestal (1), Medical Genetics and Pathology Institute, University Hospital Basel, Basel (2), Research and Development, ATARAXIS, New York (3), Breast Center, University Hospital Basel, Basel (4)

Introduction: Older patients with breast cancer are underrepresented in the validation of contemporary prognostic tools, despite substantial heterogeneity in recurrence risk and treatment fitness. Ataraxis Breast RISK (ATX) is a locked multimodal artificial intelligence model integrating digitized H&E histopathology with clinicopathological variables to estimate recurrence risk. We evaluated whether ATX maintains prognostic performance in patients aged ≥70 years compared with younger patients.

Methods: ATX was evaluated across five independent breast cancer cohorts not used for model development. Patients were stratified by age at diagnosis into ≥70 and <70 years. The primary endpoint was an approximation of recurrence-free interval (RFI), defined as time from diagnosis to first documented breast cancer recurrence. Because cause-of-death information was unavailable, deaths without prior documented recurrence were censored. Prognostic discrimination was assessed using Harrell's C-index, Cox proportional hazards models and Kaplan–Meier analysis. ATX low versus high risk was defined using a 10% predicted 5-year recurrence-risk threshold.

Results: The analysis included 2,324 patients, including 461 aged ≥70 years and 1,863 aged <70 years. ATX showed comparable prognostic discrimination in older and younger patients, with pooled C-indices of 0.723 (95% CI 0.559–0.843) and 0.725 (95% CI 0.654–0.786), respectively. Among patients ≥70 years, estimated 5-year RFI was 0.97 (95% CI 0.93–0.99) in the ATX low-risk group versus 0.83 (95% CI 0.75–0.89) in the high-risk group (log-rank p <0.001). Corresponding estimates in patients <70 years were 0.95 (95% CI 0.94–0.96) and 0.83 (95% CI 0.79–0.87; p <0.001). In multivariable analysis, ATX remained independently associated with recurrence risk (HR per 1-SD increase 1.42, 95% CI 1.14–1.77; p <0.005), whereas age group was not (HR 1.02; p = 0.93).

Conclusions: ATX demonstrated comparable prognostic performance in patients aged ≥70 and <70 years and significantly separated low- and high-risk older patients. These findings suggest that multimodal AI-based recurrence prediction captures prognostic information beyond chronological age and may provide a useful approach to risk stratification in older patients with breast cancer. Prospective validation in dedicated older-patient cohorts is warranted.

9316

Obesity Paradox on Oncological Outcomes in Patients Treated with Robotic Stereotactic Body Radiotherapy for Primary Prostate Cancer

M. Elleisy (1), N. Bachmann (1), S. Oberhansl (1), A. Althaus (1), L. Mose (2), D. Aebersold (1), M. Shelan (1)

Radiation Oncology, University Hospital of Bern, Bern (1), Radiation Oncology, University Hospital Heidelberg, Heidelberg (2)

Introduction: The prevalence of obesity is increasing rapidly worldwide. The “obesity paradox” suggests that obesity may be associated with improved outcomes in some malignancies, but evidence in prostate cancer (PCa) remains conflicting. This study evaluated the impact of body mass index (BMI) on oncological outcomes in patients treated with robotic stereotactic body radiotherapy (SBRT) for primary PCa.

Methods: Data from patients treated with robotic SBRT for primary PCa between 2014 and 2025 were retrospectively collected at our centre. Patients were stratified by BMI into normal weight (NW, <25 kg/m²), overweight (OW, 25–29.9 kg/m²), and obese (OB, ≥30 kg/m²) groups. Clinical progression-free survival (cPFS; time from end of SBRT to biochemical recurrence [Phoenix criteria] or local, nodal, or distant recurrence) and overall survival (OS) were compared using Kaplan-Meier and multivariable Cox regression, adjusted for D’Amico risk group, age, hormonal therapy, and type 2 diabetes mellitus (T2DM). Acute and late GI/GU toxicities were graded according to CTCAE v5.0.

Results: A total of 319 patients were included (median follow-up 30.8 months), of whom 115 (36%) were NW, 135 (42%) OW, and 69 (22%) OB. T2DM prevalence increased significantly with BMI (14.8% NW, 27.4% OW, 55.1% OB; p <0.001). 1-, 3-, and 5-year cPFS rates were 98.9%, 82.0% and 65.6% (NW), 94.7%, 86.0% and 74.4% (OW), and 93.1%, 76.5% and 62.3% (OB); corresponding OS rates were 99.0%, 89.9% and 85.4%, 100%, 93.2% and 89.4%, and 98.3%, 84.7% and 74.7%. On multivariable analysis, neither OW nor OB (vs. NW) was independently associated with cPFS (HR 0.66, 95% CI 0.38-1.14, p = 0.134 and HR 0.84, 95% CI 0.44-1.62, p = 0.607) or OS (HR 0.68, 95% CI 0.30-1.52, p = 0.344 and HR 1.14, 95% CI 0.46–2.85, p = 0.776), whereas T2DM independently predicted worse cPFS (HR 1.68, 95% CI 1.03-2.74, p = 0.038). Recurrence pattern (local/regional/distant) differed significantly across BMI groups (p = 0.033). No significant difference in grade ≥3 GU and GI toxicities at any time during follow-up was observed.

Conclusions: Among patients treated with robotic SBRT for primary PCa, BMI category was not independently associated with cPFS or OS, arguing against an obesity paradox in this setting. T2DM, rather than obesity itself, appears to be the more relevant independent adverse prognostic factor.

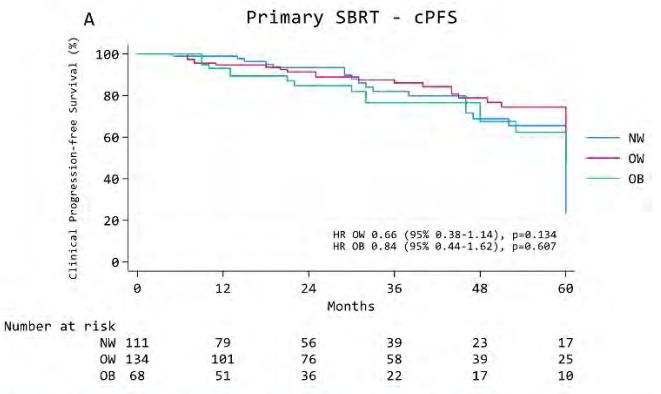


Figure 1. Clinical progression-free survival by BMI group for primary PCa.

HR with 95% CI was estimated using adjusted Cox regression.

CI, confidence interval; cPFS, clinical progression-free survival; HR, hazard ratio; NW, normal weight; OB, obese; OW, overweight; SBRT, stereotactic body radiation; PCa, prostate cancer.

Published under the CC license Attribution 4.0 International (CC BY 4.0)

8238

Avelumab first-line maintenance for locally advanced or metastatic urothelial carcinoma in Europe and Russia: Interim results from the AVENUE study

D. Zihler (1), A. Sultanbaev (2), A. L. Brachtel (3), M. Z. Poves (4), S. Rausch (5), K. Schlack (6, 7), S. Hoch (8), S. Banek (9), A. García Domínguez (10), I. González (11), N. Lainez (12), U. Anido (13), G. Niegisch (14, 15), A. Kohler (16), A. M. Diaz (17), S. Bhunia (18), T. Hack (19), J. Hoffman (20), P. J. Goebell (21), J. E. Gschwend (22), D. Zihler (1)

Department of Medical Oncology, Hematology, and Transfusion Medicine, Cantonal Hospital Aarau, Aarau (1), Department of Chemotherapy, Republican Clinical Oncology Dispensary, Ufa (2), Department of Urology, Vincent Hospital Hannover, Hannover (3), Department of Medical Oncology, Hospital Universitario Morales Meseguer, Murcia (4), Department of Urology, University Hospital Tuebingen, Tuebingen (5), Department of Urology and Pediatric Urology, University Hospital Muenster, Muenster, North Rhine-Westphalia (6), Department of Urology, West German Cancer Centre, University Hospital Muenster, Muenster (7), Uro-Oncology and Surgical Urology, UroCompass Urology Practice, Berlin (8), Department of Urology, University Hospital Dresden, Dresden (9), Department of Medical Oncology, Complejo Asistencial Universitario de Salamanca, Salamanca (10), Hospital Son Llátzer, Palma de Mallorca, Hospital Son Llátzer, Palma de Mallorca, Spain, Palma de Mallorca (11), Hospital Universitario de Navarra, Hospital Universitario de Navarra, Pamplona (12), Medical Oncology Department, Complejo Hospitalario Universitario de Santiago,, Santiago de Compostela (13), Department of Urology, Medical Faculty, University Hospital Düsseldorf, Düsseldorf (14), Department of Urology, Centre for Integrated Oncology (CIO) Düsseldorf, CIO Aachen-Bonn-Cologne-Düsseldorf, Düsseldorf (15), Department of Oncology, Cantonal Hospital Baselland, Liestal (16), Department of Medical Oncology, University Hospital of A Coruña, A Coruña (17), Department of Statistics, Merck Specialities Pvt. Ltd., Hyderabad, India, an affiliate of Merck KGaA, Hyderabad (18), Department of oncology, Merck Healthcare Germany GmbH, Weiterstadt, Germany, an affiliate of Merck KGaA, Weiterstadt (19), Department of oncology, EMD Serono, Billerica, MA, USA, an affiliate of Merck KGaA, Billerica (20), Department of Urology and Pediatric Urology, University Hospital Erlangen, Erlangen, Germany, Erlangen (21), Department of Urology, Technical University of Munich, School of Medicine and Health, Munich (22)

Introduction: Avelumab first-line maintenance (1LM) is recommended for patients with locally advanced or metastatic urothelial carcinoma (la/mUC) without disease progression after first-line (1L) platinum-based chemotherapy (PBC) based on results from the JAVELIN Bladder 100 phase 3 trial. AVENUE confirmed the effectiveness and safety of avelumab 1LM in routine practice in Germany, Spain, Switzerland, and Russia. We report ad hoc interim analyses of the first half of the enrolled overall population.

Methods: AVENUE is an ongoing, prospective, real-world study of patients with la/mUC without progression after 1L PBC who initiated avelumab 1LM before enrolment at the discretion of the treating physician, per local approval. The primary objective is to evaluate the overall survival (OS) rate at 12, 24, and 36 months. Secondary objectives include assessment of median OS, progression-free survival (PFS), and safety.

Results: At data cutoff (December 12, 2025), in the overall population (N = 177, including 17 patients from Switzerland), median follow-up was 20.1 months, median age was 70 years (range, 43–89), 78.0% were male, and 89.3% had ECOG performance status of 0/1. Primary tumour site was upper or lower tract in 27.7% and 72.3%, respectively. 1L PBC regimen was gemcitabine + cisplatin in 61.0% (split dose, 8.5%) and gemcitabine + carboplatin in 36.2% of patients. At data cutoff, 17 patients (9.6%) remained on avelumab and 72 had received subsequent therapy, most commonly with an antibody-drug conjugate (ADC; 68.1%). Effectiveness and safety outcomes are shown in the Table.

Conclusions: Interim data from AVENUE further support the effectiveness and safety of avelumab 1LM in a heterogeneous population with la/mUC.

Endpoint	Overall (N=177)
OS from avelumab start	
Median (95% CI), months	26.1 (18.5-32.5)
12-month rate (95% CI), %	66.9 (59.3-73.4)
18-month rate (95% CI), %	58.2 (50.4-65.3)
PFS from avelumab start	
Median (95% CI), months	6.2 (4.6-10.0)
12-month rate (95% CI), %	37.2 (29.8-44.5)
18-month rate (95% CI), %	28.6 (21.8-35.7)
Treatment-related adverse events, n(%)	
Any grade	111 (62.7)
Grade ≥3	29 (16.4)
Serious	27 (15.3)
Leading to permanent discontinuation	21 (11.9)
Leading to death	2 (1.1)
NE, not estimable	

2690

Beyond Chronological Age: Real-World Association Between Age and G8 Screening Scores in Older Adults With Cancer

E. D. Chiru (1), D. Hašek (1), D. Wirth (1), C. Müller (2), H. Unger (2), T. Wallrabenstein (1), M. Sonderegger (1), M. Vetter (1)

Oncology and Hematology, Cantonal Hospital Baselland, Liestal (1), Geriatrics, Cantonal Hospital Baselland, Liestal (2)

Introduction: Frailty and geriatric vulnerability are increasingly relevant to treatment decisions in older patients with cancer. The G8 screening tool is widely used to identify patients who may benefit from comprehensive geriatric assessment (CGA). However, chronological age itself contributes to the G8 score, raising the question of whether lower scores in older patients primarily reflect age or broader multidimensional vulnerability. We investigated the relationship between chronological age and G8 scores in a real-world oncology population.

Methods: We performed a retrospective single-center analysis of consecutive patients with documented G8 screening between January 2024 and April 2026 at the Cancer Center Baselland. Patients were categorized as <70, 70–≤80, >80–≤90, and >90 years. G8 scores were summarized according to age group, and associations between chronological age and total G8 score were assessed using Pearson and Spearman correlation analyses.

Results: A total of 281 evaluable G8 assessments were included. Most patients were aged 70–≤80 years (n = 167) or >80–≤90 years (n = 99). Mean G8 scores decreased from 12.58±2.64 in patients aged 70–≤80 years to 11.44±3.04 in those aged >80–≤90 years and 11.35±1.70 in patients >90 years. Chronological age demonstrated a weak but statistically significant inverse association with G8 score (Pearson $r = -0.151$, $p = 0.011$; Spearman $\rho = -0.139$, $p = 0.020$), with substantial interindividual variability across age groups.

Conclusions: Increasing age was associated with modestly lower G8 scores, but the weak correlation indicates that chronological age explains only a limited proportion of geriatric vulnerability. These findings support structured frailty screening rather than age-based assumptions when assessing older patients with cancer. In breast oncology, where treatment intensity frequently requires balancing efficacy against functional reserve and toxicity risk, routine G8 screening may help identify patients who warrant CGA and individualized supportive interventions.

 Published under the CC license Attribution 4.0 International (CC BY 4.0)

1815

Patient reported long term functional outcome after treatment of localized rectal cancer: a cross-sectional study (PROCRESS)

J. G. Gorges (1), T. J. Jumuga (2), S. B. Bastian (3), R. C. Cathomas (3)

Internal Medicine, Cantonal Hospital Graubünden, Chur (1), Biostatistic, SAKK Competence Center, Bern (2), Oncology, Cantonal Hospital Graubünden, Chur (3)

Introduction: Localized rectal cancer is commonly treated with surgery alone or neoadjuvant chemoradiotherapy followed by surgery. Total neoadjuvant therapy (TNT) including polychemotherapy followed by chemoradiotherapy with or without surgery has recently been introduced. A common complication after rectal surgery is bowel, urinary and/or sexual dysfunction which impairs the quality of life (QOL). Preoperative chemotherapy (CT) and radiotherapy (RT) might alter the functional outcome but in some cases, patients might be spared the surgery. There is a lack of data on patient reported outcomes after different treatment modalities for rectal cancer.

Methods: All patients who were treated for localised rectal cancer in curative intention at Kantonsspital Graubünden from January 2019 to January 2024 and had minimal follow up of 12 months since diagnosis were included. Baseline characteristics, treatment details, MRI findings, operation reports and histopathology results were reviewed in the electronic health record. Patient reported quality of life including bowel, urinary and sexual function after treatment was assessed with different questionnaires (FACT-C, EORTC QLQ CR29, LARS) during a personal interview. Primary endpoint was the Trial Outcome Index (TOI), a summary score of FACT-C subscales (PWB, FWB, CSS) according to the different treatment approaches. Secondary endpoints were FACT-C total score, low anterior resection syndrome (LARS) score and urinary and sexual dysfunction (CR29).

Results: 35 patients were included, interviewed between 04/2025 to 08/2025 and divided in 3 treatment groups: A (surgery only, n = 6), B (CT+CT/RT+surgery, n = 10) and C ((CT)/RT +surgery, n = 16). 3 patients had no surgery (watch & wait strategy) and were excluded from group comparison: A vs. B+C. TOI was in group A 74.5 points and 78.0 in B+C (p = 0.65). There was no significant difference between A and B+C in FACT-C (122.5 vs 128.0), major LARS (33% vs. 57%) and the median in urinary incontinence, urinary frequency, impotence and sexual interest. Real life data showed a high rate of omitted rigid rectoscopies of 26% (N = 9/35) in the staging process, mainly due to pain.

Conclusions: There was no significant difference between neoadjuvant TNT, (Chemo-)/RT and surgery alone groups in TOI and secondary endpoints. In total all groups described a good QOL, there was no significant impact on QOL due to neoadjuvant TNT.

8174

Oncogene-Driven Genomic Profiles are Linked to Poor Overall Survival in Muscle-Invasive Bladder Cancer (MIBC)

C. Poyet (1), A. S. Franzen (2), U. Bieri (2), E. Kaufmann (3), D. Eberli (4), M. Schmid (5), M. Zoche (5), H. Moch (5), M. Lork (4)

Department of Urology, Stadtspital Triemli, Zurich (1), Division of Urology, Department of Surgery, Kantonsspital Baden, Baden (2), Department of Urology, Luzerner Kantonsspital, Lucerne (3), Department of Urology, University Hospital Zurich, Zurich (4), Department of Pathology and Molecular Pathology, University Hospital Zurich, Zurich (5)

Introduction: Muscle-invasive bladder cancer (MIBC) is a genomically complex disease with limited biomarkers for predicting patient outcomes. This study aimed to identify molecular correlates of overall survival in MIBC through comprehensive genomic profiling.

Methods: Tumor DNA from cystectomy specimens of 32 MIBC patients was analyzed using the FoundationOne® CDx platform. Patients were categorized into a favorable outcome group (overall survival ≥60 months, n = 14) and a poor outcome group (overall survival <60 months, n = 18). Mutational profiles, genomic instability markers, and copy number alterations were compared between groups.

Results: Across the cohort, 279 pathogenic or likely pathogenic mutations were identified in 88 genes. Frequently altered genes - including TP53, PIK3CA, KDM6A, and FGFR3 - showed similar distributions across outcome groups. Genomic instability markers including tumor mutational burden (TMB) and microsatellite instability (MSI) were comparable and not prognostically informative. In contrast, tumors from the poor outcome group exhibited significantly higher frequency and burden of gene amplifications, often involving known oncogenes and co-amplification hotspots.

Conclusions: These exploratory findings suggest that oncogene amplifications, rather than traditional genomic instability metrics, are associated with poor overall survival in MIBC, warranting validation in larger cohorts to assess their potential relevance as prognostic markers and therapeutic targets.

5406

Real-World Prevalence of HER2 IHC 3+ in Unselected NSCLC: Implications for Testing Strategy

M. Lipp (1), L. Boos (2), O. Chijioke (1, 3), C. Pauli (1, 3), M. Haberecker (1)

Pathology and Molecular Pathology, University Hospital Zurich, Zurich (1), Medical Oncology and Hematology, University Hospital Zurich, Zurich (2), Medical Faculty, University of Zürich, Zurich (3)

Introduction: HER2 overexpression has emerged as a clinically actionable biomarker across multiple solid tumors, with trastuzumab deruxtecan (T-DXd) approved for HER2-positive (IHC 3+), unresectable or metastatic solid tumors after prior systemic therapy. However, real-world data on the prevalence, molecular context, and potential treatment implications of HER2 IHC 3+ status in unselected NSCLC remain limited.

Methods: A total of 316 consecutive NSCLC cases with documented patient consent underwent routine baseline reflex molecular testing using the Oncomine Precision Assay at a single center, including HER2 IHC testing. HER2 expression was scored according to the gastric cancer HER2 scoring criteria. Clinicopathologic features, co-occurring genomic alterations, and treatment courses were analyzed for all HER2 IHC 3+ cases.

Results: HER2 IHC 3+ was identified in 19/316 cases (6%), all adenocarcinomas. Median age was 74 years (range 54–85) and 53% of patients were male. Stage at diagnosis spanned early to advanced disease, 18/19 cases (95%) were identified at first diagnosis, with one case (5%) identified at relapse. An approved actionable driver alteration was present in 4/19 cases (21%: MET exon 14 skipping, atypical EGFR mutation, KRAS G12C (n = 2)); ERBB2 amplification was found in 2/19 cases (11%) but is not independently targetable in NSCLC. Six received systemic therapy with palliative intent. None had received T-DXd by data cut-off (09/2026): three still receiving first-line therapy (two in maintenance without progression, one after local progression), two died before or during first-line therapy, and one was lost to follow-up. One further patient treated with curative intent has suspected progression and is a potential T-DXd candidate.

Conclusions: HER2 IHC 3+ identifies a clinically relevant NSCLC subgroup, independent of ERBB2 alterations and other

 Published under the CC license Attribution 4.0 International (CC BY 4.0)

actionable drivers. However, universal reflex HER2 IHC testing at initial NSCLC diagnosis may have limited clinical utility and incurs testing costs without immediate treatment implications. HER2 IHC testing at relapse or progression, particularly in driver-negative disease, may provide a clinically feasible and cost-efficient testing strategy.

Table 1: Clinico-pathological characteristics of Her2 3+ (over expression) cases

#	Stage	Age	Sex	Histology	NGS Alterations	ERBB2 Status	Actionable Driver	PD-L1	Therapy	Follow-up
1	IA1	84	F	AC	MET ex14	no alteration	MET ex14	neg.	Local (surgery)	pT1a pN0 R0 no recurrence
2	IV	75	M	AC	TP53 G244C	no alteration	none	neg.	KEYNOTE-189 -> *2nd line T-Dxd	Lost to follow-up after 4 cycles (relocated)
3	IA2	85	M	AC	KRAS G12V; GNAS R201C	no alteration	none	neg.	Local (SBRT)	SBRT completed no recurrence
4	IIIA	75	M	AC	No alteration detected	no alteration	none	TC3	Surgery + adj. therapy IM-power001 -> *Relapse, re-biopsy	Atezolizumab maintenance; no progression
5	IIIA	65	M	AC	KRAS G12V	no alteration	none	TC2	Surgery + adj. chemotherapy -> *2nd line T-Dxd	Adj. chemotherapy completed, suspected osseous progression
6	IV	62	F	AC	FGFR1 Amp; EGFR G719C; CDK4 R24H; EGFR E709V	no alteration	EGFR G719C/ E709V	TC3	Amivantamab and Lazertinib	deceased before treatment initiation
7	IA2	75	M	AC	KRAS G12F	no alteration	none	TC1	Local (surgery + SBRT by 3 synchronous AC)	Index lesion treated with SBRT no recurrence
8	IB	79	F	AC	KRAS G12C	no alteration	KRAS G12C	TC3	Local (surgery)	pT2a pN0 R0 no recurrence
9	IV	71	F	AC	TP53 K132R; EGFR Amp.	no alteration	none	TC2	KEYNOTE-189 -> *2nd line T-Dxd	Pem/Pem maintenance no progression
10	IA	71	F	AC	BRAF G464V; TP53 G262V	no alteration	none	TC3	Local (surgery + SBRT by 2 synchronous AC)	Index lesion treated with SBRT no recurrence
11	IIA	84	M	AC	KRAS Q61L	no alteration		TC3	Local (SBRT, by 2 synchronous AC)	SBRT completed local progress under Pembrolizumab
12	IV	54	M	AC	TP53 R280Efs*65; KRAS G13C; CDKN2A del	no alteration		TC2	CheckMate 9LA -> *2nd line T-Dxd	Nivolumab maintenance no progression
13	IIA	73	F	AC	KRAS low-amp; KRAS G12C	no alteration		neg.	-> *1st line: CodeBreaK- 202 or SUNRAY-01 -> *2nd line T-Dxd	Pneumonectomy (external institution) no recurrence
14	IIIC	78	F	AC	No alteration detected	no alteration		neg.	Radio-chemotherapy followed by re-evaluation -> *2nd line T-Dxd	SBRT completed, nodal progression treated with SBRT. no recurrence
15	Local relapse	75	M	AC, SMARCA4 - def.	BRAF N581I; TP53 G262V	no alteration		TC3	Local therapy (SBRT) -> *1st ICI mono -> *2nd line T-Dxd	SBRT completed, no recurrence
16	IIIB	73	M	AC, mucinous	No alteration detected	no alteration		neg.	Neoadj. KEYNOTE-671	deceased after neoadj. therapy
17	IIB	72	F	AC, mucinous	GNAS R201S; KRAS G12D	no alteration		neg.	AEGEAN (evaluation for ADOPT-Trial)	ypT3 ypN0 R0 adj. Durvalumab ongoing
18	IA2	73	M	AC	ERBB2 Amp; TP53 R273L	amplified		neg.	Local (SBRT)	SBRT completed no recurrence
19	IV	79	F	AC	ERBB2 Amp	amplified		neg.	IPSOS-Trial	Deceased after 1 cycle of atezolizumab, immune-related hepatitis

Tumor stages at primary diagnosis as per the 9th edition of the UICC TNM classification. Asterisk (*) therapies that are planned/anticipated as the next line. AC: Adenocarcinoma, MET ex14: Met-Exon 14 Skipping Event, Amp.: amplification, PD-L1 TC1: 1-4%, PD-L1 TC2:5-49%, PD-L1 TC3: ≥50%. SBRT: stereotactic body radiotherapy. Pem/ Pem: Pemetrexed/ Pembrolizumab. T-DXd: trastuzumab deruxtecan. ICI: immune checkpoint inhibitor.

0393

Investigating Pemetrexed's Role in Maintenance Therapy for Metastatic Non-Squamous NSCLC After Platinum-Based Chemo-Immunotherapy with Pembrolizumab

L. A. Boos (1), M. Sarwary (1), L. Hempel (1), N. Miglino (1), L. Fábregas-Ibáñez (1), A. Wicki (1)

Department of Medical Oncology and Hematology, University Hospital Zurich, Zurich (1)

Introduction: For metastatic non-squamous non-small-cell lung cancer (NSCLC), pembrolizumab plus platinum-based chemotherapy is a standard first-line treatment, while the optimal maintenance strategy remains unclear. This study investigates the benefit of adding pemetrexed to pembrolizumab maintenance following platinum-based chemotherapy.

Methods: A retrospective analysis included 121 patients with metastatic non-squamous NSCLC treated with first-line platinum-doublet chemotherapy plus pembrolizumab between January 2024 and December 2025. Maintenance consisted of pembrolizumab monotherapy following de-escalation (n = 27), pembrolizumab plus pemetrexed (n = 44), or pemetrexed monotherapy (n = 8). Primary progression or death occurred in 42 patients. Overall survival (OS) and progression-free survival (PFS) were analyzed using Kaplan–Meier estimates, with subgroup analyses by PD-L1 expression (TC0, TC1–2, TC3), oncogenic driver status and Central nervous system (CNS) metastases.

Results: OS was significantly longer with pembrolizumab maintenance monotherapy compared with combination maintenance therapy (35 vs 24 months; HR 0.41, 95% CI 0.24-0.72; p = 0.002). PFS was also observed longer with monotherapy (9.0 vs 6.0; HR 0.61; 95% CI 0.38-0.99 p = 0.035). In an exploratory analysis excluding patients with high PD-L1 expression (TC3), a similar trend toward improved OS with monotherapy was observed (HR 0.41; p = 0.002). Among patients with intermediate PD-L1 expression (TC1–2), monotherapy was associated with longer OS and PFS (36 vs. 16; HR 0.43; p = 0.032 respectively 9.0 vs 5.0; HR 0.46; p = 0.016). A OS benefit was also observed in patients without targetable oncogenic drivers (32 vs. 25; HR 0.47; p = 0.028). Amid patients without CNS metastases, OS was longer with monotherapy (32.5 vs 20.0; HR 0.36; p = 0.006). No significant differences in OS (35 vs 36.8; p = 0.211) or PFS (9.5 vs 8.8; p = 0.463) were observed between pembrolizumab and pemetrexed monotherapy.

 Published under the CC license Attribution 4.0 International (CC BY 4.0)

Conclusions: In this retrospective cohort, pembrolizumab maintenance monotherapy was associated with longer survival than combination maintenance, particularly in patients with intermediate PD-L1 expression, without oncogenic drivers or CNS metastases. Given the retrospective, non-randomized design and small subgroups, further studies are needed to define the optimal maintenance strategy after first-line chemo-immunotherapy.

ONCOREHA/OPS/PALLIATIVE.CH/SNIO/SOHC POSTER PRESENTATION - NURSING, SUPPORTIVE & PALLIATIVE CARE, REHABILITATION & SURVIVORSHIP AND INTEGRATIVE ONCOLOGY

1625

Structured hypnotherapy during (neo)adjuvant chemotherapy: a randomized controlled study

C. Urech (1), I. Ge (1, 2), A. Wiencierz (3), C. Wenk (1), C. Mang (1), A. Oseledchyk (4), A. Brandt (4), D. Schäfer-Rohr (1), A. Kölle (1), C. Balmelli (1), L. Basic (5), F. D. Schwab (1, 2), C. Montavon (1), W. P. Weber (2), V. Heinzelmann (1), C. Schwegler (1), C. Kurzeder (1, 2)

Gynecology and Gynecologic Oncology, University Hospital Basel, Basel (1), Breast Clinic, University Hospital Basel, Basel (2), Department of Clinical Research, University Hospital Basel, Basel (3), Medical Oncology, University Hospital Basel, Basel (4), Faculty of Medicine, University of Basel, Basel (5)

Introduction: Chemotherapy is frequently associated with impaired health-related quality of life (QoL) and psychological distress in cancer patients. Evidence-based supportive care interventions during systemic treatment remain limited. This randomized controlled trial is the first to evaluate structured hypnotherapy delivered during chemotherapy.

Methods: Breast cancer patients undergoing neoadjuvant or adjuvant chemotherapy were randomized to standard supportive care including psycho-oncological support with or without an adjunctive structured hypnotherapy programme. The intervention comprised up to 10 face-to-face sessions. Audio recordings were provided and self-hypnosis encouraged. The primary endpoint was average global QoL during chemotherapy assessed using the EORTC QLQ-C30 global health status/QoL scale. Secondary endpoints included anxiety and depression measured by the Hospital Anxiety and Depression Scale (HADS) and psychosocial distress assessed by the Distress Thermometer (DT). Analyses followed the intention-to-treat (ITT) principle using baseline-adjusted linear regression. A per-protocol (PP) sensitivity analysis included patients who attended at least three hypnotherapy sessions.

Results: In the ITT set (n = 61), hypnotherapy was associated with a consistent trend towards higher average QoL during chemotherapy compared with standard care. The baseline-adjusted mean difference was 3.9 points (95% CI −3.4 to 11.2; p = 0.287) favoring hypnotherapy. PP analysis demonstrated a numerically larger effect size of 4.9 points (95% CI −2.7 to 12.5; p = 0.204), supporting an enhanced effect among patients adherent to the hypnotherapy intervention. Anxiety, depression and distress declined over time in both groups, with numerically greater reductions in the hypnotherapy group. Importantly, mean DT scores fell below the threshold for clinically significant distress (<4) only in patients receiving hypnotherapy at follow-up.

Conclusions: Structured hypnotherapy during chemotherapy is feasible and associated with consistent favorable trends in QoL and psychosocial outcomes, including a clinically relevant reduction in distress. These results highlight hypnotherapy as a promising integrative supportive care approach and support further evaluation in larger randomized trials.

3508

Broad in ambition, thin in commitment: what Switzerland's first national cancer plan needs before adoption

S. Schobinger (1)

SwissCAPA Board of Directors, Swiss Cancer Patient's Alliance (SwissCAPA), Berne (1)

Introduction: Switzerland is preparing its first National Cancer Plan (NCP 2027–2032). We assessed how the consultation draft compares internationally on three separate scales: patient co-design, implementation commitment and thematic scope.

Methods: Document analysis of 31 national cancer plans (27 EU member states, UK, Canada, Australia, USA) and the Swiss draft (27 May 2026). Full plan texts were coded on these scales: implementation commitment (operational depth, accountability framework, multi-year funding, national coordinating body; binary, 0–4), patient co-design (five indicators, 0/0.5/1; 0–5) and thematic scope (26 dimensions; "anchored" = dedicated objective or measure with lead and timeline). Funding counted only where the plan states committed amounts. Plans in other languages were machine-translated in full; EU plans were cross-checked against the OECD/EC Country Cancer Profiles 2025. Ambiguities were resolved conservatively; scales were not aggregated; reference values exclude Switzerland.

Results: On patient co-design the Swiss draft scored 2.5/5, below the median of 3.0 (IQR 2.0–4.3): consultation is documented, but patient organisations are not co-authors and no seat is reserved in plan oversight, which 9 of 31 plans provide; 10 plans are coded co-produced. On implementation commitment it scored 2/4, at the median of 2 (IQR 1–3): measures with leads and timelines, but no accountability framework and no committed funding; five plans quantify a dedicated multi-year budget. On thematic scope it names 17 of 26 dimensions but anchors 7, the lowest of all 31 plans (median 17). Nine dimensions are structural gaps, among them genetic counselling, tumour boards, rare cancers, adolescents and young adults, fertility preservation, a survivorship passport and the right to be forgotten. Ten more, including psycho-oncology, caregiver support and return to work, are named without an objective or measure of their own.

Conclusions: The gap is not in the topics the draft names but in how it commits to them. Before adoption it needs a reserved seat for patient representatives in plan governance, binding milestones with mandatory public reporting, a committed multi-year budget, and concrete measures for the dimensions it only mentions - each standard practice in the comparator plans. Findings reflect plan documents, not implementation or outcomes.

 Published under the CC license Attribution 4.0 International (CC BY 4.0)

1994

Emergency Department Visits and Hospitalisations in Older Adults with Cancer: A Retrospective Cohort Study

I. Besser (1), C. Müller (2), M. Sonderegger (3), H. Unger (4), D. Wirth (3), N. Geigy (5), F. Dreyer (6), M. Vetter (3, 7, 8)

Center for Aging and Rehabilitation, Cantonal Hospital Baselland, Bruderholz (1), Department of Nursing and Therapies, Cantonal Hospital Baselland, Liestal (2), Center of Oncology and Hematology, Cantonal Hospital Baselland, Liestal (3), Center for Aging and Rehabilitation, Cantonal Hospital Baselland Bruderholz, Bruderholz (4), Emergency Department, Cantonal Hospital Baselland, Liestal (5), Medical Data Science Service Center, Bielefeld University, Bielefeld (6), Medical University Clinic, Cantonal Hospital Baselland, Liestal (7), Faculty of Medicine, University of Basel, Basel (8)

Introduction: Older adults with cancer frequently require emergency department (ED) visits and unplanned hospitalisations. We evaluated acute-care utilisation and factors associated with hospitalisation, length of stay (LOS), and survival in patients aged ≥70 years treated at a community cancer centre.

Methods: We conducted a retrospective single-centre chart review of patients aged ≥70 years with an oncological diagnosis and at least one ED visit and/or hospital admission between January 2023 and December 2024. Demographic, oncological, clinical, treatment-related, social, and acute-care data were extracted from electronic health records. Repeated encounters within patients were accounted for using patient-clustered generalised estimating equation (GEE) models where appropriate. Associations between reasons for hospitalisation and LOS were assessed using a multivariable GEE model with gamma distribution and log link. Survival was evaluated using time-to-event analysis.

Results: A total of 155 patients (54.2% male) with a median age of 78 years (IQR 76-81; range 73-96) contributed 552 acute-care encounters. Of these, 321 (58.2%) were ED visits followed by hospitalisation, 84 (15.2%) were ED visits without hospitalisation, and 147 (26.6%) were direct hospitalisations. Across 468 hospitalisations, median LOS was 8 days (IQR 5-12) following ED admission and 6 days (IQR 4-9) following direct hospitalisation. Reasons for acute-care utilisation differed significantly across care pathways in patient-clustered analyses. In the multivariable model, disease progression (adjusted LOS ratio 1.38, 95% CI 1.18-1.61), infections (1.34, 95% CI 1.15-1.56), and a new tumour diagnosis (1.67, 95% CI 1.30-2.16) were independently associated with longer hospital stays (all p <0.001). Seventy patients (45.2%) died during the study period.

Conclusions: Older adults with cancer showed substantial acute-care utilisation, with hospitalisation occurring frequently after ED presentation. Acute-care utilisation was not adequately explained by chronological age or tumour stage alone, whereas specific clinical reasons for admission were associated with care pathway and LOS. These findings highlight the potential value of structured oncogeriatric assessment and multidisciplinary supportive care to identify vulnerability, inform clinical decision-making, and address potentially modifiable factors contributing to acute-care utilisation.

6174

Experiences, satisfaction and patient reported outcomes of cancer patients at a complementary and integrative medicine outpatient service

U. Wolf (1), J. Ertl (1), E. Timm (1), I. Berlowitz (1), C. Maake (2)

IKIM, University of Bern, Bern (1), Anatomy, University of Zurich, Zurich (2)

Introduction: In oncology care, integrative treatment approaches are playing an increasingly important role. For more than three decades, the respective center has provided such care by combining conventional medicine with complementary approaches, primarily anthroposophic medicine and Western phytotherapy. This study assessed the experiences and satisfaction of oncology patients receiving the integrative oncology outpatient service.

Methods: We conducted a mixed-methods cross-sectional online survey (11/2025–1/2026) sent to all center patients with a valid email address. The survey assessed experiences and satisfaction with the services, diagnosis and health issues, treatments received, and demographic characteristics. Patient experience was assessed using an adapted version of the validated EUROPEP questionnaire (items rated from 1 = poor to 5 = excellent), covering doctor-patient relationship and communication, medical care, information and support, continuity and cooperation, as well as administrative processes. Further items were added to the survey to assess satisfaction, including quantitative items (e.g., How satisfied are you with the IKIM services overall? rated from 1 = not at all satisfied to 10 = very satisfied) and open-ended questions. Quantitative data was analysed descriptively; open-ended responses were reviewed for recurring themes.

Results: Of 662 survey participants, 452 (68.3%) had cancer. Most were female (72.79%) and in the 61–80 age bracket (56.19%). Breast cancer was most frequent (44.6%), followed by colon cancer (9.7%) and prostate cancer (8.2%). Common treatments involved preparations from anthroposophic medicine (97.3%), phytotherapy (26.7%), and others. Mean EUROPEP scores were all above 4 (SD 0.48–1.28), except one (>3), indicating favourable experiences. Satisfaction with treatment (M = 8.53, SD = 1.70), support (M = 8.89, SD = 1.66), and center services overall (M = 8.95, SD = 1.58) was high. Open-ended responses included feeling seen as a whole person, improved quality of life, increased self-efficacy, and relief of cancer-treatment-related symptoms and side effects.

Conclusions: Our results demonstrate that outpatient integrative oncology services can be successfully implemented within public health services and are perceived by patients as a valuable and beneficial component of cancer care.

9142

Routine Serial ePROMs Assessment Confirms Subjective Improvement Across All Domains During Ambulatory Oncology Rehabilitation and Predicts Relative Magnitude of Benefit

R. A. Popescu (1), A. Jakob (1), A. Gutierez (2), C. Kolotas (2), G. Gruber (3), M. C. Schumacher (4), G. Popescu (1), V. Blum (1), K. Tyriakidis (1), C. Leuenberger (1), F. Weber (1), C. Zobrist (2), C. Märtz (1), C. Stein (1), E. Fiechter (1), E. Ajrovski (2), S. Rutz (2), K. Saba (4), M. Sumila (3), K. Brouwer (3), S. Abbeel (2), C. von Briel (2), M. Hickey (5), J. Lyle (5)

Medical Oncology, Haematology and Palliative Care, Tumor Zentrum Aargau, Aarau (1), Radiotherapy, Institute for Radiotherapy Aarau, Aarau (2), Radiotherapy, Institute for Radiotherapy Zurich, Zurich (3), Urology, Urology Centre Hirslanden Klinik Aarau, Aarau (4), Health Value, Health Value Alliance & Systems, Epsom (5)

Introduction: Medical Oncology, Radiotherapy and Urology at our institutions invite cancer patients during or after oncological therapy to undertake ambulatory oncological rehabilitation (OncoReha), a 4-month program of supportive care including physiotherapy, group sports, nutritional advice, psycho-oncology, etc. overseen by OncoReha coaches. Patients complete online questionnaires (ePROMs) during and after OncoReha, which are shared with providers to coordinate and evaluate care. Many patients report substantial improvement, but the degree of benefit varies. This study aimed to identify early indicators of greater or less substantial benefit, potentially enabling interventions to be modified.

 Published under the CC license Attribution 4.0 International (CC BY 4.0)

Methods: ePROMs were prospectively collected for OncoReha patients from Dec-2020 to Dec-2025. Sufficient longitudinal data were available for 310 patients (182 [59%] female; 120 [39%] aged 65+ years). Data was harmonized across 14 questionnaires. A composite symptom burden score was determined at OncoReha start, OncoReha end (4 months), 7 and 12 months. Associations between baseline symptoms and subsequent symptom burden were assessed using correlation, multivariable regression and hierarchical clustering.

Results: Overall, patients reported reduced symptom burden across all domains (physical, psychological, functional and quality of life). The greatest improvement occurred during OncoReha and was sustained thereafter. The Figure shows transitions in symptom burden over time. Although many patients improved or maintained benefit, a substantial proportion retained or transitioned to a high symptom burden at program completion and beyond. Baseline symptoms significantly predicted subsequent symptom burden, particularly at earlier timepoints. After accounting for correlations between baseline symptoms, sadness and pain emerged as independent predictors, with cognitive function and nausea providing additional discriminatory value. Patient trajectories across domains and their predictive baseline symptoms will be presented.

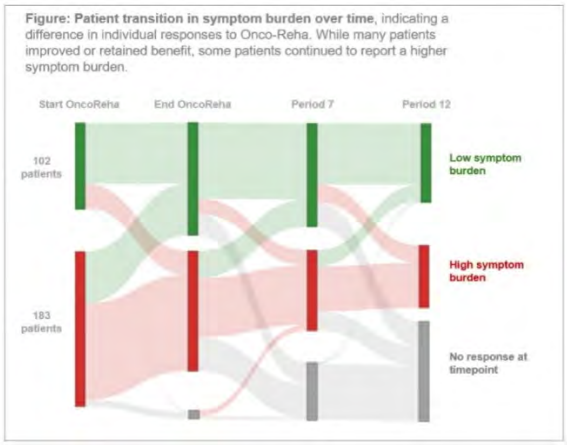


Figure: Patient transition in symptom burden over time, indicating a difference in individual responses to Onco-Reha. While many patients improved or retained benefit, some patients continued to report a higher symptom burden.

Conclusions: Many patients undertaking OncoReha reported an improvement in domain scores. We have observed that patients with a less substantial benefit may be identified from baseline symptom reporting, indicating that proactive PROMs monitoring can support program adjustment and modified interventions. We will prospectively validate this.

5458

Sleep disorders in breast cancer patients with chronic cancer-related fatigue: more than insomnia?

T. T. Rotar (1), M. Reif (2), R. Zerm (3), F. Strasser (4), M. Kröz (5)

Research, Klinik Arlesheim, Arlesheim (1), Research, Society for Clinical Research e.V., Berlin (2), Research, Research Institute Havelhöhe gGmbH, Berlin (3), Oncology, Cancer Fatigue Clinic, Schaffhausen (4), Sleep medicine, Klinik Arlesheim, Arlesheim (5)

Introduction: Sleep disturbances are - together with cancer-related fatigue - one of the most prevalent symptoms in cancer patients. They seem to have a complex relationship with each other, which may be both predisposing and perpetuating. We assessed sleep and fatigue in our study group of breast cancer survivors with chronic CRF (BCS-CRF).

Methods: In this retrospective analysis of clinical routine measures from patients with BCS-CRF, being treated in an outpatient sleep clinic, we assessed sleep-, fatigue- and regulation-measures. Inclusion criteria were at least a moderate CRF (Fatigue-Numerical-Scale ≥4 or Cancer-Fatigue-Scale – German version (CFS-D) ≥23) and completion of adjuvant cancer treatment at least six months prior. Statistical analysis was done with SPSS Version 31.0.

Results: In our study group of n = 37 patients with BCS-CRF (Tis-T3, N0-N2, M0) and a mean age of 51.3 ± 6.6 years we observed a high percentage (94.6%) of patients with chronic sleep disorders. Beside chronic insomnia, restless-legs syndrome (RLS) (40.5%) and obstructive sleep apnoea (OSA) (29.7%) were particularly common – most OSA cases being the mild form (27%). Over half of the patients (59.5%) suffered from more than one sleep disorder. The predominant symptom was severe sleep maintenance disturbance (in 74.3%). Sleep onset problems were also common with 65.7% reporting at least moderate difficulties. Fatigue measured on the CFS-D sum-scale yielded a mean of 37.8 ± 7.8 pointing to a moderate to severe gravity. On the subscales for physical and cognitive fatigue high mean scores of 17.4 ± 3.6 respective 12.7 ± 3.4 were observed. In more than 66% of patients, fatigue did not differ between the morning and the afternoon, indicating a disturbed basic rest-activity rhythm. Furthermore, patients showed an autonomic dysfunction scoring 36.1 ± 5.6 on the Trait-aR total scale (range: 18-54).

Conclusions: We assume that, alongside chronic insomnia, obstructive sleep apnoea and restless legs syndrome are frequent in breast cancer patients with chronic cancer-related fatigue. These sleep disorders predominantly present as sleep maintenance disturbances, which could perpetuate the symptoms and functional impairments associated with chronic cancer-related fatigue in breast cancer patients. We propose that chronic sleep disturbances should be evaluated as part of routine care.

1896

Use of infusion pumps to administer red blood cell concentrates; A literature review of the current evidence on the use of infusion pumps and their effects compared with administration by gravity

L. Brunner (1), S. Schönfeld (2)

Theragnostik, University Hospital Basel, Basel (1), Innere Medizin, University Hospital Basel, Basel (2)

Introduction: Millions of red blood cell concentrates are administered worldwide every year. The literature contains considerable uncertainty and conflicting findings regarding the use of infusion pumps to administer red blood cell concentrates. According to several manufacturers and the Swiss guideline for quality assurance in transfusion practice, infusion pumps may be used to administer red blood cell concentrates. However, there is very little information on the safety of this practice. Infusion pumps administer fluids in timed manner and require less supervision by trained personnel than the gravity method. The aim of this analysis is to identify the current evidence on the effects of infusion pumps on red blood cell concentrates compared with the gravity method in adult haematological patients.

Research question: How do the effects of administering red blood cell concentrates using an infusion pump differ from the effects of administering red blood cell concentrates by gravity in adult haematological patients?

Methods: A literature search was conducted in the PubMed, CINAHL, Cochrane Library and Web of Science databases. After removing duplicates, 31 publications were identified and screened; nine were assessed in full text, and seven publications were included. The included publications were subsequently evaluated using qualitative data analysis.

Results: The results show statistically significant [p = <0.05] changes in haemoglobin, free plasma haemoglobin, lactate dehydrogenase and red blood cell count with both transfusion methods. Significant findings for haemolysis and potassium

 Published under the CC license Attribution 4.0 International (CC BY 4.0)

concentration were observed only when the infusion pump was used (table 1).

Conclusions: Since the laboratory parameters show only minor differences and the significant haemolysis values after administration by infusion pump are well below the national limits, the results suggest that administration by infusion pump is relatively safe. However, the transferability of the results is limited by various factors. They are therefore insufficient to make a clear recommendation for or against the use of infusion pumps.

Publication	Hemolysis	Potassium	fHb	Hb	LDH	Red Blood Cell Count
Centrella-Nigro et al. (2018)	↔	↔	ø	ø	ø	ø
Hadjesfandiari et al. (2022)	X ↔	↔	ø	ø	X ↔	ø
Wilson et al. (2018)	↔	X ↔	X ↔	↔	ø	ø
Poder et al. (2017)	X ↔	↔	ø	ø	ø	ø
Wilson et al. (2016)	↔	ø	ø	ø	ø	ø
Pires et al. (2020)	X ↔	X ↔	X ↔	X X	↔ X	ø
Turgutoğlu Yılmaz et al. (2022)	ø	↔ ↔	X X	X X	X X	X X

Table 1: Summary of the results from the included publications. X Significant difference with an infusion pump. X Significant difference with gravity. ↔ No significant differences with an infusion pump. ↔ No significant differences with gravity. ø Not studied.

7907

Determinants of Self-Efficacy for Symptom Self-Management Among Patients Receiving Cancer Treatment: An Integrative Review

A. Ulahannan (1, 2), L. Matlet (1), C. Gremaud (1), M. De Pretto (1), M. Eicher (1, 2)

Faculty of biology and medicine, IUFRS, UNIL, Lausanne (1), Oncology, Lausanne University Hospital, Lausanne (2)

Introduction: Self-efficacy for symptom management (SESM) is defined as patients' confidence in their ability to monitor, prevent, and manage symptoms. Higher SESM is associated with better symptom self-management. This integrative review aimed to synthesise the determinants of SESM among adult oncology patients.

Methods: We conducted a systematic search of MEDLINE, PubMed, CINAHL, ProQuest, and Google Scholar up to December 2025 to identify quantitative, qualitative, and mixed-methods studies investigating self-efficacy for symptom management (SESM) during cancer treatment. Two reviewers independently screened and analysed the articles. Determinants were classified according to the consistency and convergence of findings across study designs.

Results: Fourteen studies met the inclusion criteria (11 quantitative, 3 qualitative). Symptom characteristics such as symptom distress, severity, burden, interference, cancer-related fatigue, and pain were consistently and negatively associated with SESM across quantitative studies, with convergent qualitative findings. Among patient characteristics, higher income, higher education, and absence of depression or anxiety were associated with higher SESM, whereas age, gender, cancer stage, treatment modality, and time since diagnosis showed inconclusive or null associations. Findings for treatment status, race/ethnicity, and healthcare-access disruption were directionally consistent but based on a single study with limited statistical reporting. Evidence on self-efficacy-enhancing interventions was supported across study designs: nurse-led health coaching and symptom-management support were associated with higher SESM in one observational study, with three qualitative studies reporting supportive findings. However, qualitative data also identified overly directive nursing behaviour as a potential barrier. Qualitative evidence further highlighted mastery through repeated treatment-cycle experience and family/spousal support as facilitators, with no corresponding quantitative evidence.

Conclusions: Evidence for determinants of SESM remains limited and predominantly correlational, precluding causal conclusions. Symptom characteristics and HCP-delivered support showed consistent associations. Further research is needed to clarify determinants of SESM and inform the development of self-management interventions.

Published under the CC license Attribution 4.0 International (CC BY 4.0)

7991

Key Factors and Competencies for High-Quality Palliative Care in Primary Healthcare

M. Brinovec (1, 2), P. Ovčar (1, 2)

Division of supportive care and joint healthcare activities, Oncology Institute Ljubljana, Ljubljana (1), Palliative care, Faculty of Health Sciences in Celje, Celje (2)

Introduction: Palliative care in primary healthcare is essential for providing comprehensive, timely and continuous care to patients with progressive incurable diseases and for supporting their family members. This study aimed to explore key factors associated with high-quality palliative care and the competencies and support mechanisms required for its effective delivery in primary healthcare.

Methods: A qualitative descriptive study was conducted using seven semi-structured interviews with purposively selected participants. Interviews lasted approximately 45 minutes, were transcribed verbatim and anonymised, and the data were analysed using directed thematic analysis.

Results: Participants identified comprehensive and individualised care, effective symptom management, respect for patient autonomy and dignity, early integration of palliative care, effective communication, multidisciplinary collaboration, continuity and accessibility of care, and family involvement as key quality factors. Essential competencies included clinical knowledge, communication, interpersonal and ethical skills, teamwork and care coordination. Important support mechanisms included continuing education, access to professional consultation, supervision, peer support, support from mobile palliative care teams, and clearly defined care pathways and protocols.

Conclusions: High-quality palliative care in primary healthcare depends on person-centred care, effective communication, multidisciplinary collaboration and appropriately supported professionals. Alongside clinical knowledge, communication, interpersonal, ethical and coordination competencies are essential for effective care delivery. Continuing education, supervision and access to specialist palliative care support were identified as important mechanisms for supporting effective practice.

POSTER - HEMOSTASIS, TRANSFUSION MEDICINE, VASCULAR, LABORATORY MEDICINE, BENIGN HEMATOLOGY

3098

The Swiss Red Blood Cell Disease Registry (RBCR) – an Introduction Dietliker N, Benoit T, Picotti E, Kasteler-Amrein R, Schmugge M 1Department of Medical Oncology and Hematology, University Hospital Zurich, Zurich, Switzerland 2 Department of Pediatric He

N. Dietliker (1), T. Benoit (1), R. Kasteler-Amrein (2), M. Schmugge (2), E. Picotti (2)

Hematology, Universitätsspital Zürich, Zürich (1), Department of Pediatric Hematology, Universitäts- Kinderspital Zürich – Eleonorenstiftung, Zurich (2)

Introduction: Hereditary red blood cell diseases (RBCD), including sickle cell disease (SCD), thalassemia and other rare anemia disorders (RAD), are chronic conditions associated with significant lifelong morbidity. In Switzerland, their prevalence and diversity are increasing due to migration and improved survival. However, national epidemiological data, standardized care pathways, and longitudinal outcome monitoring remain limited. The Swiss RBCR aims to collect data on epidemiology, disease characteristics, clinical course, treatment, complications and outcomes, generating real-world evidence to support standardized care, structured transition and future interventional studies.

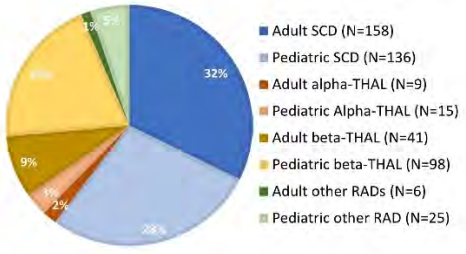
Methods: The RBCR is a nationwide, prospective, non-interventional registry. Data is collected centrally via REDCap® during routine clinical care. Funding is provided through competitive and non-competitive industry grants. Future integration of an established biobank is planned. Founding centers are the University Hospital and the University Children's Hospital Zurich. As of 10/2026, 13 further adult and pediatric centers are to be included. To estimate the national disease burden, an email-based survey on the number and type of RAD patients was conducted among 15 Swiss haematology centres in 04/2026.

Results: We identified an estimated 488 patients with RAD followed in the 15 participating centres (Figure 1). SCD was the largest group (N = 294, 60%), followed by thalassaemia (N = 163, 33%; 139 β- and 24 α-thalassemia) and other RAD (N = 31, 6%). Patients are managed across multiple adult and paediatric centres nationwide highlighting the growing clinical relevance of these disorders and the lack of a centralized infrastructure for epidemiological surveillance and outcome assessment.

Conclusions: Conclusion

This first nationwide survey identified nearly 500 RAD patients across Switzerland, underlining the need for a national registry to capture disease burden, treatment patterns and long-term outcomes. The Swiss RBCR will provide the first nationwide framework for standardized longitudinal data collection in RBCD and, through collaboration with RADeep (Rare Anemia Disorders European Epidemiological Platform), an ERN-EuroBloodNet initiative, facilitate international data sharing, research collaboration and future interventional studies to improve lifelong patient care.

Figure 1. Estimated number of patients with rare red blood cell disorders (RAD) in Switzerland across 15 participating clinics (total N=488).



 Published under the CC license Attribution 4.0 International (CC BY 4.0)

8721

Incidence of thrombosis and bleeding in patients with JAK2 V617F - positive myeloproliferative neoplasms receiving low-dose aspirin – a systematic review and meta-analysis

K. Vrotniakaite-Bajerciene (1), C. E. Marx (2), T. Tritschler (3), R. Shorr (2), M. Carrier (2), D. E. Fergusson (2), A. Delluc (2), M. Kimpton (2)

Department of Hematology and Central Hematology Laboratory, Inselspital, Bern (1), Department of General Internal Medicine, Ottawa Hospital Research Institute, Ottawa (2), Department of General Internal Medicine, Inselspital, Bern (3)

Introduction: Patients with JAK2V617F–positive myeloproliferative neoplasms (MPNs) are at increased thrombotic risk and commonly receive low-dose aspirin, yet its net clinical benefit is uncertain. We aimed to assess the risks and benefits of low-dose aspirin in this patient population.

Methods: A systematic review was performed for randomized trials and observational studies evaluating thrombotic and haemorrhagic events in patients with JAK2V617F-positive MPNs while taking low-dose aspirin. Study-level incidence rates (IR) per 100 person-years (PY) and incidence rate ratios (IRR) comparing aspirin use versus no aspirin were calculated and pooled using random-effects meta-analysis. The certainty of evidence was assessed using the Grading of Recommendations, Assessment, Development and Evaluation approach (GRADE).

Results: We included 3 randomized clinical trials and 7 observational studies (n = 1,760 with aspirin, n = 367 without aspirin). The pooled rate of thrombotic events in JAK2V617F-positive MPN patients receiving low-dose aspirin prophylaxis was 2.72 per 100 PY (95% CI 1.59 – 4.65; I2 = 93%) (Figure 1). The pooled IRR for thrombotic events comparing aspirin use versus no aspirin was 0.59 (95% CI 0.40 – 0.86, I2 = 16%). Patients with polycythemia vera (PV) had higher rates of thrombosis compared to those with JAK2 V617F-positive essential thrombocythemia (JAK2ET) (Figure 1). The pooled incidence rates of venous thromboembolism and arterial thrombosis were 1.20 (95% CI, 0.64–2.25; I^2 = 71%) and 2.06 (95% CI, 0.92–4.61; I^2 = 91%) per 100 person-years, respectively. The pooled rate of major and non-major bleeding on low-dose aspirin prophylaxis was 1.97 (95% CI 1.06 – 3.65; I2 = 90%) per 100 PY (Figure 2). The pooled IRR for bleeding events comparing aspirin use versus no aspirin was 2.43 (95% CI 1.15 – 5.11; I2 = 43%). The GRADE level of confidence for the investigated risks was low.

Conclusions: Patients with JAK2V617F-positive MPNs have ongoing high thrombosis rates while on low-dose aspirin. Aspirin was associated with a 40% reduction in thrombosis but a 2.5-fold increase in bleeding risk in patients with JAK2V617F-positive MPN with low certainty of evidence. More high-quality studies are needed to better define the role of aspirin in patients with JAK2 V617F-positive MPNs.

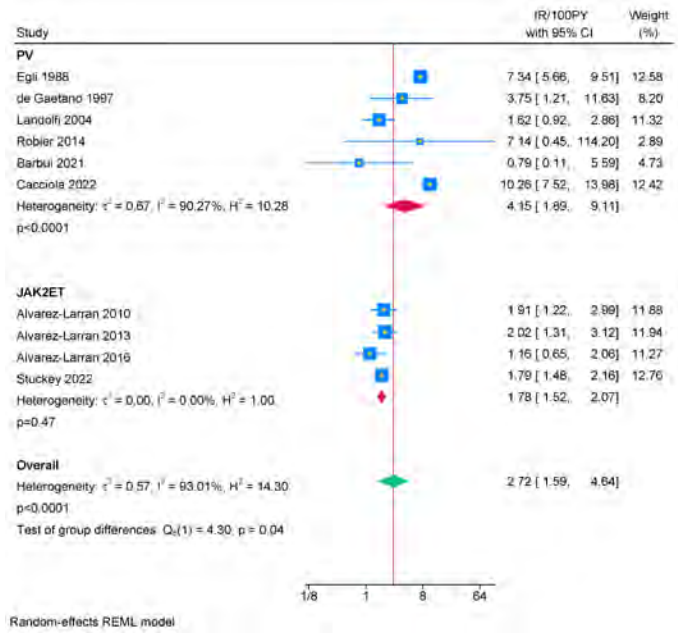


Figure 1. The IRs of thrombosis in patients with JAK2 V617F positive MPNs receiving low-dose aspirin. Abbreviations: CI, confidence interval; IR, incidence rate; JAK2ET, JAK2-positive essential thrombocythemia; PV, polycythemia vera; PY, patient-years

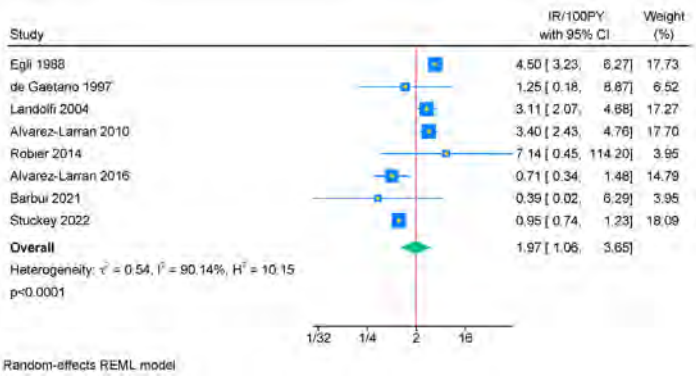


Figure 2. The IRs of major and non-major bleeding in patients with JAK2 V617F-positive MPNs receiving low-dose aspirin. Abbreviations: CI, confidence interval; IR, incidence rate; PY, patient-years

Published under the CC license Attribution 4.0 International (CC BY 4.0)

5687

Daratumumab for refractory acquired hemophilia A

J.-D. Studt (1), A. Trinchero (1)

Medical Oncology and Hematology, University Hospital Zurich, Zurich (1)

Introduction: Acquired hemophilia A (AHA) is a rare and potentially severe bleeding disorder caused by autoantibodies to endogenous factor VIII (FVIII). In addition to hemostatic treatment, immunosuppressive therapy (IST) is generally required to eradicate the FVIII autoantibody. Established IST options include corticosteroids, rituximab, and cyclophosphamide. However, some patients are refractory to these therapies.

Methods: We report three patients (one female, two male; age at diagnosis 60, 73, and 70 years) with AHA refractory to conventional IST. Hemostasis was achieved with initial recombinant activated factor VII followed by off-label emicizumab. All patients were refractory to first-line treatment with corticosteroids and subsequent anti-CD20 treatment with rituximab. Off-label anti-CD38 therapy with daratumumab was therefore administered as third-line IST. The first two patients received six and four weekly intravenous daratumumab infusions (16 mg/kg body weight), respectively, whereas the third patient received eight weekly subcutaneous injections of 1800 mg.

Results: All patients showed a rapid response, with normalization of FVIII activity and eradication of FVIII autoantibodies within 1 week after the first daratumumab dose in the two patients receiving intravenous treatment and within 4 weeks in the patient receiving subcutaneous treatment. FVIII activity and inhibitor titers were monitored using chromogenic assays insensitive to emicizumab. Apart from mild-to-moderate infusion-related reactions, no clinically significant adverse events were observed. Follow-up is now 12, 7, and 3 months, respectively, with sustained remission in all three patients.

Conclusions: In our series of patients with AHA refractory to corticosteroids and rituximab, anti-CD38 therapy with daratumumab achieved rapid eradication of FVIII autoantibodies and sustained remission and was well tolerated. Daratumumab may represent a therapeutic option for refractory AHA. Larger studies and longer follow-up are required to establish its long-term efficacy and safety.

2495

Elevated von Willebrand factor in patients with unexplained coronary stent thrombosis: A retrospective observational study and proposed diagnostic approach

N. Friedrich (1, 2), N. Dewarrat (1), F. Grandoni (1), G. Stalder (1, 3), L. Alberio (1)

Service and Central Laboratory of Haematology, Lausanne University Hospital (CHUV) and University of Lausanne (UNIL), Lausanne (1), Service of Haematology, Neuchatel Hospital (RHNe), Neuchâtel (2), Oncology and Hematology, Central Hospital Institute (ICH), Sion (3)

Introduction: Coronary stent thrombosis (ST) is a rare complication (1%), with a high mortality and recurrence rate. ST are classified based on the time of onset following stent implantation: acute (<24 hours); subacute (24 hours–30 days); late (31 days–1 year); and very late (>1 year). Risk factors are associated with (i) the procedure, (ii) the coronary lesion, (iii) antiplatelet therapy, (iv) patients-related factors. Our study focused on arterial prothrombotic factors in patients with ST without an identified mechanical cause who were treated in the Cardiology Department at the CHUV.

Methods: We included adults diagnosed with ST of undetermined origin at Lausanne University Hospital between January 2019 and April 2022. A systematic diagnostic workup was performed to characterise ST and identify underlying etiological factors.

Results: Ten patients (Table 1) experienced 16 ST episodes. At first presentation, 12/16 (75%) ST events were early, 1/16 (6%) late, and 3/16 (19%) very late. Six patients (60%) experienced recurrent ST. Only one episode (6%) was partially attributable to a mechanical cause (stent malapposition). Von Willebrand factor (VWF) activity was >150% in all episodes and >200% in 13 (93%). Factor VIII levels were >200% in 13 episodes (93%), including >300% in six. Antiphospholipid syndrome was identified in one patient (10%).

Table 1. Baseline patient characteristics

	All patients (n=10)	Patients with 1 episode of ST (n=4)	Patients with 2 episodes of ST (n=6)
Demographic data			
Age (median), (range)	55.5 (44-79)	49.5 (44-75)	61 (50-79)
Male sex	8 (80%)	4 (100%)	4 (67%)
Female sex	2 (20%)	0 (0%)	2 (33%)
Cardiovascular risk factor			
Hypertension	2 (20%)	1 (25%)	1 (17%)
Diabetes	2 (20%)	1 (25%)	1 (17%)
Smoke	8 (80%)	4 (100%)	4 (67%)
Dyslipidemia	7 (70%)	3 (75%)	4 (67%)
BMI ≥30 kg/m2	2 (20%)	1 (25%)	1 (17%)
Sex	8 (80%)	4 (100%)	4 (67%)
Age	4 (40%)	1 (25%)	3 (50%)
Familial history	2 (20%)	1 (25%)	1 (17%)
Cardiovascular history	10 (100%)	4 (100%)	6 (100%)
Obstructive sleep apnea	1 (10%)	1 (25%)	0 (0%)
Number of cumulative cardiovascular risk factors			
0	0 (0%)	0 (0%)	0 (0%)
1-3	2 (18%)	1 (25%)	1 (17%)
>3	8 (80%)	3 (75%)	5 (83%)
Comorbidities			
Venous or arterial thrombosis	0 (0%)	0 (0%)	0 (0%)
Thrombophilia	0 (0%)	0 (0%)	0 (0%)
Familial history of thrombosis	1 (10%)	0 (0%)	1 (17%)
Active cancer	0 (0%)	0 (0%)	0 (0%)
Medication at time of first ST			
Aspirin	3 (30%)	1 (25%)	2 (33%)
Clopidogrel	0 (0%)	0 (0%)	0 (0%)
Ticagrelor	0 (0%)	0 (0%)	0 (0%)
DAPT Aspirin-Clopidogrel	2 (20%)	1 (25%)	1 (17%)
DAPT Aspirin-Ticagrelor	4 (40%)	2 (50%)	2 (33%)
DAPT stopped <1 month before ST	2 (20%)	1 (25%)	1 (17%)
No antiplatelet drug	1 (10%)	0 (0%)	1 (17%)
Prophylactic anticoagulation	2 (20%)	1 (25%)	1 (17%)
Therapeutic anticoagulation	1 (10%)	0 (0%)	1 (17%)
No anticoagulation	7 (70%)	3 (75%)	4 (66%)
Medication at time of second ST			
Aspirin	NA	NA	1 (17%)
Clopidogrel	NA	NA	0 (0%)
Ticagrelor	NA	NA	0 (0%)
DAPT Aspirin-Clopidogrel	NA	NA	2 (33%)
DAPT Aspirin-Ticagrelor	NA	NA	3 (50%)
DAPT stopped <1 month before ST	*NA*	*NA*	*0 (0%)*
No antiplatelet drug	NA	NA	0 (0%)
Prophylactic anticoagulation	NA	NA	1 (17%)
Therapeutic anticoagulation	NA	NA	3 (50%)
No anticoagulation	NA	NA	2 (33%)
ABO Blood group			
A	4 (40%)	3 (75%)	1 (17%)
B	3 (30%)	1 (25%)	2 (33%)
AB	1 (10%)	0 (0%)	1 (17%)
0	2 (20%)	0 (0%)	2 (33%)

ST, coronary stent thrombosis; DAPT, double antiplatelet therapy.

Published under the CC license Attribution 4.0 International (CC BY 4.0)

Conclusions: VWF plays a central role in haemostasis. Under high shear stress and accelerated blood flow, VWF multimers unfold, interacts with the platelet GPIbα receptor, and thereby facilitates platelet aggregation. VWF's ability to bind to platelets is proportional to the size of its multimers, which is regulated by ADAMTS13, a metalloprotease that cleaves VWF, reducing the size of the multimers and thereby decreasing VWF's adhesiveness. It has been shown that, during acute myocardial infarction, intracoronary concentrations of ADAMTS13 are lower than systemic concentrations, with a reduction in the ADAMTS13 activity/VWF activity ratio. Our study showed markedly elevated systemic VWF and factor VIII levels in most patients with unexplained ST. This sustains the hypothesis that VWF plays a causal role in the development of ST, where its deployment in its activated form under shear stress would promote the formation of an arterial thrombus, and raise the possibility of VWF as a novel therapeutic target.

0319

Novel Compound Heterozygous SPTA1 Variants (c.154_159del/αLELY) Causing Severe Hereditary Red Cell Membrane Disorder in Two Brothers

M. Lork (1), D. Schmidt (2), M. Grobler (3), M. Schmugge (1), M. Amrein (1)

Diagnostic Hematology Laboratory, Department of Hematology, Oncology, Immunology, Stem Cell Transplantation and Somatic Gene Therapy, Universitäts- Kinderspital Zürich – Eleonorenstiftung, Zurich (1), Institute of Medical Virology, University of Zurich, Zurich (2), Diagnostic Oncology Laboratory, Center for Pediatric Laboratory Medicine, Universitäts-Kinderspital Zürich – Eleonorenstiftung, Zurich (3)

Introduction: Hereditary RBC membrane disorders arise from mutations in spectrin-actin cytoskeletal proteins. The hypomorphic αLELY allele is a common low-expression modifier of α-spectrin, clinically silent in isolation but capable of potentiating disease when co-inherited with a pathogenic SPTA1 variant.

Methods: Two brothers with severe transfusion-dependent hemolytic crises underwent hematological workup (EMA binding, AGLT, osmotic resistance testing) and whole exome sequencing (WES). Functional analyses included isoform-specific RT-qPCR from CD71+ reticulocytes, Western blot of RBC membrane ghosts, structural analysis of a published αβ-spectrin crystal structure (PDB: 3LBX), and co-immunoprecipitation from patient-derived ghost lysates.

Results: WES identified compound heterozygosity for the αLELY allele and a novel in-frame deletion c.154_159del (p.Ser52_Tyr53del) in the α-spectrin tetramerization domain. RT-qPCR demonstrated allelic dosage-dependent exon 46 skipping (~50% homozygous father, ~20–25% heterozygous carriers). Western blot showed comparable spectrin levels across all individuals. The αLELY-mediated reduction in functional α-spectrin is predicted to shift the membrane pool toward the defective protein, with ~two-thirds of membrane α-spectrin carrying the deletion. Structural analysis revealed Ser52 forms a direct hydrogen bond with β-spectrin at the α0/β17 interface. Co-immunoprecipitation suggests impaired αβ-spectrin interaction in patient samples.

Conclusions: This case demonstrates how a common modifier allele combined with a novel pathogenic variant produces severe hemolytic disease through a dual quantitative and qualitative mechanism, underscoring the importance of considering modifier alleles in the diagnostic workup of hereditary RBC membrane disorders.

5693

Stress-associated HbF reactivation after allogeneic haematopoietic cell transplantation in a patient with β⁺-thalassaemia trait

M. S. Bader (1), A. Stelmes (1), E. Antonopoulou (1), J. P. Halter (1), J. R. Passweg (1), P. Bättig (1), C. C. Widmer (1)

Hematology, University Hospital Basel, Basel (1)

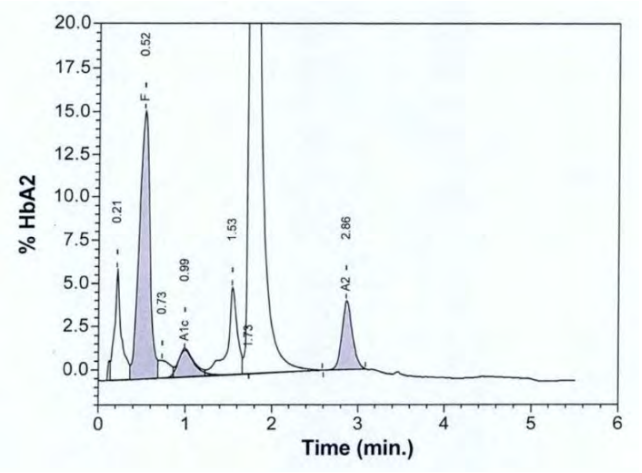
Introduction: Reactivation of fetal haemoglobin (HbF) may occur in conditions associated with increased stress on erythroid precursors. We report a case of marked HbF elevation following allogeneic haematopoietic cell transplantation (allo-HCT) in a 34-year-old man from Romania with acute myelomonocytic leukaemia who received a stem cell graft from his haploidentical sister, a heterozygous carrier of β⁺-thalassaemia.

Methods: Haemoglobin separation was performed by high-pressure liquid chromatography (HPLC) in both the patient and his donor. Molecular analysis of the HBB gene was performed by DNA sequencing in the patient.

Results: The donor showed mild hypochromic microcytic anaemia (Hb 112 g/L, MCV 75 fL, MCH 24 pg) with a relatively preserved red blood cell count (4.70 T/L). Blood smear examination demonstrated moderate anisopoikilocytosis, basophilic stippling and occasional target cells. HPLC revealed mildly increased HbA2 (4.8%) and HbF (3.0%), consistent with β⁺-thalassaemia trait.

HPLC of the patient was performed 10 months after allo-HCT. At that time, he had moderate anaemia without microcytosis or hypochromia (Hb 82 g/L, MCV 98 fL, MCH 30 pg), mild reticulocytosis (106 G/L, 39 ‰), and no evidence of iron deficiency. In contrast to the donor, HPLC revealed a marked increase in HbF to 15.5%, accompanied by increased HbA2 (4.0%). DNA sequencing identified the heterozygous HBB intronic variant c.316-106C>G, which is known to impair splicing and cause a β⁺-thalassaemia phenotype. At the time of analysis, the patient had complete donor chimerism. He was experiencing overlap graft-versus-host disease (GvHD) involving the skin and oral mucosa and was receiving treatment with ruxolitinib, a calcineurin inhibitor and extracorporeal photopheresis.

Conclusions: Despite sharing the same heterozygous HBB variant, the patient and donor exhibited markedly different erythroid phenotypes. Whereas β-thalassaemia trait is generally associated with absent or mild anaemia, the patient developed moderate anaemia and a pronounced increase in HbF following allo-HCT. The marked HbF elevation may reflect stress-induced reactivation of γ-globin production imposed by GvHD and its treatment, including JAK inhibition. The case illustrates how different erythropoietic conditions may modulate the haematological phenotype associated with an otherwise identical β⁺-thalassaemia genotype.



 Published under the CC license Attribution 4.0 International (CC BY 4.0)

1612

Clinico-serological positivity preceding laboratory functional conversion in heparin-induced thrombocytopenia: a case series

M. P. Gossin (1), L. Hayenga (1), E. Matthey-Guirao (1), F. J. Gomez (1), L. Alberio (1), A. Aliotta (1), M. G. Zermatten (1)

Central Hematology Laboratory, Lausanne University Hospital - CHUV, Lausanne (1)

Introduction: Diagnosis of heparin-induced thrombocytopenia (HIT) integrates clinical probability, immunoassays, and platelet-activating functional assays. Although functional assays are considered diagnostic gold standards, a delay may occur between clinico-serological HIT recognition and detectable platelet-activating activity. We aimed to characterize cases with delayed functional conversion and to investigate this temporal discordance using an independent flow cytometry-based functional assay.

Methods: Among HIT cases diagnosed at our center between March 2021 and September 2025, we identified four patients with initially negative platelet-activating functional assay despite clinico-serological HIT recognition, followed by delayed functional conversion on repeat testing. Available serial samples were retrospectively analyzed using the HIT antibody-induced procoagulant platelet (HIT-PCP) assay.

Results: Repeat functional testing became positive after 3–10 days in all four patients. HIT-PCP could be retrospectively assessed in three patients and was negative at initial clinico-serological recognition but became positive at the subsequent time point when HIPA and/or PIPA positivity emerged. Thus, two distinct functional tests showed a concordant negative-to-positive pattern.

Conclusions: Clinico-serological recognition of HIT may precede detectable platelet-activating activity in vitro. Concordant evolution across distinct functional tests supports a temporal change in detectable antibody-mediated platelet activation rather than an assay-specific observation. These hypothesis-generating findings warrant prospective investigation with systematic serial sampling and emphasize cautious interpretation of initially negative functional assays when clinical and serological evidence strongly supports HIT.

8180

Evaluation of the AmiCORE Apheresis System for Platelet Apheresis at a regular Blood Transfusion Service

I. Giataganzidou (1), I. Schmid (1), J. Wendler (1), E. Schindler (1), D. A. Tsakiris (1)

Blood Transfusion Service Zurich, Swiss Red Cross, Schlieren (1)

Introduction: The AmiCORE Apheresis-System is the successor model to the Amicus for platelet apheresis and offers software-based improvements as well as simplified operation. The technology in use for platelet apheresis is based on auto-elutriation different from all other separation principles in this field. Features such as storage and additive solutions used, fluid management based on weight scales and the expected product quality remain unchanged.

Methods: The AmiCORE system was evaluated at our blood donation center. Following the validation, a prospective comparison of 35 single platelet apheresis procedures with AmiCORE (n = 16) and Amicus (n = 19) was performed in an unpaired donor setting. Quality controls before pathogen inactivation (INTERCEPT® Blood System) included determination of plasma content and measurement of residual cells (leukocytes, erythrocytes, platelets).

Results: All 35 platelet products manufactured met the acceptance criteria of the Swiss Blood Transfusion service and have been transfused without any reported side effects. No clinically relevant differences were observed in donation parameters (sex, hemoglobin, total white blood cell counts, platelet precounts). Collection efficiency (precount CE2, 67±6% vs 66±6%, p = 0.49) and platelet yield (4.10 vs 4.18×10^{11}/Unit; p = 0.62) were comparable, whereas collection duration was significantly shorter for AmiCORE (54±10 vs 61±8 min, p = 0.008) and total whole blood processed significantly lower (2.52±0.32 vs 2.86±0.35 L, p = 0.006). At equivalent bag volumes (292±6 vs 290±3 mL, p = 0.07) AmiCORE products showed minimally elevated residual leukocyte counts (Lc: 0.149±0.19 vs. $0.063\pm0.07\times10^{6}$/Unit; p = 0.011) and comparable erythrocyte concentrations (0.40±0.17 vs $0.33\pm0.15\times10^{3}$/µl, p = 0.159); all values were well within the acceptance limits.

Conclusions: In single-apheresis procedures, AmiCORE achieved comparable platelet yields and collection efficiency with shorter collection times and lower processed whole blood volumes than Amicus The validation and the prospective comparison demonstrate the successful implementation of the instrument.

3050

Diagnosis and therapy of congenital TTP in pregnancy and discovery of a new mutation in ADAMTS13

V. Wester (1), A. Holbro (1, 2), N. D. Bui (3), J. Benz (3), J. A. Kremer Hovinga (4), J. van den Berg (1), N. Schmidlin (5), P. Bättig (5), O. Lapaire (3), N. R. Rusca (6), G. T. Stehle (1)

Hematology, University Hospital Basel, Basel (1), Transfusion Medicine, Blood Transfusion Service Northwestern Switzerland, Basel (2), Gynaecology, University Hospital Basel, Basel (3), Hematology and Central Hematology Laboratory, University Hospital of Bern, Bern (4), Hematology and Diagnostic Hematology, University Hospital Basel, Basel (5), Medical Genetics, University Hospital Basel, Basel (6)

Introduction: Thrombotic thrombocytopenic purpura (TTP) is a rare, life-threatening disorder that requires prompt and accurate diagnosis and treatment to reduce morbidity and mortality. As treatment differs between congenital and immune TTP, distinguishing the two subtypes is essential. cTTP is an ultra-rare subtype caused by hereditary ADAMTS13 deficiency.

Methods: In addition to the case presentation of a patient with newly diagnosed cTTP a PubMed search was conducted on cTTP and its therapeutic options.

Results: A 27-year-old previously healthy Syrian-Kurdish woman presented with vomiting and abdominal pain at 28 weeks of her second pregnancy (abortion <15. week in first pregnancy). She was diagnosed with TTP (thrombocytopenia, schistocystes in the blood smear, ADAMTS13 level <3%) and therapy with steroids and plasma exchange was started immediately. Caplacizumab crosses the placenta with a bleeding risk for the unborn and was not given as first line treatment in this clinically stable patient. After the first plasma exchange the ADAMTS13 level rose to 77% and no inhibitor was detected. Both results suggest a cTTP rather than an ongoing immune process (immune TTP). Genetic testing identified a homozygous ADAMTS13 variant c.3971A>G (NM_139027.6), classified as likely pathogenic and predicted to affect splicing. Family history was unremarkable for TTP, but the patient's parents were known to be first cousins. Therapy was switched to plasma infusions and after cost approval to Adzynma (Apadamtase alfa, a recombinant ADAMTS13). The patient had a persistent normal blood count and the ADAMTS13 level could be kept above 13-15% what allowed a normal peripartal management. The risk for the unborn for cTTP was suggested very low with an unrelated father as cTTP in the general population is ultra-rare. The child will be tested postnatal nevertheless. cTTP has been managed

 Published under the CC license Attribution 4.0 International (CC BY 4.0)

in the literature, including during pregnancy, with plasma infusions and recombinant ADAMTS13 as therapeutic options.

Conclusions: In absence of an ADAMTS13 inhibitor and normalization of ADAMTS13 activity (>50%) after the first plasma exchange cTTP should be suspected and genetic testing initiated. Novel ADAMTS13 gene mutations continue to be identified and should be reported to expand knowledge of this ultra-rare hereditary disease. This case adds to the limited experience with recombinant ADAMTS13 during pregnancy.

8752

Acquired Hemophilia A Associated With Multicentric Castleman Disease: A Case Report and Review of the Literature

T. Gerardi (1), M. Iarossi (1), A. Casini (1), P. Fontana (1)

Angiology and Hemostasis departement, Geneva University Hospital, Geneva (1)

Introduction: Acquired hemophilia A (AHA) is a rare autoimmune bleeding disorder caused by loss of immune tolerance to factor VIII (FVIII). Multicentric Castleman disease (MCD) is a systemic inflammatory disorder characterized by cytokine excess, particularly IL-6 and profound immune dysregulation. Although autoimmune manifestations are recognized in MCD, its association with AHA is exceptionally rare. We report the fifth published case and review the literature, exploring a potential shared immunopathogenesis.

Methods: PubMed was searched using "multicentric Castleman disease" and "acquired hemophilia A".

Results: A 50-year-old woman presented with constitutional symptoms, low-grade fever, generalized lymphadenopathy, systemic inflammation and macroscopic hematuria. AHA was promptly diagnosed (aPTT: 100 s, FVIII: 6%, inhibitor: 3.1 BU). Active bleeding was controlled with rFVIIa, and emicizumab was initiated for secondary prophylaxis. Lymph node histopathology subsequently confirmed idiopathic iMCD-NOS. Dual immunosuppression targeting both conditions was started with prednisone and siltuximab, leading to rapid inhibitor clearance and FVIII normalization. During corticosteroid tapering, AHA relapsed without evidence of iMCD relapse, as indicated by a decline in FVIII activity and the appearance of a right-thigh ecchymosis. This prompted an increase in the corticosteroid dose and administration of rituximab. AHA subsequently achieved complete remission, while iMCD remained stable on maintenance siltuximab. Four previously published cases were identified. Among the five patients, four had iMCD and one had HHV-8–associated MCD. All experienced clinically significant bleeding requiring hemostatic treatment, with bleeding severity not correlated with FVIII activity. Corticosteroids combined with rituximab were the most frequently used immunosuppressive regimen (4/5), whereas IL-6–directed therapy for MCD was used in only two cases (2/5). The present case is the first to report the use of emicizumab alongside prednisone, siltuximab, and rituximab. Despite shared immunopathogenesis both conditions need treatment; responses may be asynchronous.

Conclusions: AHA arising in active MCD may represent a manifestation of shared immune dysregulation. Cytokine-driven B-cell activation may facilitate loss of FVIII tolerance and autoantibody formation, supporting combined treatment of both AHA and the underlying disease.

Table 1. Clinical, hemostatic, treatment, and outcome characteristics of patients with MCD-associated AHA

Domain	Result (n = 5)
Patient characteristics	
Age, median (range), years	50 (14–71)
Female sex	3/5 (60%)
Male sex	2/5 (40%)
Castleman disease	
iMCD	4/5 (80%)†
HHV-8–associated MCD	1/5 (20%)
iMCD subtype (n = 4)	
TAFRO	1/4 (25%)
NOS	1/4 (25%)†
Not reported	2/4 (50%)
Clinical and inflammatory features	
Lymphadenopathy	5/5 (100%)†
Fever	2/5 (40%)†
Hepatosplenomegaly/organomegaly	1/5 (20%)†
Serosal effusions	3/5 (60%)
Elevated IL-6 levels	3/5 (60%)†
Bleeding phenotype	
Bleeding at presentation	5/5 (100%)†
Post-procedural bleeding	3/5 (60%)
Soft-tissue bleeding	2/5 (40%)
Serosal bleeding	1/5 (20%)
Macroscopic hematuria	1/5 (20%)†
Subsequent/recurrent bleeding	3/5 (60%)†
Hemostatic treatment required	5/5 (100%)†
Hemostatic profile	
FVIII activity, median (range)	6% (<1–16%)
FVIII inhibitor titer, median (range)	7 BU (2.3–82)
Hemostatic treatment	
rFVIIa	4/5 (80%)†
FEIBA	2/5 (40%)
Emicizumab	1/5 (20%)†
AHA/MCD-directed treatment	
Corticosteroids	5/5 (100%)†
Rituximab	4/5 (80%)†
Cyclophosphamide	2/5 (40%)
Tocilizumab	1/5 (20%)
Siltuximab	1/5 (20%)†
Cyclophosphamide and rituximab	1/5 (20%)
Outcomes	
Complete remission of both AHA and MCD	2/5 (40%)
AHA response with ongoing MCD follow-up	1/5 (20%)†
Death	2/5 (40%)

† Present case. Values are n/N (%) unless otherwise specified. Percentages are calculated using the relevant denominator. AHA, acquired hemophilia A; BU, Bethesda units; FEIBA, factor eight inhibitor bypassing activity; FVIII, factor VIII; HHV-8, human herpesvirus 8; iMCD, idiopathic multicentric Castleman disease; IL-6, interleukin-6; MCD, multicentric Castleman disease; NOS, not otherwise specified; rFVIIa, recombinant activated factor VII; TAFRO, thrombocytopenia, anasarca, fever, reticulin fibrosis/renal dysfunction, and organomegaly.

 Published under the CC license Attribution 4.0 International (CC BY 4.0)

5363

A double-hit model of neonatal bleeding: fetal and neonatal alloimmune thrombocytopenia associated with severe haemophilia A

P. Stakia (1), S. Waldvogel-Abramowski (1)

Diagnostic, Geneva University Hospital, Geneva (1)

Introduction: Fetal and neonatal alloimmune thrombocytopenia (FNAIT) is a major cause of severe neonatal thrombocytopenia and bleeding. We report a case of FNAIT with an atypical bleeding course. A male infant born at term to a 32-year-old G1P1 woman presented on day 1 with petechiae, retinal haemorrhages, a parieto-occipital scalp haematoma and a platelet count of 19 G/L. After initial platelet recovery, he developed a spontaneous buccal haematoma at 3 months, raising suspicion of an additional haemostatic disorder.

Methods: Maternal platelet antibodies were investigated by Monoclonal Antibody-specific Immobilization of Platelet Antigen (MAIPA), and parental HPA genotyping was performed by PCR specific sequence method (PCR-SSP). At 3 months, hemostatic and molecular investigations were performed in the child. Factor VIII activity was measured, and int22h and int1h rearrangements (IVS22 and IVS1 inversions) of the F8 gene were analyzed by inverse shifting-PCR (IS-PCR) and electrophoresis. Maternal carrier testing subsequently targeted the int1h rearrangement (IVS1 inversion) identified in the child.

Results: MAIPA detected maternal anti-HPA-1a alloantibodies directed against GPIIb/IIIa. The mother was HPA-1bb and the father HPA-1aa, confirming HPA-1 incompatibility and FNAIT. Further investigation diagnosed severe hemophilia A in the child associated with an IVS1 inversion of F8. The mother had normal factor VIII activity but was a heterozygous carrier of the same F8 variant. Testing of the maternal grandmother was negative for this inversion, indicating that the variant had arisen de novo in the mother. This is a chromosomal rearrangement responsible for approximately 1 to 5% of cases of severe hemophilia A.

Conclusions: This case demonstrates two independent causes of bleeding: alloimmune thrombocytopenia and inherited severe factor VIII deficiency. Recurrent or disproportionate bleeding after platelet recovery should prompt investigation for an additional hemostatic disorder. Identifying both conditions is essential for neonatal care, genetic counselling and management of future pregnancies.

7897

Uncommon mutation in dehydrated stomatocytosis

N. Dewarrat (1), J. Walker (2), J. Schoumans (2), M. Gavillet (1)

Hematology, Lausanne University Hospital, Lausanne (1), Oncogenomic Laboratory, Lausanne University Hospital, Lausanne (2)

Introduction: Macrocytic anaemia is a common referral motive to the haematology consultation. Myelodysplastic syndrome and vitamin B12 deficiency are most commonly the underlying diagnosis. However, rarer causes should also be considered, particularly in otherwise healthy young patients. These include reticulocytosis as illustrated by the present case.

Methods: We describe the diagnostic work up for red cell membrane disease as well as the discovery of an infrequent mutation.

Results: We report the case of a healthy 47-year-old female, of Spanish origin, referred to our clinic for investigation of isolated long-standing anaemia with macrocytic tendency. Personal and family history were unremarkable, without toxic exposition including alcohol. The spleen was within normal range. Haemoglobin was 110g/l (117-157g/l), with MCV 97fl (81-99fl) and mild reticulocytosis (137G/l; 20-120G/l). Other haemolysis parameters (haptoglobin, LDH, total bilirubin) were normal. Blood smear showed erythrocytic aniso-poikilocytosis (stomatocytes, spherocytes) with polychromasia. Ferritin was elevated at 360µg/l (15-150ug/l), as was transferrin saturation coefficient (46%; 15-35%), without B9 or B12 deficiency. We ruled out enzymopathy disorders (PK, G6PD deficiency). Thalassaemia or abnormal haemoglobin was unlikely and excluded on HPLC. 5-EMA test was below the normal range at 94% (95–110%), ruling out spherocytosis. We thus carried out an ektacytometry test, results suggested dehydrated hereditary stomatocytosis (DHS). Surprisingly, genetic analysis (by augmented exome sequencing) did not show mutations in the typical DHS genes (PIEZO1, KCNN4, SLC4A1) or overhydrated hereditary stomatocytosis (RHAG). However, an apparent heterozygous nonsense mutation (60% VAF) was detected in SPTA1, typically linked to hereditary elliptocytosis (HE), as well as two polymorphisms (αLeLY).

The peripheral blood morphology, and ektacytometry curve being atypical for HE, we opted for diagnosis of DHS by precaution, since clinical guidelines are more conservative. We prescribed B9 and follow-up is unremarkable up to now.

Conclusions: Reticulocytosis is a significant cause of macrocytosis; awareness makes it possible to avoid costly tests such as bone marrow examination. When diagnosing a membranopathy, it is important to determine the subtype, as some, such as DHS, are absolute contraindications to splenectomy due to thrombotic risk.

2833

From T-ALL to AML: Immunophenotypic Evolution and Contribution of Flow Cytometry after Haploidentical Transplantation

S. ENNOUHI (1, 2), M. OUBECHE (3, 2), N. WAAL (1, 2), H. CHAOUKI (1, 2), L. ENNEFFAH (1, 2), Y. KHAYAR (1, 2), A. BELMEKKI (1, 2)

Blood Transfusion Center, Cell Therapy and Flow Cytometry Unit, Mohamed V Military Hospital, Rabat (1), HEMATOLOGY, Faculty of Medecine and Pharmacy of Rabat, Rabat (2), CLINICAL HEMATOLOGY, Mohamed V Military Hospital, Rabat (3)

Introduction: Describe the change from T-ALL to AML The role of flow cytometry

Methods: Case report. Flow cytometry. Bonne marrow examination, blood counts, Karyotyping, FISH

Results: A 27-year-old woman with no past medical history was diagnosed in 2023 with poor-prognosis immature T-ALL. FCM identified 86% blasts expressing cytoplasmic CD3 and CD7, MPO-negative. Karyotype was normal, FISH was negative for KMT2A and BCR::ABL1 rearrangements, and molecular testing was not performed. She was treated according to the GRAALL-2014 protocol, followed by haploidentical allogeneic stem cell transplantation. In late 2025, she relapsed with an extramedullary mass of the dorsum of the right foot and received azacitidine–venetoclax–vincristine, with donor lymphocyte infusions planned upon complete remission (two doses administered). In 2026, blood count showed hemoglobin 13.7 g/dL, white blood cells 14.7 × 10^9/L with 26% MPO-negative circulating blasts, and platelets 38 × 10^9/L. Bone marrow aspirate showed 75% blasts, 98% of which were MPO-negative, initially suggesting T-ALL relapse. However, FCM revealed an immature myeloid blast population (CD34+, CD117+, CD33+, HLA-DR+) lacking cytoplasmic CD3 but retaining CD7, consistent with AML with minimal differentiation (AML-M0). Cytogenetic analysis showed a possible 11p abnormality, under investigation.

 Published under the CC license Attribution 4.0 International (CC BY 4.0)

Conclusions: FCM is an essential tool for immunophenotypic monitoring of acute leukemias, enabling early detection of blast phenotype changes. Definitive distinction between lineage switch and therapy-related AML requires integration of immunophenotypic, cytogenetic and molecular data to establish clonal continuity.

POSTER - EXPERIMENTAL HEMATOLOGY / ONCOLOGY

8148

Acute Myeloid Leukemia Microenvironment: Targeting the Bone Marrow Adipocyte Differentiation Axis as a Novel Strategy to Reduce AML Progression

T. Smirnova (1, 2), C. Bataclan (2), A. Martins (2), R. Sarkis (2), G. Tsilimidos (3), S. Blum (3), C. Mariangela (3), L. De Leval (4), O. Naveiras (2, 5)

Hematology Service and Hematology Translational Research Unit, Department of Laboratory Medicine, Lausanne University Hospital, Lausanne (1), Laboratory of Regenerative Hematopoiesis, Department of Biomedical Sciences, University of Lausanne, Lausanne (2), Service and Central Laboratory of Haematology, Department of Oncology and Department of Laboratories and Pathology, Lausanne University Hospital (CHUV) and University of Lausanne (UNIL), Lausanne (3), Institute of Pathology, Department of Laboratory Medicine and Pathology, Lausanne University Hospital (CHUV) and Lausanne University, Lausanne (4), Hematology Service and Hematology Translational Research Unit, Departments of Oncology and Laboratory Medicine, Lausanne University Hospital, Lausanne (5)

Introduction: Acute myeloid leukemia (AML) is a heterogeneous hematological malignancy with high relapse rates. Bone marrow adipose tissue, which expands with aging and hematopoietic stress, supports leukemic cell survival by supplying fatty acids that fuel oxidative metabolism. However, the contribution of bone marrow adipocyte (BMAd) differentiation to AML metabolic reprogramming and response to targeted therapies remains poorly understood. We investigated whether fatty acid transport contributes to AML chemoresistance and whether targeting BMAd differentiation and fatty acid oxidation (FAO) enhances therapeutic responses.

Methods: Human AML cell lines were cultured with undifferentiated or adipocyte-differentiated bone marrow stromal cells under direct or indirect coculture conditions. Drug-response assays were performed using targeted inhibitors. Pharmacological inhibition of adipogenesis and FAO was assessed for its effects on AML survival and drug sensitivity.

Results: Using stromal cell lines and primary human bone marrow stromal cells, we found that adipocyte-differentiated stromal cells protected AML cells from venetoclax-induced apoptosis. This effect was strongest in direct-contact cocultures and partially retained in indirect-contact conditions, suggesting both contact-dependent and soluble factor mechanisms. In contrast, adipocyte-differentiated stromal cells did not significantly protect FLT3-ITD+ AML cells from midostaurin-induced apoptosis. Combined inhibition of CPT1A-mediated FAO and BCL-2 signaling significantly reduced AML blast survival in the presence of mature primary BMAds. Preliminary data further suggest that inhibition of PPARγ-mediated adipogenesis decreases the supportive effect of BMAds during targeted therapy.

Conclusions: BMAds promote resistance to venetoclax-induced apoptosis in AML, primarily through direct interactions with leukemic cells. CPT1A inhibition enhances the efficacy of BCL-2 blockade in the adipocyte-rich bone marrow microenvironment, while inhibition of BMAd differentiation may reduce BMAd-mediated chemoprotection. The absence of a similar protective effect in FLT3-ITD+AML treated with midostaurin suggests therapy- and subtype-specific resistance mechanisms. Together, these findings support a context-dependent role for the BMAd differentiation axis in microenvironment-mediated drug resistance and highlight it as a potential therapeutic target in AML.

3071

ProFeaTrOL, a bioinformatic tool to help interpreting the pathogenicity of germline missense single nucleotide variants of BAP1

P. Marchal (1, 2, 3), J. Spies (1, 2), L. Bürgi (1), K. Samarasinghe (4), L. Lane (4), F. Cerciello (1)

Department of Medical Oncology, Inselspital, Bern University Hospital, Bern (1), Department of biomedical research, University of Bern, Bern (2), Graduate School for Cellular and Biomedical Sciences, University of Bern, Bern (3), SIB, SIB Swiss Institute of Bioinformatics, Lausanne (4)

Introduction: Background and Objective: Germline single nucleotide variants (SNVs) in the tumor suppressor and deubiquitinating protein BAP1 may cause the hereditary BAP1 tumor predisposition syndrome, which is characterised by an increased risk of rare cancers, such as pleural mesothelioma and uveal melanoma, among affected family members. Standard variants effect predictors (VEP) tools have limited specificity in anticipating the pathogenic impact of the variants when applied to the rare BAP1 associated cancer conditions. Therefore, we have developed the ProFeaTrOL (Protein Features based Training for Oncogenicity Likelihood) bioinformatic model, which relies on protein features relevant to the function of BAP1.

Methods: Methods: We selected the protein features relevant to the function of BAP1 based on information from the proteomics knowledgebase neXtProt. We trained and validated ProFeaTrOL using publicly available saturation genome editing experiments for the almost complete BAP1 sequence (2968 SNV for training, 1270 for validation). We tested its performance using the clinically curated SNVs reported in ClinVar (236 SNVs). We further verified the model if applied to the ClinVar curated SNVs of BRCA1or TP53.

Results: Results: ProFeaTrOL was able to discriminate between pathogenic and benign BAP1 variants in the validation set with an AUC of 0.84. For the clinical testing set from ClinVar, the AUC was 0.89, with an accuracy of 89% (92% sensitivity and 88% specificity). The two standard VEP tools, PolyPhen-2 and SIFT, performed significantly worse in the same datasets. Furthermore, we applied ProFeaTrOL to the BRCA1 protein because it belongs to the same functional complex as the BAP1 protein. The area under the curve (AUC) reached 0.89 when the model was trained on the protein. We also tested ProFeaTrOL for TP53, as it is a tumour suppressor like BAP1, but uses different mechanisms. In this case, the tool performed only modestly. These observations in BRCA1 and TP53 further confirmed that BAP1 protein function is central to ProFeaTrOL predictions.

Conclusions: Conclusion: The ProFeaTrOL tool, which is based on the functional features of the BAP1 protein, could help to interpret germline SNVs observed in individuals at risk of BAP1 tumor predisposition syndrome.

 Published under the CC license Attribution 4.0 International (CC BY 4.0)

3572

ULK1 complex inhibition restores MHC-I expression in Diffuse Large B-cell lymphomas

H. Mandhair (1, 2), J. Dengjal (3), C. Kosnopfel (4), G. Lenz (5, 6), A. Davies (7), M. P. Tschan (8), U. Novak (1, 2)

Department of Biomedical Research/Medical Oncology, University of Bern, Bern (1), Department of Biomedical Research/Medical Oncology, University Hospital of Bern, Bern (2), Department of Biology, University of Freiburg, Fribourg (3), Translational Oncology, University of Muenster, Munster (4), Translational Oncology, University of Münster, Münster (5), Department of Medicine A, Haematology and Oncology, University Hospital Münster, Münster (6), Southampton NHIR/Cancer Research UK, Experimental Cancer Medicines Centre, Faculty of Medicine, University of Southampton, Southampton General Hospital, Southampton (7), Institute of Tissue Medicine and Pathology, University Hospital of Bern, Bern (8)

Introduction: Diffuse large B-cell lymphoma (DLBCL) can evade endogenous CD8+ T-cell surveillance through defects in major histocompatibility complex class I (MHC-I) antigen presentation, thereby contributing to an immunosuppressive lymphoma microenvironment.. In DLBCL, genetic loss of HLA class I alleles and alterations in B2M can reduce surface MHC-I expression and promote immune escape. This phenotype differs across cell-of-origin subtypes: germinal-centre B-cell-like (GCB) DLBCL commonly displays low MHC-I expression, whereas activated B-cell-like (ABC) DLBCL more frequently exhibits reduced MHC-II expression. Autophagy mediates lysosomal degradation of cellular cargo and can promote MHC-I loss in solid tumours; however, its role in DLBCL antigen-presentation defects remains unknown. To determine whether ULK1-dependent autophagy suppresses MHC-I antigen presentation in B2M-intact, MHC-I-low DLBCL and whether ULK1 inhibition restores tumour immunogenicity and CD8+ T-cell recognition.

Methods: Quantitative proteomics was used to compare basal antigen-presentation pathway proteins between GCB and ABC DLBCL cell lines. Surface MHC-I expression was quantified by MHC-I (W6/32) and HLA-A2 flow cytometry following treatment with ULK1 complex inhibitors: MRT68921 and SBI-0206965, VPS34 complex: VPS34IN1, lysosomal activity inhibitors Bafilomycin A1 and Chloroquine and proteosome inhibitor MG132. GCB Oci-Ly1 B2M-knockout cells validated the MHC-I expression. Flow cytometry evaluated immune-evasion-associated surface markers in Oci-Ly1 cells treated with 625Nm MRT68921 or vehicle for 48 h. Immunoblotting confirmed the reduced autophagic activity and MHC-I enrichment. HLA-I pathway transcripts were analysed by qRT-PCR. Primary DLBCL transcriptomic data (NCT01324596) assessed correlations between ULK1-pathway and antigen-presenting genes.

Results: Quantitative proteomics revealed lower MHC-I antigen-presentation machinery in GCB than ABC DLBCL. ULK1 inhibition with MRT68921 restored B2M-dependent surface MHC-I across multiple GCB and ABC cell lines, enhanced IFN-γ-induced MHC-I upregulation, and increased HLA-I transcription. Primary GCB patient data confirmed inverse correlations between ULK1 and HLA-A/HLA-B, identifying ULK1-driven autophagy as a reversible, druggable mechanism of immune evasion in DLBCL.

Conclusions: Targeting ULK1 restores B2M-associated surface MHC-I and may enhance lymphoma immunogenicity.

2605

A Spatial Protemics Map of Novel ADC and BiTE Targets Across Longitudinal Colorectal Cancer Cohorts

C. Bothou (1), B. Ehret (2), A. Eklund (2, 3), A. Burrus (2), J. Schneider (2, 3), E. Danenberg (2), M. Daniel (2), S. Haefliger (2, 3), N. Miglino (1), G. Gut (1), B. Gosztonyi (1), D. Rutishauser (4), M. D. Brada (4), S. Dettwiler (4), M. Cieri (5), S. de Zanet (5), A. Spinelli (5), S. Piscuoglio (5), A. Jacobs (2), J. R. Fischer (2), S. Chevrier (2), H. Moch (4), A. Wicki (1), B. Bodenmiller (3)

Department of Medical Oncology and Hematology, University Hospital Zürich and University of Zürich, Zurich (1), Navignostics, AG, Horgen (2), Department of Quantitative Biomedicine, University of Zurich, Zurich (3), Department of Pathology and Molecular Pathology, University Hospital Zürich and University of Zürich, Zurich (4), Istituto Clinico Humanitas, IRCCS-Clinical and Research Hospital, Milan (5)

Introduction: Standard metastatic Colorectal Cancer (CRC) treatment relies on FOLFOX/FOLFIRI with anti-EGFR or anti-VEGF antibodies, but options beyond second-line remain restricted. Concurrently, novel antibody-drug conjugates (ADCs) and bispecific T-cell engagers (BiTEs) show promise in basket trials. Using Imaging Mass Cytometry (IMC), we spatially map single-cell ADC/BiTE target expression, co-expression, and heterogeneity across serial mCRC samples to guide therapeutic sequencing and biomarker workflow development.

Methods: Tissue is being retrieved across four centers: University Hospital Zurich and Milan (active), alongside Stadtspital Triemli and Cantonal Hospital Aarau (upcoming). The cohort will exceed 250 mCRC patients with longitudinal primary and metastatic samples collected before and after systemic therapies. FFPE blocks are assembled into TMAs and sections are profiled via IMC using a panel targeting 14 ADC/BiTE antigens: MUC1, NGFR, Her3, FOLR1, cMet, Her2, LY6E, Trop2, TF, EGFR, B7H3, AXL, Ceacam5, and Nectin4, plus TME and structural markers. IMC images are processed through a standardized pipeline including segmentation, phenotyping and QC.

Results: Here we present preliminary results that systematically characterize expression frequency and heterogeneity across distinct clinical features, including disease stage, anatomical site, treatment, and treatment outcome. In agreement with previous IHC-based studies, we find that selected markers show decreased expression in metastases when compared to primary tumor samples. We further show first trends that suggest that prior treatment with FOLFOX or FOLFIRI can have distinct effects on target expression. Finally, we quantify correlations between target expression and the state of the immune compartment.

Conclusions: Mapping target distribution across anatomical sites and lines of therapy provides a framework for evaluating biomarker dynamics and heterogeneity in CRC. Beyond surface expression, spatial context and cellular density are key to understanding response. Standardized IMC profiling will refine single-cell biomarker discovery and rational combination strategies.

 Published under the CC license Attribution 4.0 International (CC BY 4.0)

7826

Assessing Growth Modulation Index as marker for clinical activity in a Phase 1 study with a next generation BRAF inhibitor

N. H. Bischoff (1), D. Dejardin (1), N. Keshelava (2), A. Roller (1), G. Schnetzler (1)

Roche Innovation Center Basel, F.Hoffmann- La Roche AG, Basel (1), Roche Innovation Center Zurich, F.Hoffmann- La Roche AG, Zurich (2)

Introduction: Single arm EiH studies of new oncology compounds provide limited options to compare clinical activity. In previously treated patients, Growth Modulation Index (GMI) compares duration of clinical benefit (as time-to-progression, TTP) of the experimental compound with the prior treatment in the same patient. As tumor control tends to decrease with each additional treatment line, GMI >1 suggests a clinically meaningful treatment effect. This summer student project aims to assess the GMI for mosperafenib, a next generation BRAF inhibitor in patients with BRAFv600 mutation bearing solid tumors.

Methods: In this exploratory post-hoc analysis of GMI in n = 92 patients from CH, BE, SP, UK and NZ enrolled in Ph1 study WP43295 we used patient PFS for experimental treatment and recorded treatment duration of prior lines as proxy for TTP and applied a cut-off of 1.33 as evidence for improved activity over prior therapy (GMI responder).

Results: GMI could be assessed in 78/80 patients exposed to single agent mosperafenib at doses from 200mg QD to 1200mg TID, and 10/12 patients at doses of 400mg BID and 600mg BID in combination with cobimetinib 60mg QD. Patients were exposed to a median of 3 (1-6) lines of prior therapies in the single agent cohorts and 1.5 (0-4) in the combo cohorts. This included prior BRAFinh treatment in 60% and 42% of patients in the two groups. A positive GMI (>1) for mosperafenib was seen in 48.9% of all evaluable patients, with a GMI responder rate (>1.33) of 44.3%. Mean GMI was 3.38 (95%CI 1.80, 4.05) with a median GMI of 1.08 (range 0.02-20.42). A positive GMI was seen in 35.9% of patients receiving a BRAFinh in their prior lines (n = 53) with a responder rate of 24.5%. The absence of strong correlation between PFS and prior duration of treatment (r = -0.04) supports GMI as an independent, additional marker for clinical activity. The positive GMI suggests that mosperafenib has the potential to provide prolonged therapeutic effect even in patients who progressed rapidly under previous treatments.

Conclusions: GMI could be a valuable, additional tool to assess meaningful clinical activity in early development studies without a comparator arm. GMI analysis suggests relevant antitumor activity of mosperafenib, when compared to prior treatment, including BRAF inhibitors.

8773

Aged Hematopoietic Stem Cells Enhance Immunotherapy Response in a Young Host

I. Delle Fontane (1), H. Carrasco Hope (1), C. Caballero Cifuentes (1), M. Morbidelli (1), V. Núñez Quintela (1), M. Naderi (1), L. Chentout (1), N. Vannini (1)

DOF, University of Freiburg, Freiburg (1)

Introduction: Aging is associated with profound alterations of the immune system that impair immune surveillance and influence tumor evolution and response to immunotherapy. Immunosenescence, driven by chronic low-grade inflammation, metabolic and proliferative stress, telomere erosion, and DNA damage, affects both innate and adaptive immunity. Aged hematopoietic stem cells (HSCs) progressively lose lymphoid differentiation potential, acquire a myeloid bias, and contribute to reduced naïve T-cell output and restricted T-cell receptor diversity, while promoting the expansion of immunosuppressive myeloid populations. However, the specific contribution of HSC aging to tumor microenvironment composition and its impact on immunotherapy response remain poorly understood.

Methods: To specifically investigate the effects of hematopoietic aging, we transplanted young or aged HSCs into lethally irradiated young recipient mice, followed by tumor inoculation and ICB treatment

Results: Contrary to our initial hypothesis, mice reconstituted with aged HSCs developed more durable responses to ICB than those receiving young HSCs, suggesting that hematopoietic age can influence the response to immunotherapy. We hypothesize that the enhanced response to ICB observed in mice receiving aged HSCs may be associated with regenerative lymphopoiesis supported by a functionally active thymus. In young recipients with an intact thymic environment, increased progenitor availability may support the generation of newly produced, less differentiated T-cell populations that are particularly responsive to ICB. This interpretation is further supported by the complete absence of survival observed in aged mice transplanted with aged HSCs, emphasizing the critical role of a young, functional thymic environment in sustaining effective immune reconstitution. Thus, the interaction between aged HSC-derived progenitors and a young, functional thymus may promote the generation of T-cell compartments that contribute to enhanced responsiveness to immunotherapy.

Conclusions: Our findings challenge the view that hematopoietic aging uniformly impairs responses to cancer immunotherapy and highlight the importance of considering hematopoietic age together with the host environment when investigating and modulating responses to ICB.

 Published under the CC license Attribution 4.0 International (CC BY 4.0)

POSTER - CLINICAL HEMATO-ONCOLOGY

3520

Clinical evaluation of an HCT-specific evidence-linked reasoning system in allogeneic stem cell transplantation

H. Boyadzhiev (1), J. Lötscher (1), D. Ditz (1), C. Meloni (1), E. Heilmann (1), D. Pfingst (1), E. Antonopoulou (1), J. Passweg (1), J. Halter (1), P. Schlaepfer (2), D. Hauzenberger (3), J. Paschke (3), J. Kopec (3), S. Staiger (3), C. C. Widmer (1)

Hematology, University Hospital Basel, Basel (1), Laboratory Medicine, University Hospital Basel, Basel (2), AI, Viska, Stockholm (3)

Introduction: Allogeneic hematopoietic cell transplantation (allo HCT) requires integration of longitudinal patient information with evolving evidence. For clinical use, language-model-based systems must incorporate patient context while providing verifiable sources. We developed Viska SCTx, an HSCT-specific clinical reasoning system using graph-based retrieval-augmented generation (GraphRAG) to link patient information with transplant-specific concepts and evidence. We assessed evidence grounding, source traceability and concordance with real-world decisions.

Methods: In the preliminary retrospective evaluation, 10 AML allo HCT cases were represented as structured patient records. Ten questions per case covered pre-, peri- and post-transplant care. Responses were assessed for evidence support, unsupported claims and overinterpretation. Recommendations were compared with decisions and classified as concordant, partially concordant, not assessable, or not comparable. Importantly, the evidence base can be predefined by the user, allowing analysis of selected sources. In the ongoing expanded validation, diagnosis-list information is automatically mapped to longitudinal patient fields. Currently, 120 patients have been validated; results here refer to the preliminary cohort.

Results: In the preliminary cohort, the system answered all questions and displayed supporting sources. Evidence support ranged from 77.9% to 95.2% across ten question categories, and 85% of answers contained no unsupported claims. Overall, 72% showed at least partial concordance with clinical decisions: 37% fully and 35% partially concordant. Seventeen percent were not assessable because patient information was missing and 11% were not comparable with reference decisions. Lower concordance occurred when treatment-protocol information was unavailable or centre-specific or individualized strategies were applied.

Conclusions: Viska SCTx provides an evidence-linked reference tool for allo HCT decisions combining longitudinal patient information with traceable sources. Rather than replacing clinical judgement, the system may support it by facilitating access to relevant evidence, simplifying literature review and providing a framework to compare patient-specific decisions with evidence. Expanded validation is ongoing to assess performance and reproducibility in a larger cohort.

1958

A clinical case of neoehrlichiosis mimicking a lymphoma relapse in a b-cell-depleted patient

A. Sturm (1), J. Sumer (2), T. Lehmann (1)

Hematology, Kantonsspital St. Gallen, St. Gallen (1), Infectiology, Kantonsspital St. Gallen, St. Gallen (2)

Introduction: Neoehrlichiosis is an infection with intracellular bacteria Candidatus neoehrlichia mikurensis transmitted by ticks (e.g. Ixodes ricinus). The proportion of ticks in Switzerland harbouring this bacteria is estimated between 5 and 10 percent. Typical symptoms of neoehrlichiosis encompass recurring fever, fatigue and arthralgia. Venous and arterial thrombosis is a common complication of an untreated infection with Candidatus neoehrlichia mikurensis. After a tick bite immunologically compromised individuals are usually prone to a severe course of this infection.

We report a clinical case of a 63-year-old patient who suffered from recurrent fiever started during the rituximab-maintenance of a follicular lymphoma and lasted for ten months. This patient was finally diagnosed with neoehrlichiosis and successfully treated with doxycycline.

Methods: Candidatus neoehrlichia mikurensis is an intracellular bacteria. Thus it can non be detected by conventional blood culture and staining. After multiple negative blood culture samples we performed a PCR-based, commercially availiable test to screen for the bacterial 16S-rRNA in patient's blood. After the detection and the amplification of the 16S-rRNA it was possible to identify the pathogen by RNA-sequencing.

Results: The diagnosis of neoehrlichiosis was confirmed by the repetitive identification of Candidatus neoehrlichia mikurensis by 16S-rRNA-sequencing in two different blood samples of the patient. This diagnosis provided a conclusive explanation for the symptoms including recurrent fever, fatigue and thrombosis of the left renal artery. Fever and fatigue resolved permanently after the oral treatment with doxycycline. The renal thrombosis was treated by angioplasty, stenting and oral anticoagulation. The suspected relapse of the lymphoma was ruled out by CT-imaging, biopsy and histological testing.

Conclusions: Since neoehrlichiosis can not be detected by conventional blood culture and staining the onset of recurrent fever in the context of lymphoma and in the absence of the pathogen identification can be misinterpreted as a symtom of the lymphoma relapse. Therefore b-cell-depleted patients undergoing a long term b-cell-directed lymphoma-treatment should be tested for neoehrlichiosis if they suffer from recurrent fever after a tick bite. Convenient and effective therapy with doxycycline can prevent complications and further infectiological testing.

0430

When Two Rarities Collide: Hepatic Monoclonal Immunoglobulin Deposition Disease as the First Manifestation of IgG4 Multiple Myeloma

M. Costanza (1), B. Bisig (2), A. Cairoli (1)

Service and Central Laboratory of Hematology, Lausanne University Hospital (CHUV) and Lausanne University, Lausanne (1), Institute of Pathology, Lausanne University Hospital (CHUV) and Lausanne University, Lausanne (2)

Introduction: Monoclonal immunoglobulin deposition disease (MIDD) is caused by tissue deposition of monoclonal light and/or heavy chains. Unlike amyloid, deposits are non-organised and Congo red negative. The kidney is almost always involved, while liver involvement is very rare. IgG4 multiple myeloma (MM) is also rare (about 4% of IgG myelomas) and must be distinguished from IgG4-related disease (IgG4-RD). IgG4-type MIDD has been reported only exceptionally, in the kidney. We describe hepatic MIDD as the first manifestation of IgG4 MM, focusing on diagnostic challenges.

Methods: Clinical, laboratory, imaging, histopathological and genetic data were reviewed, and the literature was searched.

Results: A 50-year-old woman followed for ulcerative colitis in remission presented with progressive anicteric cholestasis (>5 x ULN), mild cytolysis and 5 kg weight loss. Ultrasound was

 Published under the CC license Attribution 4.0 International (CC BY 4.0)

normal in November 2025, but MRI in April 2026 showed new hepatomegaly (20 cm) with hypervascular lesions. MRCP excluded primary sclerosing cholangitis. Liver biopsy in June 2026 showed massive perisinusoidal hyaline deposits, Congo red negative, without birefringence. Deposits stained positively for IgG and kappa light chain, and retrospectively for IgG4. Immunofixation showed an IgG kappa monoclonal protein (10.8 g/L), with high IgG4 (7.53 g/L; normal <0.86) and low IgG2. Free kappa light chains were 166.9 mg/L (κ/λ ratio 11.1). Bone marrow biopsy showed 15-20% monoclonal IgG4 kappa plasma cells, with hyperdiploidy on cytogenetic analysis, confirming IgG4 MM. Whole-body MRI showed no bone lesions. IgG4-RD was excluded. Proteinuria and high NT-proBNP (892 ng/L) were found, but cardiac MRI showed no infiltrative disease. Treatment with daratumumab-VCd gave an unsatisfactory response; due to rising alkaline phosphatase and hepatomegaly, cyclophosphamide was replaced by lenalidomide.

Conclusions: To our knowledge, this is the first reported case of MIDD associated with IgG4 MM, revealed by hepatic involvement. Characterising the non-amyloid deposits was challenging, as it preceded the diagnosis of MM. The concurrent presence of light and heavy chain deposits complicated the diagnosis, while the marked serum IgG4 elevation raised the possibility of IgG4-RD. Close clinician-pathologist collaboration was essential to link the hepatic deposits to the IgG4 plasma cell clone.

7014

Donor-Derived TP53 Clonal Hematopoiesis after Haploidentical Transplantation for DDX41-Mutated AML: A Case Report

E. Antonopoulou (1), E. Georgieva (1), A. Stelmes (1), M. Bader (1), D. Juskevicius (1), F. Matteazzi (1), J. Tossounidis (1), P. Apostolova (1), J. Passweg (1), J. Halter (1), B. Drexler (1)

Hematology, University Hospital Basel, Basel (1)

Introduction: Clonal hematopoiesis (CH) is detectable in approx. 3 % of allogeneic HSCT donors aged ≥40 years, most often involving mutations in DNMT3A and TET2, and donor-derived clones engraft in most recipients (1). Donor cell-derived leukemia (DDL) is rare and arises predominantly when donor has an undetected germline predisposition, notably DDX41 alteration, or from rare donor CH with TP53 or splicing-factor mutations (1,2).

Methods: We performed next generation sequencing (NGS) analysis with myeloid panel assay in blood and bone marrow samples of the patient.

Results: A 67-year-old woman with AML myelodysplasia-related, a germline DDX41 variant p.K381* and somatic ASXL1, PHF6, NRAS and DDX41 p.R525H mutations, with inconspicuous karyotype, underwent haploidentical allo-HSCT from her 64-year-old sister after exclusion of the germline DDX41 variant in the donor. At 1 month post HCT myeloid NGS of bone marrow (BM) identified a donor-derived likely oncogenic DNMT3A-Variant p.R635W (VAF 6%). At 6 months post HSCT, with complete donor chimerism, an additional oncogenic TP53 p.R248Q mutation (VAF 1.2 %) was detected. At 9 months VAF of DNMT3A and TP53-Mutations were 9 % and 1.8 %, respectively, showing gradual clonal expansion. Course was complicated by acute cutaneous GvHD (month 3) and organizing pneumonia (month 6). At 8 months systemic steroids were discontinued. At 10 months the patient has no evidence of relapse or DDL, while the donor remains healthy.

Conclusions: TP53 mutations define the highest-risk category of CH, and donor TP53 CH is a recognized precursor of DDL (1). Transformation is nonetheless not inevitable: donor-derived clones, including TP53-mutated clones, can persist for decades without progression (3). In our patient, a slowly expanding low-level TP53 clone emerging under alloimmune inflammation, chemotherapy and corticosteroid exposure warrants close surveillance. It was detected by post-transplant NGS; such clones are likely missed when monitoring is restricted to recipient markers. We will apply single-cell DNA sequencing to resolve clonal architecture, including co-occurrence with DNMT3A and TP53 allelic state. Finally, case raises dilemma of whether and how donors should be tested and informed of high-risk CH, a question that current recommendations leave open and one that is particularly pressing for older related donors (4).

3086

Late diagnosis of WHIM syndrome: an odyssey and a novel targeted treatment

M. Recher (1)

Immunology, University Hospital Basel, Basel (1)

Introduction: WHIM syndrome (Warts, Hypogammaglobulinemia, Infections, Myelokathexis) is a very rare inborn error of immunity, associated with recurrent infections and high long-term risk for malignancy and lung diseases. The disease is due to gain of function germline mutations in CXCR4 causing retention of mature lymphocytes and neutrophils in the bone marrow. Although the disease was already described in 1964, it is rarely diagnosed. Until very recently, there was no CXCR4-targeted treatment to normalise the WHIM-associated immune-dysregulation.

Methods: A patient with chronic neutropenia and lymphopenia and an IgG subclass deficiency was enrolled into our prospective immune-dysregulation cohort. Detailed immune cell phenotyping was performed by multi-parameter flow cytometry and serum immunoglobulin quantification by nephelometry. Whole-exome sequencing (WES) data were filtered against an updated list of inborn error of immunity genes aligned with the most recent report of the International Union of Immunologic Societies (IUIS).

Results: We present a patient journey with early onset neutropenic infections, severe teenage year-associated papillomavirus warts responsive to G-CSF therapy, multiple adult onset pneumonias and skin and soft tissue infections. The patient had a combined lympho- and neutropenia and a IgG subclass deficiency. Serum IgM and IgA were within the normal range. Intriguingly, a genetic panel diagnostic for congenital neutropenias did not identify any pathogenic variant, since CXCR4 was not included. Our research-based WES data identified a heterozygous p.R334* nonsense variant diagnostic for WHIM syndrome. It took more than 40 years from first symptoms to molecular diagnosis. Recently, the first targeted therapy in the form of the oral CXCR4 antagonist mavorixafor has been approved by the FDA and by the EMA and first use in Switzerland is planned following health insurance approval.

Conclusions: Immune-phenotypic and genetic analysis is essential in individual patients with chronic immune-dysregulation to screen for underlying inborn errors of immunity, even if the patient is a middle-aged adult. For patients with a germline CXCR4 gain of function, there is now an approved oral targeted therapy available in the form of the CXCR4 antagonist mavorixafor, which should not be withheld. This represents a shift in WHIM care from supportive treatment to targeted mechanism-based therapy.

 Published under the CC license Attribution 4.0 International (CC BY 4.0)

5475

KMT2A Amplification on Two Distinct Ring Chromosomes in Mixed Phenotype Acute Leukemia: A rare Cytogenetic Constellation

E. Wilhelm (1, 2), B. Okamura (1, 3), B. Glaeser (4), M. Stoikou (4), J. Dirks (1), S. Dirnhofer (5), T. Junker (3), A. Stelmes (1)

Department of Haematology and Laboratory Medicine, University Hospital Basel, Basel (1), Department of Haematooncology, University Hospital Regensburg, Regensburg (2), Department of Haematology and Oncology, Cantonal Hospital Basel-Land, Liestal (3), Department of Medical Genetics, University Hospital Basel, Basel (4), Department of Pathology, University Hospital Basel, Basel (5)

Introduction: Mixed phenotype acute leukemia (MPAL) is a rare and biologically heterogeneous group of acute leukemias in which the coexistence of myeloid and lymphoid features makes accurate lineage assignment and classification particularly challenging. We report an unusual case of MPAL with KMT2A amplification distributed across two distinct ring chromosomes and a multi-hit TP53 alteration.

Methods: Diagnostic work-up included bone marrow cytomorphology, immunohistochemistry, flow cytometry, conventional karyotyping, FISH, SNP microarray, and targeted DNA/RNA next-generation sequencing.

Results: An 82-year-old man presented with pancytopenia. Bone marrow cytology showed 32% blasts with Auer rods. By flow cytometry, blasts were cCD3+, CD7++, cTCRβ+, sCD3−, CD1a−, CD8−, CD34+, CD117+, CD10+, CD33dim, CD38+ and cMPO−, formally fulfilling WHO 2022 criteria for early T-cell precursor acute lymphoblastic leukemia. In contrast, immunohistochemistry demonstrated MPO positivity in the majority of blasts with co-expression of CD3, CD7, CD34 and CD117, consistent with POX positivity and Auer rods observed in the cytomorphology. NGS detected a TP53 splice-site mutation but none of the investigated fusion transcripts.

SNP microarray demonstrated multiple genomic alterations, including 5q deletion, high-level KMT2A amplification (>5 copies) on 11q, and TP53-associated 17p copy-neutral loss of heterozygosity. Cytogenetics showed a complex karyotype with 5q deletion, 11q gain, monosomy 13, and two ring chromosomes. FISH revealed KMT2A amplification, but no rearrangement, with amplified signals distributed across both ring chromosomes.

An individualized, less intensive treatment alternating P(O)MP with isatuximab and azacitidine/venetoclax was initiated. The patient died from neutropenic fever during the first cycle without hematologic recovery.

Conclusions: This case describes KMT2A amplification across two distinct ring chromosomes in MPAL, associated with multi-hit TP53 alteration. To our knowledge, this is a rare finding indicative of genomic instability in MPAL. It also illustrates the difficulty of lineage assignment when MPO results differ between diagnostic methods. Treatment efficacy could not be assessed because the patient died before response evaluation; absent count recovery may have reflected refractory disease, treatment-related myelosuppression, or both.

6136

Belumosudil for chronic graft-versus-host disease: a case report with excellent response

E. Georgieva (1, 2), G. Nair (1), S. Werner (1, 3), M. Fricker (1), P. Charitos-Fragkakis (1), A. Stelmes (1), R. Mathew (1), B. Drexler (1), J. Halter (1)

Hematology, University Hospital Basel, Basel (1), Faculty of Medicine, University of Basel, Basel (2), Clinical Pharmacy, University Hospital of Basel, Basel (3)

Introduction: Chronic graft-versus-host disease (cGvHD) is a major complication after allogeneic hematopoietic stem-cell transplantation (allo-HCT), and effective options are limited after corticosteroid and ruxolitinib failure. Belumosudil, a selective ROCK2 inhibitor, is approved for cGvHD by FDA and EMA after at least 2 lines of prior systemic therapy. In Switzerland access depends on health insurance approval.

Methods: Since 2022, 25 patients with severe cGvHD after at least two lines of systemic therapy were treated with belumosudil. 11 of them obtained cost coverage. We present a patient with an impressive improvement of cGvHD-manifestations under tripple therapy with Belumosudil, Ruxolitinib and extracorporeal photopheresis (ECP).

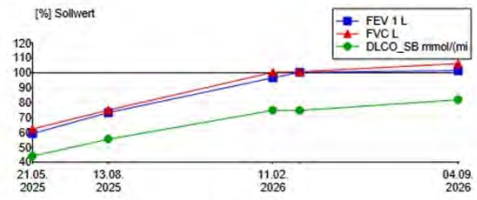
Results: A 27-year-old man underwent allo-HCT three years ago abroad for T-cell acute lymphoblastic leukemia. Three months later, acute and later severe cGvHD developed, predominantly manifesting as sclerodermatous skin involvement. Treatment with steroids, ruxolitinib and ECP stabilized the condition without improvement. Prior to belumosudil he had severe cGvHD with the following organ scores: skin 3 (generalized deep sclerosis with impaired activities of daily living), eyes 2, liver 1, lungs 2 (FEV1: 59%), joints/fascia 1. Belumosudil 200 mg once daily was added to prednisone 15mg, ruxolitinib, and ECP. Within 6 months, prednisone could be tapered. Belumosudil was well tolerated without any dose interruptions or modifications. Almost 8 months after initiation, cGvHD has remarkedly improved with skin softening allowing for normal daily activities. Improvement of soft tissue conditions is also illustrated by a complete normalization of the pulmonary function.(Fig 1, Tab 1). According to NIH classification, overall cGvHD grade decreased from severe to moderate. (organ scoring: skin 2 (deep sclerosis 5% of BSA), joints/fascia score 1, liver 0, lungs 0.

Conclusions: Overall response with belumosudil after two and more prior lines of therapy is found in about 75% of patients with significant differences by organ manifestations. An increasing number of anecdotal reports suggest a beneficial effect of combination therapy of belumosudil with ruxolitinib and/or ECP but so far this practice is not established by data from randomized trials. Although just a single case, our observation supports the need for studying combination therapies with belumosudil in a systematic manner.

Table 1. Pulmonary function test

Parameter	TLC (L)	RV (L)	sR eff (kP*s)	FVC (L)	FEV 1 (L)	FEV 1%M (%)	DLCO_SB (mmol/(mi)	DLCO_SB %Soll
Before study inclusion	4.85	1.22	0.83	3.79	2.98	77.12	5.34	44.1
At follow-up	7.48	1.30	0.44	6.04	4.97	80.42	8.93	74.7

Figure 1. Pulmonary function test



Published under the CC license Attribution 4.0 International (CC BY 4.0)

1906

BCR::ABL1-Positive Megakaryoblastic Leukemia: When AML and CML Blasts Become Indistinguishable

R. Latscha (1), D. Ditz (1), J. Dirks (1), B. Kopp (1), A. Handschin (2), A. Tzankov (3), T. Menter (3), C. Widmer (1)

Division of Hematology, University Hospital Basel, Basel (1), Hematology, Kantonsspital Baselland, Liestal (2), Institute of Medical Genetics and Pathology, University Hospital Basel, Basel (3)

Introduction: BCR::ABL1-positive acute leukemia with megakaryocytic differentiation is rare and difficult to distinguish from CML presenting in blast phase. De novo AML with BCR::ABL1 and megakaryoblastic CML blast phase may show substantial morphologic and immunophenotypic overlap. Absence of a known chronic phase does not exclude CML.

Methods: We investigated a patient referred with severe anemia by peripheral blood and bone marrow morphology, histopathology, flow cytometry, cytogenetics including FISH, molecular genetics and NGS. Historical blood counts were reviewed and discordant findings reassessed interdisciplinary.

Results: A 63-years-old male patient presented with hemoglobin of 68 g/L, leukocytes of 6 G/L and platelets of 567 G/L. His peripheral blood showed 8% blasts, dysplastic neutrophils, giant hypogranular platelets and circulating megakaryocytic nuclei. Platelet counts had declined from 375 G/L in 2021 to 129 G/L in 2025, followed by rapidly developing thrombocytosis in 2026. Splenomegaly and peripheral basophilia were absent.

The bone marrow was hypercellular with MF-2 fibrosis and increased dysplastic megakaryocytes and megakaryoblasts (~30%). Aspirate reassessment identified 10% myeloid blasts and 21% megakaryoblasts. Flow cytometry detected 6% aberrant myeloid blasts and 3.2% marrow basophils, but no distinct megakaryoblastic population (sample error). Cytogenetics showed 46,XY,t(9;22)(q34;q11.2)[20], BCR::ABL1 p210 was detected, and NGS revealed no additional pathogenic variants. Only the detection of BCR::ABL1 by FISH in mature megakaryocytes and in mature granulocyte-rich areas devoid of blasts of the bone marrow biopsy further supported CML blast phase as the favored diagnosis.

Conclusions: This case illustrates the diagnostic complexity of BCR::ABL1-positive acute leukemia with megakaryocytic differentiation without documented antecedent CML. Discordant and overlapping diagnostic findings highlight the need for integrated interpretation of the clinical history and laboratory data. Assessment of BCR::ABL1 distribution across differentiated hematopoietic compartments, together with longitudinal monitoring of BCR::ABL1 clone size during therapy, may help distinguish de novo AML from CML blast phase.

8214

Tracheal Involvement in Chronic Lymphocytic Leukemia: A Case Report

D. Heim (1), L. Stutz (1), P. Konermann (2), T. Menter (3), J. R. Passweg (1), M. Pradella (4), A. Holbro (5), L. Stutz (1)

Hematology, University Hospital Basel, Basel (1), Pneumology, University Hospital Basel, Basel (2), Pathology Institute of Medical Genetics and Pathology, University Hospital Basel, Basel (3), Radiology, University Hospital Basel, Basel (4), Hematology and Blood Transfusion Service, University Hospital Basel, Basel (5)

Introduction: Extranodal/extramedullary manifestations of chronic lymphocytic leukemia (CLL) are rare and are considered an indication for treatment. We present an uncommon case of tracheobronchial extranodal/extramedullary involvement in CLL with with a description of the diagnostic work-up, including CT imaging, bronchoscopy, and histopathological correlation. To date, no standard treatment has been established for tracheobronchial manifestations of CLL. Reporting such uncommon presentations expands clinical evidence and may improve their recognition and management.

Methods: Literature research and description of the clinical case.

Results: A 75-year-old patient presented with hoarseness, dyspnea, productive cough and subsequently developed obstructive pneumonia. The diagnosis of the extranodal involvement was established by endobronchial biopsy of the tracheal lesions whereas tracheobronchial wall thickening was also noted on CT. Treatment with obinutuzumab and venetoclax resulted in rapid and complete resolution of symptoms.

Conclusions: This case highlights that rare extranodal/extramedullary manifestations of CLL should be considered in the differential diagnosis of atypical lesions, even if a more common diagnosis appears likely. It adds to the available clinical evidence and to the evidence on treatment responsiveness, thereby improving the recognition and management of uncommon extranodal and extramedullary CLL.

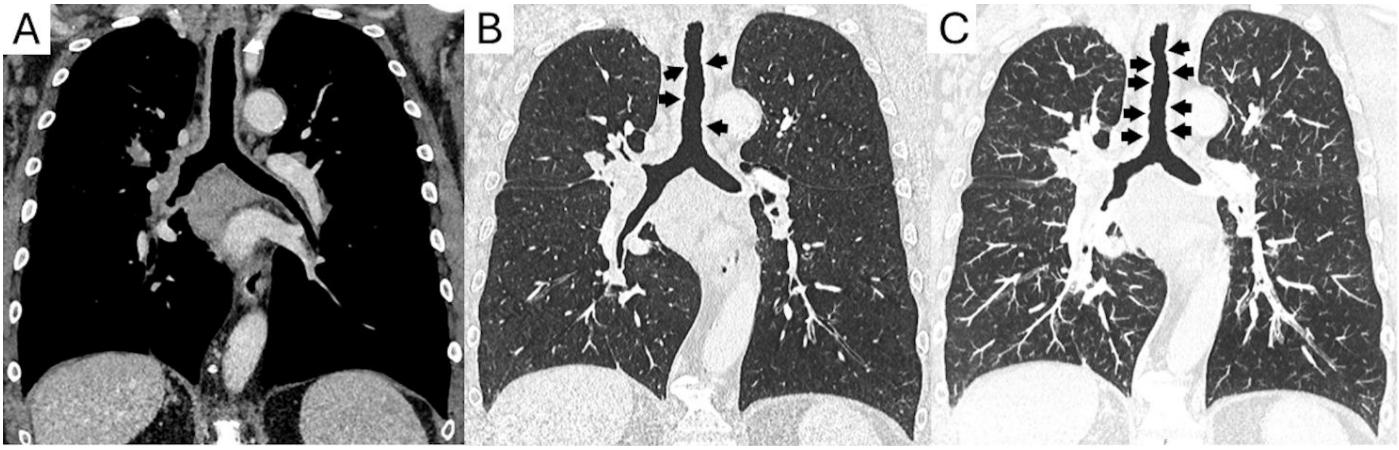


Figure 1 shows the trachea and main bronchi on coronal reformations of a chest CT. In soft tissue kernel (A) the wall thickening of the trachea (e.g. white arrow) and main bronchi can be seen. Nodular changes (black arrows) of the tracheal endothelium can be depicted on standard image (B) and are highlighted on the maximum intensity projection (MIP) image (C). These findings represent the involvement of the CLL.

 Published under the CC license Attribution 4.0 International (CC BY 4.0)

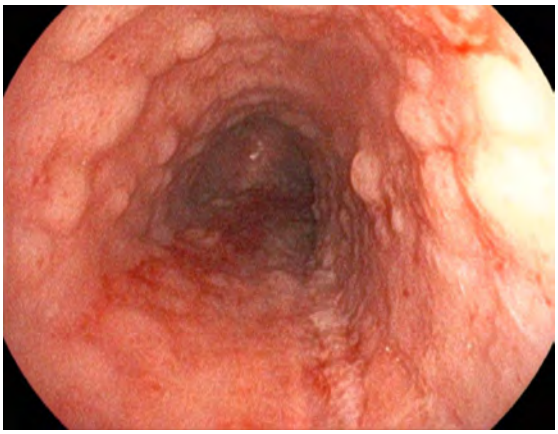


Figure 2 Endobronchial appearance at bronchoscopy: nodular changes of the trachea.

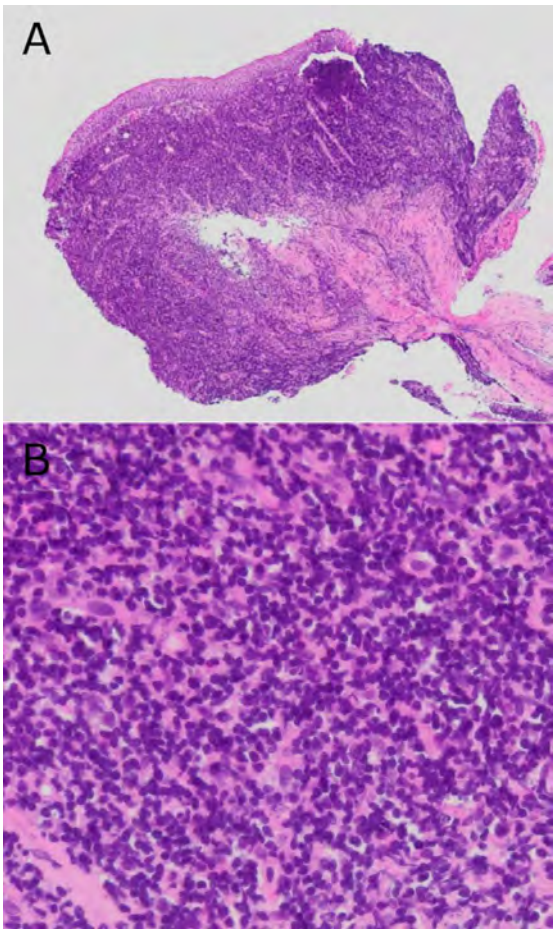


Figure 3 Hematoxylin and eosin (H&E)-stained section showing dense infiltration of small, monomorphic lymphocytes within the tracheal mucosa, consistent with CLL infiltration (A, overview; B, detail).

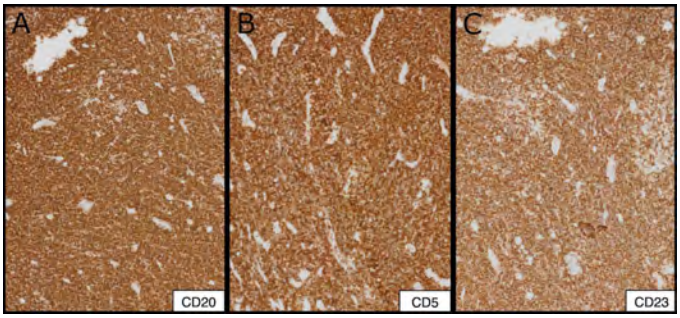


Figure 4 Immunohistochemical staining of the tracheal mucosa demonstrates the typical CD20 (A), CD5 (B), and CD23 (C) expression pattern of the CLL cells.

4522

Targeting the Clone to Target the Bone: Early Biological and Skeletal Changes with Avapritinib in Indolent Systemic Mastocytosis

T. Gerardi (1), E. Biver (2), M. Mappoura (1), Y. Beauverd (1)

Hematology departement, Geneva University Hospital, Geneva (1), Bone Diseases Unit, Geneva University Hospital, Geneva (2)

Introduction: Systemic mastocytosis (SM) is a clonal mast-cell disorder associated with osteoporosis and fragility fractures. Bisphosphonates remain the cornerstone of treatment for SM-related osteoporosis, although they target bone remodelling rather than the underlying mast-cell clone. Avapritinib, a potent KIT D816V inhibitor, reduces mast-cell disease burden in indolent systemic mastocytosis (ISM) and exploratory PIONEER data suggest a potential effect on bone density. We report the 6-month biological and skeletal changes of a patient with ISM and severe osteoporosis treated with avapritinib.

Methods: A 73-year-old woman with longstanding osteoporosis despite prolonged antiresorptive therapy developed severe vertebral fractures (T9 grade III and L1 OF4). Investigations revealed elevated basal serum tryptase, a peripheral-blood KIT D816V-positive clone (VAF 0.06% by ddPCR) and bone-marrow mast-cell aggregates, establishing ISM. Avapritinib 25 mg once daily was initiated, with prospective biological and densitometric assessment over 6 months.

Results: At 6 months, serum tryptase decreased from 49.3 µg/L to 25 µg/L (−49.3%, nadir 20 µg/L). Peripheral-blood KIT D816V VAF decreased from 0.060% to 0.014% (−76.7%). CTX decreased from 361 to 289 ng/L (−20%), although interpretation was limited by concomitant antiresorptive treatment and potential post-denosumab rebound. DXA assessment showed lower BMD values than the last pre-avapritinib assessment, but the interpretation was limited by several confounding factors, including denosumab discontinuation, subsequent zoledronic acid treatment and incident vertebral fractures. No new vertebral fracture occurred. Avapritinib was well tolerated, without treatment-related adverse events or dose modifications.

Conclusions: Avapritinib induced a marked biochemical and molecular response, with substantial reductions in serum tryptase and KIT D816V VAF. Although 6 months is too early to demonstrate a skeletal benefit, these findings support the biological rationale for targeting the KIT-mutated mast-cell clone as a potential disease-directed approach to mastocytosis-related bone disease. Longer-term prospective evaluation is warranted.

Parameter	Pre-avapritinib	Post-avapritinib, 6 months FU
Tryptase	49.3 µg/L	25 µg/L
KIT D816V VAF	0.060%	0.014%
CTX	361 ng/L	289 ng/L
Lumbar spine DXA	0.801 / -2.2	0.765 / -3.1
Femoral neck DXA	0.637 / -1.9	0.606 / -2.2
Total hip DXA	0.795 / -1.2	0.762 / -1.5
Skeletal events	T9 grade III; L1 OF4	No new vertebral fracture

DXA values are reported as BMD (g/cm²) / T-score.

Published under the CC license Attribution 4.0 International (CC BY 4.0)

9378

Diagnostic Uncertainty and Transfusion Independence With Momelotinib in a Myeloid Disorder Without a Detectable Clonal Marker

L. J. Drück (1), M. M. Bühler (2), S. Gundermann (1)

Medical Oncology and Haematology, Cantonal Hospital Winterthur, Winterthur (1), Pathology, University Hospital Zurich, Zurich (2)

Introduction: Myeloid disorders without detectable clonal markers may remain difficult to classify, complicating treatment selection and reimbursement. We report transfusion independence with momelotinib after reassessment of an initial diagnosis of primary myelofibrosis (PMF).

Methods: In 2020, a 73-year-old man presented with severe anaemia, thrombocytosis and red blood cell (RBC) transfusion dependence. Bone marrow examination showed hypercellularity, prominent granulopoiesis and megakaryopoiesis, reduced and left-shifted erythropoiesis, and grade 2 fibrosis. Cytogenetics and targeted next-generation sequencing detected no clonal marker. PMF was diagnosed, and danazol normalised blood counts, maintaining transfusion independence for approximately five years.

Results: In late 2025, severe anaemia and thrombocytosis recurred despite danazol, requiring twice-weekly RBC transfusions. Repeat investigation, including assessment for reactive and secondary causes, demonstrated impaired erythroid maturation without a detectable clonal marker. Expert review of the 2020 and 2025 biopsies did not confirm PMF. Following multidisciplinary discussion, myelodysplastic/myeloproliferative neoplasm, not otherwise specified (MDS/MPN, NOS), was considered the most likely provisional diagnosis. Momelotinib was selected for its activity in myelofibrosis-associated anaemia and its JAK1/2 and activin A receptor type 1 (ACVR1) inhibition. These actions attenuate cytokine signalling and reduce hepcidin production, respectively, improving iron availability for erythropoiesis. An individual reimbursement request was approved. The last RBC transfusion was administered two weeks after treatment initiation; the patient has remained transfusion-independent during follow-up.

Conclusions: This case illustrates how diagnostic reassessment, multidisciplinary evaluation and individual reimbursement can enable a biologically informed treatment approach despite uncertain disease classification. Transfusion independence followed momelotinib initiation, but does not establish the underlying diagnosis or prove correction of erythroid maturation through ACVR1 inhibition.

9161

Simultaneous presence of t(5;9) and t(9;14) in a patient with B-lineage acute lymphoblastic leukemia :case report and literature review

J. T. Liu (1), H. R. Li (1), L. Jiang (1), P. Zhang (1)

Cytogenetics Laboratory, Wuhan Kindstar Clinical Diagnostic Institute, wuhan (1)

Introduction: To investigate the clinical characteristics of B-lineage acute lymphoblastic leukemia (ALL) with t(5;9) and t(9;14), and to provide the reference for the diagnosis and treatment of the disease.

Methods: The clinical data of a pediatric ALL patient were retrospectively analyzed.

Results: A 1-year-old girl was admitted to our hospital complaining of lymphadenectasis and hepatosplenomegaly in December 2025. A peripheral blood examination showed the following counts: white blood cell count (WBC) 66.97×109/L, neutrophil count 1.07×109/L, lymphocyte count 64.09×109/L, red blood cell count (RBC) 1.72×1012/L, hemoglobin 44g/L, platelet count 171×109/L, and 33% of leukemic blasts were stained gray-blue. Leukemic blasts accounted for 86% of the bone-marrow cells. The patient demonstrated a B-cell phenotype, and showed expression of HLA-DR, CD10, CD19, CD20, CD22, CD34, CD38, CD58, CD123, cCD79a and TDT. A G-band-staining chromosomal analysis revealed 46,XX,t(5;9)(q14.1;p24),t(9;14)(p21;q11). A fluorescence in situ hybridization (FISH) analysis revealed MLL(-), BCR::ABL(-), PBX1::TCF3(-), ETV6::RUNX1(-). A RNA-seq analysis uncovered two fusion, SSBP2::JAK2 and CDKN2A::TRAC. According to the Chinese Children's Cancer Group study ALL 2020(CCCG-ALL-2020), the patient was divided into high risk group. Complete remission was achieved after PVDL induction regimen. The patient received consolidation therapy with methotrexate and 6-mercaptopurine, then continued to achieve remission. To July 2026, the patient remained MRD negative after a total of seven months of treatment.

Conclusions: The t(5;9)(q14.1;p24) is a recurrent abnormality in ph-like ALL that fuses SSBP2 to JAK2. JAK2 fusion ph-like ALL patient is associated with high relapse risk and poor clinical outcomes. The t(9;14)(p21;q11) is a recurrent abnormality in ALL that fuses CDKN2A to TRAC. CDKN2A::TRAC fusion may lead to the inactivation of the CDKN2A gene. Some studies have shown that the deletion of CDKN2A is associated with a poor prognosis in both adult and childhood ALL patients.

0783

Clinical Outcomes in Patients with BRCA2-Altered mHSPC Treated with Niraparib Plus Abiraterone and Prednisone: AMPLITUDE Subgroup Analysis

A. Omlin (1), D. E. Rathkopf (2), N. Agarwal (3), J. N. Graff (4, 5), S. Sandhu (6), E. Efstathiou (7), M. Özgüroğlu (8), A. J. Pereira de Santana Gomes (9), K. Vianna (10), H. Luo (11), G. T. Gotto (12), H. H. Cheng (13, 14), K. S. Gries (15), B. Baron (16), F. Shen (17), S. D. Mundle (15), S. A. McCarthy (15), D. Olmos (18), K. N. Chi (19), G. Attard (20)

University of Zurich and Tumorzentrum Hirslanden Zurich, Onkozentrum Zurich AG, Zurich (1), Department of Medicine, Memorial Sloan Kettering Cancer Center, New York (2), Huntsman Cancer Institute, University of Utah, Salt Lake City (3), Knight Cancer Institute, Oregon Health & Science University, Portland (4), Hematology/Oncology, Veterans Affairs Portland Health Care System, Portland (5), Genitourinary Oncology Service, Peter MacCallum Cancer Centre, Melbourne (6), Genitourinary Oncology, Houston Methodist Cancer Center, Houston (7), Cerrahpaşa Faculty of Medicine, Istanbul University Cerrahpaşa, Istanbul (8), Oncologia Clinica, Liga Norte Riograndense Contra o Câncer, Natal (9), Oncologia Clinica, Centro Integrado de Oncologia de Curitiba, Curitiba (10), Department of Urology, Chongqing University Cancer Hospital, Chongqing (11), Department of Oncology, University of Calgary, Calgary (12), Division of Hematology and Oncology, University of Washington, Seattle (13), Clinical Research Division, Fred Hutchinson Cancer Center, Seattle (14), R&D, Johnson & Johnson, Raritan (15), R&D, Johnson & Johnson, Leiden (16), R&D, Johnson & Johnson, Spring House (17), I+12 Biomedical Research Institute, Hospital Universitario 12 de Octubre, Madrid (18), BC Cancer – Vancouver Center, University of British Columbia, Vancouver (19), Cancer Institute, University College London, London (20)

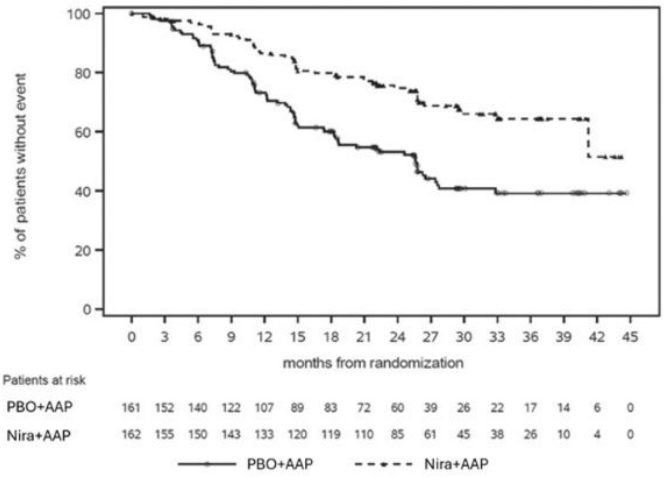
Introduction: AMPLITUDE, a phase 3, randomized, double-blind study, evaluated niraparib plus abiraterone acetate and prednisone (Nira+AAP) versus placebo plus abiraterone acetate and prednisone (PBO+AAP) with ongoing androgen deprivation therapy in patients with metastatic hormone-sensitive prostate cancer (mHSPC) harboring homologous recombination repair (HRR) gene alterations. The primary analysis demonstrated significant clinical benefit with Nira+AAP, particularly in BRCA1/2 altered patients1. BRCA2 is the most common HRR alteration in mHSPC. This analysis evaluated niraparib plus AAP in BRCA2-altered mHSPC.

 Published under the CC license Attribution 4.0 International (CC BY 4.0)

Methods: AMPLITUDE's primary endpoint was investigator-assessed radiographic progression-free survival (rPFS). Key secondary endpoints included time to symptomatic progression (TSP) and overall survival (OS). This subgroup analysis included patients with BRCA2 alterations (n = 163 per arm). Time-to-event outcomes were analysed using stratified Cox models and Kaplan-Meier methods. Safety was assessed in all BRCA subgroups; BRCA2-specific safety data were not reported separately.

Results: In the exploratory BRCA2 subgroup, Nira+AAP significantly improved rPFS versus PBO+AAP. rPFS events occurred in 48/163 (29.5%) patients receiving Nira+AAP versus 83/163 (50.9%) receiving PBO+AAP (HR 0.456; 95% CI 0.319-0.652). Median rPFS was not reached (NR) with Nira+AAP versus 25.63 months with PBO+AAP. TSP was also improved with Nira+AAP, with events observed in 27/163 (16.6%) versus 59/163 (36.3%) patients, respectively (HR 0.417; 95% CI 0.264-0.658). Median TSP was NR in both arms. At the first OS interim analysis, deaths occurred in 36/163 (22.1%) patients receiving Nira+AAP and 55/163 (33.7%) receiving PBO+AAP (HR 0.658; 95% CI 0.432-1.002). Median OS was NR in both arms. Safety was consistent with the known safety profile of Nira+AAP. Grade 3/4 adverse events (AEs) occurred in 75.9% versus 57.1% of patients and serious adverse events in 35.1% versus 27.0% in the Nira+AAP and PBO+AAP arms, respectively. No new safety signals were observed.

Conclusions: In patients with BRCA2- altered mHSPC, Nira+AAP improved rPFS, TSP and showed a favorable OS trend versus PBO+AAP, with no new safety signals. These findings further support biomarker-directed use of PARP inhibition combined with androgen-signaling inhibition in patients with BRCA2-altered mHSPC.



POSTER - CLINICAL SOLID TUMOR ONCOLOGY

9135

Comparison of Child–Turcotte–Pugh Score and Albumin–Bilirubin Index for Prognostication in Advanced Hepatocellular Carcinoma: A Five-Year Prospective Cohort Study from a Tertiary Cancer Centre in a Low- and Middle-Income Country

X. Sinha (1)

Medical Oncology, SMIH SGRRU, Dehradun (1)

Introduction: To compare the prognostic performance of the Albumin-Bilirubin (ALBI) grade and the Child–Turcotte–Pugh (CTP) score in assessing hepatic functional reserve and predicting overall survival in patients with advanced hepatocellular carcinoma, and to evaluate their utility for clinical risk stratification.

Methods: In this prospective observational study, consecutive patients with newly diagnosed advanced hepatocellular carcinoma treated between January 2020 and December 2024 were enrolled. Patients were stratified by Child–Turcotte–Pugh (CTP) class and Albumin–Bilirubin (ALBI) grade. Overall survival was analysed using the Kaplan–Meier method and Cox proportional hazards regression. Prognostic performance was compared using Harrell's concordance index (C-index) and receiver operating characteristic (ROC) analysis. Bootstrap validation and propensity score matching were performed to assess model robustness and minimize confounding.

Results: A total of 236 patients were included (median age, 61 years; 79.2% male). Cirrhosis was present in 76.3%, portal vein thrombosis in 58.1%, and macrovascular invasion in 63.6%. Increasing ALBI grade was significantly associated with poorer ECOG performance status, higher AFP levels, greater tumour burden, vascular invasion, and advanced BCLC stage (all P <0.001). Median overall survival declined significantly across ALBI grades (18.6, 10.9, and 4.9 months for grades 1–3; P <0.001) and CTP classes (17.5, 9.8, and 4.7 months for classes A–C). On multivariable analysis, ALBI grade 3 independently predicted worse overall survival (adjusted HR 2.36, 95% CI 1.62–3.43; P <0.001), whereas CTP class was not independently prognostic. ALBI demonstrated superior prognostic discrimination compared with CTP (C-index 0.712 vs. 0.669; ROC AUC 0.782 vs. 0.704; P = 0.018). These findings remained consistent following bootstrap validation and propensity score–matched analysis (adjusted HR 2.11, 95% CI 1.41–3.17; P <0.001).

Conclusions: ALBI demonstrated superior prognostic performance over the CTP score and independently predicted survival in advanced hepatocellular carcinoma. As a simple and objective measure of hepatic reserve, ALBI may be the preferred tool for routine prognostic assessment and treatment decision-making.

6214

Exploring Microbial and Metabolic Signatures in Non-Muscle-Invasive Bladder Cancer: A Pilot Study

M. Lork (1), Y. Morsy (2), J. Surber (1), M. Scharl (2), V. Wu (3), N. Zamboni (3), J. H. Rüschhoff (4), A. Ebner (5), D. S. Engeler (6), B. Förster (7), L. J. Hefermehl (5), J. Langenauer (6), F. Obrecht (7), R. Seiler-Blarer (8), D. Eberli (1), B. Kaufmann (1), C. Poyet (9), U. Bieri (5, 1)

Department of Urology, University Hospital Zurich, Zurich (1), Department of Gastroenterology and Hepatology, University Hospital Zurich, Zurich (2), Department of Biology, Institute of Molecular Systems Biology, Swiss Federal Institute of Technology/ETH Zurich, Zurich (3), Department of Pathology and Molecular Pathology, University Hospital Zurich, Zurich (4), Division of Urology, Department of Surgery, Cantonal Hospital Baden, Baden (5), Department of Urology, HOCH Cantonal Hospital of St. Gallen, St. Gallen (6), Department of Urology, Cantonal Hospital Winterthur, Winterthur (7), Department of Urology, Hospital Center Biel, Biel (8), Department of Urology, Triemli City Hospital, Zurich (9)

Introduction: Bladder cancer remains a significant health challenge, with non-muscle-invasive bladder cancer (NMIBC) representing the most common subtype. Although Bacillus

 Published under the CC license Attribution 4.0 International (CC BY 4.0)

Calmette-Guérin immunotherapy reduces recurrence and progression to muscle-invasive bladder cancer (MIBC), many patients experience treatment failure or adverse effects, underscoring the need for predictive biomarkers. Emerging evidence suggests that the gut microbiome and host metabolome may influence cancer development and immunotherapy response. This pilot study aimed to characterize gut microbial and systemic metabolic features associated with NMIBC and to explore their potential as candidate biomarkers.

Methods: We analyzed the microbiome and metabolome profiles of fecal and plasma samples from 10 NMIBC patients and 10 healthy controls. Shotgun metagenomic sequencing assessed microbial composition and diversity, while flow-injection mass spectrometry was used for untargeted metabolomic profiling. Clinical metadata - including age, sex, smoking history, and tumor grade - were collected to explore potential associations with omics profiles.

Results: While overall microbial diversity did not differ significantly between groups, specific bacterial taxa were differentially abundant. Multiple species within the phylum Bacillota, including Ruminococcus torques, Dorea longicatena, and Blautia producta, were enriched in NMIBC patients. Notably, many of the upregulated species belonged to the family Lachnospiraceae, well known for short-chain fatty acid production. Plasma metabolomic profiling identified several differentially regulated metabolites: healthy controls exhibited higher levels of the medium-chain fatty acid octanoic acid and decanoic acid, whereas NMIBC patients showed increased levels of p-cresol and p-cresol sulfate.

Conclusions: This hypothesis-generating pilot study identifies preliminary microbial and metabolic differences in NMIBC. These findings provide a rationale for larger, longitudinal studies to evaluate the clinical relevance of these alterations for disease monitoring and BCG response prediction.

8102

Early Circulating Tumour DNA Dynamics Predict Outcomes After Anti-EGFR Rechallenge in Metastatic Colorectal Cancer: A Systematic Review and Meta-Analysis

M. M. BILAL (1), M. S. Patel (2), S. Firdos (3), S. Zaidhulla (4), A. A. Khaleelullah (4), M. NAVEED (5), A. A. Patel (6), T. A. Mukadam (7), D. L. Kotak (1)

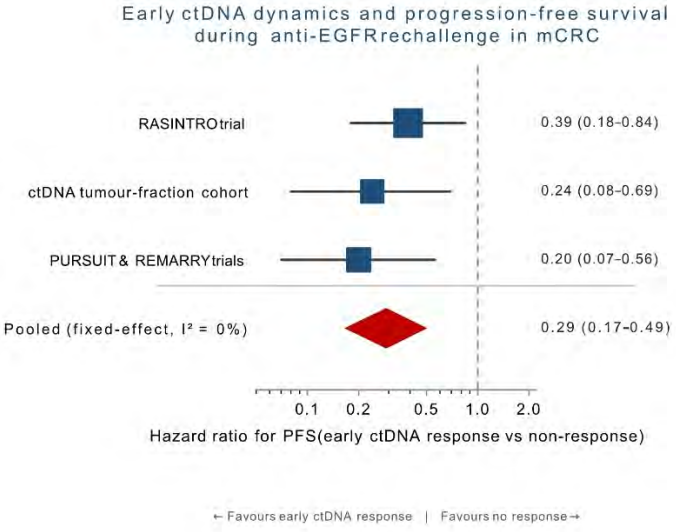
Medicine, Caucasus International University, Tbilisi (1), Medicine, Dr Kiran C Patel Medical College & Research Institute, Gujarat (2), Medicine, King Saud University, Riyadh (3), Medicine, Ken Walker International University, Tbilisi (4), Medicine, Petre Shotadze Tbilisi Medical Academy, Tbilisi (5), Medicine, government medical college gujarat, Gujarat (6), Medicine, Ivane Javakhishvili Tbilisi State University, Tbilisi (7)

Introduction: Anti-EGFR rechallenge is used in RAS/BRAF wild-type metastatic colorectal cancer (mCRC) after an anti-EGFR-free interval, but patient selection has relied mainly on a single pre-treatment circulating tumour DNA (ctDNA) sample. Whether ctDNA measured serially after rechallenge begins adds prognostic value is unclear. We performed a systematic review and meta-analysis to determine whether early, on-treatment ctDNA dynamics predict progression-free survival (PFS), overall survival (OS), objective response rate (ORR) and disease control rate (DCR) during anti-EGFR rechallenge.

Methods: PubMed, Scopus and Cochrane Library were searched for studies of anti-EGFR rechallenge in mCRC that measured ctDNA at more than one time point during treatment and reported its relationship to PFS, OS, ORR or DCR. Hazard ratios (HRs) with 95% confidence intervals (CIs) were extracted for early ctDNA response versus non-response and pooled on the log HR scale using a fixed-effect, generic inverse-variance model; heterogeneity was assessed with I^2.

Results: Three independent, non-overlapping prospective cohorts (32, 38 and 47-50 ctDNA-evaluable patients) reported serial ctDNA sampling during rechallenge. Early ctDNA decline, variously defined as a greater than 50% fall in mutant allele fraction, any or an 80% or greater fall in methylation-based tumour fraction, or clearance of plasma RAS positivity by treatment cycle 3, predicted better outcomes in every cohort. The pooled PFS HR for early responders versus non-responders was 0.29 (95% CI 0.17-0.49, p <0.001), with no statistical heterogeneity (I^2 = 0%). The two cohorts reporting OS showed a concordant association (individual HRs 0.39 and 0.13; pooled HR 0.27, 95% CI 0.13-0.53). Response rates were consistently higher among early ctDNA responders (23.8% versus 0% in the largest cohort), although overall response rates remained modest (ORR 9.5-22.0%; DCR up to 80.0%).

Conclusions: Early on-treatment ctDNA dynamics predict PFS and OS during anti-EGFR rechallenge in mCRC, independently of baseline molecular selection, and the effect is consistent despite differences in assay platform and response threshold across studies. These findings support prospective validation of early ctDNA response as a real-time biomarker to guide continuation or early discontinuation of rechallenge therapy.



1831

Health care costs by treatment pathways in men with localized prostate cancer: a Swiss claims data analysis (2015–2024)

M. Stucki (1), L. Cakir (2), A. Omlin (3), M. Pratsinis (4), D. Zwahlen (5), S. Wieser (1)

Winterthur Institute of Health Economics, ZHAW Zurich University of Applied Sciences, Winterthur (1), Faculty of Health Sciences and Medicine, University of Luzern, Luzern (2), -, Onkozentrum Zürich AG, Zürich (3), Klinik für Urologie, Kantonsspital St. Gallen, St. Gallen (4), Klinik für Radio-Onkologie, Kantonsspital Winterthur, Winterthur (5)

Introduction: Prostate cancer (PC) is the most common solid cancer in men in high-income countries and imposes a substantial economic burden. There is only scarce data on care practices and treatment costs for localized and locally advanced PC in Switzerland. This in-depth analysis quantifies total and PC-specific health care costs across distinct treatment pathways for men with localized PC treated with radical prostatectomy (RP) or radiotherapy (RT) as initial therapy.

Methods: This retrospective study used Swiss mandatory health insurance claims data (2015–2024) from a large insurer. The data includes all billed services. Patients initiating either RP or RT as primary treatment for localized PC were identified

 Published under the CC license Attribution 4.0 International (CC BY 4.0)

based on their health service use and attributed to mutually exclusive pathways. The available data did not allow for attribution to the underlying risk groups – though higher risk groups may be inferred in cases of intensive upfront multimodal treatment. Total and PC-specific costs were estimated at 1 and 3 years from treatment initiation.

Results: We identified 2965 PC patients of whom 1971 (66.5%) had RP, and 994 (33.5%) had RT or brachytherapy as initial therapy. The patients were attributed to the following pathways: RP without adj. therapy (59%); RP with adj. RT (4%); RP with adj. androgen deprivation therapy (ADT) or new hormonal therapy (NHT) (3%); RT without adj. therapy (9%); brachytherapy (2%), RT with concurrent ADT for <12 months (10%), 12–36 months (7%), >36 months (2%); RT with adj. NHT (3%). Mean 1-year cumulative total costs by pathway were CHF 32349 (RP, no adj.); CHF 57410 (RP, adj. RT); CHF 46593 (RP with ADT/NHT); CHF 29925 (RT, no adj.); CHF 27220 (brachytherapy); CHF 34449-38715 (RT with ADT); CHF 68166 (RT with NHT). PC-specific costs followed a similar pattern. At 3 years after initial RP or RT, cost differences across pathways widened.

Conclusions: Health care costs in localized PC increase with treatment intensity and presumed disease risk. Patients without adjuvant therapy incur the lowest and comparable costs. Costs escalate progressively in pathways with adjuvant treatments, consistent with the presumed higher-risk disease profiles requiring additional care beyond the initial therapy. These findings provide important real-world information on treatment practices and costs in localized PC in Switzerland.

4005

Synchronous MSI-H Ampullary and Colonic Adenocarcinomas with Concurrent Germline MSH2 and RAD51C Pathogenic Variants in a Young Patient

I. Huber (1), B. Ramos (2), R. K. de Lima (2), F. C. Pelloso (3), M. E. Consolaro (4), A. C. Alarcao (5), M. R. Bitencout (6), R. K. Cuman (7), M. D. Carvalho (4), V. D. Marques (6), S. M. Pelloso (4)

Onkologie, Hämatologie und Transfusion, Cantonal Hospital Aarau, Aarau (1), Oncology, Santo Antonio Hospital, Blumenau (2), Secretaria Municipal de Saúde, Secretaria Municipal de Saúde de Curitiba, Curitiba (3), Universidade Estadual de Maringá, Universidade Estadual de Maringá, Maringá (4), Faculdade Adventista do Parana, Faculdade Adventista do Parana, Maringá (5), Medicine, Universidade Estadual de Maringá, Maringá (6), Health Science, Universidade Estadual de Maringá, Maringá (7)

Introduction: Lynch syndrome, caused by germline mismatch repair (MMR) variants, is the commonest hereditary colorectal cancer (CRC) syndrome. RAD51C pathogenic variants impair homologous recombination repair (HRR) and predispose to ovarian and breast cancer, being rarely described in CRC. We report a young patient with synchronous MSI-H ampullary and colonic adenocarcinomas and co-occurring germline MSH2 and RAD51C pathogenic variants, illustrating the complexity of concurrent MMR and HRR defects.

Methods: A 34-year-old woman presented in September 2025 with jaundice, abdominal pain and 13 kg weight loss. Imaging showed a pancreatic head lesion, colonoscopy revealed a synchronous stenotic transverse colon mass. She underwent combined gastroduodenopancreatectomy and right colectomy. Tumour immunohistochemistry, somatic next-generation sequencing and a 42-gene germline panel were performed.

Results: Two independent primaries were confirmed: intra-ampullary intestinal-type adenocarcinoma (G2, pT3b pN1, 2/20 nodes; LVI+/PNI+) and ascending colon adenocarcinoma (G2, focal mucinous, pT4a pN2b, 10/56 nodes). Both tumours showed loss of MSH2/MSH6 with preserved MLH1/PMS2; the colonic tumour was MSI-H, RAS/BRAF wild-type, with somatic ERBB2 and TP53 variants. Germline testing identified two heterozygous pathogenic variants, MSH2 c.2152C>T (p.Gln718*) and RAD51C c.709C>T (p.Arg237*), plus a BLM variant of uncertain significance. Family history included gastrointestinal and haematological malignancies across three generations. Following the recent ATOMIC trial, the addition of atezolizumab to adjuvant chemotherapy was discussed, the case was referred to multidisciplinary tumour board and oncogenetics. Reduced-dose adjuvant mFOLFOX was discontinued after 7 cycles owing to grade 2–3 asthenia and persistent diarrhoea. At last follow-up the patient had no evidence of disease with normalised tumour markers.

Conclusions: This case supports comprehensive multi-gene germline panel testing in young-onset gastrointestinal malignancies, where actionable variants beyond the Lynch spectrum can be uncovered. It also highlights the need for multidisciplinary tumour boards equipped to manage overlapping hereditary cancer syndromes, since concurrent MMR and HRR defects raise unresolved questions, including the comparative roles of MSI-H-directed immunotherapy and HRR-directed strategies, that warrant prospective investigation.

Table 1. Germline molecular findings

Results of a 42-gene germline hereditary cancer panel performed on peripheral blood in a young patient with synchronous MSI-H ampullary and colonic adenocarcinomas. Variant classifications follow ACMG/ClinVar standards at the time of submission.

Gene	Variant (HGVS, MANE Select)	Consequence	Classification
MSH2	NM_000251.3:c.2152C>T p.Gln718Ter	Nonsense heterozygous	PATHOGENIC ★★★ · ClinVar 90909
RAD51C	NM_058216.3:c.709C>T p.Arg237Ter	Nonsense heterozygous	PATHOGENIC ★★ · ClinVar 186364
BLM	NM_000057.4:c.572G>T p.Arg191Ile	Missense heterozygous	VUS ★★ · ClinVar 454157

Interpretation

- Dual DNA-repair pathway involvement: concurrent germline defects in mismatch repair (MSH2) and homologous recombination repair (RAD51C).
- MSH2 p.Gln718Ter confirms Lynch syndrome; reviewed by the InSiGHT expert panel.
- RAD51C p.Arg237Ter is a pathogenic HRR-gene variant, rarely reported in colorectal cancer.
- BLM p.Arg191Ile is a variant of uncertain significance, reported for completeness; not clinically actionable.

Both synchronous tumours showed loss of MSH2 and MSH6 with preserved MLH1 and PMS2 on immunohistochemistry; the colonic tumour was MSI-high and RAS/BRAF wild-type on somatic sequencing.

ACMG: American College of Medical Genetics and Genomics; HGVS: Human Genome Variation Society; HRR: homologous recombination repair; MANE: Matched Annotation from NCBI and EMBL-EBI; MSI: microsatellite instability; VUS: variant of uncertain significance. ClinVar review status: ★★★ expert panel; ★★ multiple submitters, no conflicts.

 Published under the CC license Attribution 4.0 International (CC BY 4.0)

1609

Evaluation of the effectiveness of radio-oncological therapy concepts in geriatric head and neck cancer patients

M. Bürstner (1)

Radioonkology, Technical University Munich, Munich (1)

Introduction: The clinical heterogeneity of elderly patients poses a major challenge for selecting an appropriate treatment, particularly in head and neck cancer patients. The goal of this retrospective analysis was to compare various treatment approaches and to bring out the outcomes and advantages of each therapeutic approach.

Methods: This retrospective analysis included 301 patients (211 men, 90 women) diagnosed with a head and neck cancer at the age of at least 70 years. These patients were treated between July 2010 and December 2024 and were analyzed based on their medical records. Kaplan-Meier was used for evaluation, with the overall survival as endpoint.

Results: Five treatment approaches were evaluated: Definitive Radiotherapy (RT) +- Chemotherapy (CT), adjuvant RT+- CT and palliative RT. The best 3-year overall survival with a rate of 82% was achieved with adjuvant Chemoradiotherapy (CRT), followed by definitive CRT with 75%. RT alone performed worse in terms of long term survival, although adjuvant RT with 64% was superior to definitive RT with 56%. As the only non-curative treatment method, palliative RT, as expected, showed the worst overall survival.

Conclusions: Patients treated with a combination of RT and CT showed better overall survival compared to those treated with RT alone , both in the adjuvant and the definitive setting. However, a certain degree of selection bias must be taken into account here, as fitter patients were deemed capable of undergoing more intensive therapy. To make an informed treatment decision, both the patient's age and individual cofactors, such as comorbidities and polypharmacy, should be taken into account.

4209

A Shared BRIP1 Variant in Father–Son Pancreatic Cancer: A Familial Molecular Observation with Potential Implications for Homologous Recombination Repair

N. Degrauwe (1), G. Dei Tos (2), M. Trimech (3), K. Homicsko (2), A. Digklia (2)

Oncology, CHVR, Sion (1), Oncology, CHUV, Lausanne (2), Pathology, CHUV, Lausanne (3)

Introduction: Familial pancreatic ductal adenocarcinoma (PDAC) may reveal uncommon cancer-predisposition mechanisms. BRIP1 participates in homologous recombination repair, but its contribution to pancreatic cancer susceptibility and therapeutic sensitivity remains poorly defined. We report an unusual father–son occurrence of PDAC with the same tumor BRIP1 variant.

Methods: Clinical, pathological and molecular data from two first-degree relatives with PDAC were retrospectively reviewed. Tumor next-generation sequencing included comprehensive cancer-gene profiling and assessment of variant allele frequencies (VAF).

Results: PDAC was diagnosed in the father at age 70 and in his son at age 39. Both tumors independently harbored the identical BRIP1 c.475A>G (p.Lys159Glu) variant of uncertain significance, with VAFs of 48% and 49%, respectively, despite estimated tumor cellularities of only 30% and 20%. This pattern suggested a possible constitutional heterozygous variant. The tumors otherwise showed distinct molecular profiles, notably KRAS G12D in the father and KRAS G12V in the son. No clear second BRIP1 alteration or loss was identified, although low tumor cellularity limited assessment of loss of heterozygosity. Both patients experienced clinically meaningful disease control with platinum-containing chemotherapy. The father achieved a partial response to FOLFIRINOX but died within one year. The son underwent prolonged multimodal treatment and survived approximately five years. Short exposure to olaparib, limited by thrombocytopenia, did not allow assessment of PARP-inhibitor sensitivity.

Conclusions: The occurrence of PDAC in two first-degree relatives, including early-onset disease, together with the same BRIP1 p.Lys159Glu variant at approximately 50% VAF in both tumors represents an unusual familial molecular observation. Although germline inheritance, pathogenicity and BRIP1-related HR deficiency cannot be established, this finding supports further investigation of BRIP1 in familial and early-onset PDAC and highlights the limitations of assigning therapeutic actionability to individual HRR-gene VUS

9365

Cisplatin-gemcitabine versus MVAC Regimen as neoadjuvant therapy in Muscle-Invasive Bladder Cancer: Systematic Review and Meta-Analysis

A. Sakh (1), F. Faza (2)

School of Medicine, University of Pelita Harapan, Tangerang (1), Nanotechnology department, University of Airlangga, Surabaya (2)

Introduction: This Systematic review and meta-analysis evaluates the comparative efficacy, survival benefits, and surgical safety of these two regimens to clarify the optimal therapeutic approach.

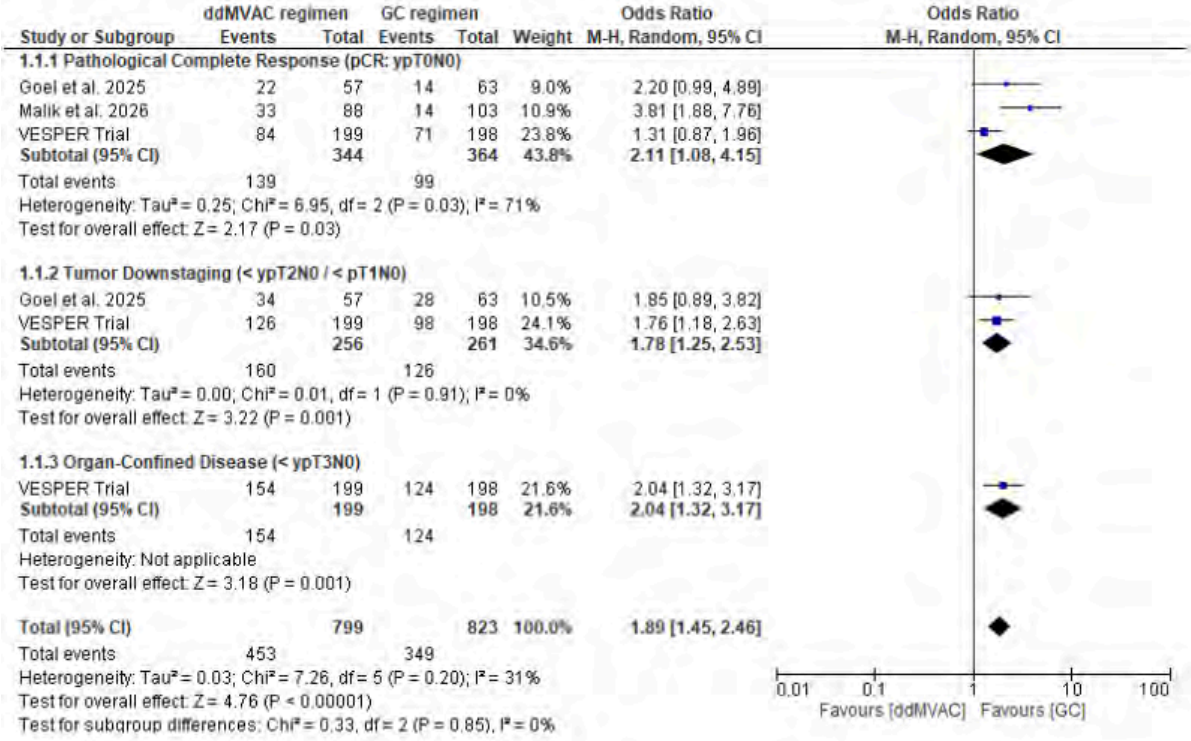
Methods: Conducted in accordance with PRISMA 2020 standards, this review pooled data from four studies encompassing 1,019 patients. We utilised random-effects modelling (Mantel-Haenszel and inverse-variance methods) to calculate pooled odds ratios (OR) and hazard ratios (HR) alongside their 95% confidence intervals (CI). Risk of bias was assessed utilizing the RoB2 tool for randomised controlled trials and the ROBINS-I tool for non-randomised studies.

Results: ddMVAC yielded significantly higher pathological complete response (ypT0N0: OR 2.11, 95% CI 1.08-4.15, p = 0.03), tumor downstaging (<ypT2N0: OR 1.78, 95% CI 1.25-2.53, p = 0.001), and organ-confined disease rates (<ypT3N0: OR 2.04, 95% CI 1.32-3.17, p = 0.001) than GC. Furthermore, ddMVAC significantly improved overall survival (HR 0.74, 95% CI 0.63-0.87, p = 0.0004) and progression-free survival (HR 0.74, 95% CI 0.55-1.00, p = 0.05). Disease-free survival (HR 0.85, 95% CI 0.68-1.06, p = 0.15) and event-free survival (HR 0.66, 95% CI 0.38-1.15, p = 0.14) favoured ddMVAC but lacked statistical significance. Surgical feasibility was comparable; there were no significant differences in cystectomy execution (OR 1.28, 95% CI 0.85-1.94, p = 0.23), negative margin (R0) resections (OR 2.62, 95% CI 0.80-8.57, p = 0.11), or chemotherapy completion (OR 0.71, 95% CI 0.49-1.02, p = 0.06).

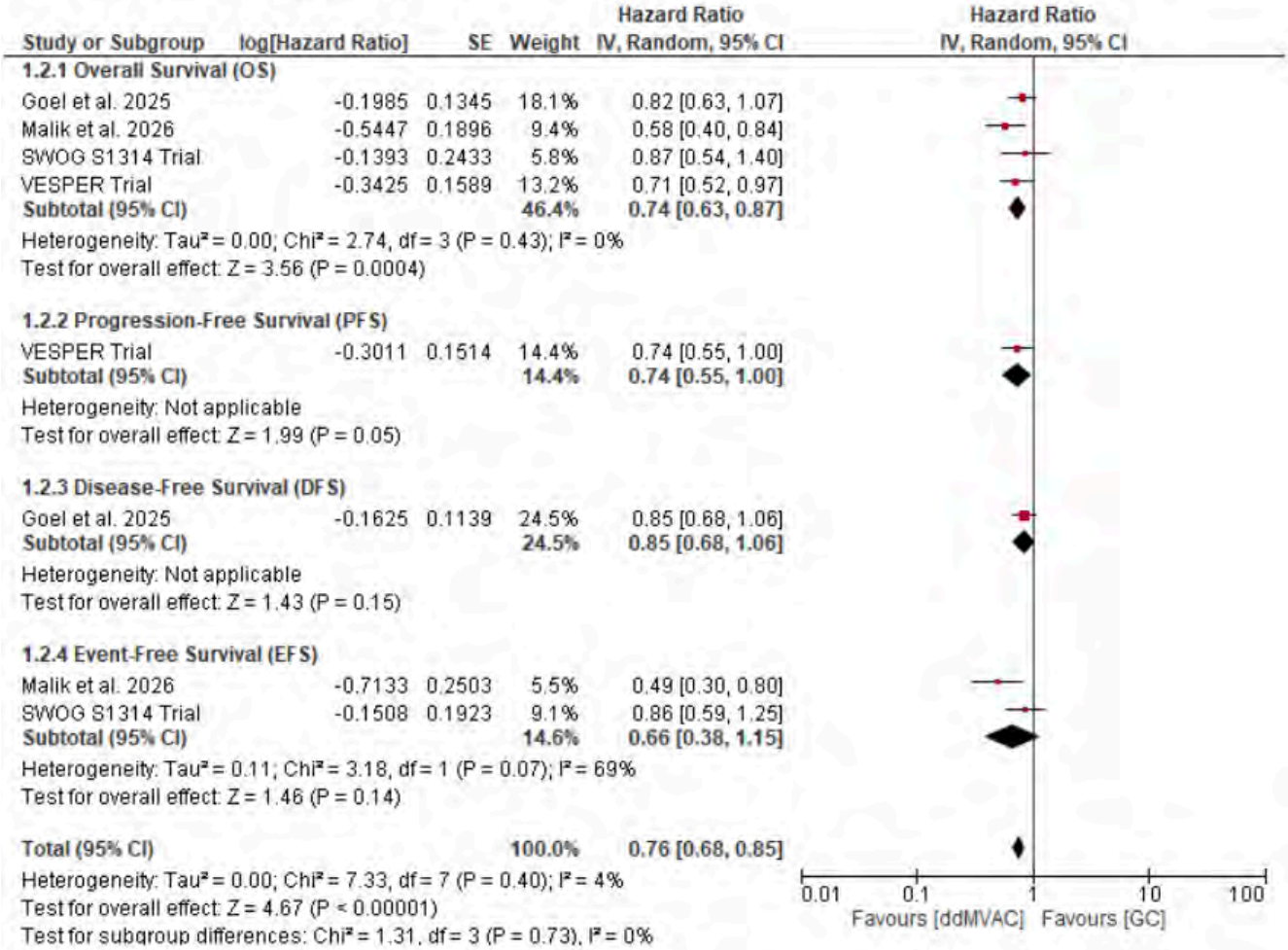
Conclusions: Compared with GC, neoadjuvant ddMVAC yields superior pathological downstaging and significantly extends overall survival in patients with MIBC. Crucially, this enhanced oncological efficacy does not negatively impact the feasibility, safety, or success rates of subsequent radical cystectomies.

 Published under the CC license Attribution 4.0 International (CC BY 4.0)

A. Pathological Response Outcomes

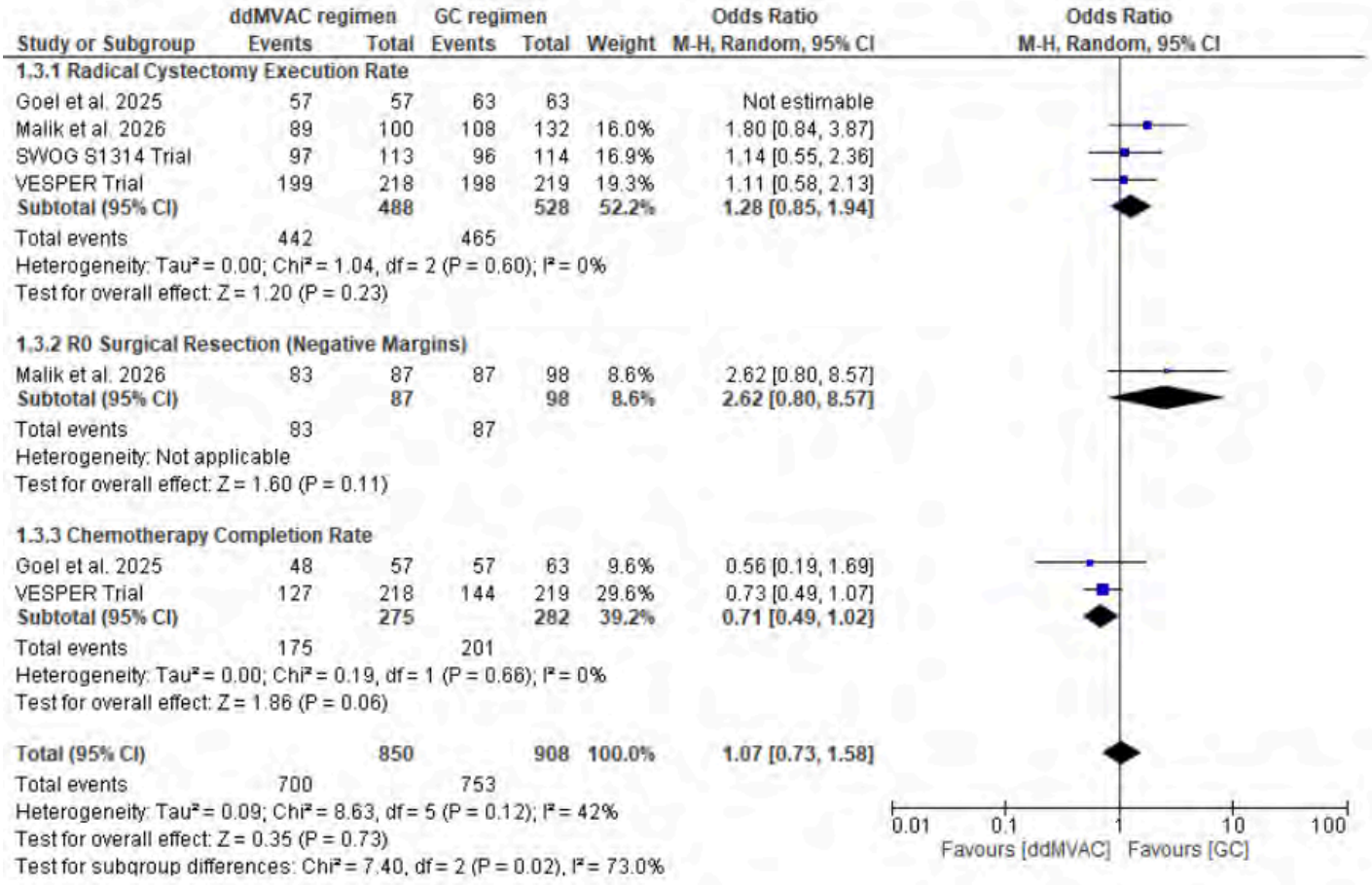


B. Survival Outcomes



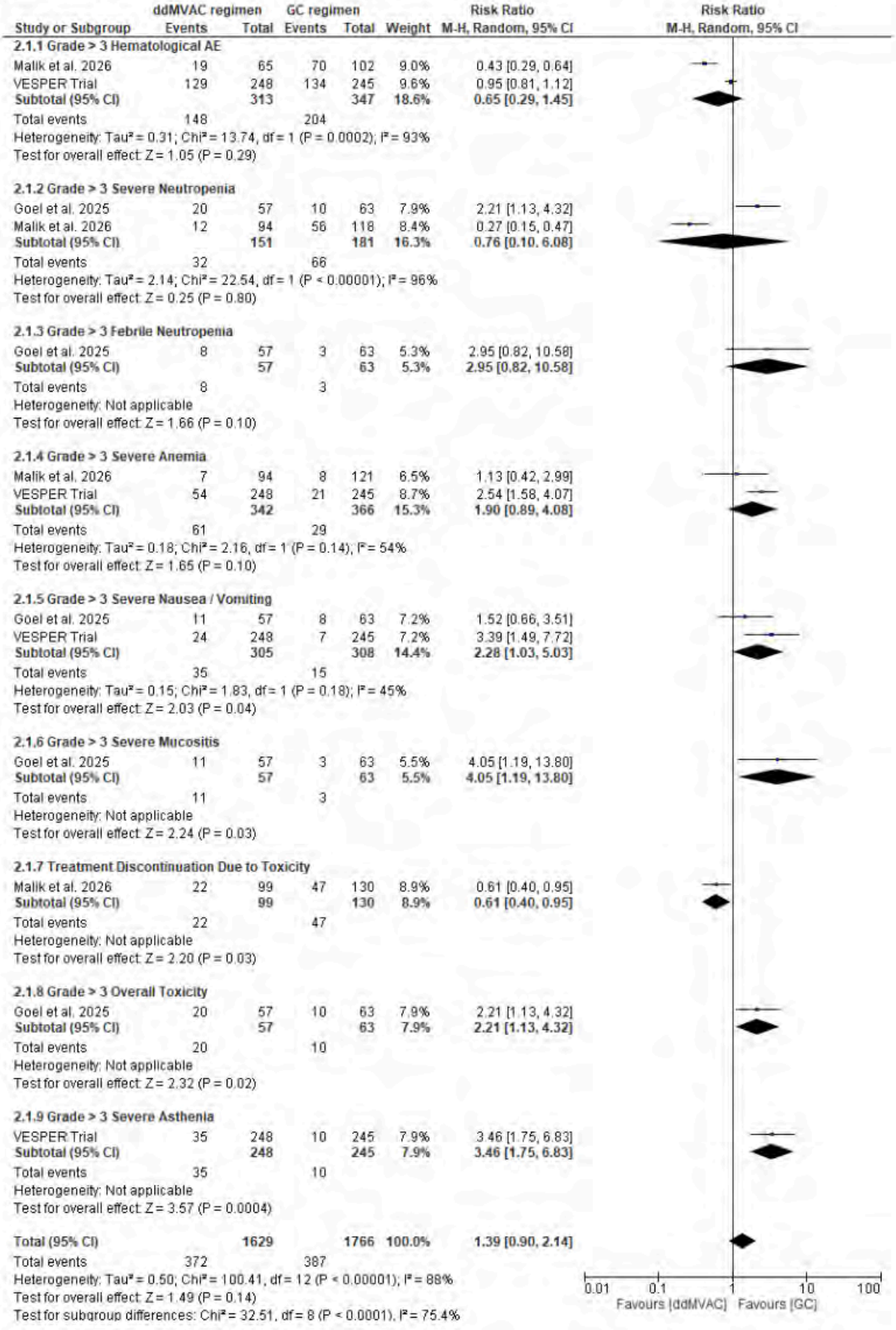
Published under the CC license Attribution 4.0 International (CC BY 4.0)

C. Surgical Outcomes



Published under the CC license Attribution 4.0 International (CC BY 4.0)

D. Safety and Toxicity Outcomes



Published under the CC license Attribution 4.0 International (CC BY 4.0)

7982

Heart Rate Variability and Systemic Inflammation as Non-Invasive Biomarkers of Physiological Burden and Resilience in Lung Cancer Patients

L. Hunakova (1), M. Zvarik (2), I. Mikolaskova (1), E. Zurkova (1)

Institute of Immunology, Faculty of Medicine Comenius University, Bratislava (1), Faculty of Mathematics, Physics and Informatics, Comenius University, Bratislava (2)

Introduction: Lung cancer and its systemic therapies induce systemic inflammation and autonomic nervous system (ANS) dysregulation. Heart rate variability (HRV) serves as a non-invasive window into ANS balance and physiological stress.

Objective: To evaluate HRV parameters and systemic inflammatory markers in lung cancer patients compared with healthy controls, assessing their potential as monitoring biomarkers for physiological burden.

Methods: In this pilot study, 5-minute resting ECG recordings (1000 Hz, Bittium Faros 180) were analyzed using Kubios Premium (v3.5.0) in 19 lung cancer patients (predominantly stage III-IV lung cancer) and 23 healthy volunteers. Autonomic indices—including parasympathetic nervous system (PNS) index and sample entropy (SampEn)—and inflammatory markers—neutrophil-to-lymphocyte ratio (NLR) and systemic immune-inflammation index (SII)—were compared after adjustment for age and sex.

Results: Compared to healthy controls, patients demonstrated significantly higher heart rates, lower SampEn complexity, and a reduced PNS index. Concurrently, patients exhibited markedly elevated NLR and SII values. These findings reflect sympathetic modulation, impaired cardio-vagal control, and heightened systemic immune-inflammation in lung cancer patients.

Conclusions: Reduced HRV and elevated inflammatory indices suggest possible autonomic impairment and systemic stress in lung cancer. Non-invasive HRV monitoring represents a valuable tool to evaluate physiological resilience and overall systemic burden, supporting clinical management in lung cancer patients.

2448

Liver Transplantation (LT) for Colorectal Liver Metastases (CRLM): A Case Report

O. Novosad (1), P. Majno-Hurst (2), A. De Gottardi (3), G. Bedino (4), A. Cristaudi (5), P. Compagnon (6), J. Roggero (7), A. Pedrazzini (8), E. Roggero (1)

Oncology and Hematology, Private Practice, Fondazione Oncologia Lago Maggiore, Bellinzona (1), Department of Surgery, Faculty of Biomedical Sciences, Ente Ospedaliero Cantonale (EOC) , Università della Svizzera Italiana (USI), Lugano (2), Gastroenterology and Hepatology, Cantonal Hospital Lucerne, Lucerne (3), Nephrology, Cantonal Hospital Lugano, Lugano (4), Department of Surgery, Regional Hospital of Lugano, Lugano (5), Division of Transplantation, Geneva University Hospital, Geneva (6), Oncology and Hematology, Cantonal Hospital Aarau, Aarau (7), Oncology and Hematology, Private Practice, Fondazione Oncologia Lago Maggiore, Locarno (8)

Introduction: LT is established treatment for selected primary and metastatic liver tumors, neuroendocrine tumors, but its role in CRLM remains controversial.

Methods: We describe a patient with pT3N2M0 RAS/BRAF wild-type pMMR CRC followed over 24 years. Decisions were guided by MDT review, molecular profiling, and ethics committee approval. Staging used PET, MRI, and CT.

Results: We report the case of a 42-year-old woman with pT3N2M0 CRC, RAS/BRAF wild-type, HER2-negative, pMMR/MSS, who underwent left hemicolectomy in 2001 followed by adjuvant 5-fluorouracil/leucovorin/irinotecan. Metachronous liver metastases were detected in 2011, the patient received FOLFOX plus cetuximab, achieving a rapid CR, and underwent right hepatectomy with en bloc resection of segment IV. Intrahepatic recurrence was treated by partial hepatectomy in 2014, and a new recurrence in 2017 was treated with modified FOLFIRINOX plus panitumumab, again achieving a CR sustained for more than 2 years, followed by maintenance capecitabine and panitumumab. In 2019, given sustained remission and absence of extrahepatic disease, she underwent orthotopic LT following multidisciplinary and ethics committee review and thorough discussion with the patient and her family. PET, MRI, and CT showed no evidence of microscopic residual disease in the perihepatic and parabiliary territory, further supporting the rationale for a radical surgical approach. LT resulted in a four-year disease-free interval. In 2025, progression involved the lungs, mediastinal and retroperitoneal lymph nodes and additional surgery to remove a peritoneal implant causing obstruction of the biliary loop. Molecular re-profiling revealed an acquired TP53 mutation with unchanged RAS/BRAF status. She received first-line post-transplant FOLFOX plus panitumumab, and she is currently on second-line bevacizumab, irinotecan, and 5-fluorouracil.

Conclusions: This case, with its prolonged clinical history spanning 24 years and a four-year disease-free interval following LT, supports the view that CRLM should not be regarded as an absolute contraindication to transplantation. Carefully selected patients — particularly those with RAS/BRAF wild-type tumors, documented complete responses, and strictly intrahepatic disease — may achieve meaningful long-term survival. Further prospective studies are needed to refine selection criteria and optimize post-transplant systemic strategies.

3977

Bone Marrow Carcinomatosis in Essential Thrombocythemia Revealing Claudin-18.2-Positive Malignancy: From Diagnostic Clues to Biomarker-Guided Therapy

T. Materski (1), J. Roggero (1), R. Grobholz (1, 2), C. Pauli (3, 2), N. Cantoni (1), C. Bothou (1)

Department of Oncology, Hematology and Transfusion Medicine, Cantonal Hospital Aarau, Aarau (1), Medical Faculty, University of Zurich, Zurich (2), Department of Pathology and Molecular Pathology, University Hospital Zurich, Zurich (3)

Introduction: A 45-year-old man with JAK2-positive essential thrombocythaemia (ET) developed progressive bone pain, marked alkaline phosphatase (ALP) elevation, and rapidly changing haematological and radiological findings. This case highlights the challenge of distinguishing MPN progression from concomitant malignancy and describes the response to CLDN18.2-directed treatment despite an occult primary.

Methods: Diagnostic work-up included serial CT/MRI, bone marrow biopsy, serial ALP assessment, and comprehensive immunohistochemical characterization.

Results: The patient had JAK2-positive ET treated with anagrelide. Eighteen months later, he developed progressive bone pain, an abrupt ALP rise (>2300 U/L), declining platelets, and features suggestive of myelofibrotic transformation. CT/MRI showed progressive skeletal abnormalities. Circulating blasts prompted a repeat bone marrow biopsy, revealing extensive adenocarcinoma infiltration (two-thirds of trephine core) alongside known MPN and myelofibrosis. FDG-PET/CT and MRI demonstrated diffuse skeletal uptake, an L2 lesion with posterior wall destruction, and transformation into a gland-forming tumour. No primary was identified on imaging or endoscopy. The tumour was MSS, CK7+/CDX2+, HER2 1+, ARID1A-loss, and showed moderate-to-strong membranous CLDN18.2 expression in 100% of cells; PSA, TTF-1, and PD-L1 were negative,

 Published under the CC license Attribution 4.0 International (CC BY 4.0)

supporting metastatic adenocarcinoma of suspected gastric/hepatobiliary origin. FOLFOX plus zolbetuximab (from cycle 2) resulted in a marked biochemical and haematological response, with ALP dropping from >2300 to 190 U/L and rapid normalisation of platelets.

Conclusions: New bone pain, biochemical abnormalities, or changing blood counts in MPN patients should not automatically be attributed to disease progression, and discordant findings warrant histological reassessment. Biomarker profiling can identify actionable targets despite an occult primary. Strong CLDN18.2 expression enabled effective zolbetuximab treatment in metastatic adenocarcinoma without a proven gastric primary.

0328

Targeted therapies in metastatic pancreatic ductal adenocarcinoma and cholangiocarcinoma: a visual comparison of actionable molecular alterations

M. Fivaz (1), V. Genoud (1), T. Koessler (1)

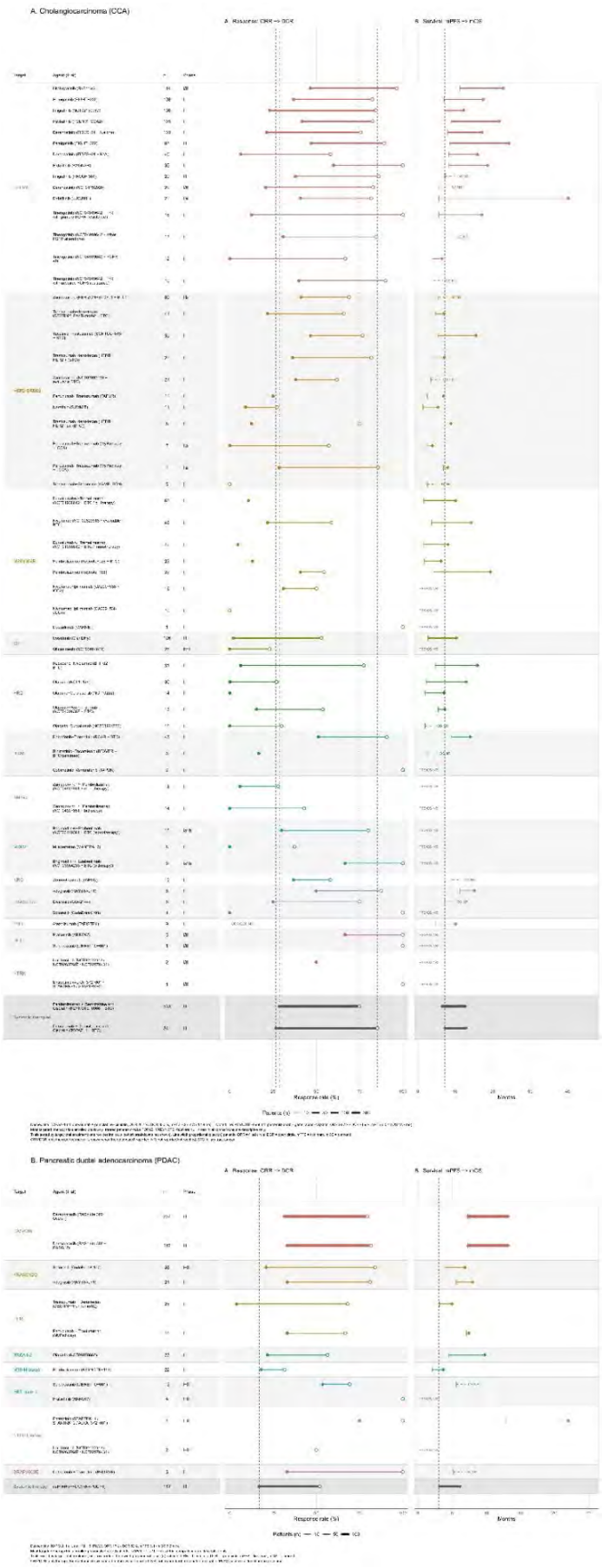
Oncology, Geneva University Hospital, Geneva (1)

Introduction: Pancreatic ductal adenocarcinoma (PDAC) and cholangiocarcinoma (CCA) are both aggressive malignancies of the pancreas and biliary tract, respectively, and primarily treated with standard chemotherapy. However, these tumors differ markedly in their genomic landscape and eligibility for precision oncology. Over the last decade, the molecular features of these diseases have been thoroughly characterized, and targeted therapies have emerged as potential new treatment strategies.

Methods: We reviewed phase I-III clinical trials published through 2026 that evaluated targeted therapies in PDAC and CCA, focusing primarily on reported efficacy (ORR and DCR) and survival outcomes (mPFS and mOS). These data are plotted against the standard second-line chemotherapy regimen to provide a visual comparison of expected clinical outcomes.

Results: In CCA, 49 trials covering 13 different molecular targets reported clinical outcomes, compared with 13 trials covering 8 targets in PDAC. Overall, the data are highly heterogeneous but appear to show higher ORR and mPFS than standard treatment in both tumors.

Conclusions: Treatment for CCA and PDAC is progressively moving toward biomarker-driven strategies. However, CCA currently offers a broader range of actionable targets and higher response rates than PDAC, where targeted therapies remain limited to rarer molecular subgroups, but may improve with the arrival of RAS inhibitors. Comprehensive molecular profiling at diagnosis is essential in both tumous, and future research should prioritize subtype-specific trials, standardized biomarker testing, and strategies to expand the proportion of patients eligible for targeted therapy.



Published under the CC license Attribution 4.0 International (CC BY 4.0)

2866

RASolve 301: Phase 3 trial in progress of daraxonrasib vs. docetaxel in previously treated RAS mutant non-small cell lung cancer

A. Curioni-Fontecedro (1), F. Skoulidis (2), K. C. Arbour (3), S. Popat (4), C. R. Lindsay (5), H. Hironouchi (6), G. Zalcman (7), J. Naidoo (8), A. J. de Langen (9), L. Tao (10), E. Su (10), M. Hiremath (10), A. Rittmeyer (11), M. Johnson (12)

Department of Oncology, HFR Fribourg, Kantonsspital Fribourg, Villars-sur Glâne (1), Department of Thoracic-Head & Neck Medical Oncology, The University of Texas MD Anderson Cancer Center, Houston (2), Department of Thoracic Oncology, Memorial Sloan Kettering Cancer Center, New York (3), Department of Oncology, Royal Marsden Hospital-Sutton, Sutton (4), Department of Thoracic Medical Oncology, The Christie Hospital, Manchester (5), Department of Thoracic Oncology, National Cancer Center Hospital, Tokyo (6), Department of Thoracic Oncology, Hôpital Bichat – Claude Bernard, Paris (7), Department of Medical Oncology, Beaumont Hospital, Dublin (8), Department of Pulmonary Medicine, Antoni van Leeuwenhoek, Amsterdam (9), Department of Oncology, Revolution Medicines, Inc., Redwood City (10), Department of Thoracic Oncology, LKI Lungenfachklink Immenhausen, Immenhausen (11), Department of Medical Oncology, SCRI Oncology Partners, Nashville (12)

Introduction: Patients with previously treated NSCLC represent a significant unmet need. RAS mutations occur in ~30% of NSCLC cases. Common oncogenic mutations in RAS are substitutions at glycine 12 (G12), glycine 13 (G13), or glutamine 61 (Q61). Other than KRAS G12C, there are no approved targeted therapies available for RAS mutant NSCLC. Daraxonrasib (RMC-6236) is an oral, RAS(ON) multi-selective, tri-complex inhibitor of GTP-bound mutant and wild-type RAS. In a Phase 1 monotherapy trial (NCT05379985), daraxonrasib at 160–220 mg daily showed manageable safety and preliminary efficacy in NSCLC patients. As of 21 July 2025 (N = 59), Grade ≥3 adverse events reported in ≥2 patients included rash (n = 5, 8%), vomiting (n = 5, 8%), and diarrhoea (n = 2, 3%) with no Grade 4 or Grade 5 treatment-related adverse events (TRAEs). In 38 patients with RAS mutant NSCLC previously treated with 1 or 2 lines of therapy, daraxonrasib achieved an ORR of 42% (95% CI: 26–59), with a median duration of response of 11.5 (95% CI: 4.6–not estimable [NE]) months. Responses were seen across G12, G13, and Q61 codons. PFS and OS were 8.3 (95% CI: 4.0–12.5) and 16.0 (95% CI: 9.5–NE) months. These results provide strong rationale for the continued development of daraxonrasib in RAS mutant NSCLC patients.

Methods: RASolve 301 is a global, multicentre, open-label, randomised Phase 3 study (NCT06881784) evaluating efficacy and safety of daraxonrasib vs. docetaxel (1:1 randomisation) in patients with previously treated, locally advanced or metastatic RAS mutant NSCLC. Key inclusion criteria: pathologically confirmed NSCLC, age ≥18 years, ECOG performance status 0–1, prior anti-PD(L)-1 therapy and platinum chemotherapy, and an eligible RAS mutation (defined as nonsynonymous mutations in KRAS/NRAS/HRAS at codons 12, 13, or 61) by local testing. Key exclusion criteria: untreated central nervous system metastases, prior RAS-directed therapy, or actionable driver mutation with approved targeted therapy. Dual primary endpoints: PFS (per RECIST v1.1 assessed by Blinded Independent Central Review [BICR]) and OS in patients with RAS G12X mutations excluding G12C. Key secondary endpoints: PFS (per RECIST v1.1 by BICR) and OS in patients with all RAS mutations, and ORR (per RECIST v1.1 by BICR).

The study will enrol ~590 patients, including from sites in Switzerland.

Results: Trial in progress; none.

Conclusions: Trial in progress; none.

0794

Bone Marrow Carcinomatosis with Bicytopenia Mimicking a Haematological Disorder as the Initial Presentation of Metastatic Breast Cancer

B. Okamura (1, 2), G. Favre (1), S. Ebner (3), R. Zanetti (3), M. Vetter (1)

Department of Haematology and Oncology, Cantonal Hospital Basel-Land, Liestal (1), Department of Haematology and Laboratory Medicine, University Hospital Basel, Basel (2), Department of Obstetrics and Gynecology, Cantonal Hospital Basel-Land, Liestal (3)

Introduction: Bone marrow carcinomatosis (BMC) with cytopenia represents a rare finding in one of the most prevalent oncologic diseases – breast cancer. Even more rare being present at the initial diagnosis – the BMC might lead to findings attributable to a haematologic disease, thus possibly leading to a more convoluted diagnostic pathway.

Methods: We present a rare case of a 59-year-old patient with an estrogen receptor- (ER), progesterone receptor- (PR) and GATA3-positive ductal carcinoma with BMC and the dual-track haematologic and oncologic diagnostic process ahead of establishing the final diagnosis.

Results: The Patient initially presented to the emergency department with symptoms attributed to benign paroxysmal positional vertigo; with an incidental co-finding of mildly reduced haemoglobin and thrombocyte values. After four weeks, an ENT-evaluation was performed due to symptom persistence; with a subsequent finding of bone lesions suspicious for a haematologic malignancy or for metastatic origin in a brain MRI. A haematologic evaluation including a bone marrow puncture was going on simultaneously with a gynaecologic evaluation, which showed a possibly malignant lesion in her right breast tissue (BI-RADS 5 according to a mammograph). A PET-CT scan was performed, showing FDG-avidity in the breast lesion as well as in the bone marrow, hence bringing the differential diagnosis of a BMC due to a primary breast tumor. The immunohistochemic findings in a fine needle biopsy of the breast lesion (ER positive (100%), PR positive (25%), Her2 negative (1+), Ki-67: 30%, GATA3 positive) were consistent with the findings in the bone marrow sample showing tumor cells (ER positive (100%), PR positive (15%), Her2 negative (0), Ki-67 30%, GATA3 positive) while bringing no morphologic or flowcytometric evidence for a heamatologic malignancy. A first line treatment with Ribociclib 600 mg per day (d1-21) and Letrozole 2.5 mg per day was initiated, leading to a rapid improvement of the thrombocyte counts.

Conclusions: This case highlights the importance of a multidisciplinary diagnostic approach in patients with an atypical and diagnostically challenging presentation of breast cancer with BMC. Furthermore, the concordant immunohistochemical findings in the breast and bone marrow biopsies supported the diagnosis of bone marrow involvement by metastatic breast cancer.

 Published under the CC license Attribution 4.0 International (CC BY 4.0)

POSTER - NURSING, SUPPORTIVE & PALLIATIVE CARE, REHABILITATION & SURVIVORSHIP AND INTEGRATIVE ONCOLOGY

1929

Distraction with Virtual Reality and Tablet Devices During Routine Needle Procedures in Children with Cancer: A Protocol for a Randomized Controlled Trial

S. Aljomaa (1), M. Garami (1)

Pathological Sciences, Semmelweis University, Budapest (1)

Introduction: Frequent needle-related procedures during cancer treatment are a significant source of pain and distress for children. Approximately 50%–60% of pediatric patients experience pain and anxiety during nursing puncture procedures. Virtual reality (VR) is a promising distraction technique that may help reduce procedural pain and anxiety. This study aims to compare the effects of VR and a tablet-based distraction intervention with standard care on procedural pain and anxiety in paediatric oncology patients.

Methods: This three-arm, parallel-group randomized controlled trial will include 200 pediatric oncology patients undergoing needle-related procedures during hospitalization for chemotherapy. Participants will be randomly allocated in a 1:1:1 ratio to (1) VR plus standard care, (2) tablet-based intervention plus standard care, or (3) standard care alone. Standard care will consist of topical application of lidocaine 25 mg/g and prilocaine 25 mg/g cream before the procedure and will be provided to all participants. The primary outcome will be procedural pain intensity, assessed using the Visual Analog Scale (VAS) immediately before and after the procedure. Secondary outcomes will include change in anxiety, assessed using the Multidimensional Anxiety Scale for Children (MASC), observer-rated procedural pain assessed using the VAS, and participant satisfaction measured using a 4-point Likert scale following the intervention. Statistical analyses will follow the intention-to-treat principle. The study has been approved by the Scientific and Research Ethics Committee of Hungary (TUKEB) (Approval No. NNGYK/30533-6/2026).

Results: The study will compare procedural pain across the three study arms and evaluate changes in pain and anxiety between groups, as well as participant satisfaction following the procedure. The trial is currently ongoing, with participant recruitment underway.

Conclusions: VR is a promising non-pharmacological intervention that may help alleviate procedural pain and anxiety in children with cancer undergoing repeated needle-related procedures. This trial will provide evidence on the potential effectiveness of VR and tablet-based distraction in paediatric oncology supportive care.

3559

Liminality – A concept to understand patient life transitions after cancer treatment

T. Mathieu (1), S. Cairo Notari (1), N. Favez (1)

Faculty of Psychology and Educational Sciences, University of Geneva, Geneva (1)

Introduction: Individuals who experienced a cancer frequently face persistent difficulties after the end of treatment, which can affect their quality of life. Three profiles have been described. Some individuals manage to regain a satisfactory quality of life; some face major difficulties; finally, some oscillate between a difficult and a satisfactory quality of life and struggle to feel cured. The experience of this last profile might be understood through the concept of liminality. So far, the applications of liminality across studies vary and no clear definition emerge. In order to operationalize liminality and to help identifying individuals who struggle to have a satisfactory life, we conducted a scoping review. Our aim was to define how liminality has been conceptualized, how the concept has been used, and the characteristics that have been associated with it.

Methods: We carried a scoping review. Five databases were explored: Pubmed, PsycNet, Embase, Web of Science and CINAHL. We used keywords related to cancer and liminality. 454 studies were identified. After the screening, 22 studies were considered as relevant according to our inclusion and exclusion criteria. We extracted the definition of liminality, its use and the associated characteristics.

Results: Liminality is applied and conceptualized differently across studies. Several terms (e.g., state, experience and space) are employed with the concept. Liminality use relates to various cancer trajectory: treatment, post-treatment and end-of-life. The concept is most employed to describe negative consequences: uncertainties, changes in identity, fear of recurrence or death, biographical disruption. However, it is also used to depict posttraumatic growth.

Conclusions: We formulate a tentative definition: liminality is a state where individuals who experienced a cancer face persistent difficulties and vulnerabilities, marked by uncertainty, social and identity disruption, marginalization and challenges in planning for the future. Individuals who experienced cancer might remain in this liminal state until they redefine their identity. Following this definition, we will try to create a questionnaire in order to assess liminal state, with the aim of helping health professional to identify and support patients.

 Published under the CC license Attribution 4.0 International (CC BY 4.0)

INDEX OF FIRST AUTHORS

The numbers refer to the pages of the supplement.

Aliotta A 35 S
Aljomaa S 95 S
Alonso Calleja A 41 S
Ambrosini S 17 S
Andermatt T 23 S
Antonini E 27 S
Antonopoulou E 80 S
Arber C 18 S

Bader MS 72 S
Baldenweg M 39 S
Barrera P 51 S
Bataclan C 45 S
Besemer B 16 S
Besser I 63 S
Bilal MM 56 S, 86 S
Bischoff NH 78 S
Bitsina C 47 S
Boos LA 23 S, 61 S
Bothou C 77 S
Boyadzhiev H 79 S
Brinovec M 66 S
Brunn S 15 S
Brunner L 64 S
Burger A 49 S
Bürgin M 30 S
Bürstner M 88 S

Camarillo-Retamosa E 22 S
Casini A 36 S
Checinska W 16 S
Chiru ED 58 S, 59S
Costanza M 79 S
Couzens A 30 S
Curioni-Fontecedro A 94 S

de Jong-Bakker DP 28 S
Degrauwe N 88 S
Delle Fontane I 78 S
Devin Meier DM 52 S
Dewarrat N 75 S
Diab R 6 S, 8 S
Dietliker N 66 S
Drück LJ 84 S
Duygu Yildiz Özkaya DY 34 S

Eggebrecht GL 24 S
Elleisy M 58 S
Ennouhi S 75 S

Fathi M 2 S
Ferrari TF 54 S
Fivaz M 93 S
Friedrich N 70 S

Gafner L 6 S
Gautier LA 39 S
Gavillet M 51 S
Genthon A 49 S
Georgieva E 81 S
Gerardi T 74 S, 83 S
Giataganzidou I 73 S
Gorges JG 60 S
Gossin MP 73 S
Gremelspacher T 13 S

Haeri K 12 S
Hafezi M 15 S
Hahn SH 18 S
Hale BD 46 S
Hayenga L 34 S
Heim D 82 S
Hodel N 53 S
Hörtensteiner L 41 S
Huber I 87 S
Hugi D 21 S
Hunakova L 92 S
Hussung S 24 S

Jauch AJ 42 S

Kampa-Schittenhelm KM 44 S
Karantzelis N 54 S
Koch C 20 S

Latscha R 82 S
Lechner J 4 S
Lee S-Y 48 S
Legardeur H 12 S
Lipp M 60 S
Liu JT 84 S
Lork M 72 S, 86 S

Mandhair H 77 S
Marchal P 76 S
Materski T 92 S
Mathieu T 95 S
Meinlschmidt GM 26 S
Mena A 19 S
Mikula S 55 S
Monnin-Respen F 36 S
Müller S 57 S

Nieves-Ortega R 38 S
Novosad O 92 S

Okamura B 94 S
Omlin A 84 S
Orloff M 22 S

Patel S 15 S
Pellegrino C 48 S
Popescu RA 63 S
Poyet C 60 S

Rahimi S 10 S
Rasiah R 51 S
Recher M 80 S
Roser K 26 S, 29 S
Rotar TT 64 S

Sakh A 88 S
Schiess LC 27 S
Schobinger S 62 S
Schultheiss C 42 S
Shehwar D 12 S
Sinha X 85 S
Smirnova T 76 S
Stakia P 75 S
Stucki M 86 S
Studt J-D 70 S
Sturm A 79 S

Tripodo M 32 S

Ulahannan A 65 S
Urech C 62 S

Veillard J 19 S
Veyron T 38 S
von Moos R 5 S
Vrotniakaite-Bajerciene K 40 S, 67 S

Wester V 73 S
Wilhelm E 81 S
Wolf U 63 S

Zhang Y 46 S
Zielinska KA 4 S
Zihler D 59 S

SWISS MEDICAL WEEKLY

Editor in chief:
Prof. Gérard Waeber

Deputy editor in chief:
Prof. Stefan Weiler

Academic editors: see www.smw.ch

Managing editors:
Natalie Marty, MD
Jan Roth, MD

doi: https://doi.org/10.57187/5878
ISSN online supplement: 2504-1622

Published under the CC license Attribution 4.0 International (CC BY 4.0)
You are free to share (copy and redistribute the material in any medium or format) and adapt (remix, transform, and build upon the material) for any purpose under the following terms: Attribution – You must give appropriate credit, provide a link to the license, and indicate if changes were made. You may do so in any reasonable manner, but not in any way that suggests the licensor endorses you or your use.

No additional restrictions – You may not apply legal terms or technological measures that legally restrict others from doing anything the license permits.

Guidelines for authors and online submission: www.smw.ch

Cover image: © Neydtstock | Dreamstime.com

© SMW supporting association, 2026.